AFWAL-TR-85-3125

AIRCRAFT TRANSPARENCY TEST METHODOLOGY

K. I. Clayton
B. S. West
D. R. Bowman

University of Dayton Research Institute
300 College Park Avenue
Dayton, Ohio 45469

March 1986

Final Technical Report for Period June 1984 - September 1985

Approved for public release; distribution is unlimited.

FLIGHT DYNAMICS LABORATORY
AIR FORCE WRIGHT AERONAUTICAL LABORATORIES
AIR FORCE SYSTEMS COMMAND
WRIGHT-PATTERSON AIR FORCE BASE, OHIO 45433

UNCLASSIFIED
SECURITY CLASSIFICATION OF THIS PAGE

REPORT DOCUMENTATION PAGE

1a. REPORT SECURITY CLASSIFICATION UNCLASSIFIED	1b. RESTRICTIVE MARKINGS NONE
2a. SECURITY CLASSIFICATION AUTHORITY N/A	3. DISTRIBUTION/AVAILABILITY OF REPORT APPROVED FOR PUBLIC RELEASE: DISTRIBUTION IS UNLIMITED.
2b. DECLASSIFICATION/DOWNGRADING SCHEDULE N/A	
4. PERFORMING ORGANIZATION REPORT NUMBER(S) UDR-TR-85-122	5. MONITORING ORGANIZATION REPORT NUMBER(S) AFWAL-TR-85-3125
6a. NAME OF PERFORMING ORGANIZATION UNIVERSITY OF DAYTON RESEARCH INSTITUTE 6b. OFFICE SYMBOL (If applicable) N/A	7a. NAME OF MONITORING ORGANIZATION Air Force Wright Aeronautical Laboratories Flight Dynamics Laboratory
6c. ADDRESS (City, State and ZIP Code) DAYTON, OHIO 45469	7b. ADDRESS (City, State and ZIP Code) WRIGHT-PATTERSON AIR FORCE BASE, OHIO 45433-6553
8a. NAME OF FUNDING/SPONSORING ORGANIZATION FLIGHT DYNAMICS LABORATORY 8b. OFFICE SYMBOL (If applicable) AFWAL/FIER	9. PROCUREMENT INSTRUMENT IDENTIFICATION NUMBER F33615-84-C-3409
8c. ADDRESS (City, State and ZIP Code) WRIGHT-PATTERSON AIR FORCE BASE, OHIO 45433-6553	10. SOURCE OF FUNDING NOS. PROGRAM ELEMENT NO.: 62201F PROJECT NO.: 2402 TASK NO.: 03 WORK UNIT NO.: 55
11. TITLE (Include Security Classification) AIRCRAFT TRANSPARENCY TEST METHODOLOGY (U)	
12. PERSONAL AUTHOR(S) K. I. CLAYTON, B. S. WEST, D. R. BOWMAN	
13a. TYPE OF REPORT FINAL	13b. TIME COVERED FROM 84JUN TO 85SEP
14. DATE OF REPORT (Yr., Mo., Day) March 1986	15. PAGE COUNT 188
16. SUPPLEMENTARY NOTATION	

17. COSATI CODES		
FIELD	GROUP	SUB. GR.
11	09	
14	02	

18. SUBJECT TERMS (Continue on reverse if necessary and identify by block number)
AIRCRAFT TRANSPARENCY TESTING, EXPOSURE SIMULATION, TRANSPARENCY DURABILITY, IN-SERVICE ENVIRONMENT, ACCELERATED WEATHERING, (see reverse)

19. ABSTRACT (Continue on reverse if necessary and identify by block number)

This program centered around a test matrix of 364 coupon type specimens to assess the degree of validity of the existing durability test methodology. Laboratory generated test data, for comparison to available in-service failure data, was produced from tests performed on specimens cut from the following actual transparency designs: F-16A coated monolithic polycarbonate canopy with the original production coating, manufactured by Texstar; F-16A laminated canopy, manufactured by Sierracin; F-15 monolithic stretched acrylic windshield, manufactured by Swedlow; F-15 monolithic stretched acrylic canopy, manufactured by Swedlow; and F-111 laminated ADBIRT windshield, manufactured by Sierracin. Various simulated environmental conditions were combined with the following test parameters: surface/chemical craze, haze/transmittance, high-rate impact, falling weight impact, coating adhesion, flatwise tension, torsional shear, wedge peel, thermal shock, in-flight abrasion, flightline abrasion, and edge attachment. The durability evaluation of monolithic stretched acrylic, coated monolithic polycarbonate, and acrylic faced/polycarbonate laminated

20. DISTRIBUTION/AVAILABILITY OF ABSTRACT UNCLASSIFIED/UNLIMITED ☐ SAME AS RPT. ☒ DTIC USERS ☐	21. ABSTRACT SECURITY CLASSIFICATION UNCLASSIFIED
22a. NAME OF RESPONSIBLE INDIVIDUAL MALCOLM E. KELLEY	22b. TELEPHONE NUMBER (Include Area Code) (513)255-5060 22c. OFFICE SYMBOL AFWAL/FIER

DD FORM 1473, 83 APR EDITION OF 1 JAN 73 IS OBSOLETE.

UNCLASSIFIED
SECURITY CLASSIFICATION OF THIS PAGE

CONTINUATION, BLOCK 18.

ACRYLIC
POLYCARBONATE
LAMINATED CONSTRUCTION

CONTINUATION, BLOCK 19.

transparencies is highly dependent on a realistic accelerated weathering exposure. During this program, accelerated weathering was simulated using QUV, 120°F, 7 hour UV/5 hour condensation cycles with 168 hours run time equaling one equivalent year of in-service exposure. The proposed accelerated weathering exposure alone appears too severe; the proposed accelerated weathering exposure combined with normal cleaning cycles appears to be representative of in-service usage.

PREFACE

The efforts reported herein were performed by the Aerospace Mechanics Division of the University of Dayton Research Institute (UDRI), Dayton, Ohio, under Air Force Contract F33615-84-C-3409. The program was sponsored by the Air Force Wright Aeronautical Laboratories, Flight Dynamics Laboratory, Wright-Patterson Air Force Base, Ohio. Air Force administrative direction and technical support was provided by Mr. Malcolm E. Kelley, AFWAL/FIER, the Air Force Project Engineer.

The work described herein was conducted during the period 25 June 1984 to 25 September 1985. University of Dayton project supervision was provided by Mr. Dale H. Whitford, Supervisor, Aerospace Mechanics Division, and Mr. Blaine S. West, Head, Applied Mechanics Group. Technical effort was accomplished under Messrs. B. S. West and K. I. Clayton as Principal Investigators, with Mr. D. R. Bowman being responsible for the overall coordination of experimental exposure/test. In addition, the authors wish to acknowledge the following major contributors: Peter Muth, Machine Shop fabrication; Theresa Dietz and Marianne Piekutowski, environmental conditioning and Nonmetallic Laboratory testing; Paul Johnson, Structures Laboratory testing; and Michael Bouchard and Dee Pike, Test Method consultation.

TABLE OF CONTENTS

TABLE OF CONTENTS (continued)

TABLE OF CONTENTS (concluded)

LIST OF ILLUSTRATIONS

LIST OF ILLUSTRATIONS (Continued)

LIST OF ILLUSTRATIONS (continued)

LIST OF ILLUSTRATIONS (concluded)

LIST OF TABLES

SECTION 1
INTRODUCTION

1.1 BACKGROUND

The U.S. Air Force, recognizing that high performance aircraft transparencies are a high cost item, is committed to achieving lower cost-of-ownership for aircraft transparencies. A means of achieving this goal would be to incorporate a realistic laboratory test methodology which adequately addresses and simulates all applicable in-service mission environmental factors, either sequentially or in combination as appropriate, into the acquisition cycle of any transparency system.

Since 1981, the University of Dayton Research Institute (UDRI) conducted a survey of developmental testing and in-service durability of F-15, F-16, and F-111 transparencies for AFWAL/FIER (Reference 1). The following organizations were visited and informal discussions held to identify areas of concern relating to in-service durability and test method deficiencies: six Air Force bases, namely Wright-Patterson, Hill, McClellan, Luke, Mountain Home, and Cannon; two prime aircraft manufacturers, namely General Dynamics and McDonnell Aircraft; and five transparency suppliers, namely Goodyear Aerospace, PPG Industries, Sierracin/Sylmar, Swedlow, Inc., and Texstar Plastics. These visits provided valuable insight into the primary types of in-service failures such as crazing, scratching, and haze associated with monolithic stretched acrylic; protective surface coating adhesion, abrasion resistance, and embrittlement associated with monolithic coated polycarbonate; and delamination and optical deterioration associated with acrylic faced/polycarbonate laminated construction.

Subsequently, from January 1982 to February 1983, UDRI defined a methodology and criteria for testing and evaluating the durability of high performance aircraft transparencies for AFWAL/FIER using simulated in-service environmental conditioning

(Reference 2). It was designed to provide the maximum amount of reliable data, in a timely manner, using a minimum amount of coupon, subscale, and full-scale testing. Some aspects of the resultant methodology remained to be validated, such as simulated in-service exposure correlation and acceptance criteria. It is the coupon test portion of this methodology that forms the basis for the program documented herein.

The objective of this program was to assess the degree of validity of the existing test methodology defined in Reference 2 through the evaluation of laboratory generated test data when compared to available in-service failure data; subsequent recommendations being made to yield improvements in a revised methodology.

1.2 OBJECTIVE

This program was based on a test matrix of approximately 364 coupon type specimens, as shown in Table 1.1, which were fabricated, conditioned, and tested in accordance with a comprehensive test plan. The experimental test phase was primarily based on the recommended aircraft transparency test methodology for durability evaluation as documented in Reference 2. Tests were performed on specimens cut from the following full-scale production transparency designs:

- F-16a coated monolithic polycarbonate with the original production coating, manufactured by Texstar;
- F-16a laminated canopy manufactured by Sierracin;
- F-15 monolithic stretched acrylic windshield manufactured by Swedlow;
- F-15 monolithic stretched acrylic canopy manufactured by Swedlow; and
- F-111 ADBIRT windshield manufactured by Sierracin.

Laboratory generated test data was evaluated and compared with in-service failure data to assess the degree of validity of

TABLE 1.1

TEST MATRIX

TEST PARAMETER	F-15 Monolithic Stretched Acrylic Windshield	F-15 Monolithic Stretched Acrylic Canopy	F-16A Coated Monolithic Polycarbonate Canopy	F-16A Laminated Canopy	F-111 Laminated ADBIRT Windshield
SURFACE/CHEMICAL CRAZE					
Isoropyl Alcohol	5	5	5	5	5
Ethylene Glycol	5	5	5	5	5
HAZE/TRANSMITTANCE	5	5	5	5	5
IMPACT - MTS BEAM					
Baseline	5	5	5	5	5
Exposed	5	5	5	5	5
IMPACT - FALLING WEIGHT					
Baseline		10	10	10	
Exposed		10	10	10	
COATING ADHESION			10		
INTERLAMINAR BOND INTEGRITY					
Flatwise Tension				5	5
Torsional Shear				5	5
Wedge Peel				5	5
THERMAL SHOCK					
Standard	5	5	5	5	5
Plus Partial Vacuum	5	5	5	5	5
ABRASION RESISTANCE					
In-Flight	5	5	5	5	5
Flightline	5	5	5	5	5
EDGE ATTACHMENT	3	12	10	11	3
SUBTOTAL	48	77	85	91	63
TOTAL					364

the test methodology. Recommendations have been made for achieving improved laboratory testing realism.

SECTION 2

TEST TRANSPARENCY DESIGNS AND SPECIMEN PREPARATION

2.1 MATERIAL PROCUREMENT FOR EXPERIMENTAL TESTS

Purchase orders were issued and the following five production transparencies obtained for specimen fabrication:

Swedlow, Inc., one F-15 monolithic stretched acrylic windshield and one F-15 monolithic stretched acrylic forward canopy;

Texstar Plastics, one F-16A forward coated monolithic polycarbonate canopy with the original production C254 coating;

Sierracin/Sylmar, one F-111 ADBIRT windshield, and

One Sierracin laminated F-16A canopy, Serial No. 31, was furnished GFE.

Figure 2.1 presents the nominal cross-section of each transparency.

2.2 SPECIMEN IDENTIFICATION AND LAYOUT

All specimens were identified using the following code: "ij-k" where i denotes transparency design (A-E); j denotes test parameter (O-Z); and k denotes specimen number. These identification codes were scribed on each specimen after machining.

Transparency Design:

A = F-15 monolithic stretched acrylic windshield
B = F-15 monolithic stretched acrylic canopy
C = F-16A coated monolithic polycarbonate canopy
D = F-16A laminated canopy
E = F-111 laminated ADBIRT windshield

Test Parameter:

O = Surface/chemical craze
P = Haze/transmittance
Q = Impact - MTS beam
R = Impact - falling weight
S = Coating adhesion
T = Flatwise tension

Material Identification Number	Description	Nominal Cross-Section (inches)
A	F-15 Monolithic Stretched Acrylic Windshield	0.90
B	F-15 Monolithic Stretched Acrylic Canopy	0.40
C	F-16A Coated Monolithic Polycarbonate Canopy	0.74
D	F-16A Laminated Canopy	0.76
E	F-111 Laminated ADBIRT Windshield	0.78

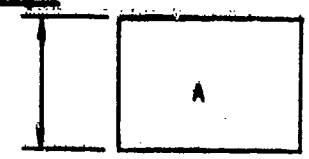

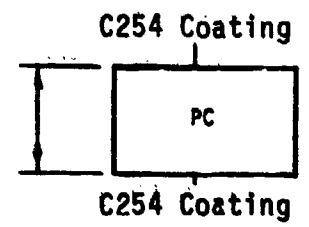

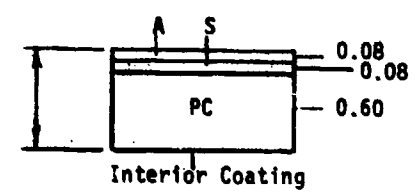

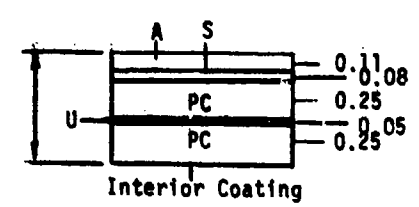

A = Acrylic
PC = Polycarbonate
U = Urethane
S = Silicone

Figure 2.1. Nominal Transparency Cross-Section.

U = Torsional shear
V = Wedge peel
W = Thermal shock
X = In-flight abrasion
Y = Flightline abrasion
Z = Edge attachment

Figures 2.2 through 2.16 show photographs which were taken of all transparencies to document specimen location.

2.3 SPECIMEN FABRICATION AND SEALING

All specimen fabrication was accomplished in the UDRI machine shop. Specimens were first cut from the full-size transparencies by jig-sawing and/or band-sawing. As necessary, selected edges of specimens, such as beam sides, were milled. Cutting temperature was controlled during milling through the use of cooling air. Edges were machined dry in a vertical mill using a four flute 1-inch diameter cutter at 900 RPM and a table feed of 6-1/2 inches/minute. Care was taken to minimize heat-up by removing less than 0.030-inch of material per cut. Polarized light inspection was used in conjunction with the milling operation to ensure that the level of residual machining stress was negligible along the milled edges. In addition, the corners of machined edges were deburred using #400 emery paper. All specimen edges were sealed with General Electric RTV 630 silicone prior to environmental conditioning.

Figure 2.2. Specimen Layout, F-15 Windshield L/H Side.

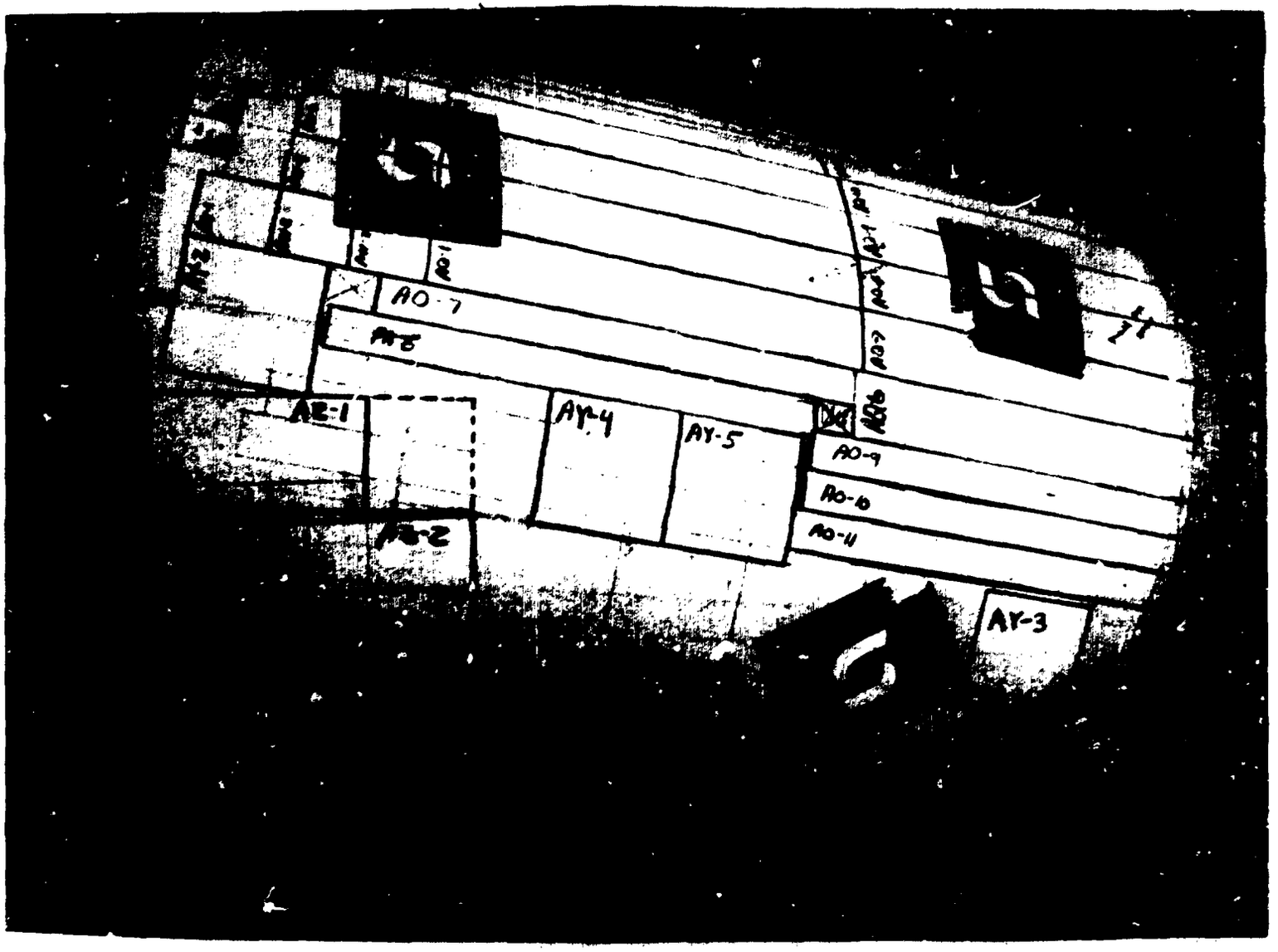

Figure 2. 3. Specimen Layout, F-15 Windshield R/H Side.

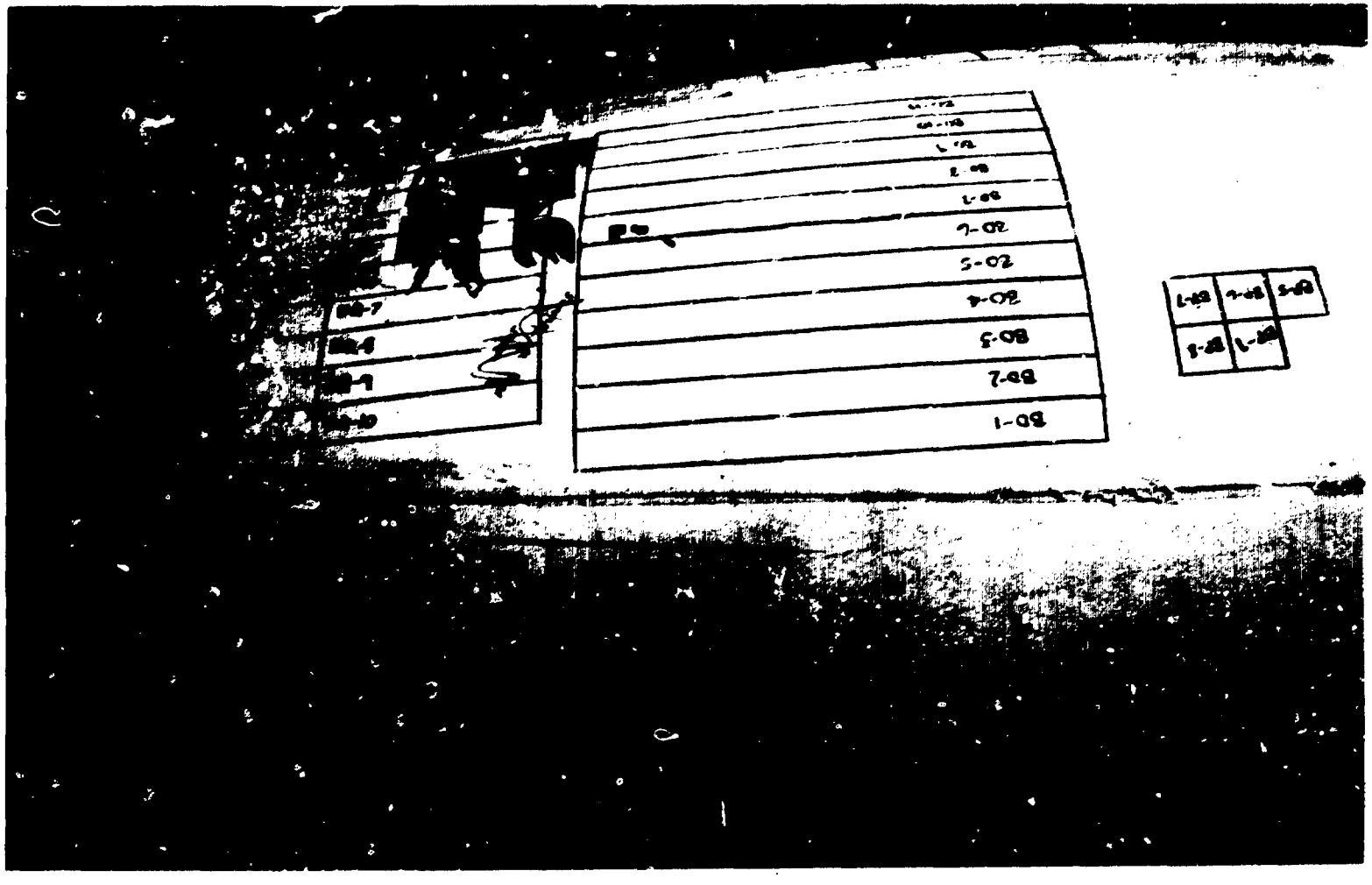

Figure 2.4. Specimen Layout, F-15 Canopy L.H. Side.

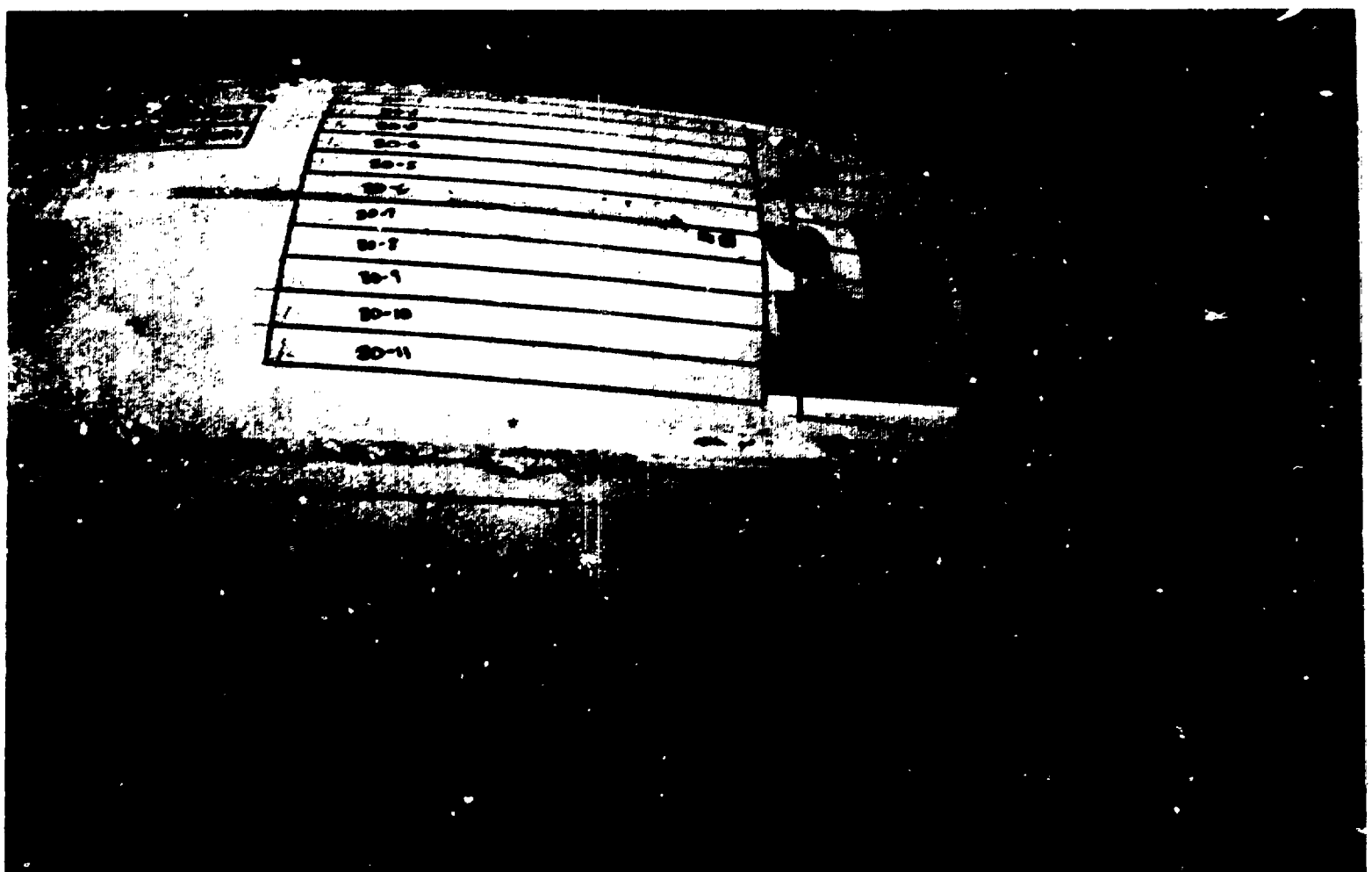

Figure 2.5. Specimen Layout, F-15 Canopy R.H. Side.

Figure 2.6. Specimen Layout, F-16A Monolithic Canopy.

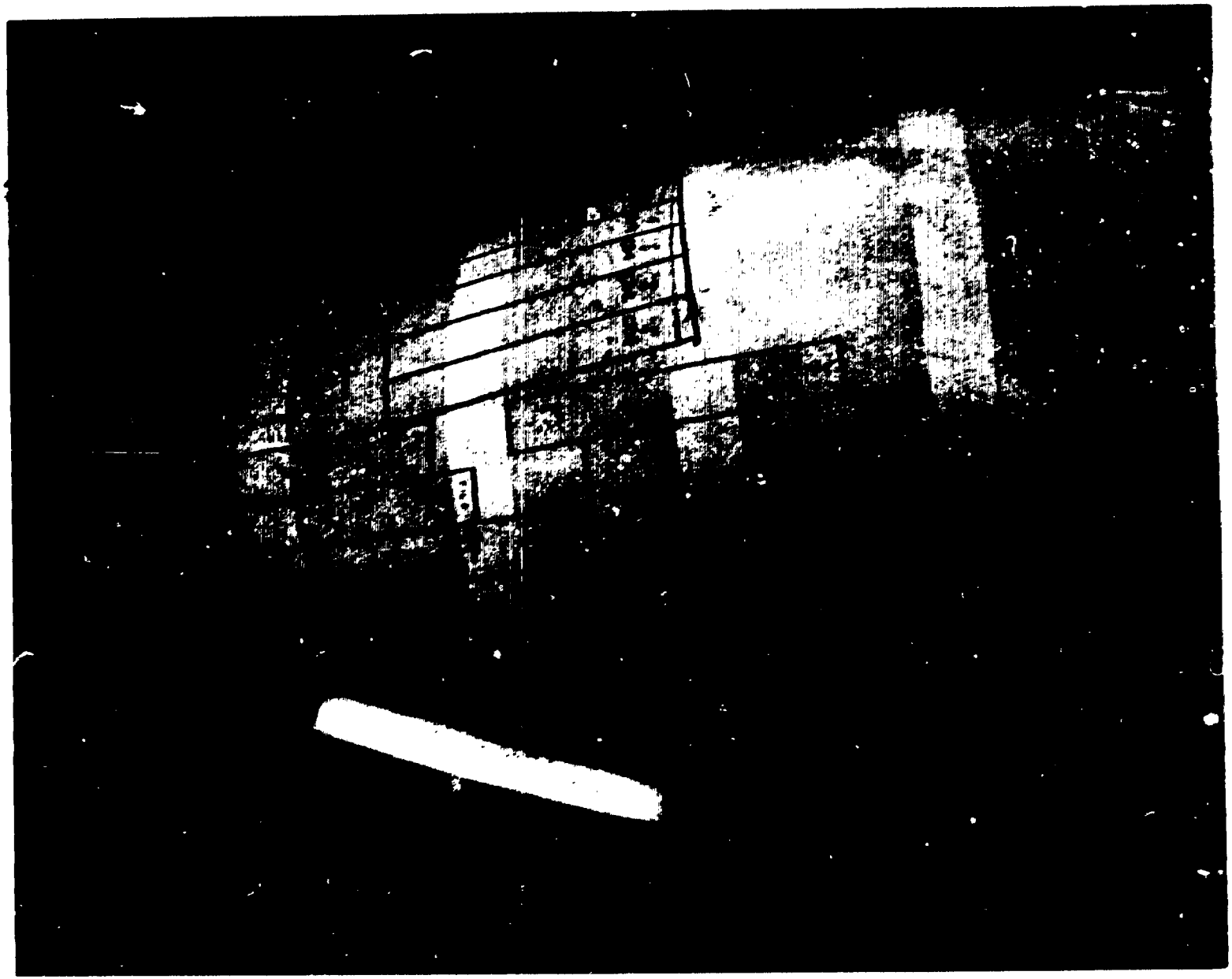

Figure 2.7. Specimen Layout, F-16A Monolithic Canopy, Forward L.H. Side.

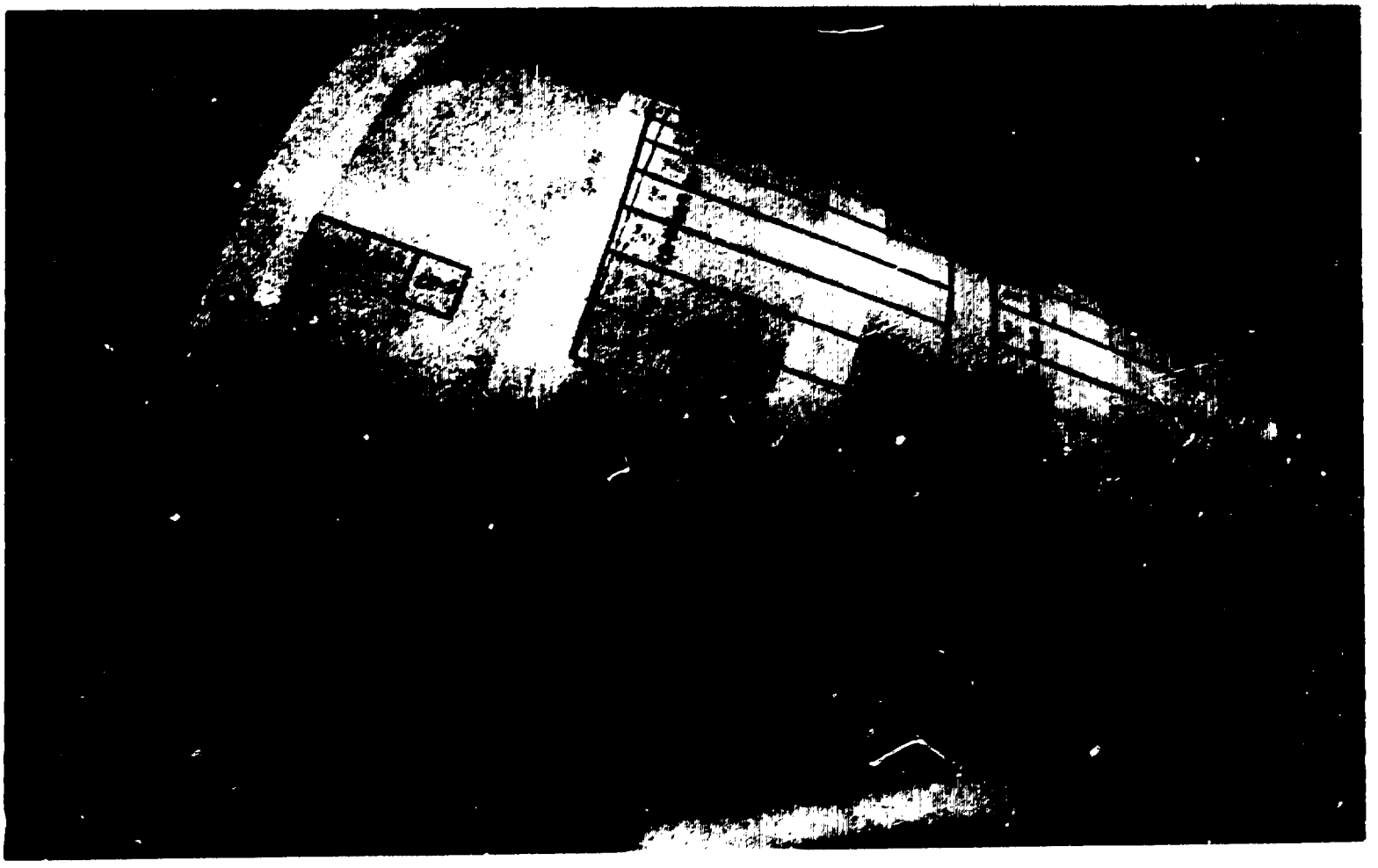

Figure 2.8. Specimen Layout, F-16A Monolithic Canopy, Forward R.H. Side.

Figure 2.9. Specimen Layout, F-16A Monolithic Canopy, Aft L.H. Side.

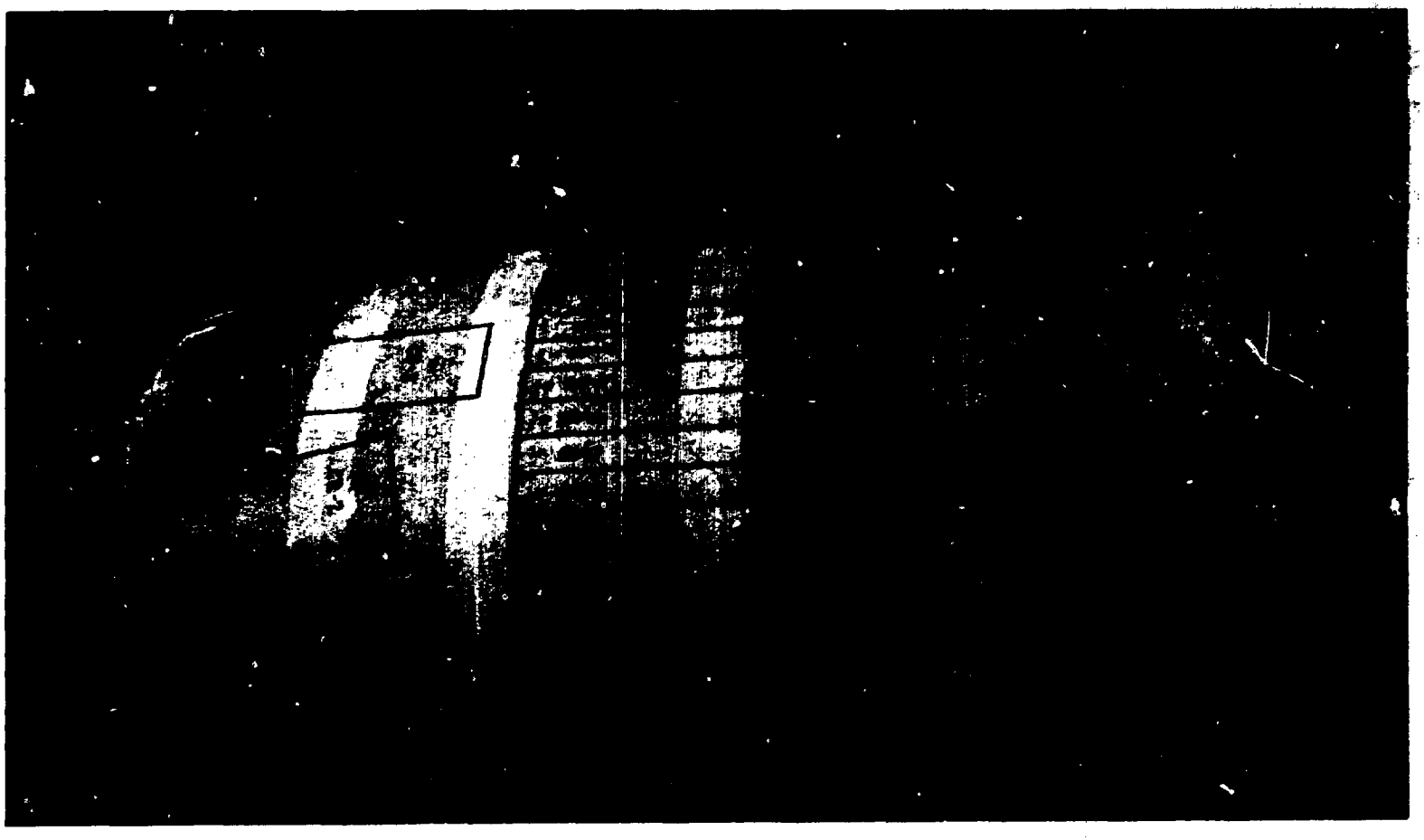

Figure 2.10. Specimen Layout, F-16A Monolithic Canopy, Aft R.H. Side.

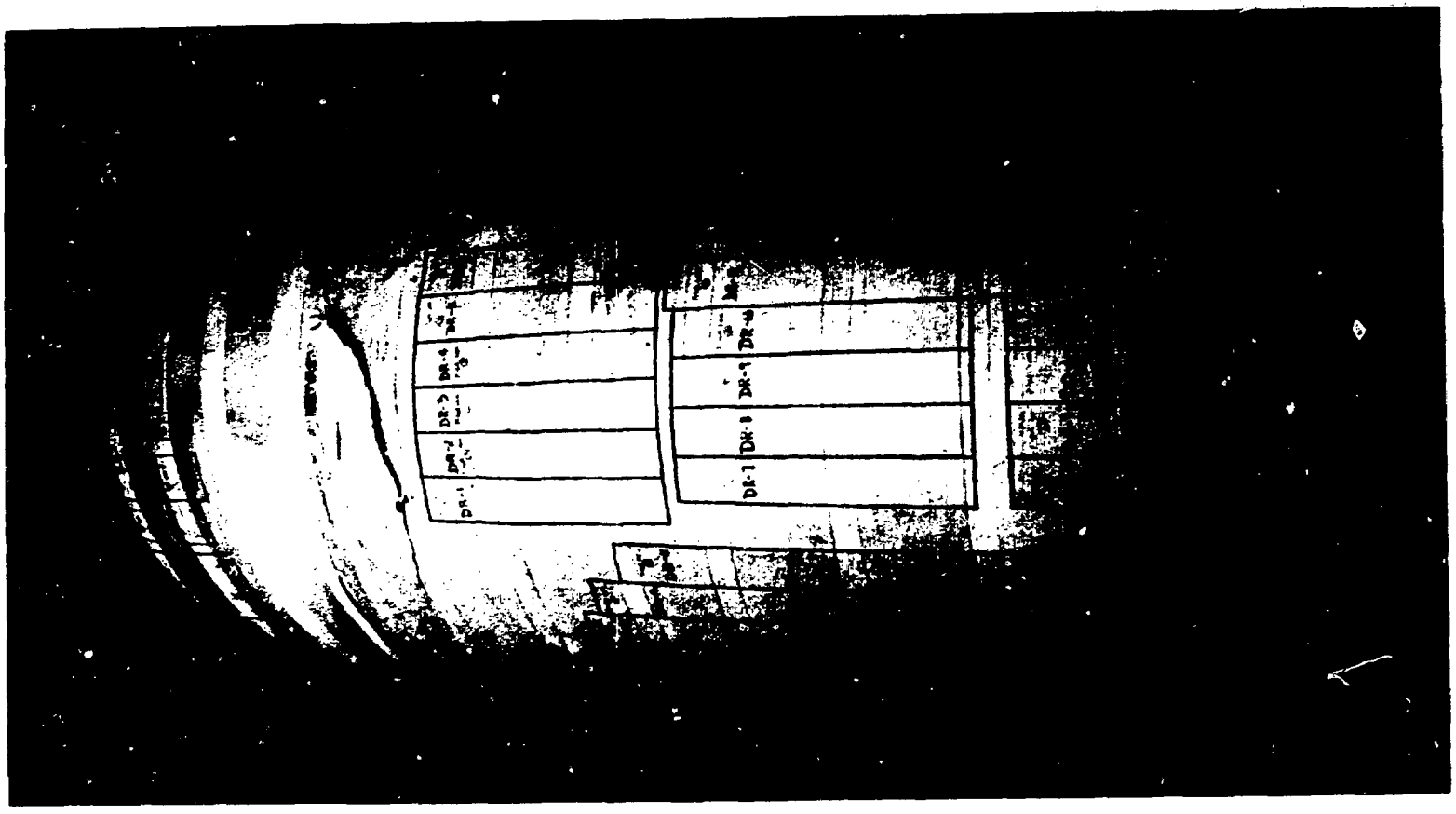

Figure 2.11. Specimen Layout, F-16A Laminated Canopy.

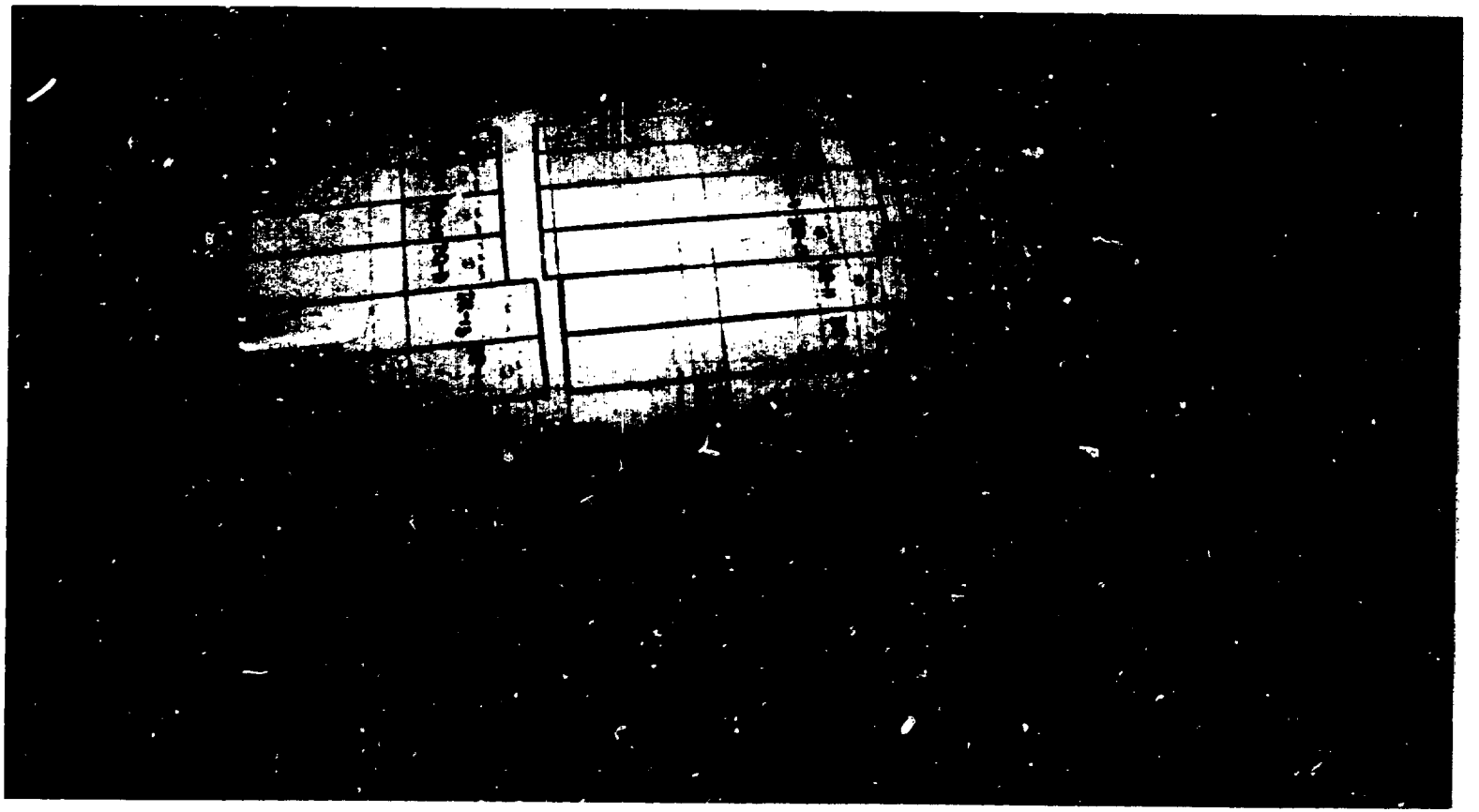

Figure 2.12. Specimen Layout, F-16A Laminated Canopy, Forward L.H. Side.

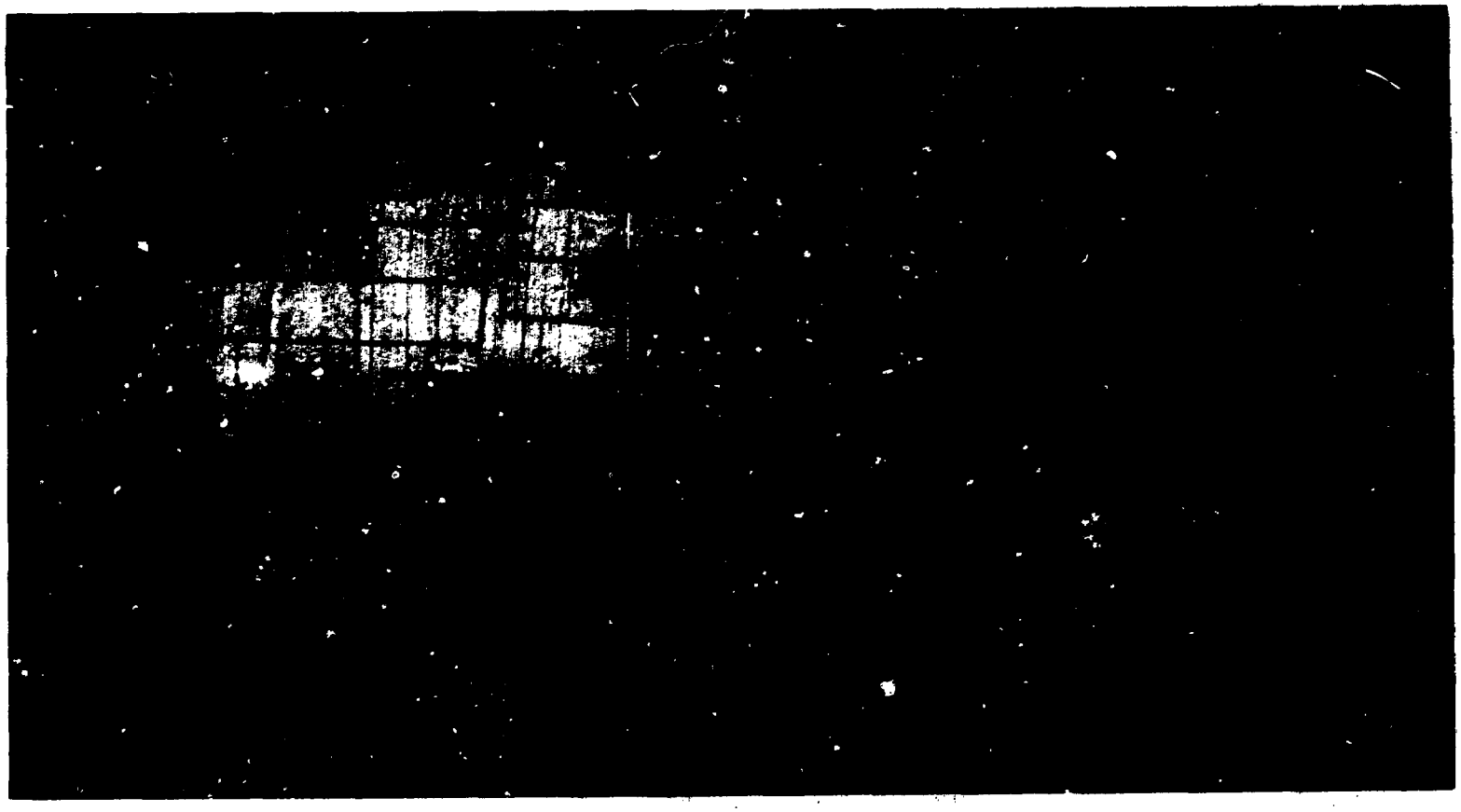

Figure 2.13. Specimen Layout, F-16A Laminated Canopy, Forward R.H. Side.

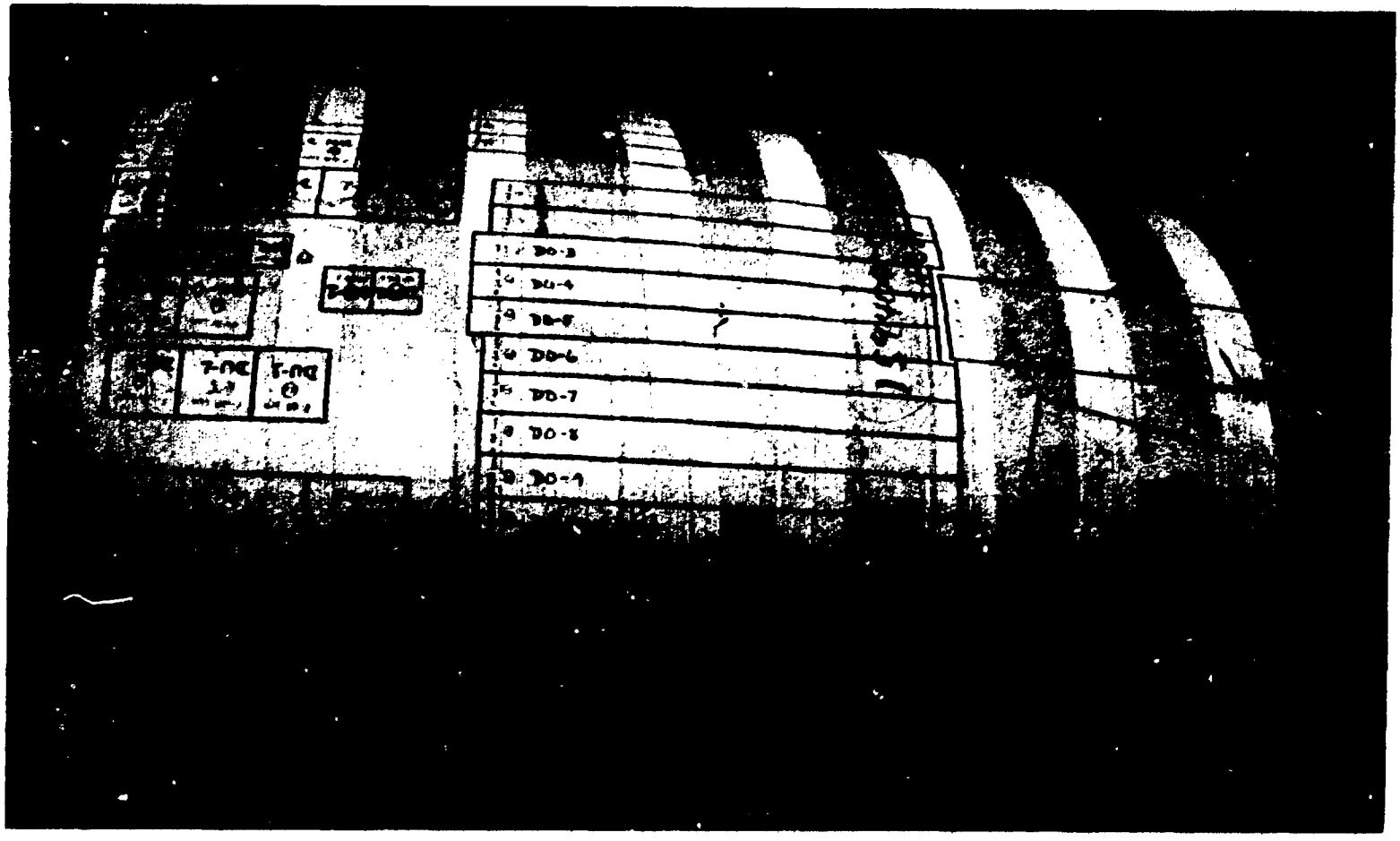

Figure 2.14. Specimen Layout, F-16A Laminated Canopy, Aft L.H. Side.

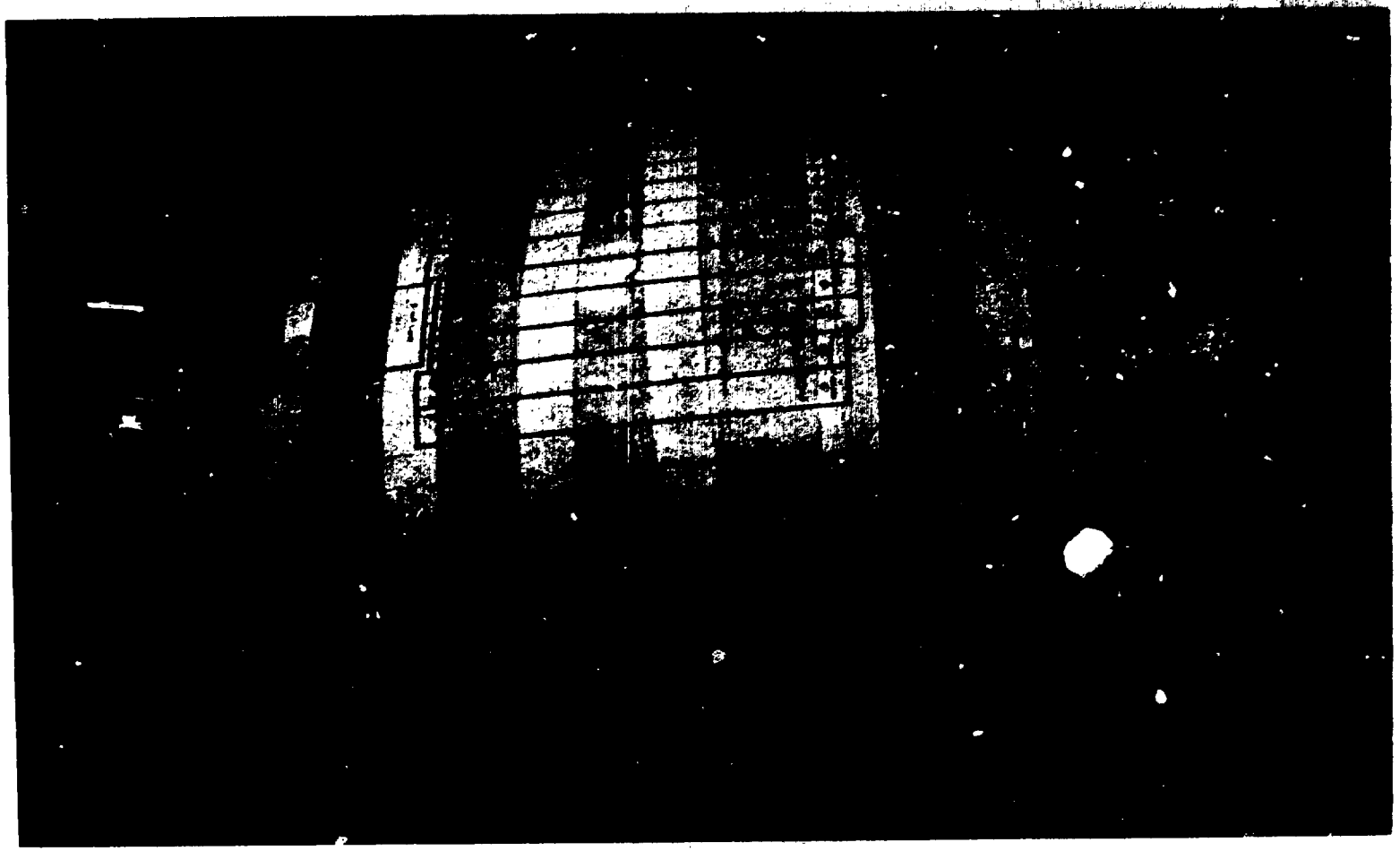

Figure 2.15. Specimen Layout, F-16A Laminated Canopy Aft R.H. Side.

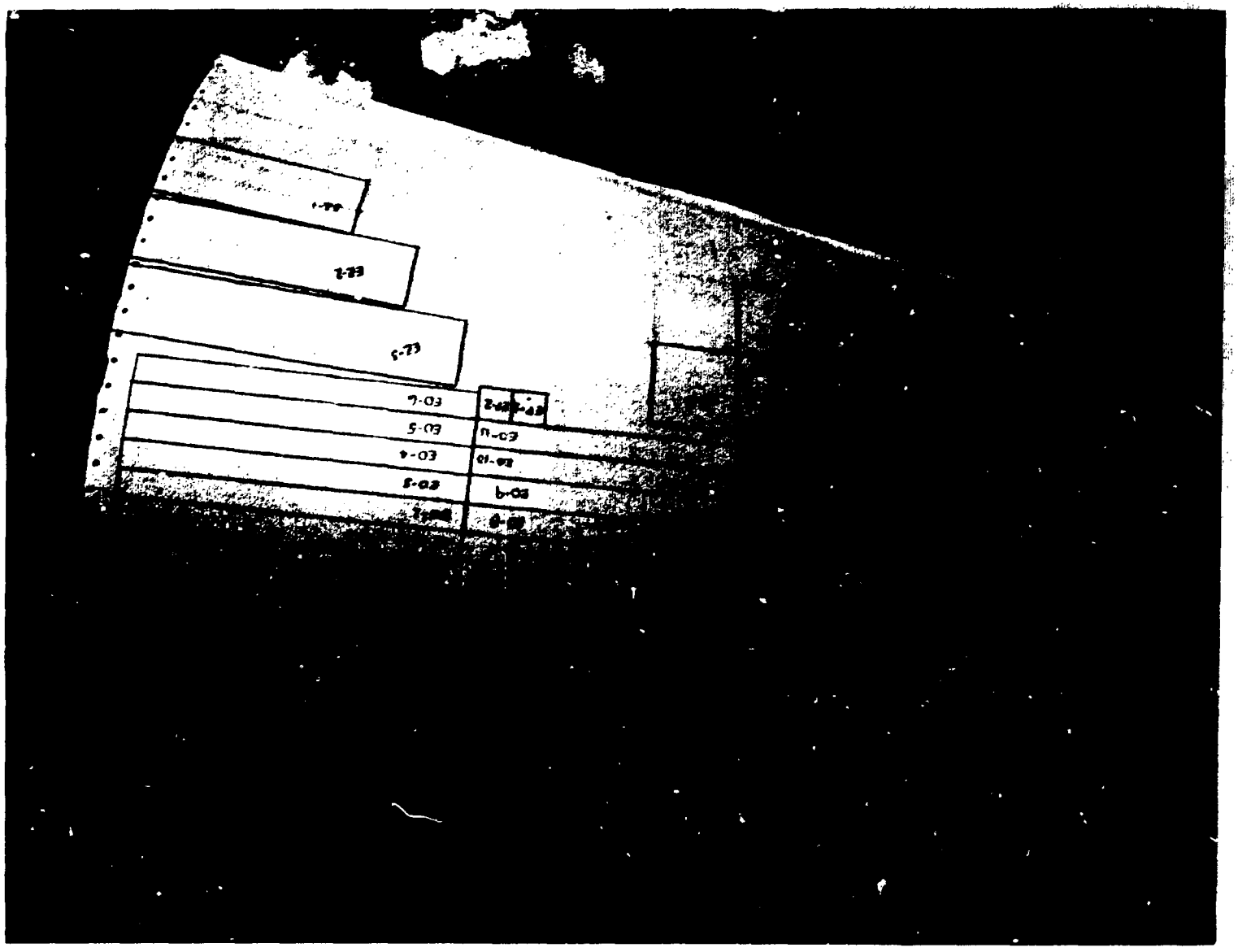

Figure 2.16. Specimen Layout, F-111 Windshield.

SECTION 3
EXPERIMENTAL TESTS

3.1 SURFACE/CHEMICAL CRAZE (INCREMENTAL STRESS CRAZE TEST METHOD)

3.1.1 Specimen Configuration

The standard ASTM F484 beam dimensions were modified, with the width being 1±0.03 in. and the length being 15±0.05 in. The thickness remained that of the as-received transparency material. Specimens were cut from locations on the actual transparencies so as to minimize curvature along the beam length and equalize the curvature between replicates.

3.1.2 Test Method

Bending stress decreases along the length of a cantilever beam specimen from a maximum value at the fulcrum to a minimum of zero at the point of load application (neglecting locally induced stresses at the point of load application). Thus, discrete points along the beam's length have unique values of bending stress associated with them.

A chemical applied along the length of the beam would cause crazing first at higher stressed points and then progressively at lower stressed points. By recording time for crazing to occur at each point, many stress versus time-to-craze points (in fact, an entire curve) can be obtained from a single specimen and test.

The hardware for the incremental stress craze test method (Figure 3.1) is very similar to that of the standard test method. The fixturing, including cantilever supports and load application gear, are identical. The extended specimen length facilitates correlation of craze location with discrete points (and thus values of bending stress) along the beam. These points are marked at one-quarter and one-half inch intervals as shown in Figure 3.2. Both laminated and monolithic specimens were tested.

Figure 3.1. Hardware for Modified Crazing Test.

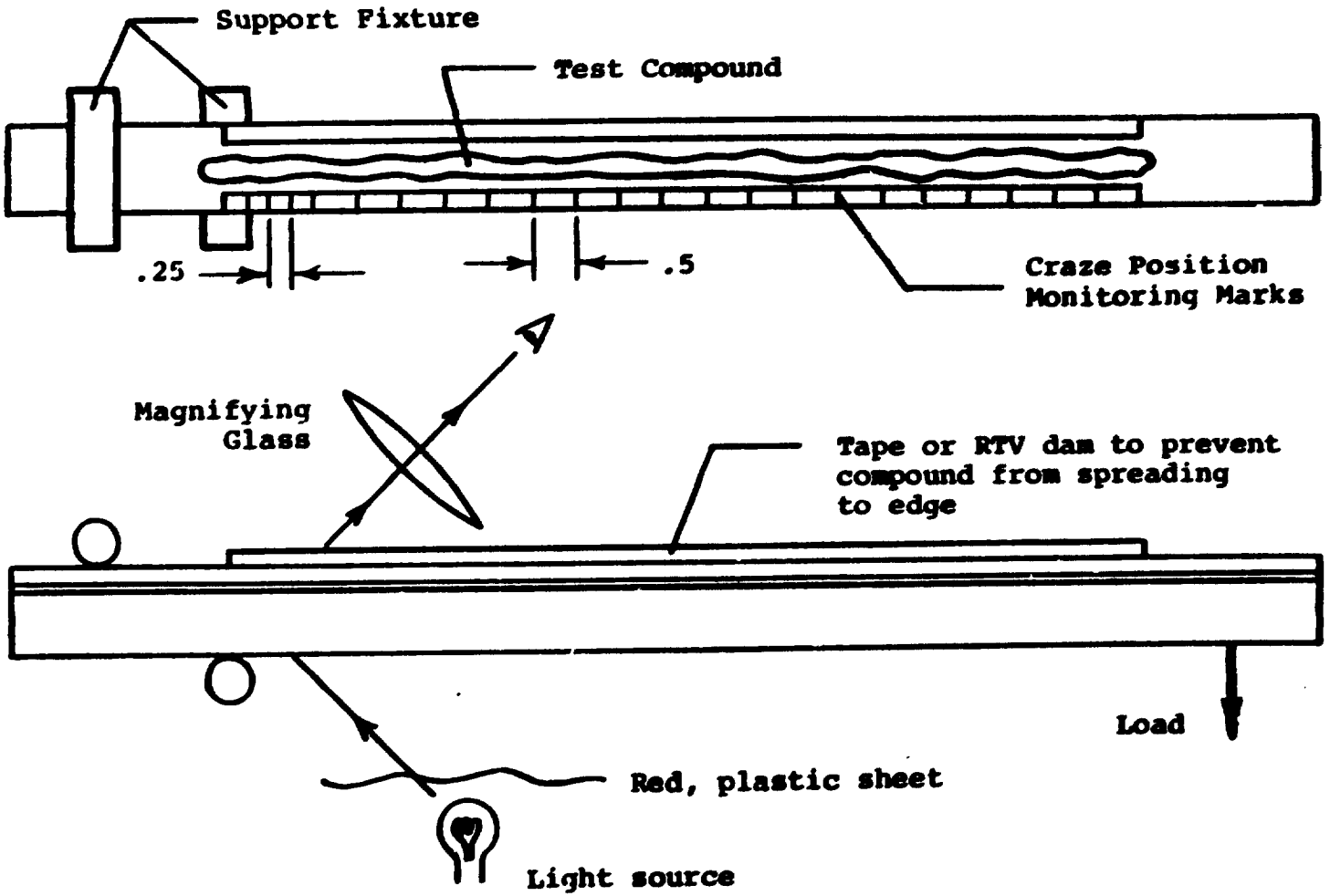

Figure 3.2. Setup for Modified Crazing Tests.

Calibration beams were loaded to determine the bending stress distribution over the beam length so that crazing locations could be matched with stress values. This distribution could not be computed using elementary beam theory for laminated material since low-modulus interlayers cause plane sections normal to the specimen axis to warp severely under test load and for the monolithic specimens, because of the large scale deflections, the validity of small deflection theory was questionable.

Five strain gages were, therefore, employed to determine the bending stress distribution (see Figure 3.3) for each of the specimens. For the strain-gaged beam, a load that would result in a nominal maximum fiber stress of 2,000 psi at gage 3 was used. The strain readings do not stabilize, but increase continuously under constant load. Due to the duration of actual testing, it is necessary to account for this viscoelastic behavior ("creep").

The increase in strain was monitored and percent "creep" curves computed for the gages; the percent "creep" being defined as

$$\frac{\varepsilon_t - \varepsilon_o}{\varepsilon_o} \times 100\%$$

where ε_o is the strain at the instant of load application and ε_t is the strain at some later time. An average of "creep" was determined from the computed curves and used to correct the strain reading recorded for each gage at the instant of load application. The corrected strains were converted to stresses using Hooke's law.

The specimens were loaded and allowed to stabilize for 10 minutes. Isopropyl alcohol and ethylene glycol were then applied along the length of the beams. The time for crazing to initiate at each craze-propagation mark was recorded; the test

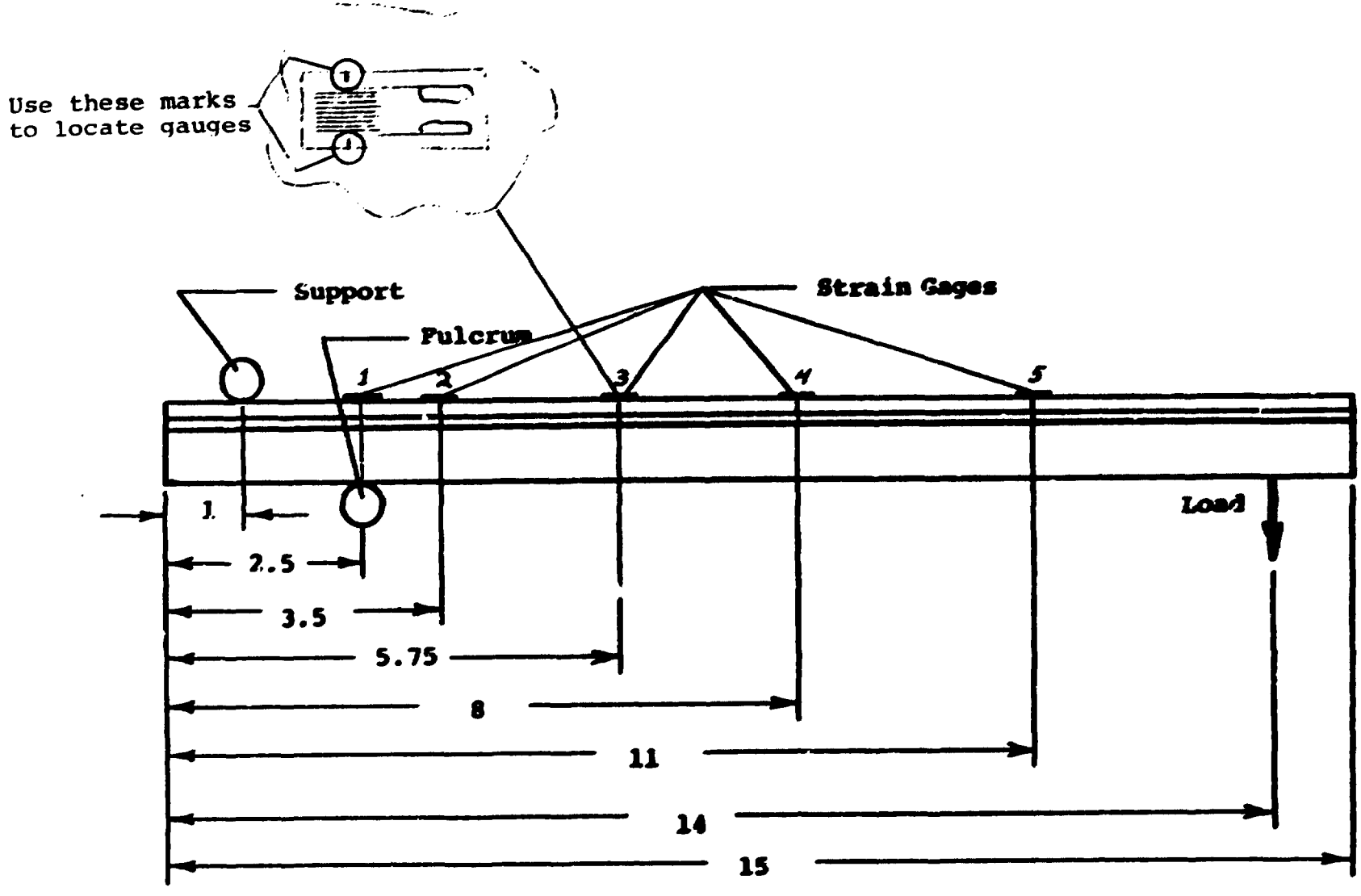

NOTE: All dimensions in inches.

Figure 3.3. Setup for Stress Calibration of Beam.

being completed when crazing reached the point of load application or when the time elapsed from the beginning of chemical application was 30 minutes. The chemicals used were renewed during testing as follows:

Isopropanol: From 0 to 300 seconds, 1 ml of alcohol was applied every 20 seconds, for a total of 15 ml for the first 300 seconds. From 301 to 700 seconds, 1 ml of alcohol was applied every 30 seconds. A total of 13 ml of alcohol was applied. From 701 to 1,000 seconds, 1 ml of alcohol was applied every 60 seconds. A total of 5 ml was applied. From 1,001 to 1,800 seconds, 1 ml of alcohol was applied every 120 seconds. A total of 7 ml was applied. For the duration of the test, a grand total of 40 ml was applied.

Ethylene Glycol: From 0 to 180 seconds, 1 ml of ethylene glycol was added every 30 seconds. A total of 6 ml was applied. From 181 to 600 seconds, 1 ml of ethylene glycol was applied every 60 seconds. A total of 7 ml was applied. From 601 to 1,800 seconds, 1 ml was applied every 120 seconds. A total of 10 ml was applied. For the duration of the test, a grand total of 23 ml was applied to the specimen.

Time-to-craze versus upper-ply surface stress along the length of the beam specimen was plotted.

3.1.3 Environmental Conditioning

The Q.U.V. Accelerated Weathering Tester, manufactured by the Q-Panel Company, Cleveland, Ohio, and shown in Figure 3.4, combines the effects of the UV wavelengths of sunlight with heat and condensation to simulate accelerated weathering. Using the Q.U.V. tester with Q-Panel UVB-313 lamps, an operating temperature of 120°F, alternating cycles of 7 hours UV followed by 5 hours condensation, and based on a year of natural weathering being simulated by 168 hours run time, the specimens were conditioned for 504 hours or 3 equivalent

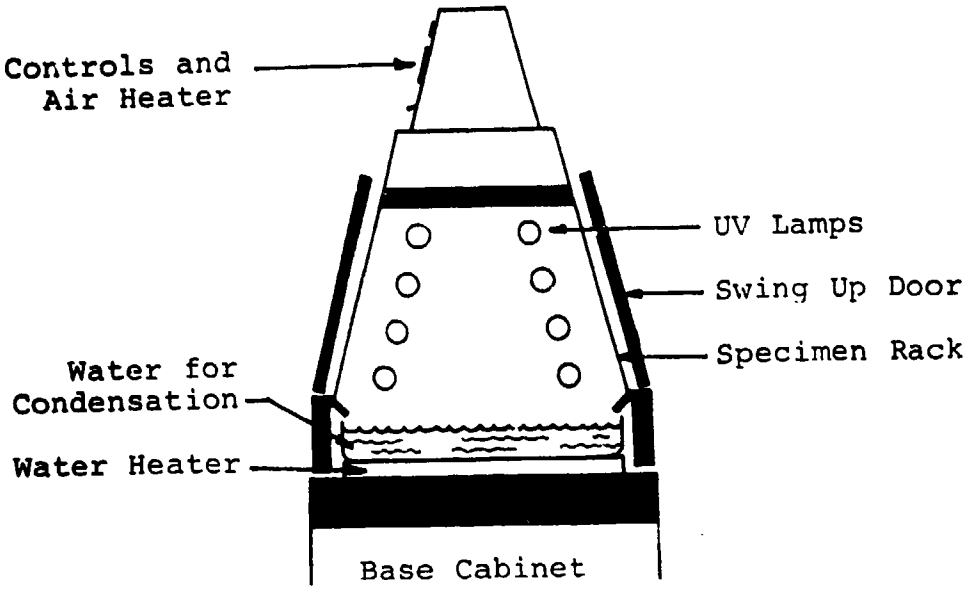

Schematic Cross Section

Figure 3.4. QUV Accelerated Weathering Tester.

years of accelerated weathering prior to test. Figure 3.5 shows typical specimen mounting.

3.1.4 Test Data

Table 3.1 presents the time to craze at 2,000 psi for surface/chemical craze specimens cut from the five actual transparencies and subjected to isopropyl alcohol and ethylene glycol after 504 hours of accelerated weathering (Q.U.V.) exposure, Data, in more detail, is plotted as shown in Appendix A.

3.1.5 Data Analysis/Correlation

The proposed acceptance criteria specified that there would be no crazing from isopropyl alcohol or ethylene glycol at an outer fiber stress of 2,000 psi after 3 equivalent years of accelerated weathering exposure. With isopropyl alcohol, all of the specimens crazed at this outer fiber stress. With ethylene glycol, crazing was less severe. Crazing did occur, however, on most of the specimens beyond the 2,000 psi outer ply stress, although some of the crazes were very small, "dot" crazes, almost unnoticeable to the untrained eye. This "dot" crazing is not necessarily prevalent enough to create detrimental visual aberation. The monolithic stretched acrylics showed the greatest resistance to crazing with both solvents. The coated polycarbonate showed the least resistance with many of the specimens showing some crazing even before the 10 minute stabilizing period was through, and almost instantaneous crazing of the entire specimen when the solvents were added. The acrylic outer faces of the laminated F-16A canopy specimens all cracked during the test with the isopropyl alcohol solvent. For all of the specimens, either the proposed acceptance criteria was too high or the Q.U.V. cycle was too severe. Most of the beams crazed even at an outer fiber stress of 1,000 psi. Typical tested beams are shown in Figure 3.6; Figures 3.7 through 3.9 showing resultant surface/chemical craze in detail.

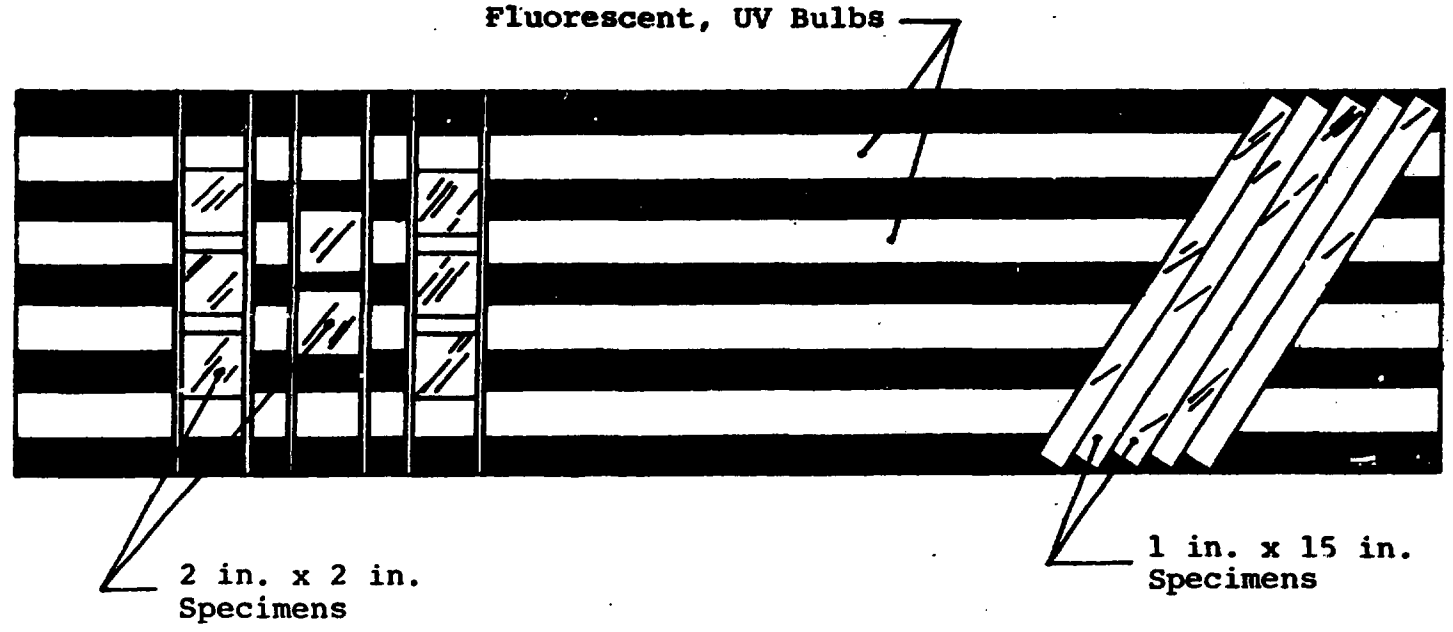

Figure 3.5. Specimen Mounting for the QUV Tester.

TABLE 3.1

SURFACE/CHEMICAL CRAZE DATA

Isopropyl Alcohol		Ethylene Glycol	
Specimen	Time (sec) *	Specimen	Time (sec) *
A0-1	139	A0-6	200
A0-2	64	A0-7	did not craze
A0-3	76	A0-8	did not craze
A0-4	86	A0-9	53
A0-5	65	A0-10	none
B0-1	114	B0-6	none
B0-2	86	B0-7	541
B0-3	93	B0-8	none
B0-4	104	B0-9	none
B0-5	111	B0-10	none
C0-1	**	C0-6	**
C0-2	**	C0-7	**
C0-3	**	C0-8	**
C0-4	**	C0-9	**
C0-5	**	C0-10	**
D0-1	15	D0-6	crazed
D0-2	15	D0-7	16
D0-3	13	D0-8	15
D0-4	18	D0-9	23
D0-5	16	D0-10	did not craze
E0-1	9.5	E0-6	505
E0-2	14	E0-7	495
E0-3	6	E0-8	528
E0-4	9	E0-9	108
E0-5	7	E0-10	527

* Time to craze at 2,000 psi outer fiber stress.

** Crazed immediately after addition of chemical.

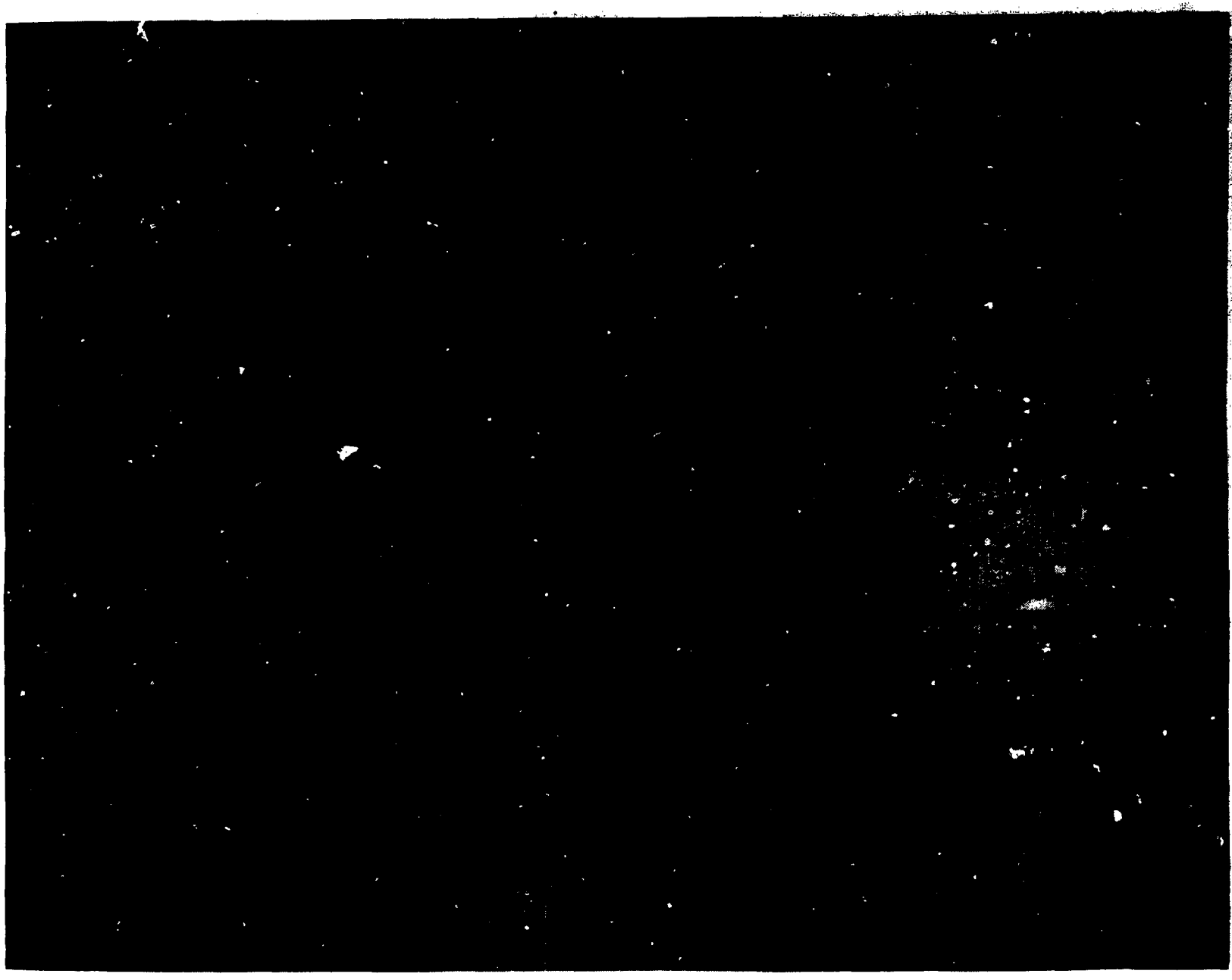

Figure 3.6. Typical Surface/Chemical Craze Beams.

F—15 MONOLITHIC
STRETCHED ACRYLIC
WINDSHIELD

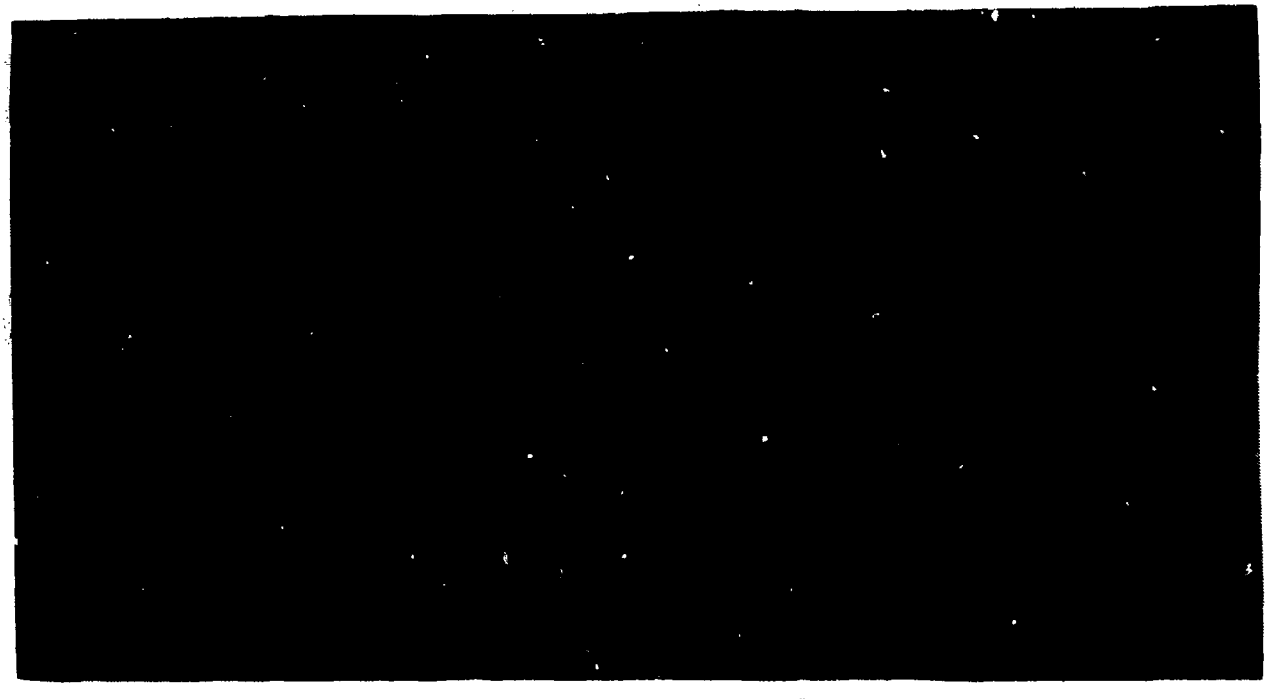

F—15 MONOLITHIC
STRETCHED ACRYLIC
CANOPY

Figure 3.7. Detail of F-15 Crazing.

F-16A COATED
MONOLITHIC POLY-
CARBONATE CANOPY

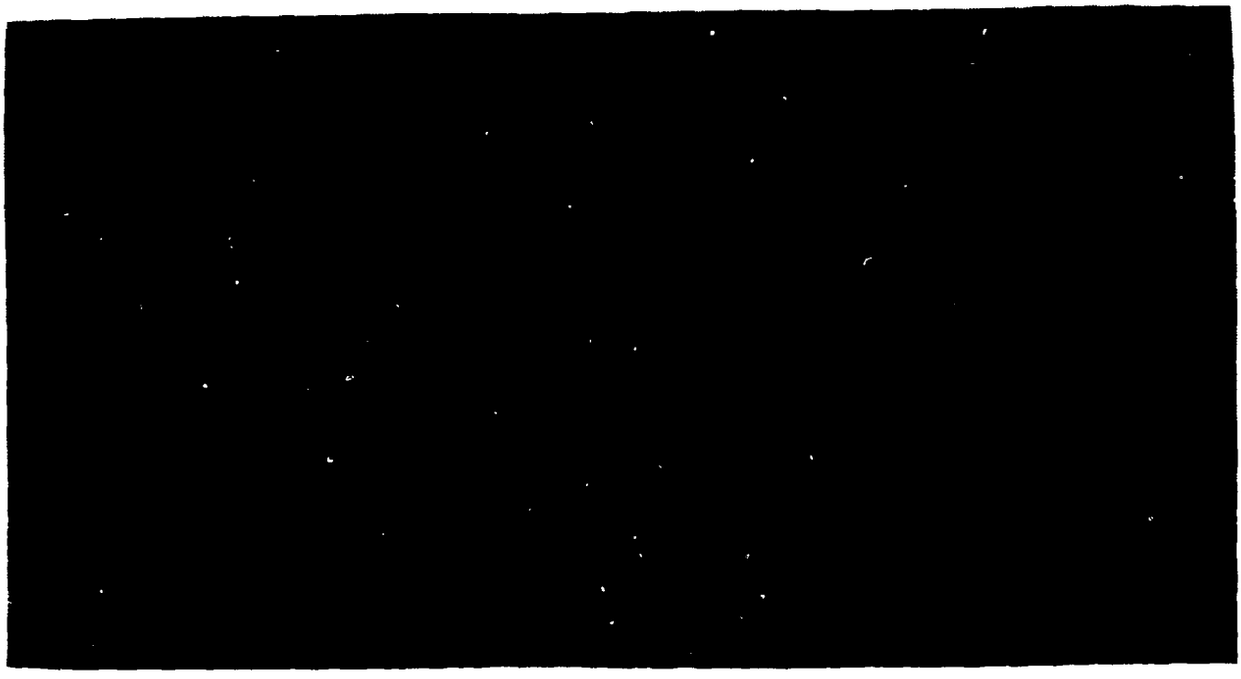

F-16A LAMINATED
CANOPY

Figure 3.8. Detail of F-16A Crazing.

F—111 LAMINATED
ADBIRT WINDSHIELD

Figure 3.9. Detail of F-111 Crazing.

3.2 HAZE/TRANSMITTANCE

3.2.1 Specimen Configuration

The standard FTM406-Method 3022 coupon, 1-1/2" square was used.

Initially, four unexposed calibration coupons, two having a maximum radius of curvature and two having a minimum radius of curvature, were cut from the F-15 stretched acrylic canopy and tested to measure the effect of specimen curvature on haze and transmittance; resultant data shown below being comparable to flat specimens.

Specimen	Radius	% Haze	% Transmittance
BP-1	max	0.70	92.8
BP-2	max	1.00	92.9
BP-5	min	0.71	93.2
BP-6	min	0.74	93.0

3.2.2 Test Method

Federal Test Method Standard FTM406, Method 3022, or equivalent. Figure 3.10 shows the Hazemeter used to measure haze/transmittance.

3.2.3 Environmental Conditioning

Accelerated weathering was conducted in accordance with Paragraph 3.1.3, with readings taken after 0, 1, 2, and 3 years of simulated exposure.

3.2.4 Test Data

Table 3.2 presents the complete haze and transmittance results; this data being summarized in Table 3.3.

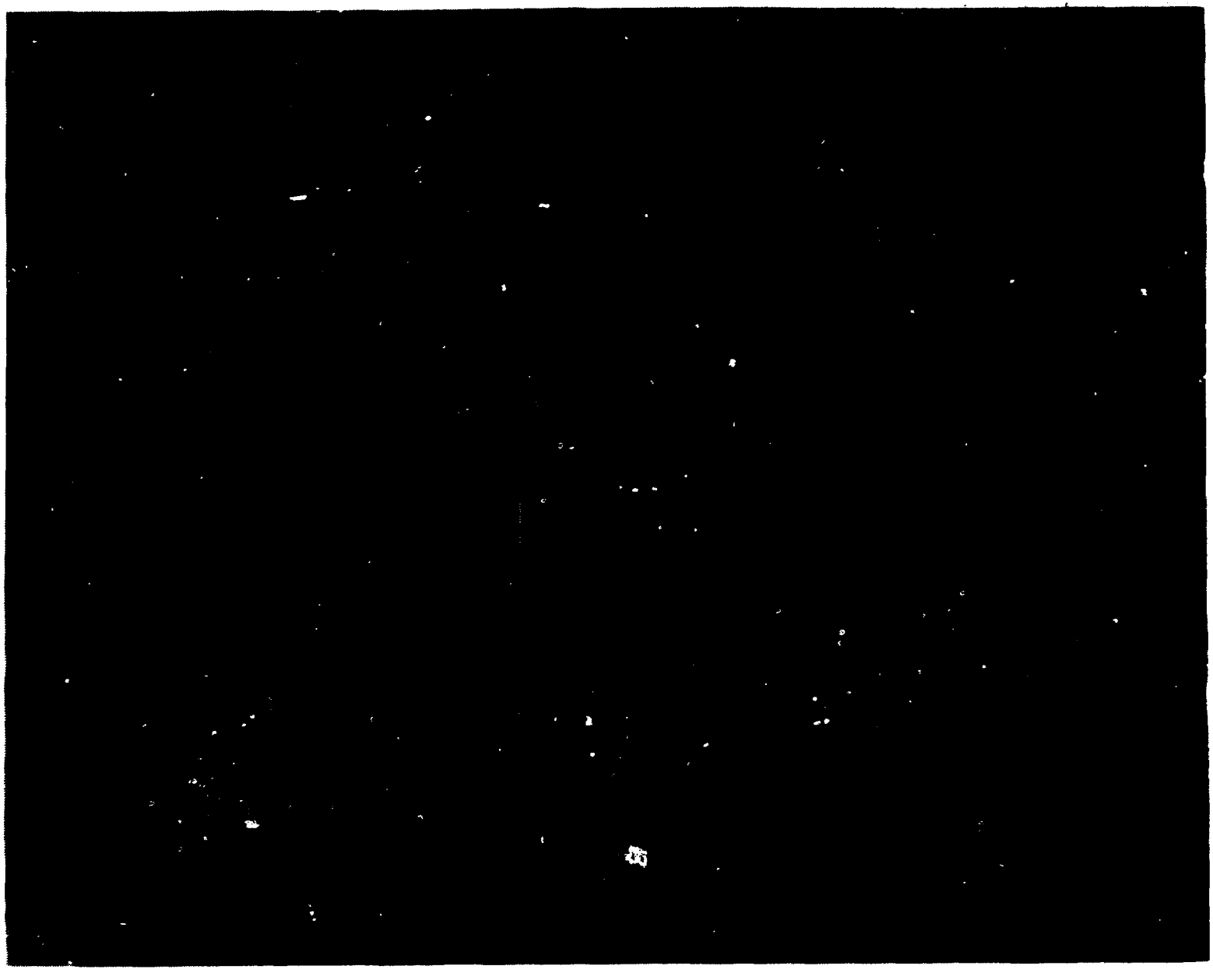

Figure 3.10. XL 211 Hazeguard System Hazemeter.

TABLE 3.2

HAZE AND TRANSMITTANCE RESULTS

Specimen Identification No.	Equivalent Exposure Years	Trans. %	Average	Standard Dev.	Haze %	Average	Standard Dev.
AP-1	0	91.7			1.17		
AP-2		91.7			0.90		
AP-3		91.7	91.680	0.045	1.96	1.428	0.536
AP-4		91.6			2.05		
AP-5		91.7			1.06		
AP-1	1	91.5			3.28		
AP-2		91.4			2.91		
AP-3		91.4	91.480	0.084	3.76	3.444	0.442
AP-4		91.6			3.25		
AP-5		91.5			4.02		
AP-1	2	91.2			3.28		
AP-2		91.3			4.24		
AP-3		91.2	91.280	0.084	4.37	4.218	0.358
AP-4		91.3			4.51		
AP-5		91.4			4.37		
AP-1	3	91.5			3.36		
AP-2		91.4			4.17		
AP-3		91.4	91.44	0.055	5.31	5.350	2.139
AP-4		91.4			4.98		
AP-5		91.5			8.93		
BP-1	0	92.8			0.70		
BP-2		92.9			1.00		
BP-3		92.9			0.99		
BP-4		92.8			0.89		
BP-5		93.2	92.967	0.132	0.71	0.808	0.132
BP-6		93.0			0.74		
BP-7		93.1			0.63		
BP-8		93.0			0.75		
BP-9		93.0			0.86		

TABLE 3.2 (continued)

Specimen Identification No.	Equivalent Exposure Years	Trans. %	Average	Standard Dev.	Haze %	Average	Standard Dev.
BP-1	1		no 1-year readings taken.				
BP-2							
BP-3							
BP-4							
BP-5							
BP-6							
BP-7		92.9			3.47		
BP-8							
BP-9							
BP-1	2	92.9			3.38		
BP-2		92.4			5.25		
BP-3		92.6			8.79		
BP-4		92.3			5.97		
BP-5		92.9	92.41	0.756	5.18	6.05	1.587
BP-6		92.6			5.29		
BP-7		90.5			6.39		
BP-8		92.5			6.31		
BP-9		93.0			7.88		
BP-1	3	92.7			3.51		
BP-2		92.2			5.60		
BP-3		92.5			9.03		
BP-4		92.4			6.28		
BP-5		92.7	92.58	0.199	5.56	6.12	1.930
BP-6		92.5			6.72		
BP-7		92.6			3.23		
BP-8		92.8			6.89		
BP-9		92.8			8.27		

TABLE 3.2 (continued)

Specimen Identification No.	Equivalent Exposure Years	Trans. %	Average	Standard Dev.	Haze %	Average	Standard Dev.
CP-1	0	88.6			1.29		
CP-2		88.7			1.40		
CP-3		88.7	88.600	0.122	1.40	1.372	0.0705
CP-4		88.4			1.46		
CP-5		88.6			1.31		
CP-1	1	86.6			12.7		
CP-2		85.9			17.1		
CP-3		85.5	86.660	0.991	17.8	13.540	3.738
CP-4		87.8			10.1		
CP-5		87.5			10.0		
CP-1	2	79.9			36.6		
CP-2		80.3			36.6		
CP-3		80.6	80.680	0.939	34.9	35.740	1.167
CP-4		82.3			34.1		
CP-5		80.3			36.5		
CP-1	3	83.1			36.0		
CP-2		80.8			38.0		
CP-3		81.3	81.580	1.406	46.9	39.600	4.641
CP-4		82.9			35.8		
CP-5		79.8			41.3		
DP-1	0	87.5			3.18		
DP-2		87.7			2.86		
DP-3		87.4	87.540	0.114	3.00	2.930	0.167
DP-4		87.5			2.74		
DP-5		87.6			2.87		

TABLE 3.2 (continued)

Specimen Identification No.	Equivalent Exposure Years	Trans. %	Average	Standard Dev.	Haze %	Average	Standard Dev.
DP-1	1	87.5			3.95		
DP-2		87.5			4.63		
DP-3		87.6	87.600	0.122	4.86	4.494	0.490
DP-4		87.8			4.01		
DP-5		87.6			5.02		
DP-1	2	87.5			4.68		
DP-2		87.8			4.95		
DP-3		87.7	87.720	0.148	5.12	4.814	0.262
DP-4		87.7			4.44		
DP-5		87.9			4.88		
DP-1	3	88.0			5.86		
DP-2		87.7			5.86		
DP-3		88.2	87.940	0.230	3.78	5.282	0.865
DP-4		88.1			5.39		
DP-5		87.7			5.52		
EP-1	0	84.9			3.22		
EP-2		85.0			3.41		
EP-3		84.7	84.900	0.122	3.37	3.314	0.085
EP-4		85.0			3.23		
EP-5		84.9			3.34		
EP-1	1	84.5			5.47		
EP-2		84.3			6.03		
EP-3		84.2	84.400	0.141	4.57	5.290	0.705
EP-4		84.5			4.53		
EP-5		84.5			5.85		

TABLE 3.2 (concluded)

Specimen Identification No.	Equivalent Exposure Years	Trans. %	Average	Standard Dev.	Haze %	Average	Standard Dev.
EP-1	2	84.2			5.50		
EP-2		83.4			7.57		
EP-3		83.6	83.760	0.305	6.61	6.310	0.921
EP-4		83.7			5.31		
EP-5		83.9			6.56		
EP-1	3	84.0			11.24		
EP-2		83.7			10.33		
EP-3		83.8	83.680	0.259	7.76	9.742	1.629
EP-4		83.3			9.61		
EP-5		83.6			9.77		

TABLE 3.3

HAZE AND TRANSMITTANCE DATA SUMMARY

Specimen Identification No.	Equivalent Exposure Years	Average % Transmittance	Standard Dev.	Average % Haze	Standard Dev.
AP 1-5	0	91.68	0.045	1.428	0.536
	1	91.48	0.084	3.444	0.442
	2	91.28	0.084	4.128	0.358
	3	91.44	0.055	5.35	2.139
BP 1-10	0	92.967	0.132	0.808	0.132
	1	91.9	(one reading)	3.47	(one reading)
	2	92.41	0.756	6.05	1.587
	3	92.58	0.199	6.12	1.93
CP 1-5	0	88.6	0.122	1.372	0.0705
	1	86.66	0.991	13.54	3.738
	2	80.68	0.939	35.74	1.167
	3	81.58	1.406	39.6	4.641
DP 1-5	0	87.54	0.114	2.93	0.167
	1	87.6	0.122	4.494	0.49
	2	87.72	0.148	4.814	0.262
	3	87.94	0.230	5.282	0.865
EP 1-5	0	84.9	0.123	3.314	0.085
	1	84.4	0.141	5.29	0.705
	2	83.76	0.305	6.31	0.921
	3	83.68	0.259	9.742	1.629

3.2.5 Data Analysis/Correlation

The proposed acceptance criteria specified that after three equivalent years of accelerated weathering exposure, the percent haze shall not exceed 4% and transmittance shall be within 2% of the unexposed baseline reading. All transparency designs exceeded 4% haze after 3 years of simulated exposure with the coated polycarbonate experiencing the most degradation. Further discussion is presented in Section 4. All transparency designs met the proposed transmittance requirement except for the coated polycarbonate. Typical tested coupons are shown in Figure 3.11; Figure 3.12 shows resultant haze in detail.

3.3 IMPACT-HIGH RATE MTS BEAM

3.3.1 Specimen Configuration

The three-point loaded beam specimens were machined to t inches thick, 2t inches wide, and 14t inches long, where t equals the as-received thickness. Beam edges were milled and inspected using polarized light to ensure that the level of residual machining stress was low; beam ends remained as band-sawed. Additionally, the lengthwise corners of the specimen edges were deburred using #400 emery paper in the region of critical loading; the goal being to initiate failure from the central surface and not the edges. Specimens were cut from the actual transparencies so as to minimize curvature along the beam length and equalize the curvature between replicates.

3.3.2 Test Method

The "high-rate" MTS beam test is an instrumented flexure test utilizing three-point simply-supported loading. The MTS test machine used to conduct these tests is a high performance electrohydraulic closed loop test system with high level control and data gathering capabilities (reference Figure 3.13). It consists of the following major components: a servohydraulic power pump, a specimen holding fixture, a reaction

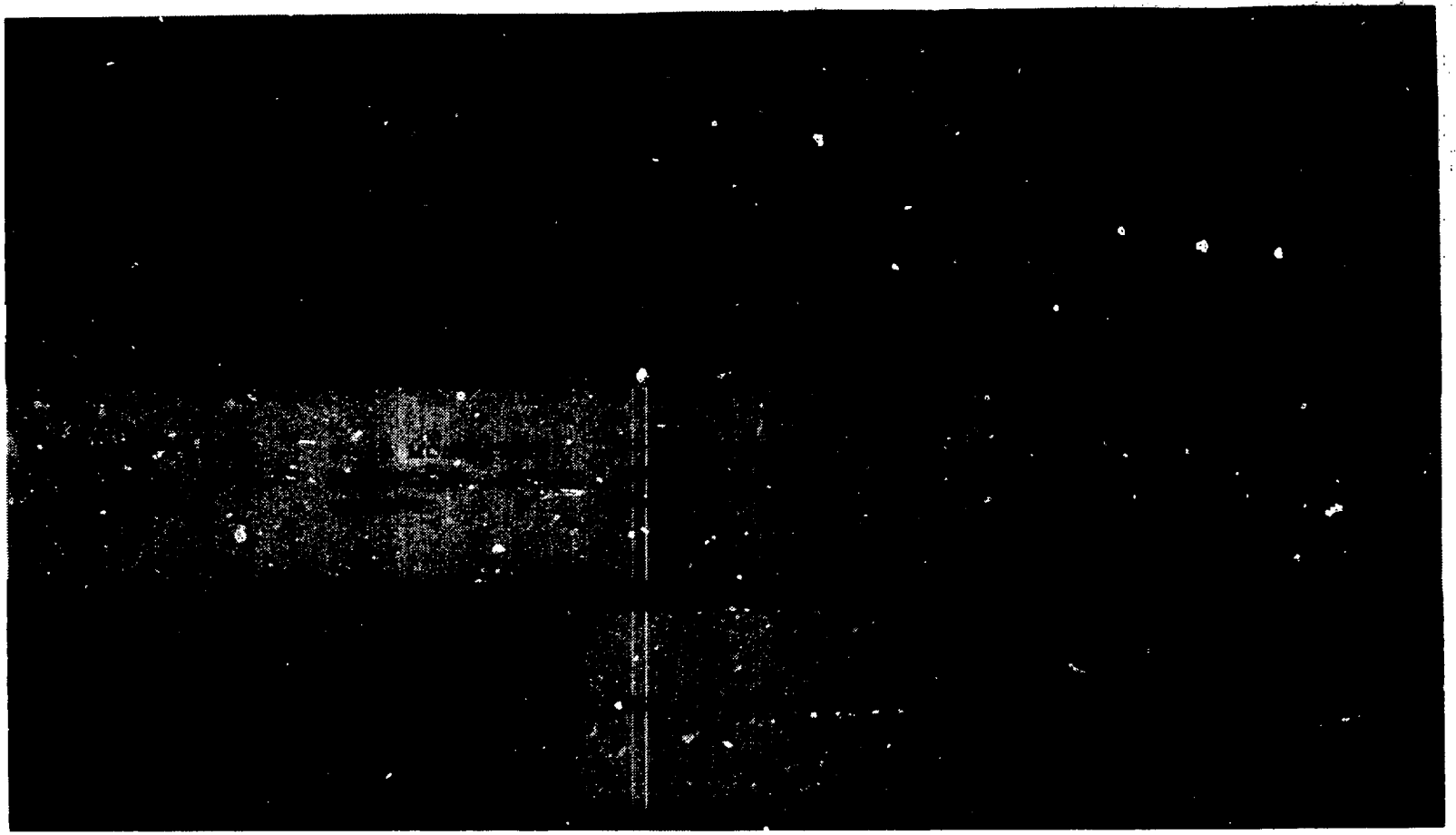

Figure 3.11. Typical Tested Haze/Transmittance Coupons.

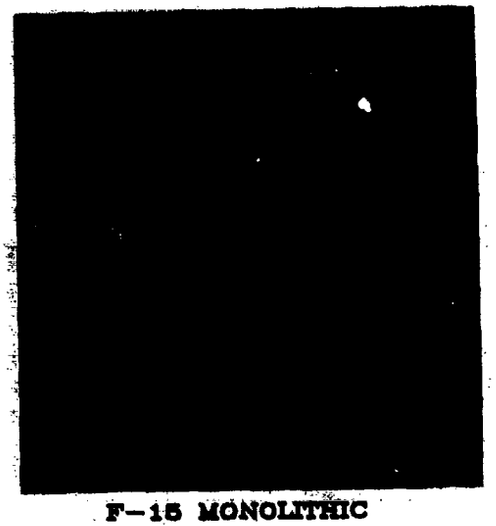

F-15 MONOLITHIC
STRETCHED ACRYLIC
WINDSHIELD

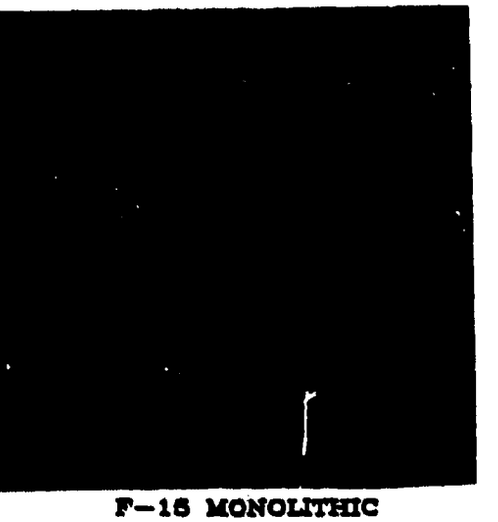

F-15 MONOLITHIC
STRETCHED ACRYLIC
CANOPY

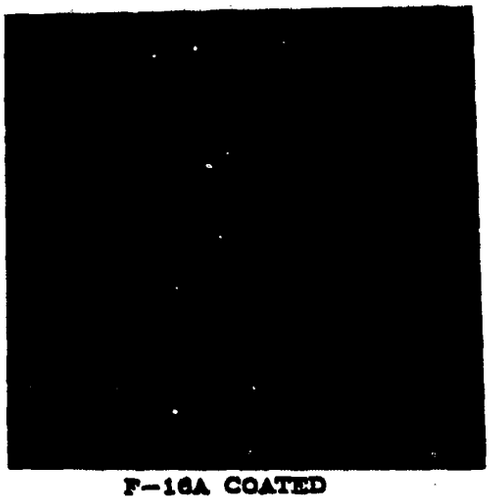

F-16A COATED
MONOLITHIC POLY-
CARBONATE CANOPY

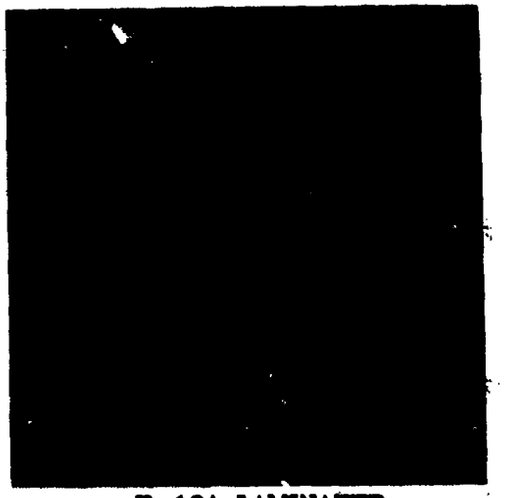

F-16A LAMINATED
CANOPY

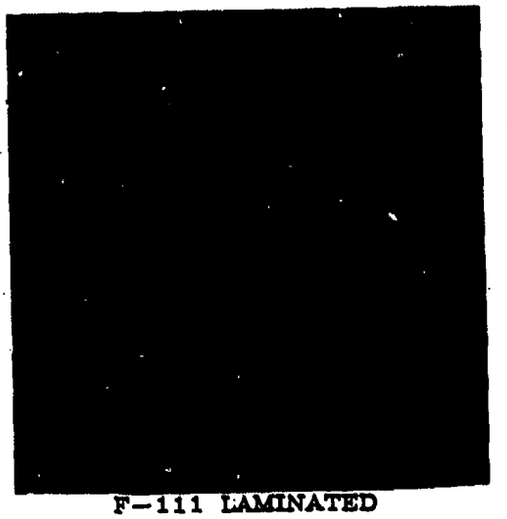

F-111 LAMINATED
ADBIRT WINDSHIELD

Figure 3.12. Haze/Transmittance Detail.

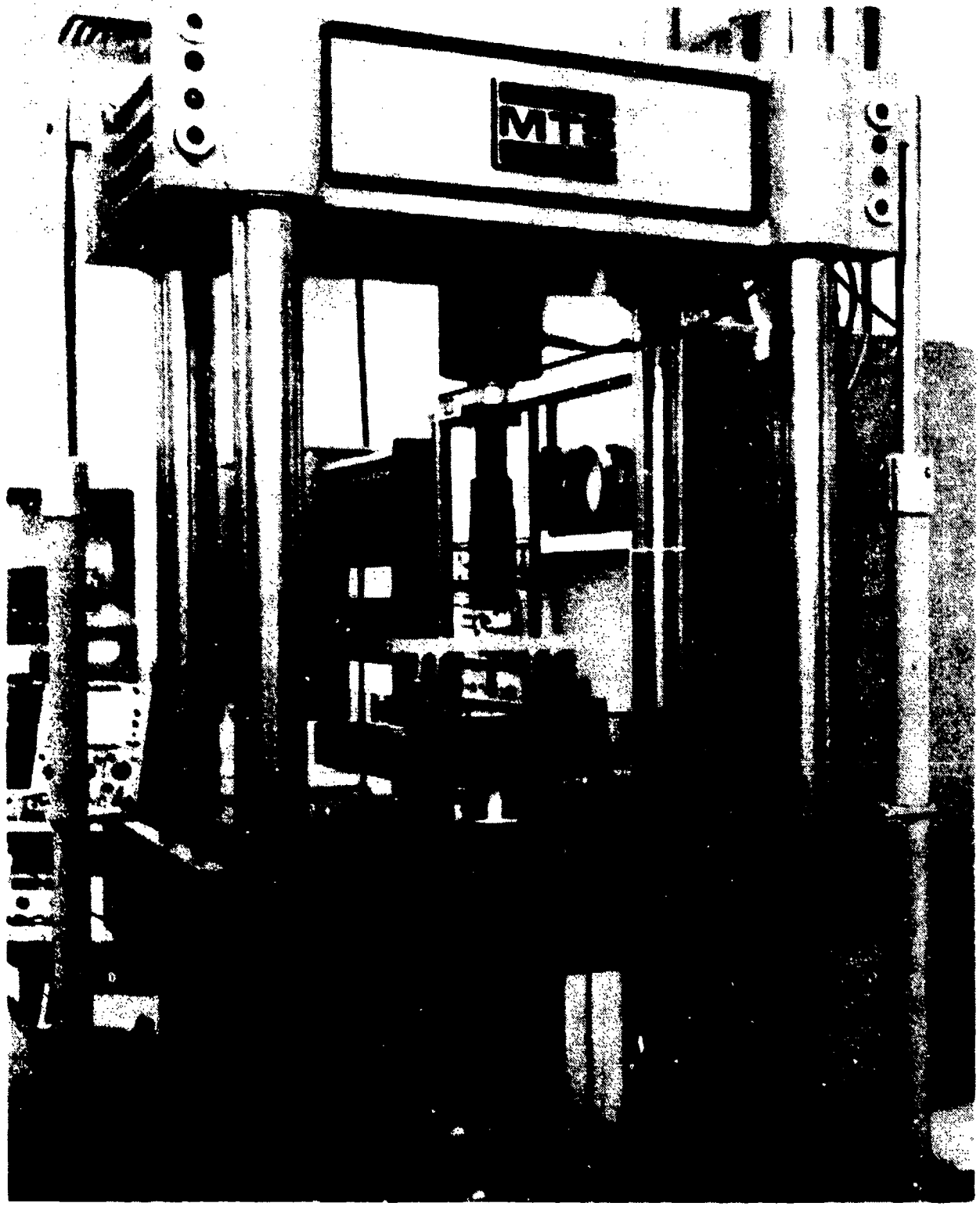

Figure 3.13. High Performance Electrohydraulic Closed Loop Test System.

load frame, appropriate transducers, an electronic feedback controller operating the actuator through an electrically controlled hydraulic servovalve, and suitable data gathering, storage, and recording instrumentation. It is a system of matched components manufactured by MTS Systems Corporation, Minneapolis, Minnesota. A mounting fixture was used to provide three-point simply-supported loading to the center of each beam specimen; the contact radius of each loading support being 3/8 inch (reference: Figure 3.14). The span between supports was 6t with an overhang of 4t at each end, where t equals as-received thickness. The specimen was centered in the fixture with the test surface down, producing tension in the test surface under investigation. The two outer supports are part of the loading yoke below the specimen. This yoke is positioned above the vertically mounted actuator, and is attached to the top of the ram; the yoke moving upward to load the specimen. Ram position is measured by an LVDT (Linear Variable Differential Transformer), with this signal being sent as the feedback signal to the analog electronic feedback controller for the actuator; the command signal for the controller being generated by a selectable function generator. Displacement rate was controlled to be 2,000 inches/minute. Peak displacement was set at a selected value of 3.00 inches. The center loading support remained stationary during testing. The upper part of the center support is attached to the stationary load frame. Both load and displacement were set at zero when the specimen just touched the loading fixture. The calibrated output signals of both the LVDT and the load cell were captured in a dual channel digital transient waveform recorder and then played back on an X-Y recorder to document load versus displacement for each high-rate MTS beam test specimen.

3.3.3 Environmental Conditioning

To fully realize the contributing effects of stress, UV, moisture, and temperature, five test specimens from each of the five transparency designs were restrained to induce

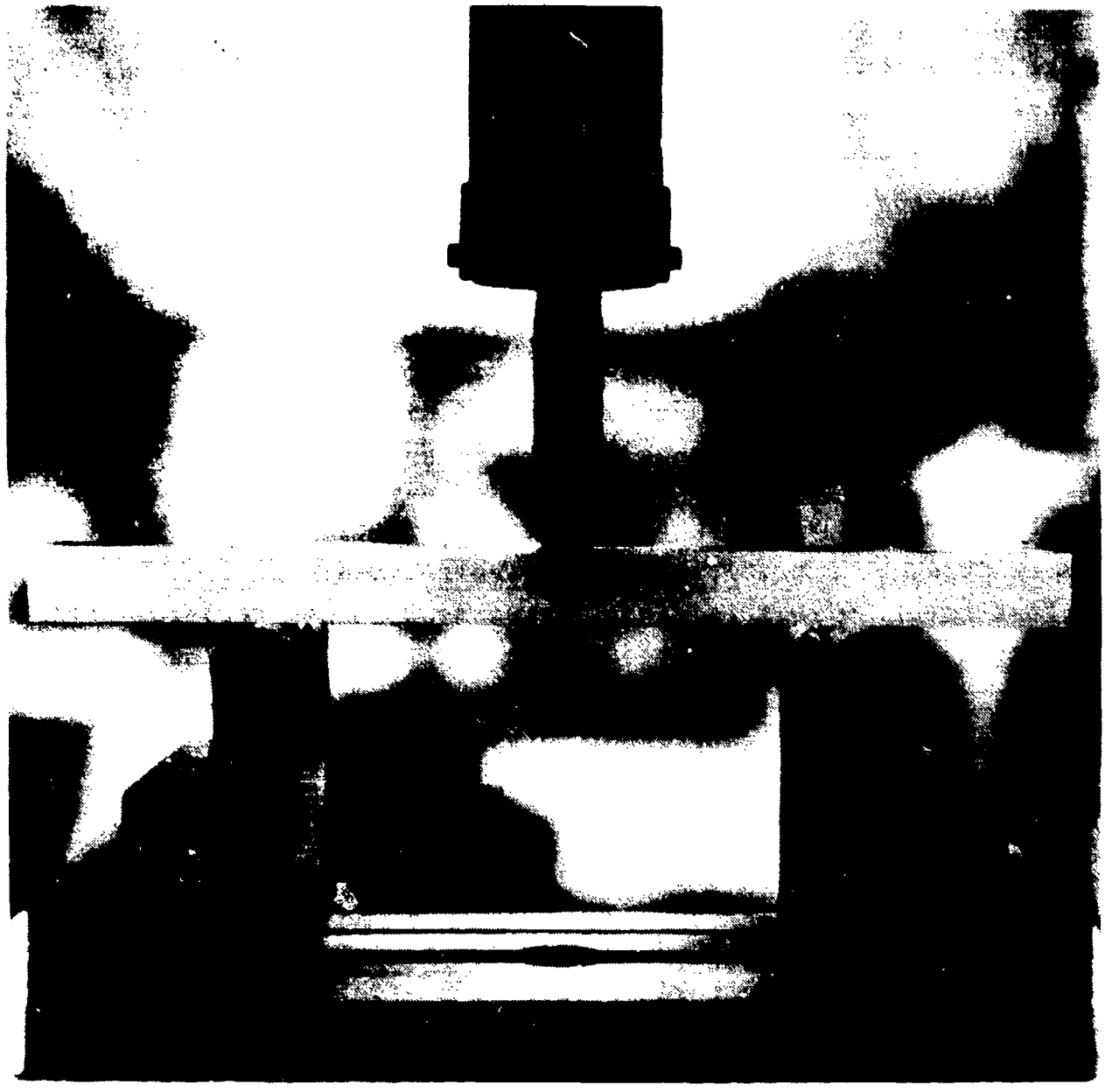

Figure 3.14. Test Setup: Simply-Supported MTS Beam.

an initial outer tensile fiber stress of 1,000 psi prior to being exposed to the accelerated weathering condition of Paragraph 3.1.3. Figure 3.15 shows the fixtures used to induce outer fiber stress into the impact beam specimens. Three different size loading fixtures were designed to induce stress in the impact beams. The fixtures fit into the Q.U.V. weathering machine so that the outer surfaces of the specimens, which were in tension, faced the UV lamps. A strain gage was mounted at the center of one unexposed coupon from each specimen type so that the stress fixtures could be calibrated for each material system. Using Hooke's law, $\sigma=E\varepsilon$, the strain at 1,000 psi outer fiber stress was calculated, and the deflection required to obtain that strain was determined for each specimen type. The specimens were then mounted in the fixtures, deflected to achieve the required stress, and then loaded into the Q.U.V. machine.

3.3.4 Test Data

Table 3.4 presents the MTS impact data generated for both baseline (unexposed) and environmentally conditioned beams tested at 2,000 inches per minute. Figures 3.16 through 3.20 show typical load versus displacement curves for each of the transparency designs.

3.3.5 Data Analysis/Correlation

The proposed acceptance criteria for the high rate impact test specified that after 3 equivalent years of accelerated weathering plus stress, the change in impact resistance determined by threshold-of-failure energy shall not exceed 15% of the unexposed baseline value. Based on the Table 3.4 data, the F-15 stretched acrylic windshield and the F-16A laminated canopy satisfied this criteria; the F-111 laminated windshield did not. As seen on other programs, the F-16A coated monolithic polycarbonate canopy increased in ductility and energy absorption after exposure, indicative of coating removal/debonding from the substrate. Figure 3.21 shows typical

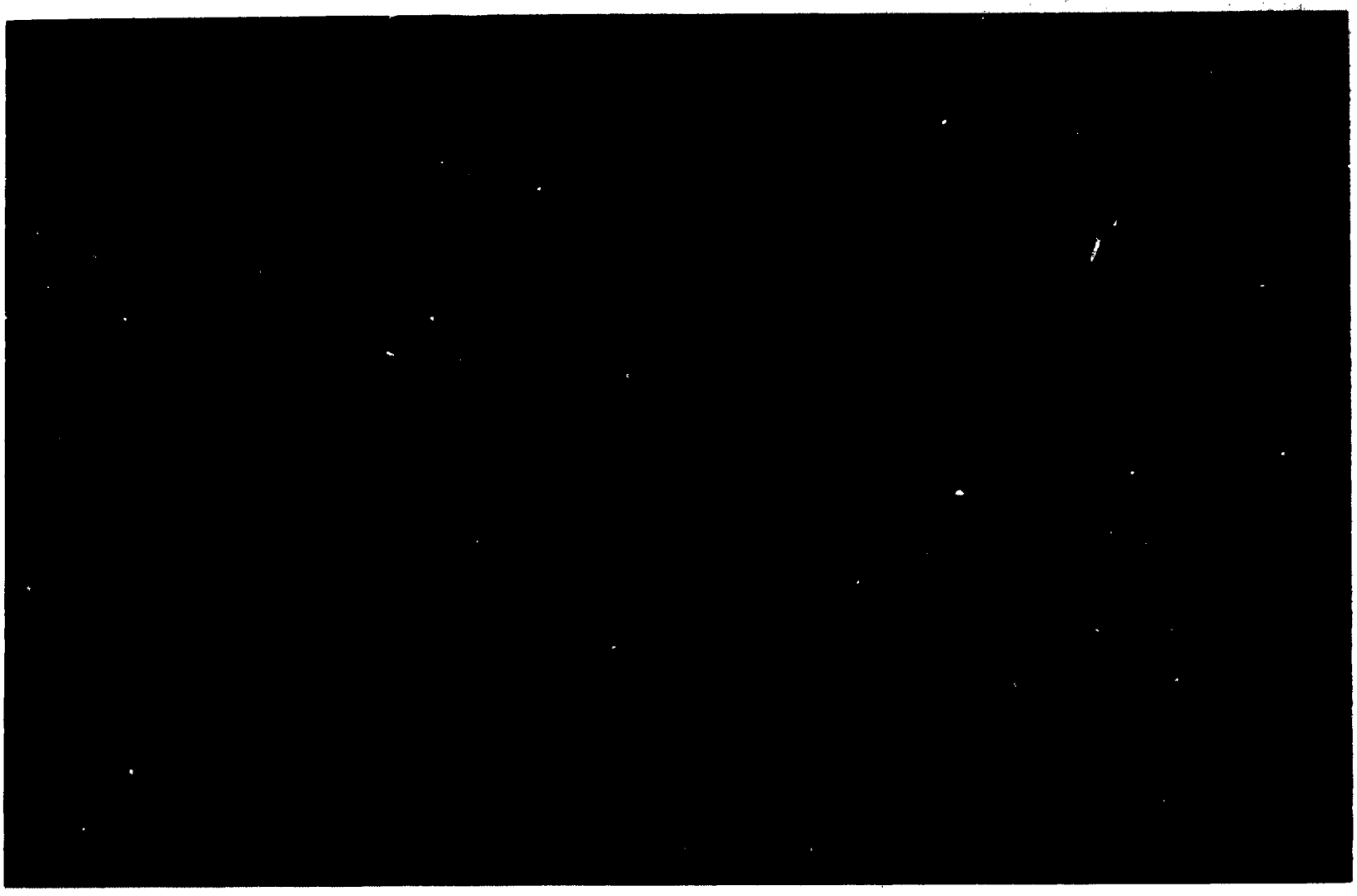

Figure 3.15. Fixtures for Inducing Stress Into the Impact Specimens During Conditioning.

TABLE 3.4

IMPACT BEAM RESULTS

BASELINE				EXPOSED (3 equivalent years of QUV)					
ID No.	Energy ft-lbs	Average (Std.Dev.)	Failure	ID No.	Energy ft-lbs	Average (Std.Dev.)	Failure	% Change	Nominal Strain $in/in\ sec^{-1}$
AQ-1	70.6		BF	AQ-7	35.3		BF		
-2	71.6		BF	-8	55.7		BF		
-3	76.6	71.9 (3.32)	BF	-9	80.8	64.5 (19.09)	BF	-10	6.27
-4	73.2		BF	-10	78.8		BF		
-5	67.6		BF	-11	72.1		BF		
BQ-1	2.0		BF	BQ-7	1.2		BF		
-2	1.5		BF	-8	1.7		BF		
-3	3.0	2.1 (0.62)	BF	-9	1.3	1.6 (0.50)	BF	-24	13.89
-4	1.6		BF	-10	1.3		BF		
-5	1.4		BF	-11	2.4		BF		
CQ-1	200.8		DF	CQ-7	261.3		DF		
-2	176.6		DF	-8*	285.9		DF		
-3	180.6	180.9 (11.61)	DF	-9	238.2	291.8 (54.96)	DF	+61	8.19
-4	175.6		DF	-10	382.6		DF		
-5	171.1		DF	-11	291.7		DF		
DQ-1	223.7		DF	DQ-7	200.0		DF		
-2	244.1		DF	-8	225.8		DF		
-3	165.4	202.2 (31.51)	DF	-9	220.8	223.2 (20.27)	DF	+10	6.80
-4	184.3		DF	-10	214.2		DF		
-5	193.3		DF	-11	255.		DF		
EQ-1	247.1		D	EQ-7	170.0		DF		
-2	250.8		D	-8	152.5		DF		
-3	242.3	244.4 (7.35)	D	-9	148.3	147.5 (15.55)	DF	-40	4.53
-4	249.3		DF	-10	137.5		DF		
-5	232.6		DF	-11	129.2		DF		

DF denotes ductile failure (of tension surface)
BF denotes brittle failure
D denotes ductile deformation below threshold of failure

* test surface tested in compression

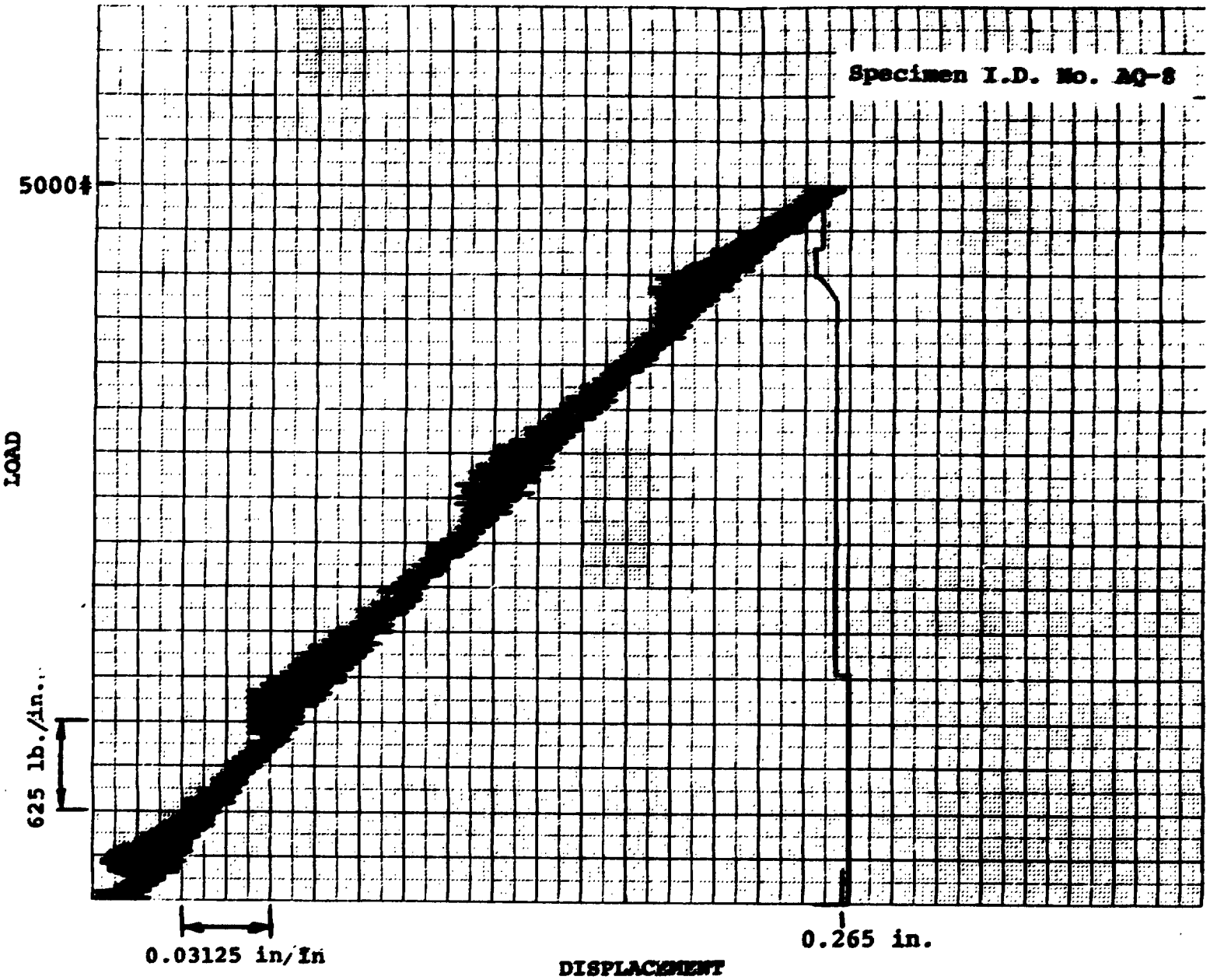

Figure 3.16. Typical Load vs. Displacement Plot, MTS Beam, F-15 Monolithic Stretched Acrylic Windshield.

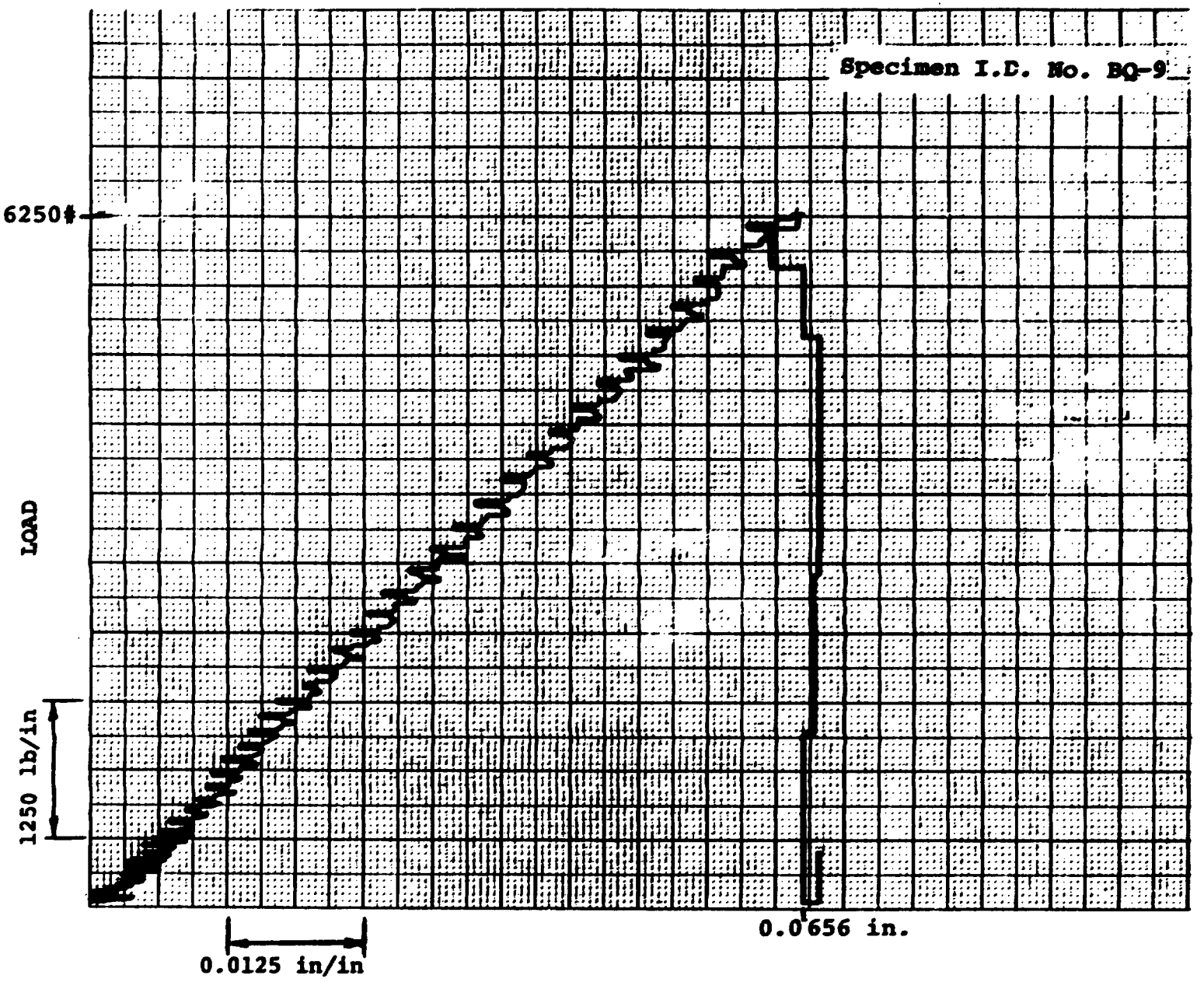

Figure 3.17. Typical Load vs. Displacement Plot, MTS Beam, F-15 Monolithic Stretched Acrylic Canopy.

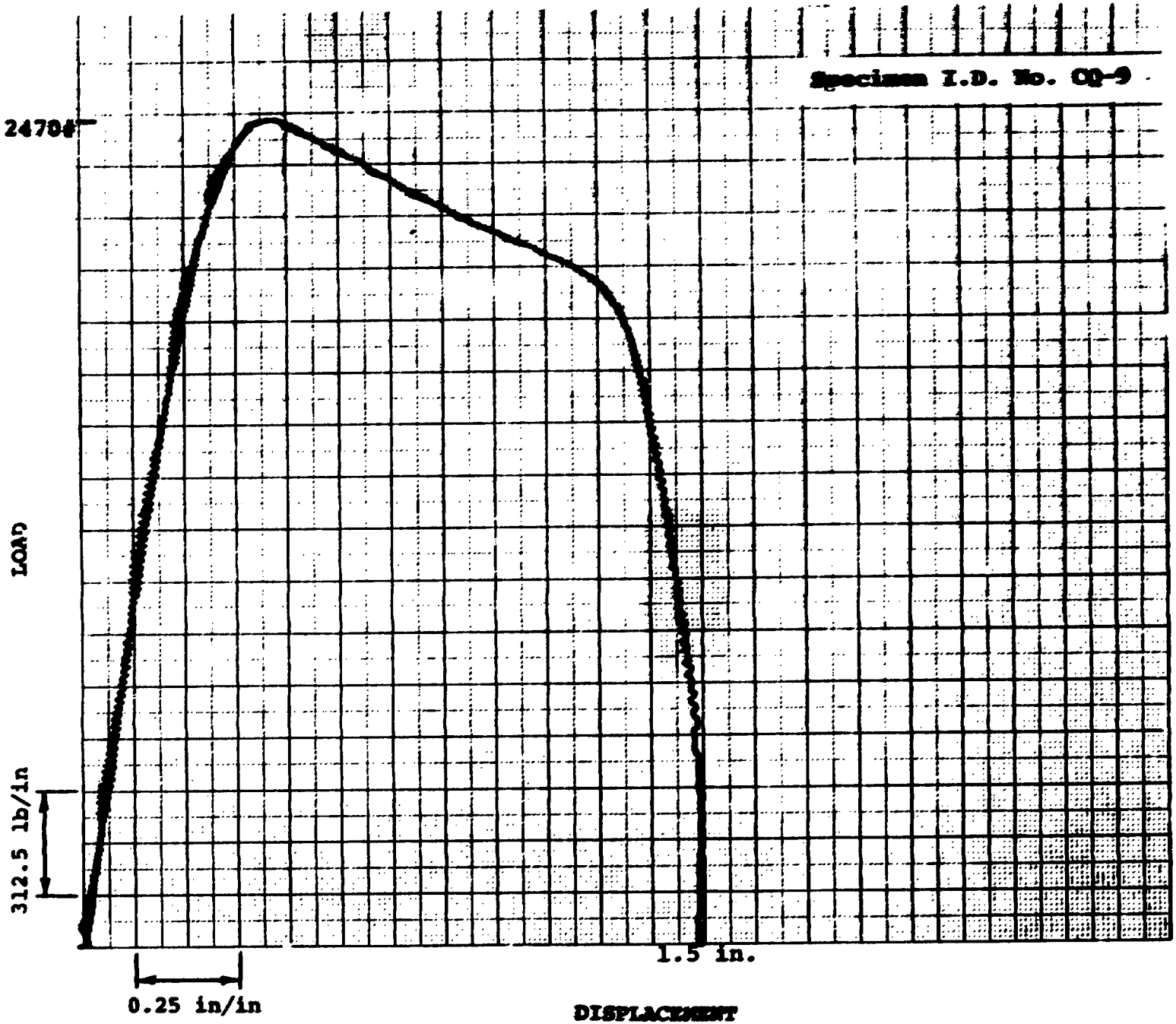

Figure 3.18. Typical Load vs. Displacement Plot, MTS Beam, F-16A Coated Monolithic Polycarbonate Canopy.

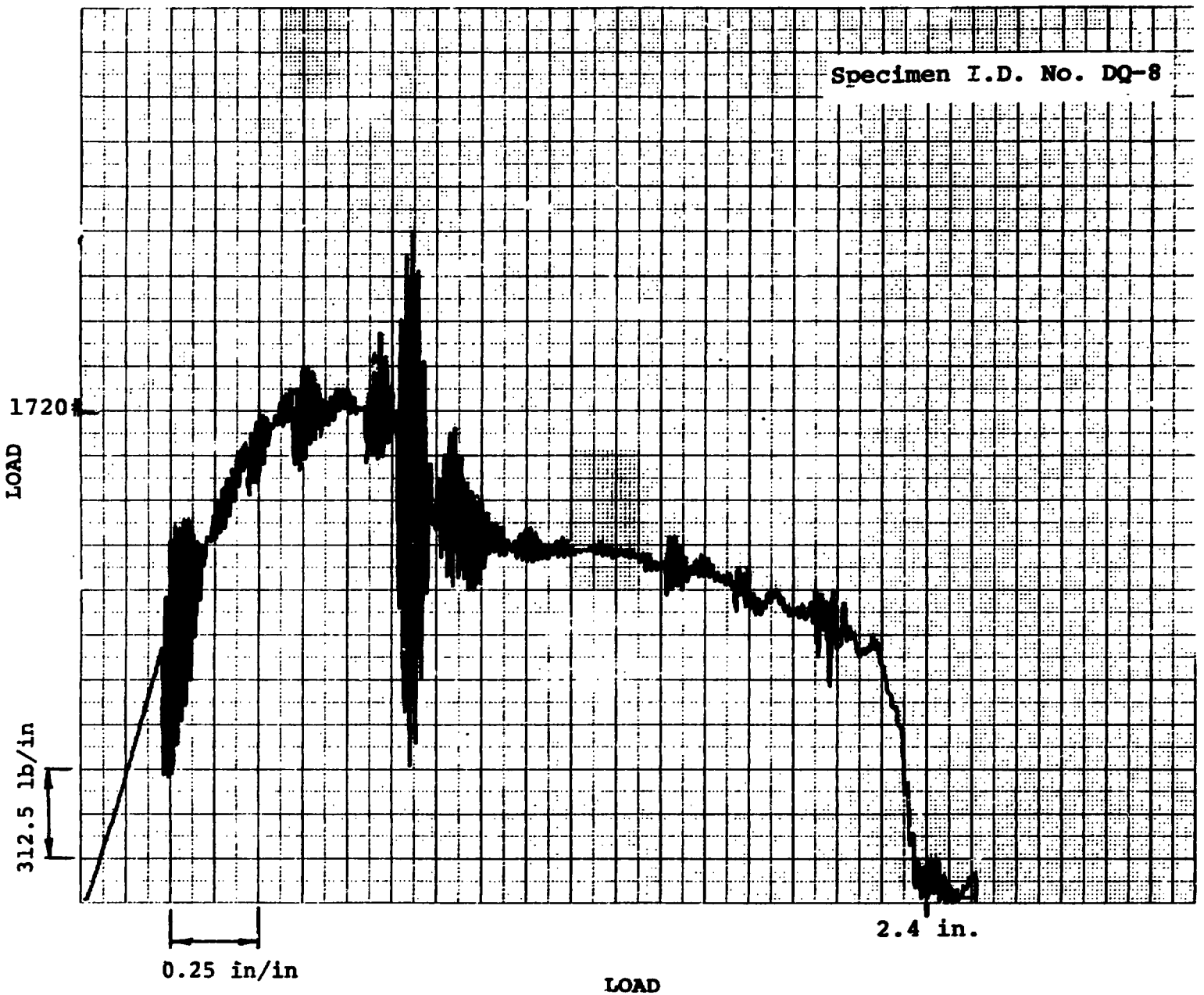

Figure 3.19. Typical Load vs. Displacement Plot, MTS Beam, F-16A Laminated Canopy.

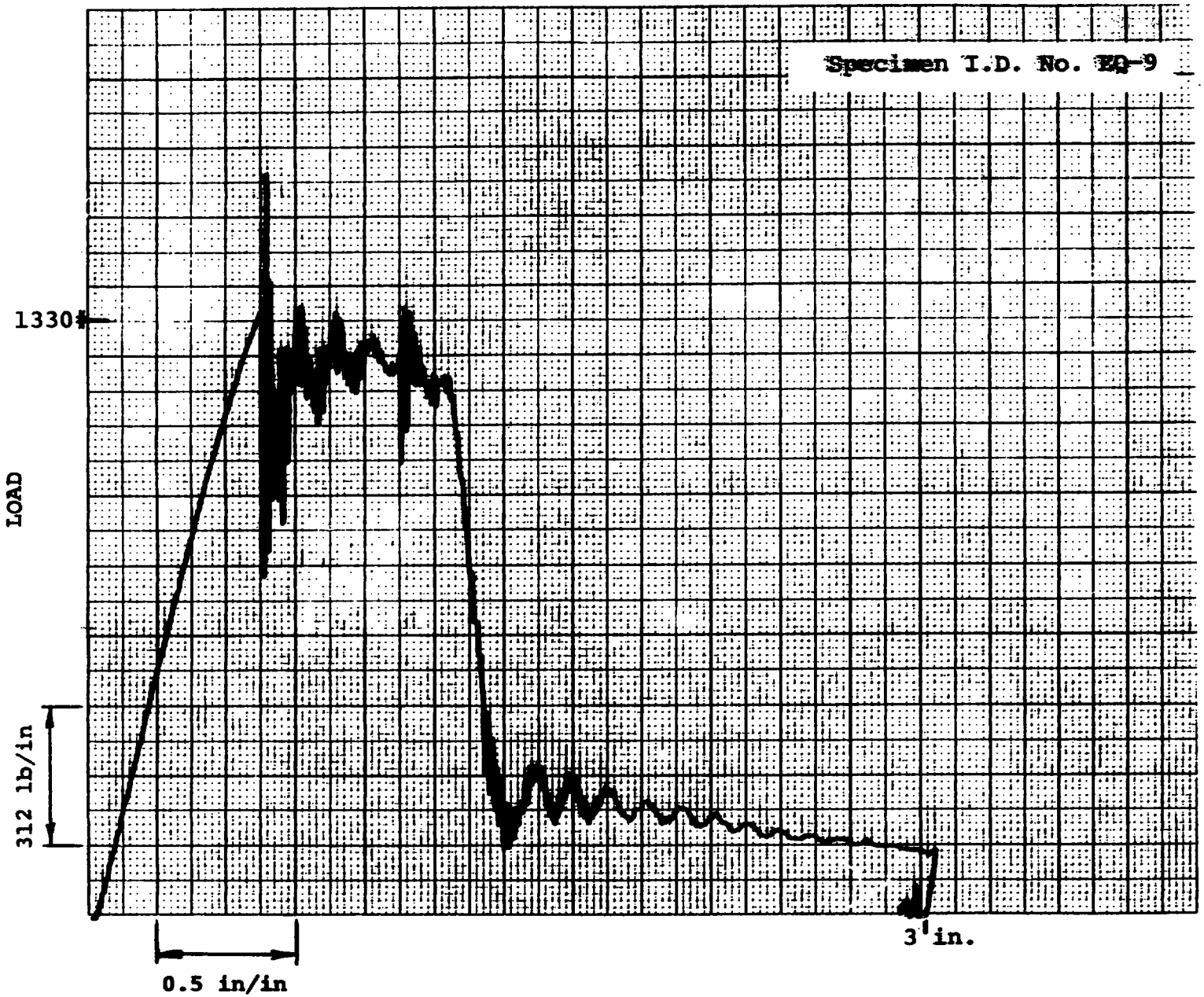

Figure 3.20. Typical Load vs. Displacement Plot, MTS Beam, F-111 Laminated ADBIRT Windshield.

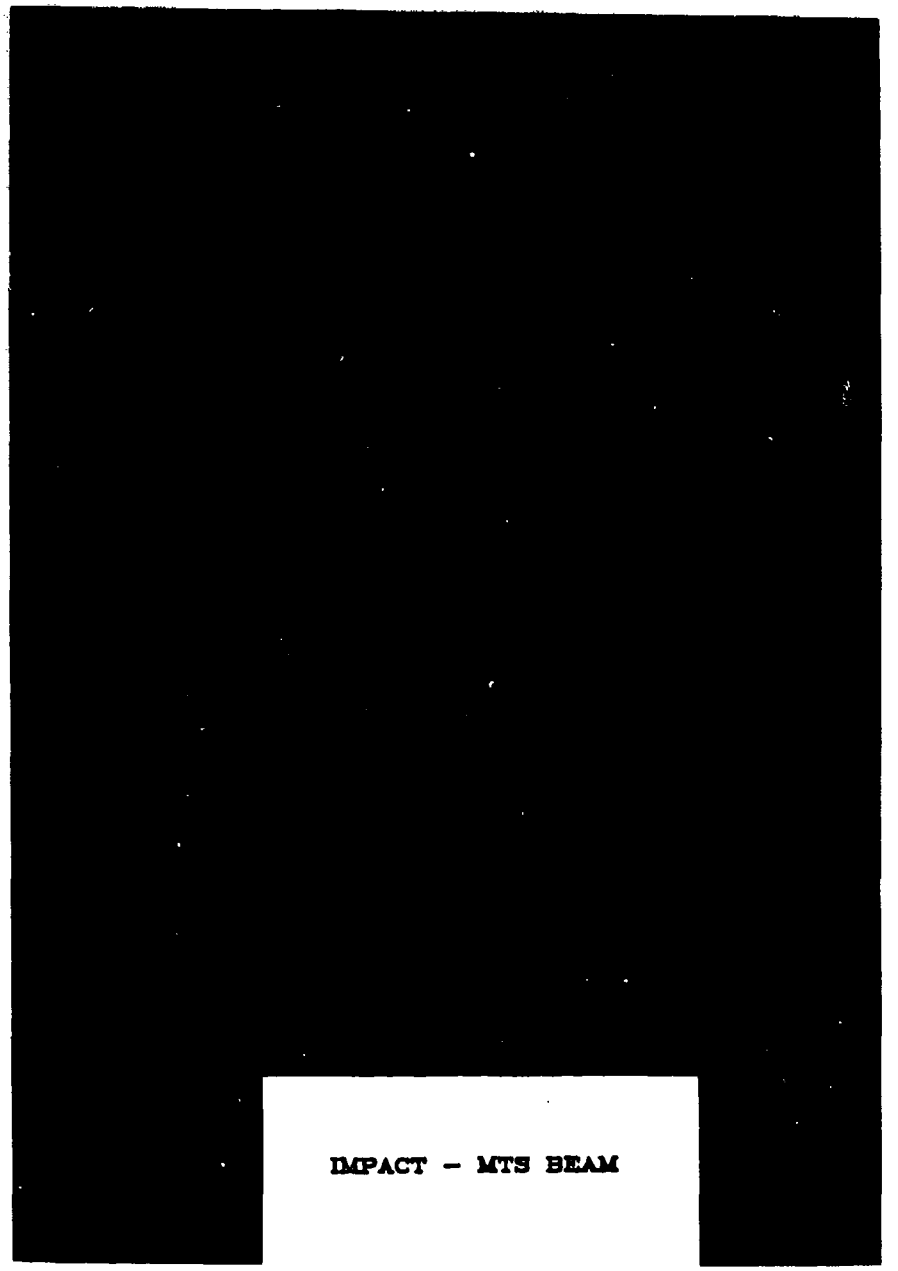

Figure 3.21. Typical Failed MTS Impact Beam Specimens.

failed beam specimens, tested after exposure, and Figures 3.22 through 3.24 show specimen failure detail.

3.4 IMPACT-FALLING WEIGHT

3.4.1 Specimen Configuration

In accordance with Paragraph 3.3.1.

3.4.2 Test Method

In accordance with ASTM Test Method F736-81. Figure 3.25 shows the test apparatus. Figure 3.26 shows the test setup.

3.4.3 Environmental Conditioning

Accelerated weathering plus stress, 10 required from each design in accordance with Paragraph 3.3.3; and baseline, 10 required from each design.

3.4.4 Test Data

Table 3.5 presents the falling weight test data presented for baseline (unexposed) and environmentally conditioned beams cut from the F-15 monolithic stretched acrylic canopy, the F-16A coated monolithic polycarbonate canopy, and the F-16A laminated canopy. Sufficient material was not available for testing the F-15 windshield or the F-111 windshield. Typical failed specimens are shown in Figure 3.27.

3.4.5 Data Analysis/Correlation

The proposed acceptance criteria for the falling weight impact test specified that after 3 equivalent years of accelerated weathering plus stress exposure, the change in impact resistance as determined by threshold-of-failure energy shall not exceed 15% of the unexposed baseline value. Based on the Table 3.5 data, both the F-15 stretched acrylic canopy and the F-16A laminated canopy satisfied the proposed criteria. The F-16A

F—15 MONOLITHIC
STRETCHED ACRYLIC
WINDSHIELD

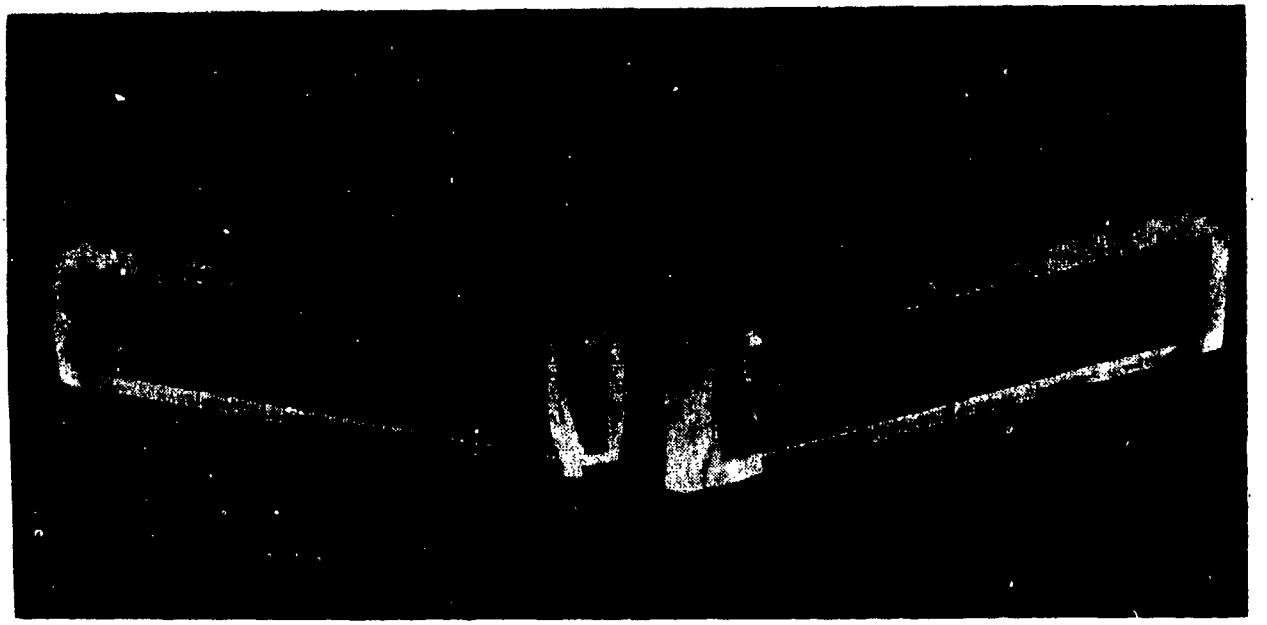

F—15 MONOLITHIC
STRETCHED ACRYLIC
CANOPY

Figure 3.22. Detail of F-15 MTS Impact Beam Failed Specimens.

F—16A COATED
MONOLITHIC POLY—
CARBONATE CANOPY

F—16A LAMINATED
CANOPY

Figure 3.23. Detail of F-16A MTS Impact Beam Failed Specimens.

Figure 3.24. Detail of F-111 MTS Impact Beam Failed Specimens.

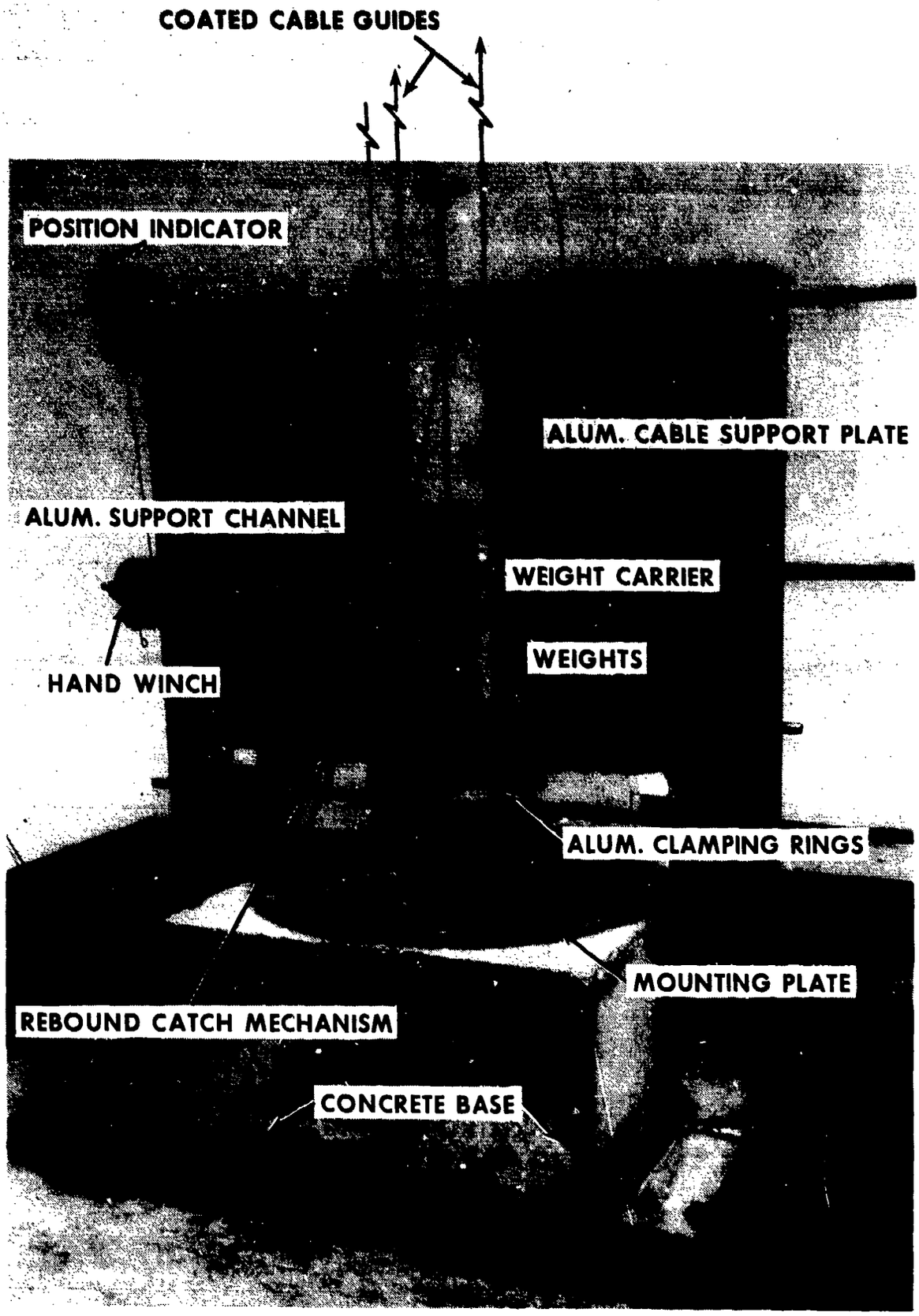

Figure 3.25. UDRI Falling Weight Impact Test Apparatus.

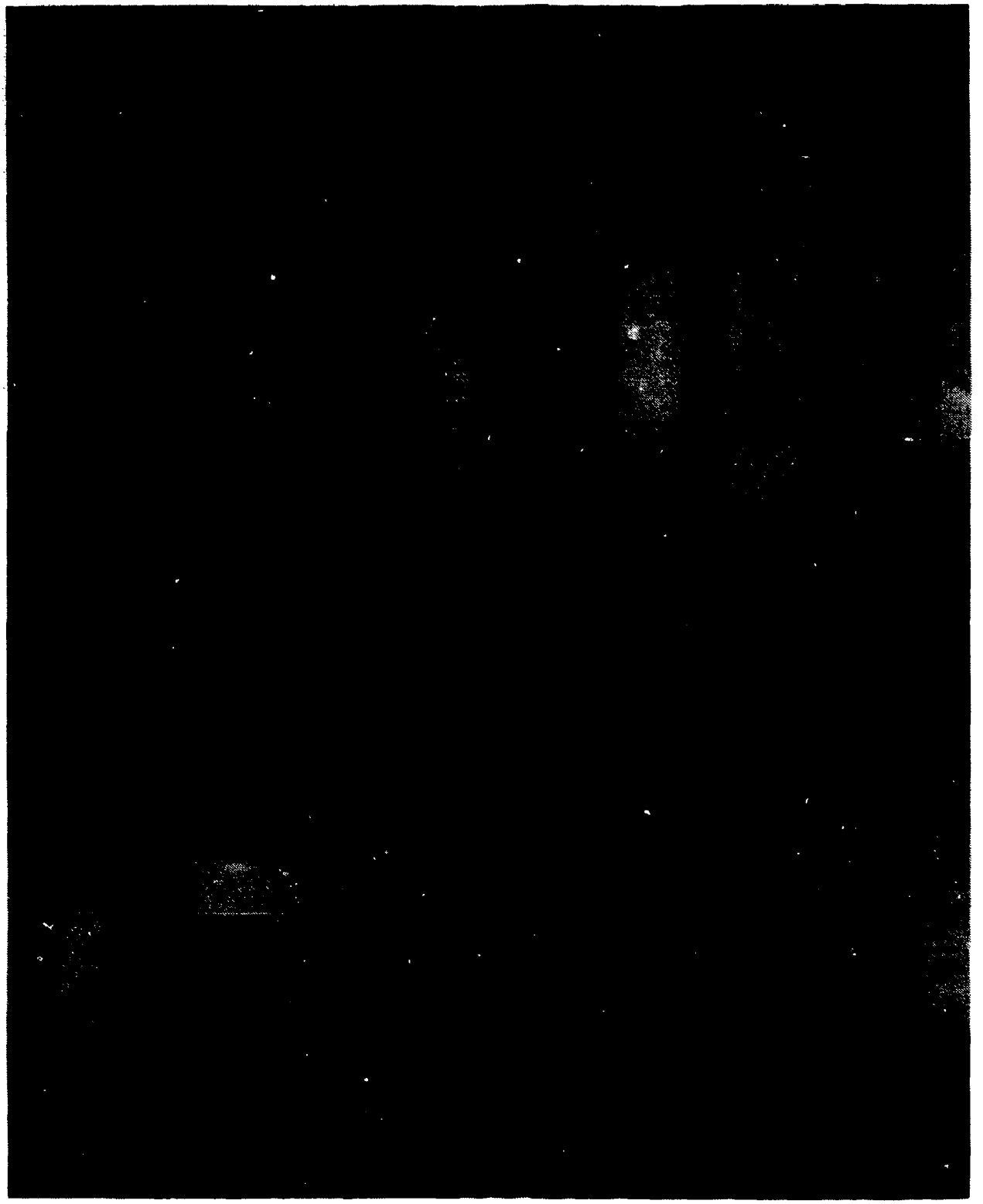

Figure 3.26. Test Setup: Falling Weight Impact.

TABLE 3.5

FALLING WEIGHT TEST RESULTS

Specimen ID Number	Energy ft-lbs	Threshold of Failure Energy ft-lbs	Strain Rate $in/in\ sec^{-1}$	Failure	Specimen ID Number	Energy ft-lbs	Threshold of Failure Energy ft-lbs	Strain Rate $in/in\ sec^{-1}$	Failure	Change
BR-1	2.10		98.3	NF	BR-11	4.20		89.7	NF	
-1	3.07		98.3	NF	-11	4.48		92.7	NF	
-1	5.04		98.3	P	-11	4.65		94.5	P	
BR-2	4.20		89.7	P	BR-12	4.55		93.4	P	
BR-3	2.52		69.5	NF	BR-13	4.48		92.7	P	
-3	3.36		80.3	NF	BR-14	4.34		91.2	P	
-3	3.78		85.1	P	BR-15	4.20		89.7	NF	
BR-4	3.78		85.1	NF	-15	4.34		91.2	P	
-4	3.99		87.5	NF	BR-16	4.27		90.5	NF	
-4	4.20		89.7	P	-16	4.34		91.2	P	
BR-5	4.06		88.3	P	BR-17	4.34		91.2	NF	
BR-6	3.99	4.14	87.5	NF	-17	4.48	4.56	92.7	NF	+10%
-6	4.13		89.0	NF	-17	4.62		94.1	NF	
-6	4.27		90.5	NF	-17	4.76		95.5	NF	
-6	4.41		91.9	P	-17	4.90		96.9	P	
BR-7	4.20		89.7	P	BR-18	4.62		94.1	NF	
BR-8	4.13		89.0	P	-18	4.83		96.2	NF	
BR-9	4.06		88.3	NF	-18	5.04		98.3	P	
-9	4.20		89.7	NF	BR-19	4.76		95.5	P	
-9	4.34		91.2	P	BR-20	4.48		92.7	P	
BR-10	4.20		89.7	NF						
-10	4.41		91.9	NF						
-10	4.62		94.1	P						

TABLE 3.5 (concluded)

Specimen ID Number	Energy ft-lbs	Threshold of Failure Energy ft-lbs	Strain Rate in/in sec^{-1}	Failure	Specimen ID Number	Energy ft-lbs	Threshold of Failure Energy ft-lbs	Strain Rate in/in sec^{-1}	Failure	Change
CR-1	142		74.9	D	CR-11	176		83.6	D	
CR-2	170		82.1	F	CR-12	176		83.6	D	
CR-3	171		82.2	F	CR-13	225		94.6	D	
CR-4	168		81.6	F	CR-14	301		83.6	D	
CR-5	166	171	81.1	D	CR-15	337	330	88.5	D	+93%
CR-6	167		81.4	D	CR-16	385		94.6	F	
CR-7	168		81.6	D	CR-17	361		91.6	F	
CR-8	171		82.2	D	CR-18	349		90.1	F	
CR-9	172		82.5	F	CR-19	341		89.1	F	
CR-10	175		83.1	F	CR-20	334		88.2	F	
DR-1	230		79.4	P	DR-11	230		79.4	D	
DR-2	198		73.6	D	DR-12	239		81.0	F	
DR-3	212		76.2	D	DR-13	232		79.8	D	
DR-4	219		77.4	D	DR-14	234		80.2	D	
DR-5	226	229	78.6	D	DR-15	238	238	80.8	F	+4%
DR-6	230		79.2	P	DR-16	238		80.9	D	
DR-7	228		79.0	F	DR-17	240		81.2	F	
DR-8	227		78.8	D	DR-18	239		81.0	F	
DR-9	229		79.1	D	DR-19	239		81.1	F	
DR-10	230		79.2	F	DR-20	239		81.1	F	

D denotes ductile deformation; below failure
F denotes threshold of failure; visible open crack
P denotes penetration; beam split in two; exceeds failure
NF denotes no failure (below elastic limit)

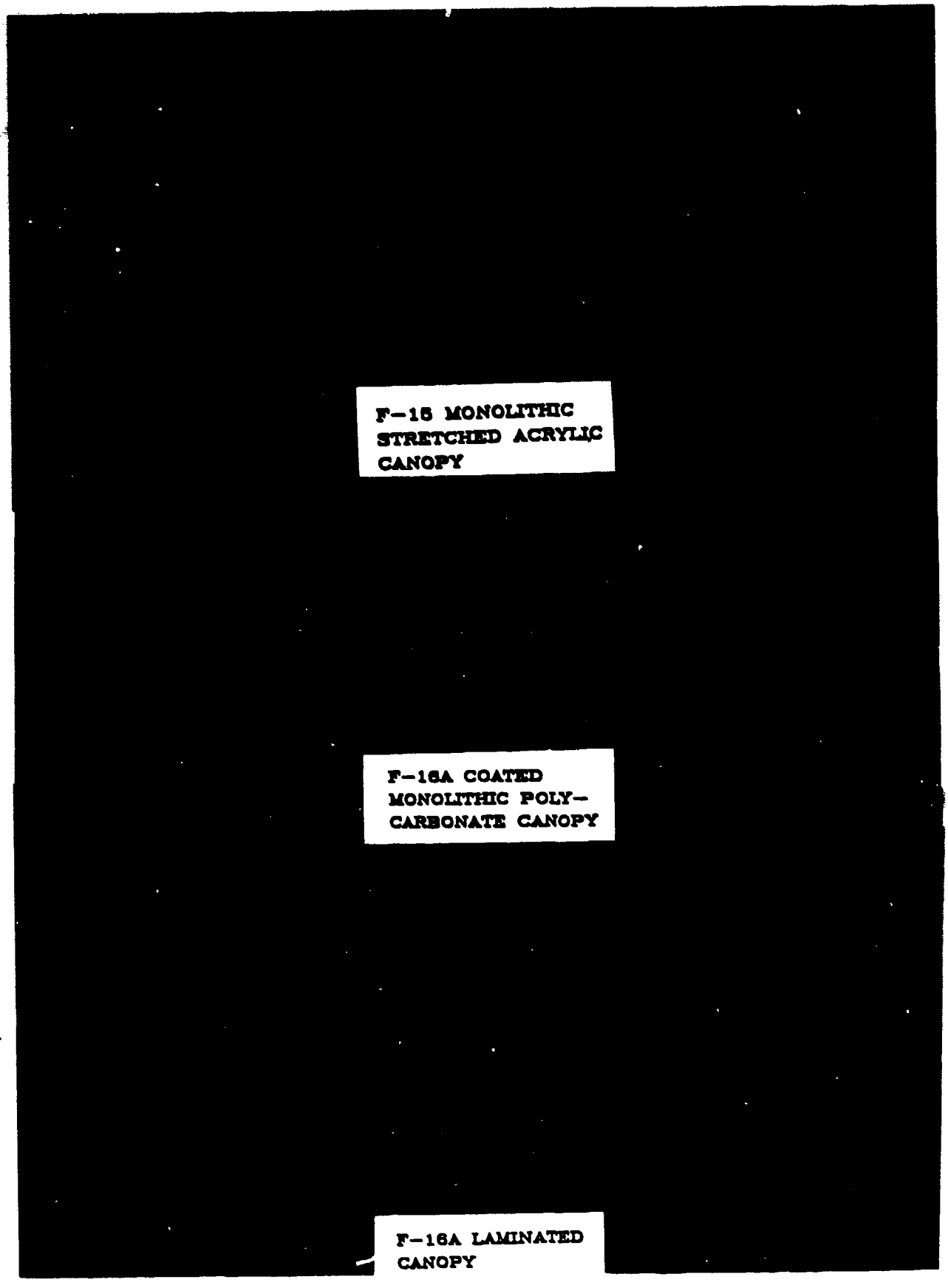

Figure 3.27. Typical Failed Falling Weight Impact Beam Specimens.

coated polycarbonate canopy data was consistent with results from the high rate impact tests; indicating a significant increase in energy absorption (ductility) after exposure.

For the exposed (artificially weathered) impact specimens, the failure energies for the falling weight beams were greater than those for the MTS beams. Results were similar for the baseline (unweathered) beams, except the coated polycarbonate failure energies for the MTS beams were higher than those for the falling weight beams. These differences in failure energies may be attributed to several factors: the differences in strain rate and the "threshold-of-failure" definitions. As shown in Table 3.6, strain rates for the falling weight tests were between 5 and 11 times faster than strain rates for the MTS beam tests. The expected effect of a fater strain rate is to increase the response stiffness of the test specimen; also, the peak load which can be sustained by the specimen would be expeted to increase. These expectations held true for all specimens except the baseline coated polycarbonate as noted above. The coating on the polycarbonate is strain-rate sensitive and brittle. At higher strain rates the coating causes earlier failure of the polycarbonate. After exposure, however, as the coating is degraded, this embrittling effect of the coating disappears. The definitions of "failure" for the two impact beam tests are different. For MTS beams, the stroke is limited to 2-1/2 inches. The failure mode of tested beams reflects this stroke limitation. In contrast, the falling weight beams are tested such that a well-defined failure is achieved. For brittle materials such as acrylic, the failure energy is the amount of energy the material can withstand just before fracture. For ductile materials such as polycarbonate, threshold-of-failure is defined as the energy at which visible open cracks start to develop in the material (reference Figure 3.2.7, F-16A coated monolithic polycarbonate canopy). These differences make the comparison between the two impact tests difficult and valid only when the differences between the tests are realized.

TABLE 3.6

COMPARISON OF MTS IMPACT BEAM AND FALLING WEIGHT IMPACT BEAM STRAIN RATES AND FAILURE ENERGIES

BASELINE

		MTS	Falling Weight	% Difference = $(\frac{F.W.-I.B.}{I.B.})x100\%$
F-16 Stretched Acrylic Canopy	Strain Rate*	13.9	90.7	+553%
	Failure Energy**	2.1	4.14	+ 97%
F-16A Poly-carbonate Canopy	Strain Rate	8.2	82.3	+904%
	Failure Energy	180.9	171	-5.4%
F-16A Laminated Canopy	Strain Rate	6.8	79.2	+1065%
	Failure Energy	202.2	229	+13.3%

EXPOSED

F-15 Stretched Acrylic Canopy	Strain Rate	13.9	93.8	+575%
	Failure Energy	1.6	4.56	+185%
F-16A Poly-carbonate Canopy	Strain Rate	8.2	90.7	+1006%
	Failure Energy	291.8	330	+13.7%
F-16A Laminated Canopy	Strain Rate	6.8	81.0	+1091%
	Failure Energy	223.2	238	+6.6%

*Strain rate in in/in sec^{-1}

**Failure energy in ft-lbs

3.5 COATING ADHESION

(F-16A Coated Monolithic Polycarbonate Canopy Only)

3.5.1 Specimen Configuration

Five sets of 2 each per the following geometry:

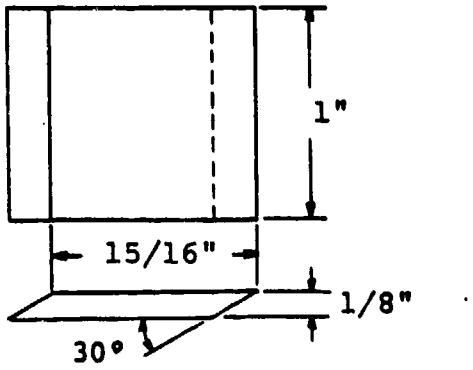

3.5.2 Test Method

Rain impingement tests at 500 mph on test specimens inclined at 30 degrees to the direction of motion were conducted on the rotating arm apparatus at Wright-Patterson Air Force Base (Reference Figure 3.28). This rotating arm apparatus consists of an 8-foot diameter double arm blade. It is designed to produce high tip velocities with negative lift and low drag coefficient. Five sets of mated test specimens were mounted at the leading edge tip sections of the double rotating arm. The double arm is mounted horizontally on a vertical drive shaft. Simulated rainfall is produced by four curved manifold quadrants. Each manifold quadrant has 24 equally spaced capillaries. Raindrop size and drop rate are controlled by the capillary orifice diameter and the head pressure of the water supply. The manifold quadrants are mounted above the tips of the double rotating arm. Raindrops from the simulation apparatus impact the test specimens throughout their

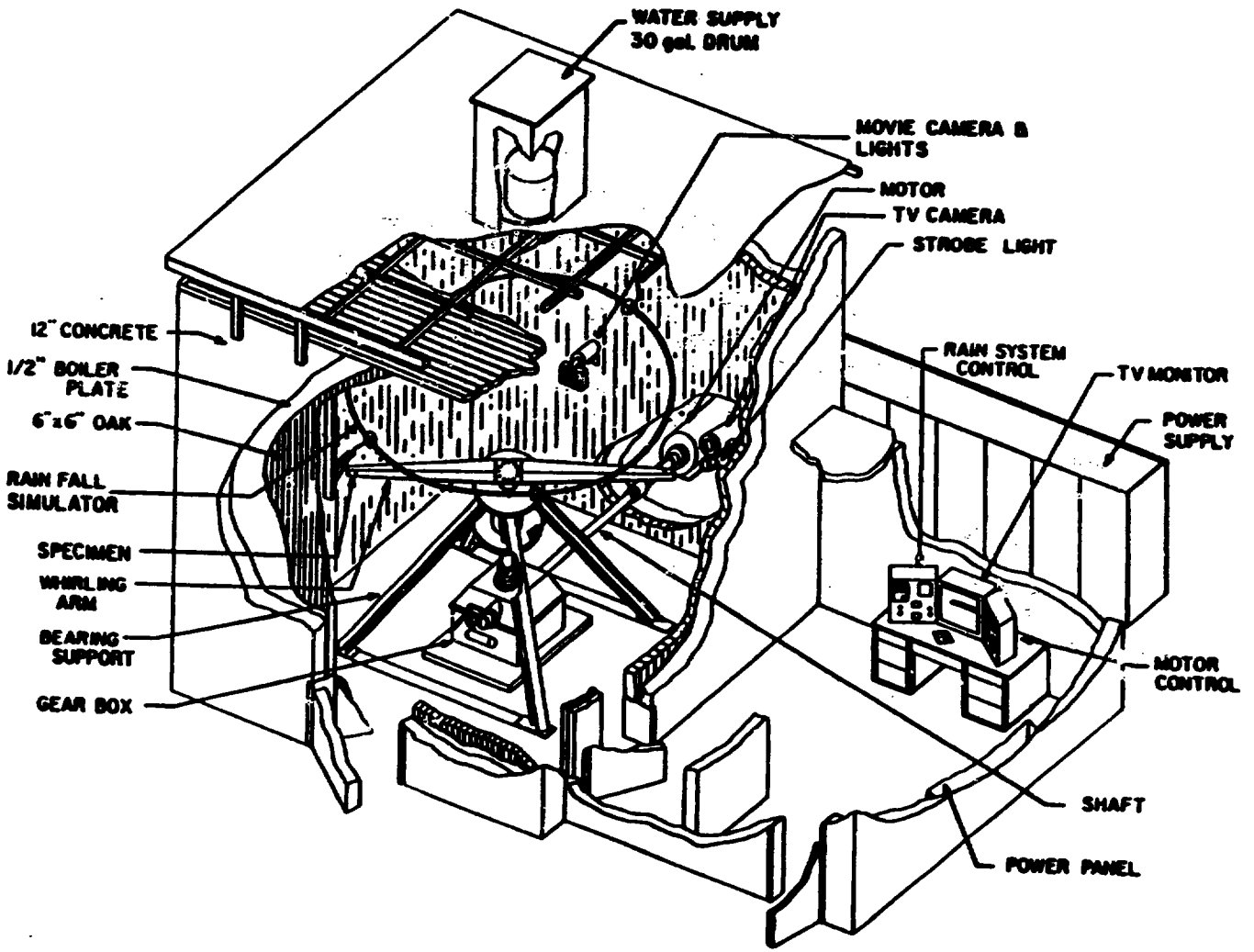

Figure 3.28. Mach 1.2 Rain Erosion Test Apparatus.

entire annular path. Rain droplets are 3.0 mm in diameter and generated at the rate of 1 inch/hour of simulated rainfall.

At test intervals of 1 and 2 minutes, all specimens were examined visually to determine the percentage of coating removal. After 5 minutes of testing, all specimens were subjected to optical examination and scanning electron microscope to determine the percentage of coating removal.

3.5.3 Environmental Conditioning

Accelerated weathering plus stress in accordance with Paragraph 3.3.3. A special fixture was fabricated to accommodate the small specimens.

3.5.4 Test Data

Table 3.7 presents the coating adhesion data generated by the rain erosion test apparatus; the percentage of coating removal being noted.

3.5.5 Data Analysis/Correlation

After five minutes of testing, all specimens failed to satisfy the proposed acceptance criteria that tested specimens experience no substantial amount of coating removal; resultant data being consistent with corresponding Reference 3 test results.

3.6 INTERLAMINAR BOND INTEGRITY (DELAMINATION) (F-16A Laminated Canopy and F-111 Laminated ADBIRT Windshield Only)

3.6.1 Flatwise Tension

3.6.1.1 Specimen Configuration

Using ASTM F521-77 as a guidelines, the 2-inch square standard specimen was modified to 1-inch square to minimize the effects of transparency curvature. The specimen test area was undercut, as shown in Figure 3.29, to ensure

TABLE 3.7

COATING ADHESION (RAIN EROSION) TEST DATA

Speed: 500 mph

Rainfall: 1 in/hr

Exposure: 3 equiv. yrs. of accelerated weathering plus stress

Specimen Number	Coating Removal, Percent Test Time, Minutes		
	1	2	5
CS-1	5	30	64
CS-2	1	5	33
CS-3	5	25	85
CS-5	3	20	91
CS-6	2	10	69
CS-7	10	30	84
CS-8	2	25	68
CS-9	2	20	76
CS-10	1	10	30
CS-11	1	10	70

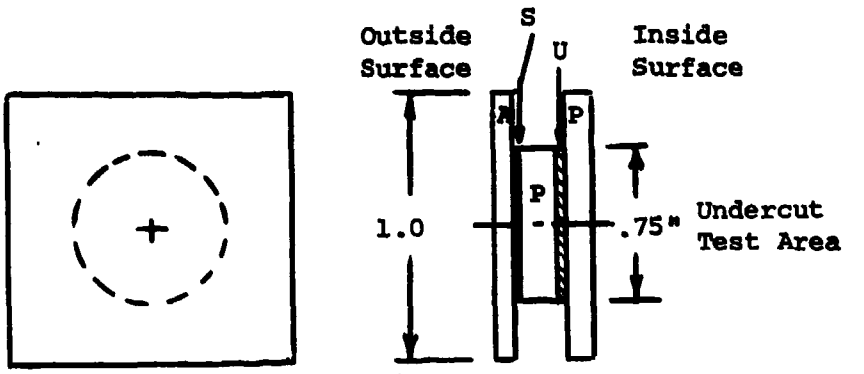

A = Acrylic
P = Polycarbonate
S = Silicone
U = Urethane

Figure 3.29. Modified Flatwise Tension Specimen.

failure in the test interlayer and to eliminate specimen-to-fixture bondline failure.

3.6.1.2 Test Method

Using ASTM F521-77 as a guideline, specimens were bonded to one-inch square loading blocks using a room temperature curing adhesive. An alignment fixture was used to center the specimen and align the loading blocks to ensure a true tensile load. Tests were conducted at a loading rate of 100 lb/sec in an MTS electrohydraulic closed loop test machine (reference Figure 3.30). Load versus displacement data was recorded.

3.6.1.3 Environmental Conditioning

Accelerated weathering in accordance with Paragraph 3.1.3.

3.6.1.4 Test Data

Table 3.8 presents the flatwise tension data generated for both laminated transparency designs; typical load versus displacement curves being shown as Figures 3.31 and 3.32. Displacement measurements, measured internal to the machine, represent the sum of the displacements in the fixture and specimen (including all interlayers), and cannot be used for calculating the elastic modulus. Because of the possibility of the displacement measurements being misinterpreted, they have not been tabulated. Force measurements, also measured internal to the machine, were subject only to instrumentation-type errors which were considered to be negligible.

3.6.1.5 Data Analysis/Correlation

Failures occurred in the silicone interlayer for both the F-16 and F-111 laminated transparencies; an adhesive failure at an average ultimate tensile stress of 392 psi for the F-16 and a cohesive failure at an average ultimate

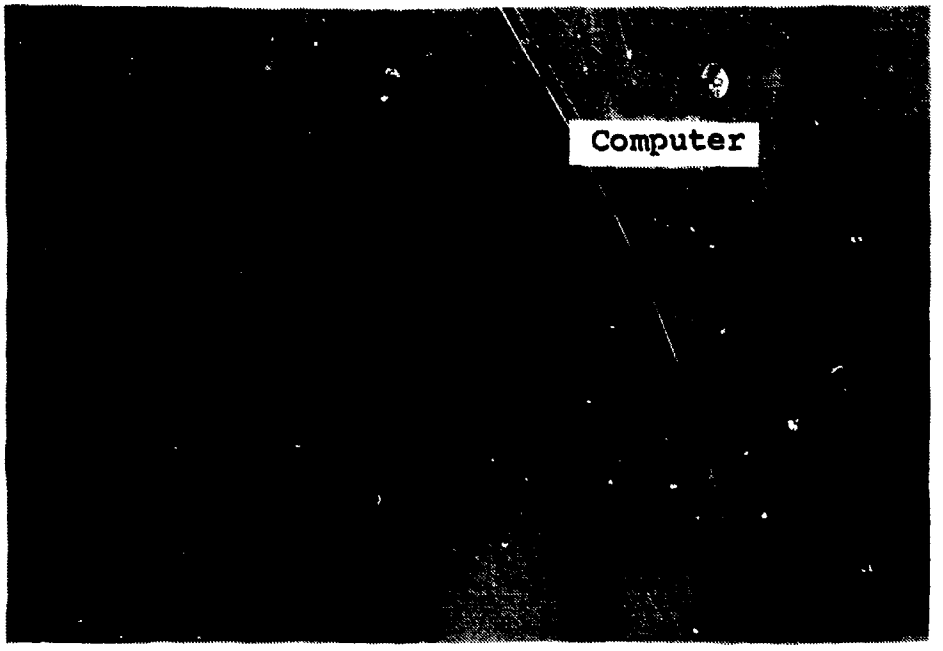

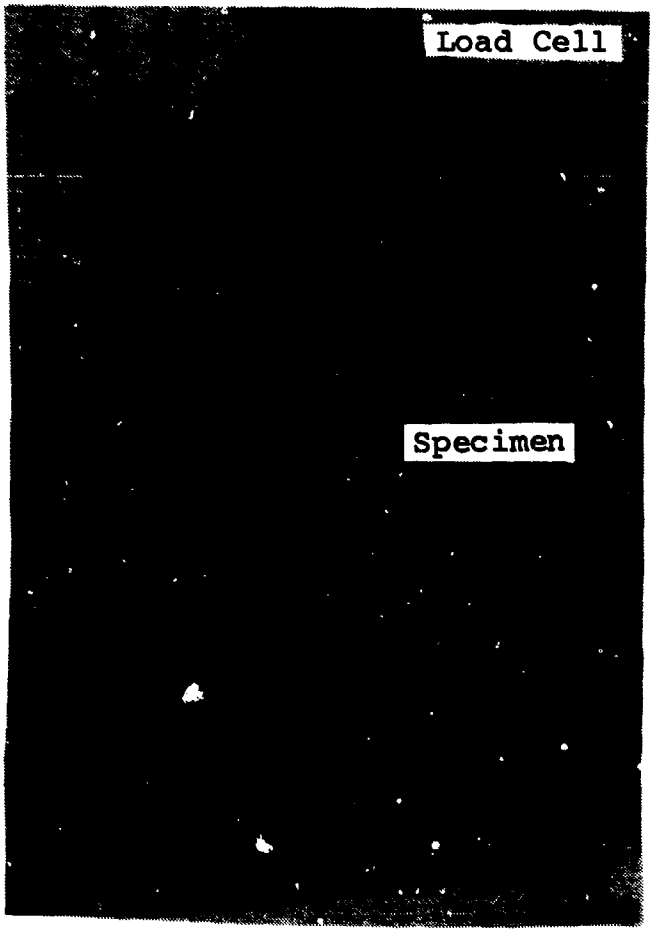

Figure 3.30. Test Set-up: Flatwise Tension.

TABLE 3.8

FLATWISE TENSION

Specimen ID	Failure Type	Failure Location	Ultimate Tensile Stress (psi)	Average Ultimate Tensile Stress, psi (Standard Deviation)
DT-1*	A	A,P	355	
DT-2	A	P	no data	
DT-3	A	A	437	
DT-4	A	A,P	396	392 (38.14)
DT-5	A	A,P	419	
DT-6	A	A	351	
ET-1*	C		398	
ET-2	C		278	
ET-3	C		265	307 (74.2)
ET-4	C		396	
ET-5	C		215	
ET-6	C		290	

Failure Type

A denotes adhesive failure
C denotes cohesive failure

Location

A - adhesive failure at acrylic interface
P - adhesive failure at polycarbonate interface

*Note: All specimen failures at silicone interlayer.

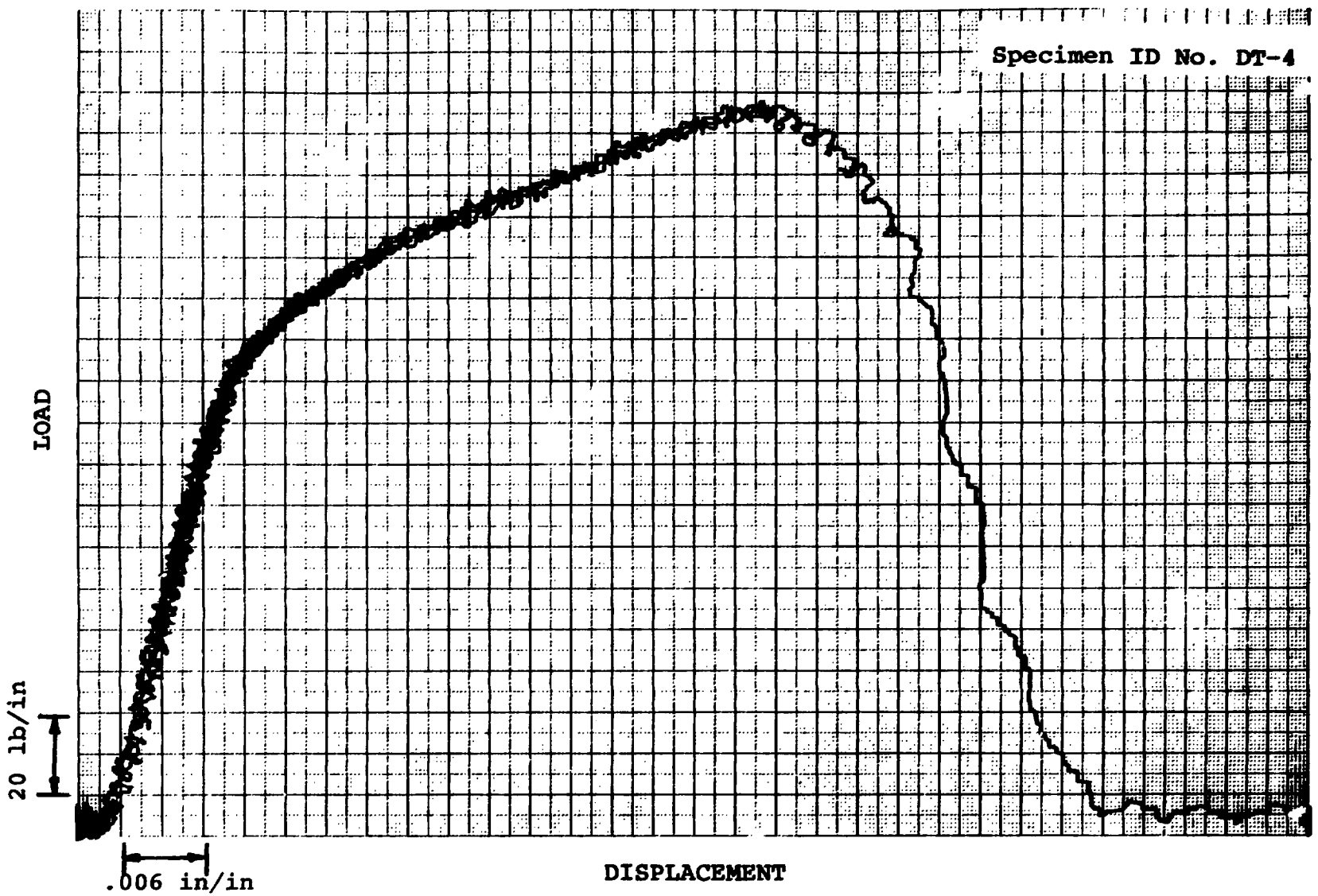

Figure 3.31. Typical Load vs. Displacement Plot, Flatwise Tension, F-16A Laminated Canopy.

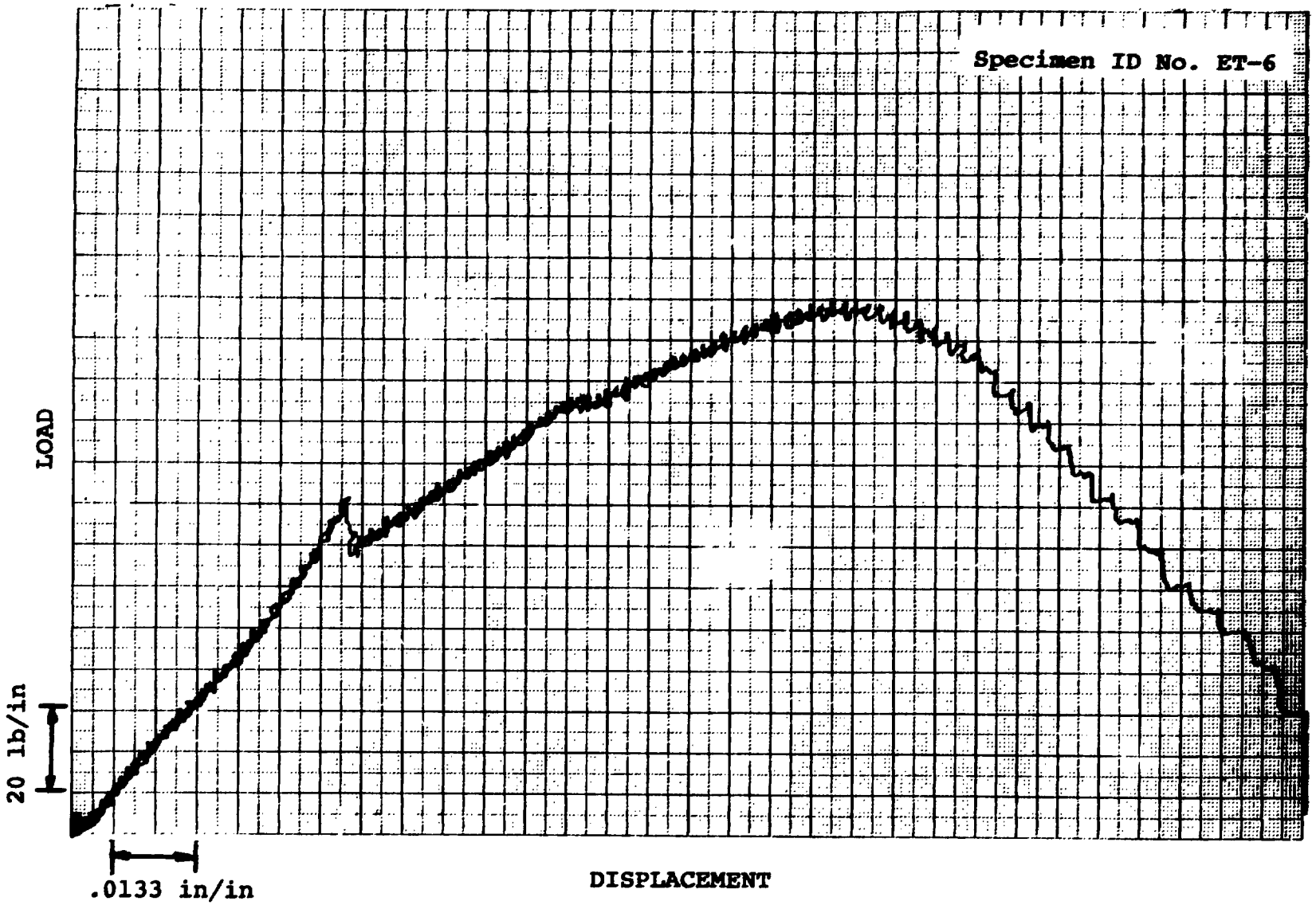

Figure 3.32. Typical Load vs. Displacement Plot, Flatwise Tension, F-111 Laminated ADBIRT Windshield.

tensile stress of 307 psi for the F-111. Compared to previous test results from the Reference 3 program conducted on flat sheet material, these values appear low; previous data showing 570 psi ultimate for the F-16. However, the Reference 3 program used a loading rate of 10,000 lbs/sec compared to 100 lbs/sec used for this testing program. The silicone is strain-rate sensitive, and at a higher strain rate can withstand a higher peak load. Both of these transparencies are manufactured by Sierracin; it is not obvious why the interlayer failures were differrent--adhesive at a higher strength for the F-16 laminated transparency and cohesive at a lower strength for the F-111 laminated transparency. Typical failed specimens are shown in Figure 3.33.

3.6.2 Torsional Shear

3.6.2.1 Specimen Configuration

Using ASTM D229-76 as a guideline, specimens were machined to the configuration as shown in Figure 3.34, having an annular test area of 0.245 sq. in.

3.6.2.2 Test Method

Torsional shear tests were conducted at an angular displacement rate of 10 degrees/minute, resulting in an equivalent average linear shear displacement rate (equivalent average linear shear displacement rate = average angular displacement rate x $(\pi/360)$ x $(r_i+r_o)/2$) of 0.055 in/min.

Specimens were tested by holding one surface ply stationary with an aluminum fixturing socket attached to the closed loop MTS system load cell and applying a torque to the other ply through a fixturing socket attached to the actuator (reference Figure 3.35).

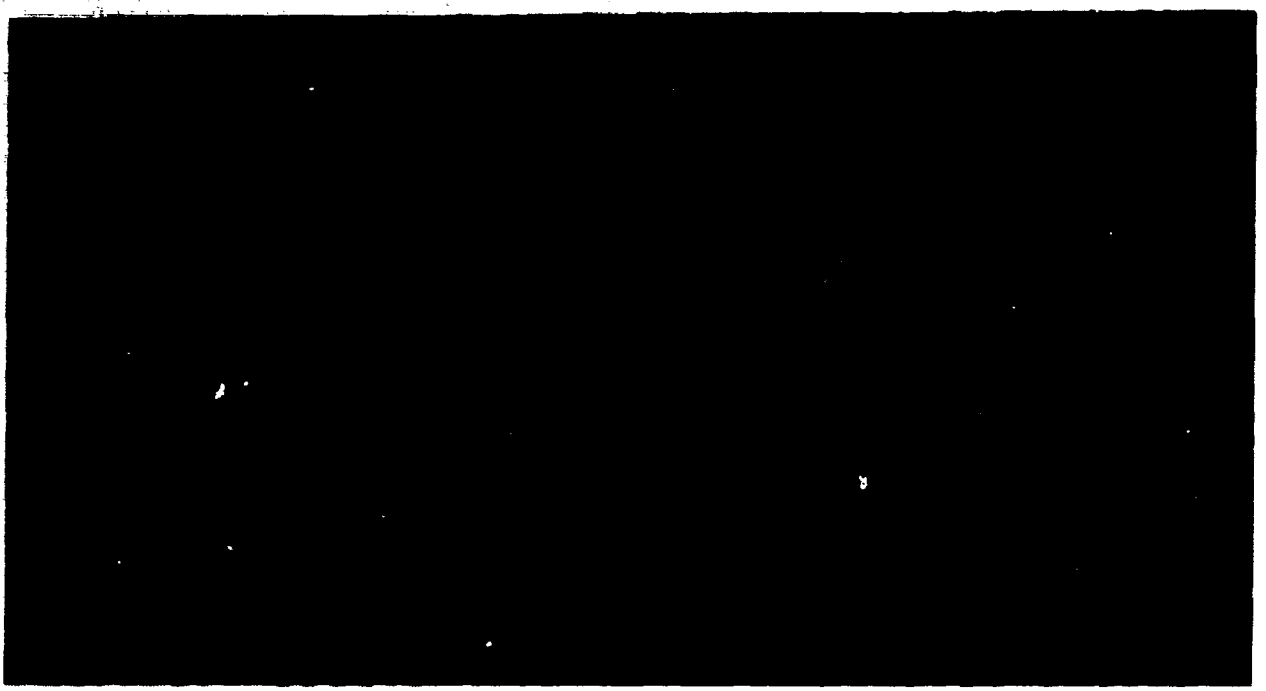

F-16A LAMINATED CANOPY

F-111 LAMINATED ADBIRT WINDSHIELD

Figure 3.33. Typical Failed Flatwise Tension Specimens.

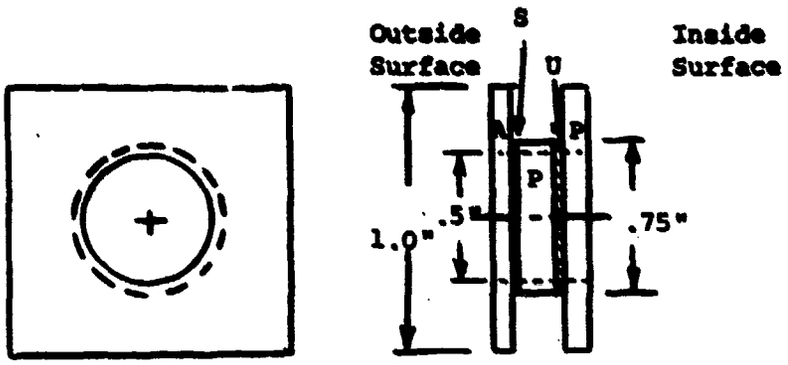

▨ - Tested Interlayer
(not to scale)

A = Acrylic
P = Polycarbonate
S = Silicone
U = Urethane

Figure 3.34. Modified Torsion Shear Specimen.

Figure 3.35. Torsional Shear Specimen Mounted in Test Machine.

3.6.2.3 Environmental Conditioning

Accelerated weathering in accordance with Paragraph 3.1.3.

3.6.2.4 Test Data

Table 3.9 presents the torsional shear data generated for both laminated transparency designs; typical load versus displacement curves being shown as Figures 3.36 and 3.37. The angular displacement was measured internal to the machine and represents the sum of the angular displacements in the fixture and specimen. Due to the relative stiffness of the fixture and the magnitude of the displacement, the measured angular displacement was representative of the actual interlayer displacement of laminated F-16A canopy and the sum of the interlayer displacements of the two tested interlayers in the F-111 ADBIRT transparency. Torque was measured with a load cell between the stationary fixturing socket and the machine frame, and was subject only to instrumentation-type errors which were considered negligible.

3.6.2.5 Data Analysis/Correlation

Failures occurred in the silicone interlayers for both the F-16 and F-111 laminated transparencies; at an average ultimate shear stress of 230 psi for the F-16 and 184 psi for the F-111. Compared to previous results from the Reference 3 program, conducted on flat sheet material, these values appear low; previous data showing 349 psi ultimate for the F-16. However, the Reference 3 torsional shear tests were run at an angular displacement rate of 500 °/sec, while for this test program torsional shear tests were run at 10 °/min. As noted before, the silicone is strain-rate sensitive and higher peak stress values would be expected at higher strain rates. Typical specimen failures are shown in Figure 3.38.

TABLE 3.9

TORSIONAL SHEAR DATA

Specimen ID	Failure Type	Failure Location	Angular Displacement (degrees)	Ultimate Shear Stress (psi)	Average Ultimate Shear Stress, psi (Standard Deviation)
DU-1	C,A	A	15.0	244.5	
DU-2	C		13.9	225.7	
DU-3	C		14.6	244.5	
DU-4	C,A	A	14.4	236.9	230.0 (22.82)
DU-5	C,A	A	14.6	184.3	
DU-6	C,A	A	16.5	252.0	
DU-7	C,A	A	15.5	221.9	
EU-1	C		36.3	206.9	
EU-2	C		32.3	184.3	
EU-3	C		34.5	225.7	184.3 (43.61)
EU-4	C		30.0	135.4	
EU-5	C		40.8	225.7	
EU-6	C		31.3	127.9	

Failure Type

A denotes adhesive failure
C denotes cohesive failure

Location

A - adhesive failure at acrylic interface

NOTE: All failures in silicone interlayer.

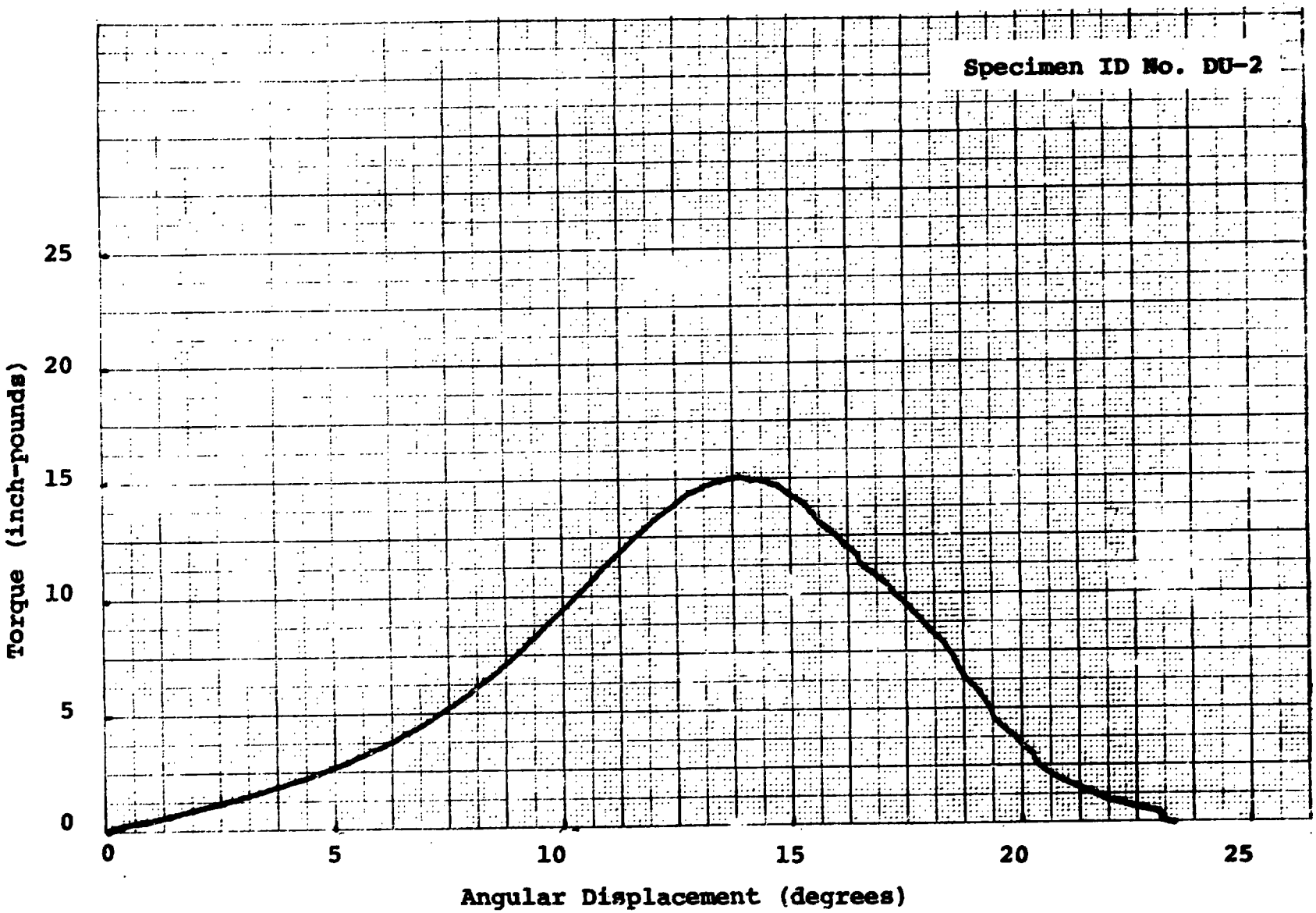

Figure 3.36. Typical Torque vs. Angular Displacement Plot, Torsional Shear, F-16A Laminated Canopy.

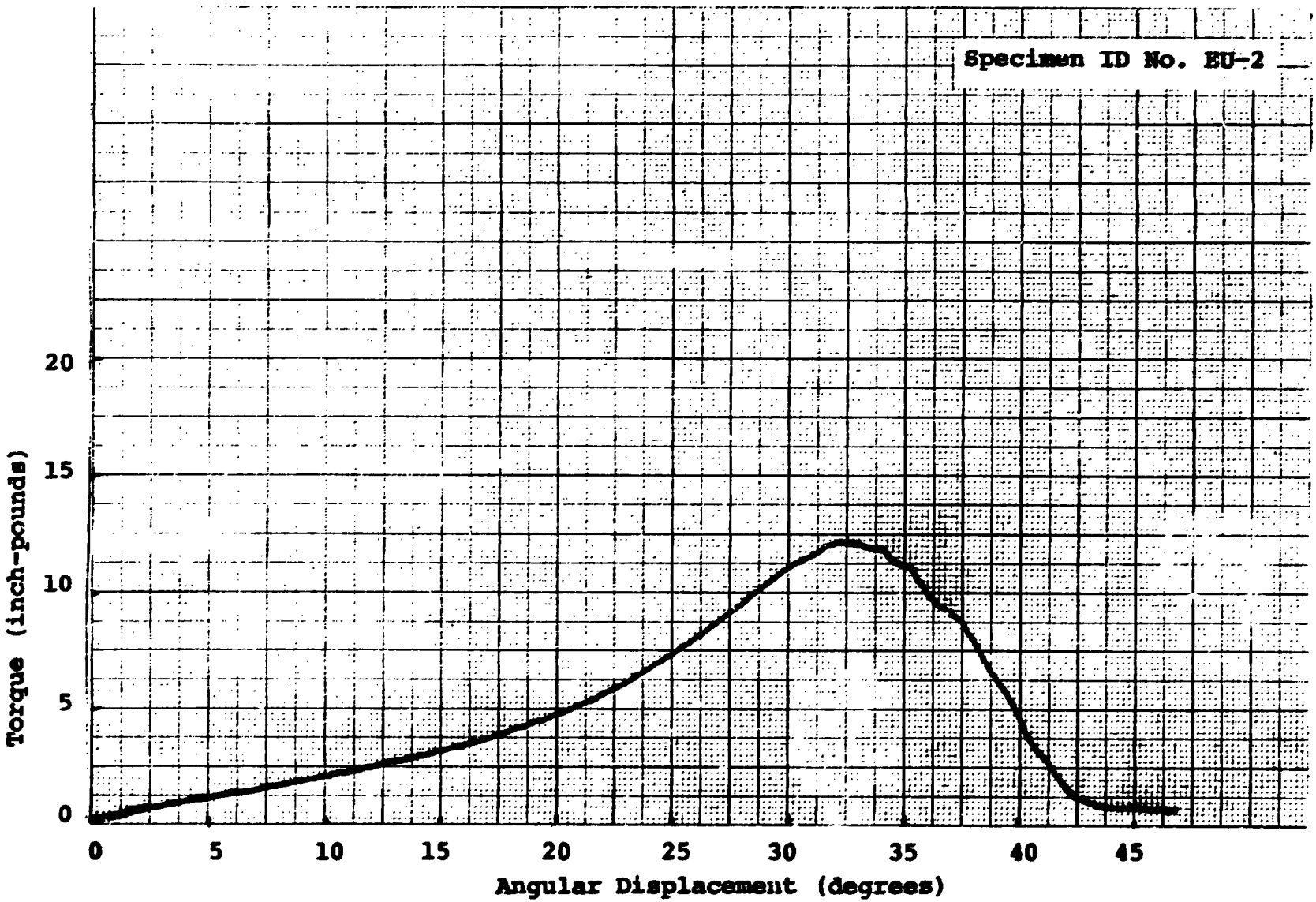

Figure 3.37. Typical Torque vs. Angular Displacement Plot, Torsional Shear, F-111 Laminated ADBIRT Windshield.

Figure 3.38. Typical Failed Torsional Shear Specimens.

3.6.3 Wedge Peel

3.6.3.1 Specimen Configuration

Using ASTM D3762-79 as a guideline, specimens and wedges were machined to the configuration shown in Figure 3.39. A slot, centered on the interlayers to be tested, was machined 1-3/16 inches into the end of each specimen. The specimens and aluminum wedges were sized to expand the stress gradient for various points of delamination so as to maximize the differences in the delamination lengths of the various materials.

3.6.3.2 Test Method

Wedge peel tests were conducted by inserting the wedge into the specimen slot, thereby causing delamination of the specimen along the interlayer. The wedges were inserted flush with the edge of each specimen. A fixture held the wedges in position for the duration of the test. The delamination length was measured at time intervals of 0.1, 1, 2, 4, 7, 12, 24, 48, 72, and 100 hours after insertion of the wedge.

3.6.3.3 Environmental Conditioning

Accelerated weathering in accordance with Paragraph 3.1.3.

3.6.3.4 Test Data

Table 3.10 presents the wedge peel test results generated for both laminated transparency designs. Plots of delamination length versus time are shown as Figures 3.40 and 3.41.

3.6.3.5 Data Analysis/Correlation

Test results from the wedge peel tests are inconsistent. The acrylic facing snapped off at the end of

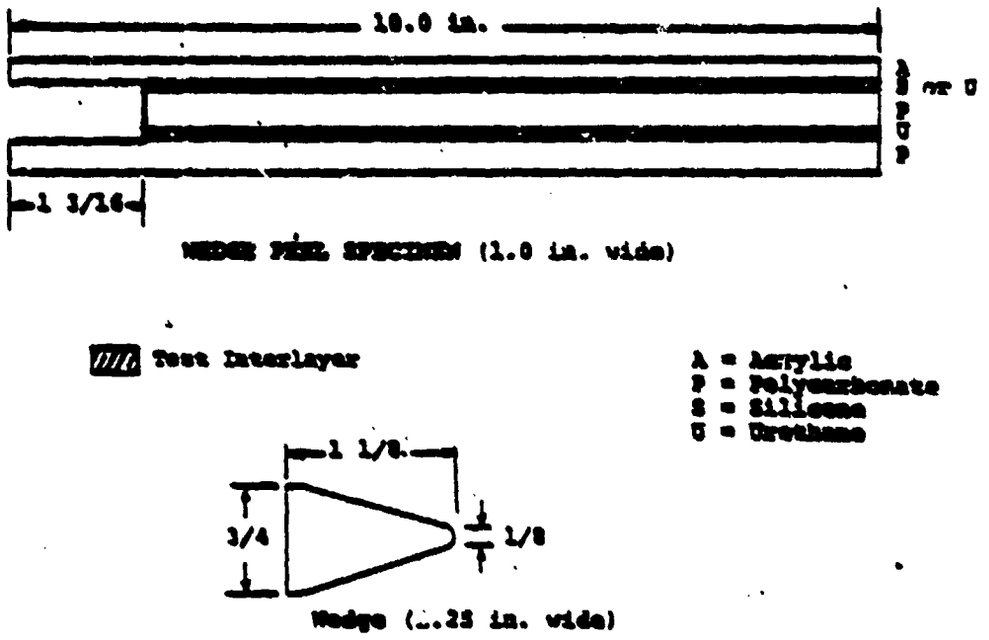

Figure 3.39. Modified Wedge Peel Specimen and Wedge Configuration.

TABLE 3.10

WEDGE PEEL RESULTS

TIME HOURS	SPECIMEN ID NO.	DV-1	DV-2*	DV-3*	DV-4	DV-5*	EV-1	EV-2*	EV-3	EV-4	EV-5
0		0			0		0		0	0	0
0.1		0			0.12		0.05		0	0	0.05
1		0.52			0.61		0.07		0.4	0	0.17
2		0.73			0.79		0.08		0.61	0	0.20
4		1.08			1.10		0.09		0.9	0	0.23
7		1.14			1.20		0.42		1.02	0	0.29
12		1.28			1.32		0.86		1.10	0.02	0.31
24		1.36			1.41		1.02		1.22	0.16	0.39
48		1.45			1.50		1.10		1.26	0.25	0.42
72		1.48			1.57		1.17		1.29	0.29	0.47
100		1.52			1.63		1.21		1.33	0.36	0.51

*Acrylic broke immediately after insertion of the wedge

Note: Delamination length in inches

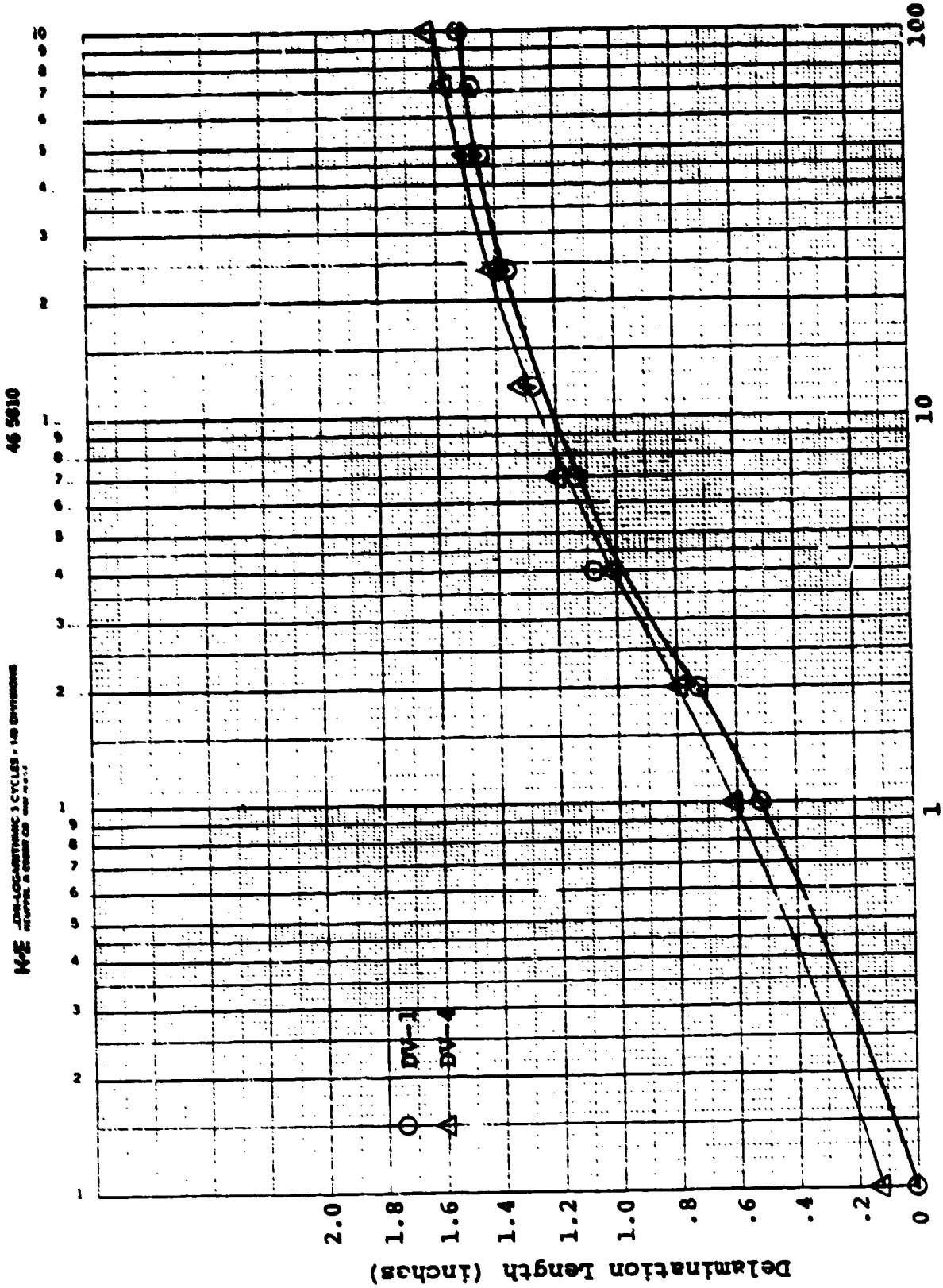

Figure 3.40. Summary of Wedge Peel Tests for F-16A Laminated Canopy

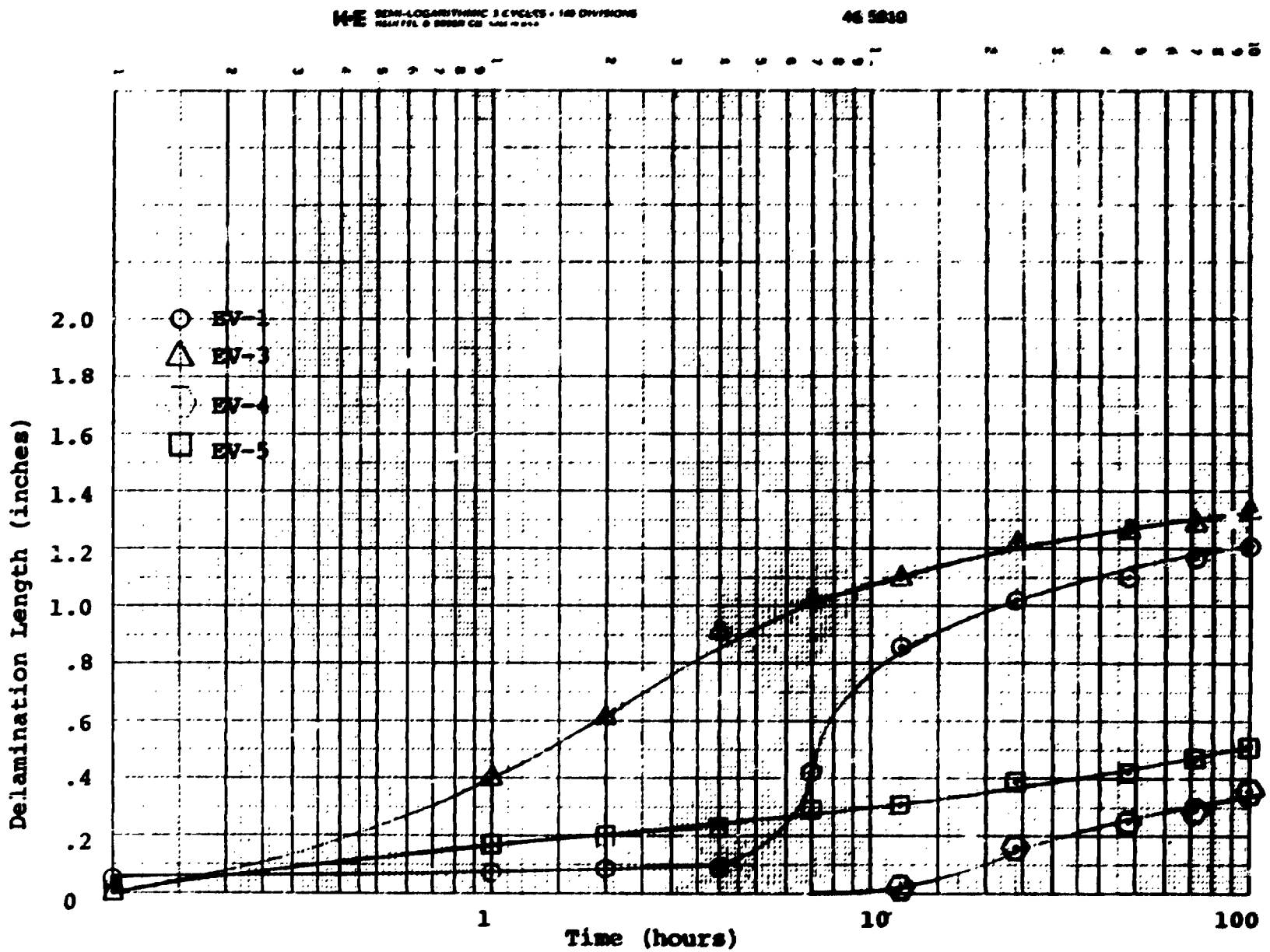

Figure 3.41. Summary of Wedge Peel Tests for F-111 ADBIRT Windshield.

the slot on three F-16 specimens and one F-111 specimen, all of which had been exposed, immediately upon insertion of the wedge. Two F-111 specimens experienced small, less than 0.6-inch, delamination along the silicone interlayer after 100 hours, while the remaining F-111 and F-16 specimens delaminated over 1-inch along the silicone interlayer after 100 hours. Delaminated wedge peel specimens are shown in Figures 3.42 and 3.43.

3.7 THERMAL SHOCK

3.7.1 Specimen Configuration

ASTM F520-77, Type B (2 X 2-inches as-received thickness).

3.7.2 Test Method

ASTM F520-77, Paragraph 7.5.3 and 7.6, and modified to include drying in partial vacuum during cold exposure. One coupon from each transparency design was screened to determine what pressure condition would be incorporated into the cold exposure cycle. Surface temperature versus time was recorded for atmospheric pressure and partial vacuum pressures of 3, 5, and 7 psig. There was no significant difference in the cool-down time for the three vacuum pressures. Thermal shock testing was then completed on 49 specimens from the five different transparencies. The test involved two cycles; each cycle consisted of a -65°F cold soak for 20 minutes in a cold box, immediately followed by a 20-minute soak in a 160°F oven. Twenty-four of the specimens were placed in vacuum bags maintained at a 5 psig partial vacuum during the cold soak. The other 25 specimens were also placed in vacuum bags for handling convenience during the testing, but were tested at atmospheric pressure.

3.7.3 Environmental Conditioning

Accelerated weathering in accordance with Paragraph 3.1.3.

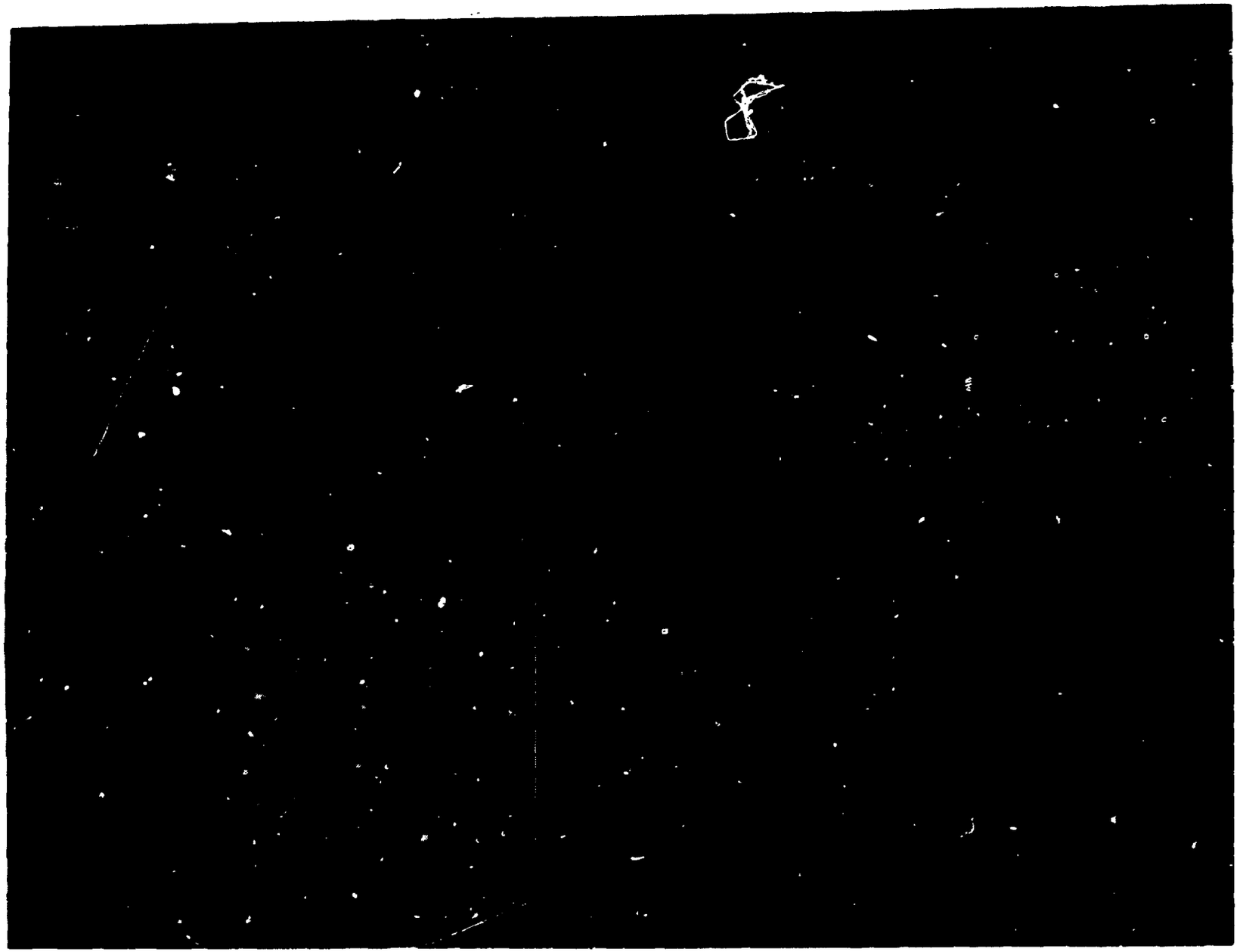

Figure 3.42. Typical Delaminated F-16A Wedge Peel Test Specimens.

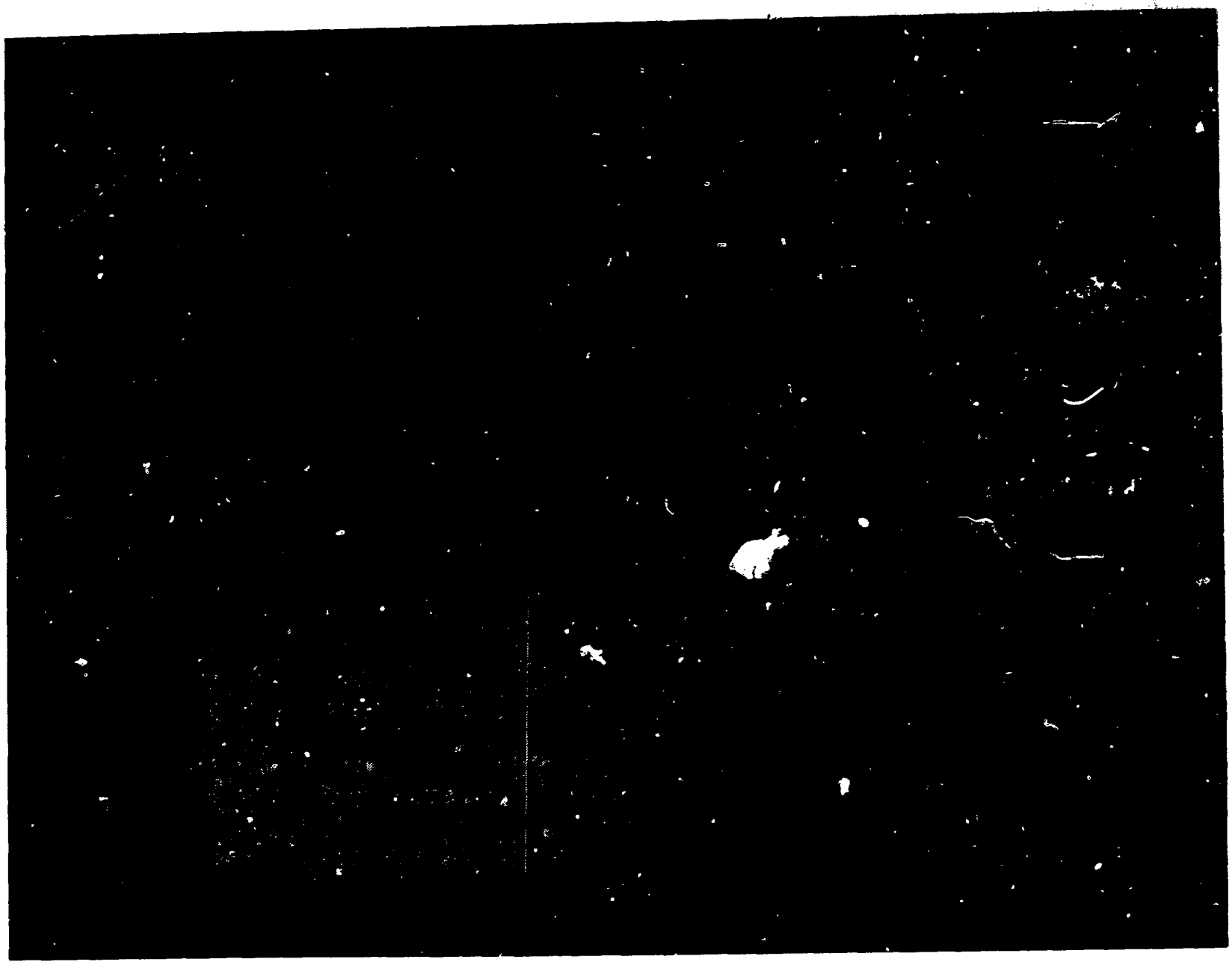

Figure 3.43. Typical Delaminated F-111 Wedge Peel Test Specimens.

3.7.4 Test Data

Table 3.11 presents the thermal shock test results for specimens taken from the five transparency designs.

3.7.5 Data Analysis/Correlation

Several of the F-15 monolithic stretched acrylic specimens showed surface fracturing at the corners of the specimens. This may have been caused by minor residual machining stresses at the corners of the specimens that were not removed by deburring, or the fracturing may have been caused by the residual stress inherent to stretched acrylic. Neither of the cast acrylic surface plies on the laminated specimens exhibited this behavior. These fractures probably would not accur in service because the fracturing was limited to specimen corners; in-service transparencies would not have this type of discontinuity. The sharp edges and corners could be rounded for future testing to avoid this problem and provide more characteristic test results. The coating on most of the F-16A coated monolithic polycarbonate specimens peeled in the vicinity of the engraved specimen numbers. This type of behavior would be expected around any surface flaw where coating delamination could be initiated. The F-16A laminated polycarbonate canopy specimens, which were tested in the vacuum, delaminated opposite the engraved surface; those specimens which were not in the vacuum showed no damage. Overall, the addition of a partial vacuum only affected this material type significantly; no discernable difference was evident for any of the other transparency designs. There was no significant visible damage to either of the laminated designs. Typical test coupons are shown in Figure 3.44 with several closeups shown in Figures 3.45 and 3.46.

TABLE 3.11

THERMAL SHOCK TEST RESULTS

Specimen Identification Number	Pressure (psig)	Results
AW-1	0	No visible damage
-2	0	
-3	0	Fracturing at corners
-4	0	
-5	0	No visible damage
-6	-5	Fracturing at edge
-7	-5	No visible damage
-8	-5	
-10	-5	
-11	-5	
BW-1	0	Fracturing at corners
-2	0	
-3	0	No visible damage
-4	-5	
-5	0	
-6	-5	
-7	-5	
-8	-5	
-10	-5	Fracturing at corners on bottom side
-11	0	No visible damage
CW-1	0	Coating degradation
-2	0	No further degradation after environmental conditioning

TABLE 3.11 (concluded)

Specimen Identification Number	Pressure (psig)	Results
-3	0	Coating degradation
-4	0	
-5	0	
-6	-5	
-7	-5	
-8	-5	
-10	-5	No further degradation after environmental conditioning
-11	-5	Coating degradation
DW-1	0	No visible damage
-2	-	Not tested
-3	0	No visible damage
-4	0	
-5	0	
-6	-5	Minor coating degradation with some pitting on polycarbonate
-7	-5	
-8	-5	
-10	-5	
-11	-5	
EW-1	0	No visible damage
-2	0	
-3	0	
-4	0	
-5	0	
-6	-5	
-7	-5	
-8	-5	
-10	-5	
-11	-5	

F-15 MONOLITHIC STRETCHED ACRYLIC WINDSHIELD

F-15 MONOLITHIC STRETCHED ACRYLIC CANOPY

F-16A COATED MONOLITHIC POLY-CARBONATE CANOPY

F-16A LAMINATED CANOPY

F-111 LAMINATED ADBIRT WINDSHIELD

Figure 3.44. Thermal Shock Specimens.

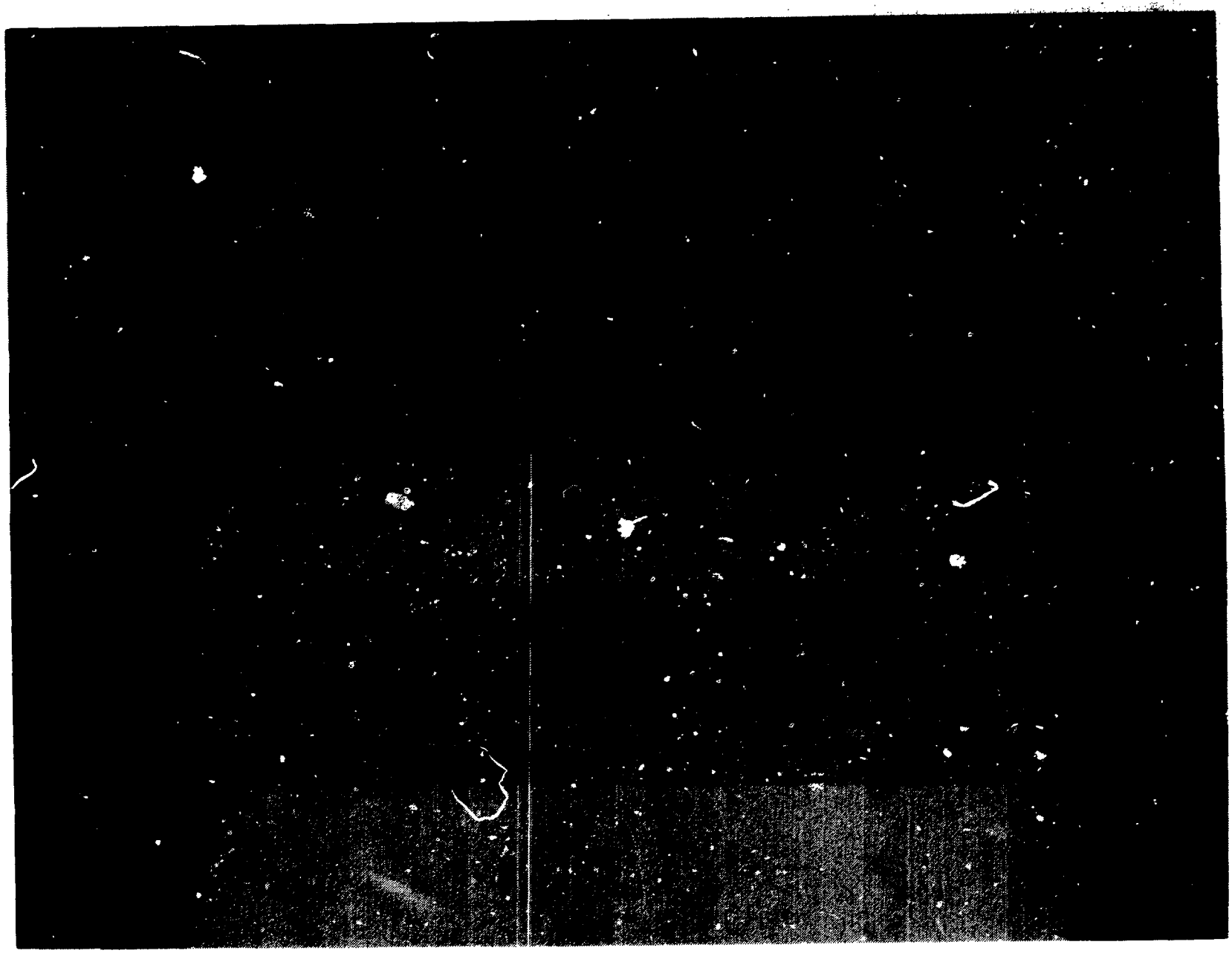

Figure 3.45. F-15 Canopy Specimen Showing Corner Fractures After Thermal Shock Testing.

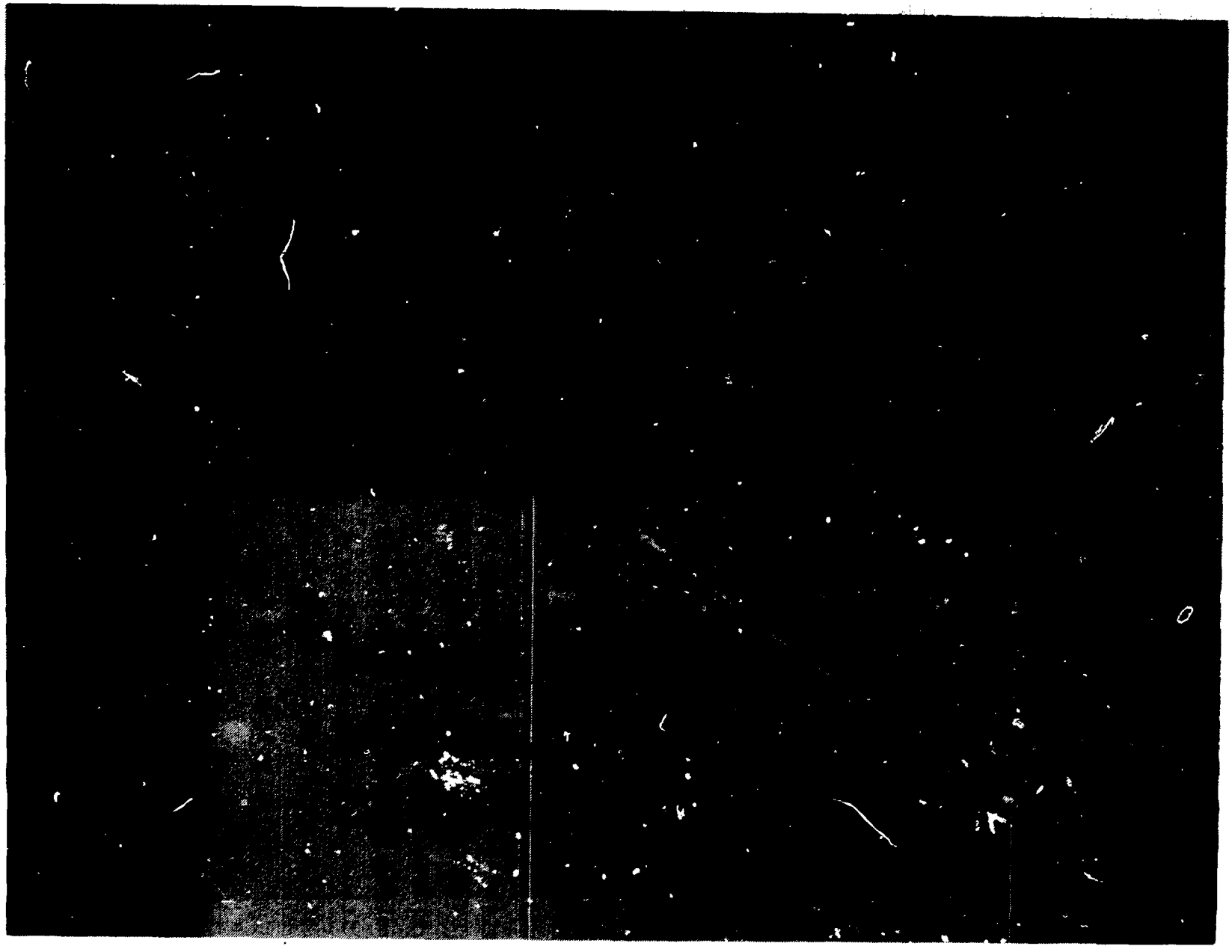

Figure 3.46. F-16A Monolithic Polycarbonate Canopy Showing Spotting and Coating Degradation After Thermal Shock Testing.

3.8 ABRASION RESISTANCE

3.8.1 In-Flight

3.8.1.1 Specimen Configuration

Three-inch square x as-received thickness.

3.8.1.2 Test Method

Measure haze before and after specified cycles of Q.U.V. exposure plus salt blast abrasion. Salt blast abrasion was conducted in accordance with the proposed ASTM Test Method, "Abrasion Resistance of Transparent Plastics and Coatings Using the Salt Impingement Method." Figure 3.47 shows the UDRI Salt Impingement Abrasion apparatus.

3.8.1.3 Environmental Conditioning

Accelerated weathering plus salt blast abrasion was conducted as follows: 168 hours of accelerated weathering in accordance with Paragraph 3.1.3 followed by a specified number of salt blast cycles x 1 = 1 equivalent year of in-flight exposure; x 2 = 2 equivalent years; x 3 = 3 equivalent years. Four different salt blast cycles were screened to determine the relative severity of the different cycles, and to determine a realistic number for simulation of actual conditions. The cycles were: 2 cycles after each year of equivalent weathering; 4 per year; 8 per year; and the proposed ASTM Standard Test Method of 2, 4, 8, 16, 25, 50, and 100 cumulative cycles per year with readings taken after each test.

3.8.1.4 Test Data

Table 3.12 presents the in-flight abrasion resistance test results based on accelerated weathering plus 2, 4, and 8 salt blasts per year of simulated service life. Test data generated per the proposed ASTM Test Method is presented as Appendix B.

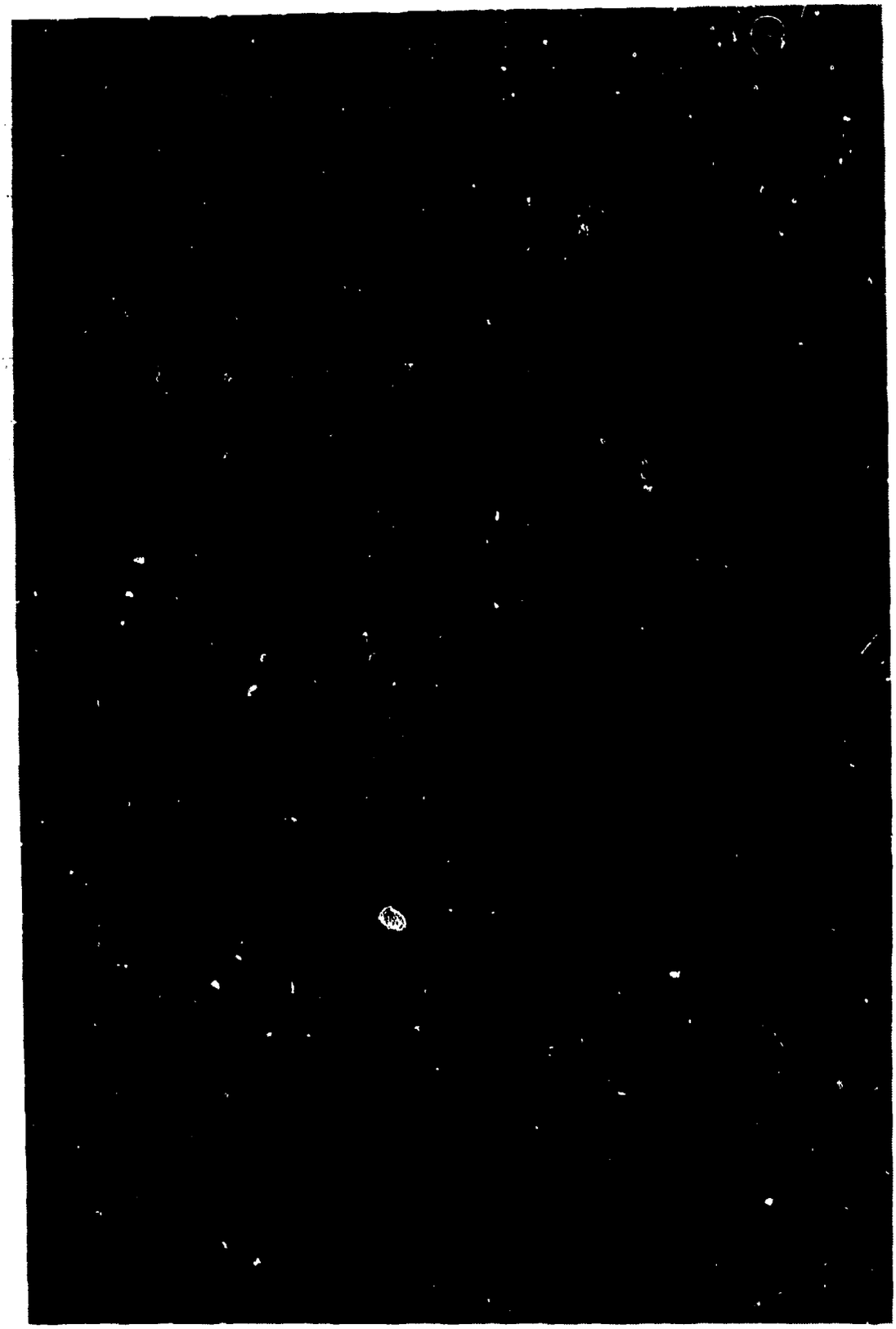

Figure 3.47. UDRI Salt Impingement Abrasion Apparatus.

TABLE 3.12

IN-FLIGHT ABRASION RESULTS

Specimen ID No.	No. of Years Exposure	No. of Salt Blasts (total)	Percent Haze		Percent Transmittance	
			Standard Deviation	Mean	Standard Deviation	Mean
AX-6	1	0	0.123	1.88	0.100	91.75
		2	0.177	2.43	0.096	91.63
	2	0	0.131	2.20	0.082	91.60
		2	0.116	2.42	0.082	91.50
	3	0	0.172	2.64	0.129	91.85
		2	0.187	2.81	0.141	91.60
AX-7	1	0	0.037	1.74	0.126	91.78
		4	0.539	2.86	0.096	91.53
	2	0	0.395	2.31	0.050	91.58
		4	0.573	2.96	0.126	91.48
	3	0	0.536	2.88	0.096	91.83
		4	0.504	3.51	0.082	91.40
AX-8	1	0	0.292	2.69	0.100	91.45
		8	0.738	4.82	0.096	91.23
	2	0	0.633	3.81	0.126	91.48
		8	0.793	4.89	0.082	91.10
	3	0	0.152	3.37	0.058	91.65
		8	0.579	4.62	0.082	91.30
BX-7	1	0	0.210	1.66	0.082	92.90
		2	0.531	2.49	0.082	92.90
	2	0	0.517	2.38	0.050	92.73
		2	0.593	2.88	0.050	92.73
	3	0	0.370	3.30	0.058	92.95
		2	0.200	3.48	0.058	92.85

TABLE 3.12 (continued)

Specimen ID No.	No. of Years Exposure	No. of Salt Blasts (total)	Percent Haze		Percent Transmittance	
			Standard Deviation	Mean	Standard Deviation	Mean
BX-8	1	0	1.132	2.15	0.058	92.85
		4	1.352	3.66	0.058	92.63
	2	0	1.286	3.21	0.050	92.68
		4	1.181	3.64	0.058	92.63
	3	0	1.089	3.41	0.050	92.83
		4	1.080	3.99	0.082	92.70
BX-9	1	0	0.267	1.64	0.050	92.88
		8	0.192	3.28	0.050	92.78
	2	0	0.266	2.88	0.082	92.70
		8	0.293	4.01	0.050	92.68
	3	0	0.395	3.04	0.000	92.90
		8	0.467	4.62	0.058	92.75
CX-6	1	0	0.503	3.90	0.222	87.88
		2	0.314	4.34	0.058	87.85
	2	0	0.956	6.29	0.126	87.53
		2	0.824	7.02	0.096	87.13
	3	0	1.652	17.38	1.025	82.75
		2	1.630	17.85	1.139	81.95
CX-7	1	0	0.715	3.00	0.163	88.00
		4	0.525	3.48	0.058	87.85
	2	0	1.859	5.93	0.096	87.38
		4	1.488	6.72	0.096	87.08
	3	0	2.278	15.85	1.080	83.60
		4	2.086	16.90	1.159	82.95

TABLE 3.12 (continued)

Specimen	No. of Years Exposure	No. of Salt Blasts (total)	Percent Haze		Percent Transmittance	
			Standard Deviation	Mean	Standard Deviation	Mean
CX-8	1	0	1.050	3.15	0.150	87.89
		8	0.673	4.02	0.058	87.75
	2	0	0.981	4.48	0.126	87.43
		8	1.212	5.74	0.183	87.10
	3	0	2.560	16.90	0.661	83.35
		8	1.603	20.33	0.678	82.40
DX-6	1	0	0.145	3.10	0.129	86.95
		2	0.186	3.62	0.096	86.83
	2	0	0.152	3.17	0.141	87.00
		2	0.062	3.48	0.126	86.98
	3	0	0.245	3.13	0.096	87.18
		2	0.246	3.34	0.058	87.05
DX-7	1	0	0.414	3.36	0.141	86.80
		4	0.637	4.04	0.126	86.63
	2	0	0.216	3.46	0.096	86.68
		4	0.189	3.78	0.129	86.65
	3	0	0.472	3.73	0.263	87.43
		4	0.097	4.78	0.171	86.93
DX-8	1	0	0.071	3.09	0.096	86.68
		8	0.117	4.18	0.096	86.58
	2	0	0.142	3.67	0.126	86.68
		8	0.217	4.32	0.082	86.60
	3	0	0.258	3.78	0.096	86.93
		8	0.179	4.55	0.058	86.85

TABLE 3.12 (concluded)

Specimen ID No.	No. of Years Exposure	No. of Salt Blasts (total)	Percent Haze		Percent Transmittance	
			Standard Deviation	Mean	Standard Deviation	Mean
EX-6	1	0	0.238	3.56	0.096	84.93
		2	0.201	4.64	0.082	84.90
	2	0	0.239	3.89	0.050	84.68
		2	0.218	4.08	0.100	84.65
	3	0	0.282	3.97	0.082	84.70
		2	0.119	4.23	0.050	84.68
EX-7	1	0	0.111	3.41	0.191	85.05
		4	0.158	3.88	0.129	84.95
	2	0	0.308	3.50	0.058	84.85
		4	0.227	3.84	0.100	84.75
	3	0	0.208	3.94	0.126	84.78
		4	0.221	4.26	0.096	84.73
EX-8	1	0	0.113	3.58	0.096	84.98
		8	0.148	4.82	0.096	84.78
	2	0	0.161	4.07	0.082	84.70
		8	0.242	4.41	0.050	84.58
	3	0	0.111	3.61	0.050	84.68
		8	0.135	4.56	0.050	84.58

3.8.1.5 Data Analysis/Correlation

The proposed acceptance criteria specifies that the percent haze shall not exceed 4%, 5%, and 6% after 1, 2, and 3 equivalent years of exposure (weathering plus abrasion), respectively. Only the F-16A coated monolithic polycarbonate specimens failed to satisfy the proposed acceptance criteria.

3.8.2 Flightline

3.8.2.1 Specimen Configuration

Four-inch square x as-received thickness.

3.8.2.2 Test Method

At 33-hour intervals, during the accelerated weathering exposure, the test samples were subjected to 50 normal cleaning operations using a solution of 1 part water to 1 part isopropyl alcohol with Kaydry disposable towels.

3.8.2.3 Environmental Conditioning

Accelerated weathering in accordance with Paragraph 3.1.3 plus cleaning at specified intervals.

3.8.2.4 Test Data

Table 3.13 presents the results for flightline abrasion resistance tests conducted on specimens taken from all five transparency designs.

3.8.2.5 Data Analysis/Correlation

After 1, 2, and 3 equivalent years of accelerated weathering plus normal cleaning operations, all coupons met the proposed acceptance criteria; namely, there was no visible damage to the specimens and the resultant haze did not exceed 4%. Figure 3.48 shows typical specimens after test.

TABLE 3.13

ABRASION RESISTANCE FLIGHTLINE RESULTS

Specimen ID Number	Equivalent Exposure (years)	Trans-mittance (%)	Average	Standard Deviation	Haze (%)	Average	Standard Deviation
AY-1	0	90.9			2.52		
-2		90.9			2.47		
-3		91.2	91.0	0.277	2.38	2.49	0.220
-4		90.7			2.84		
-5		91.4			2.25		
AY-1	1	91.2			2.31		
-2		91.2			2.16		
-3		91.1	91.1	0.164	0.21	1.61	1.356
-4		91.1			0.16		
-5		90.8			3.19		
AY-1	2	91.0			2.62		
-2		90.8			2.45		
-3		91.1	91.0	0.270	1.52	2.53	0.739
-4		91.3			2.46		
-5		90.6			3.60		
AY-1	3	90.9			2.83		
-2		90.8			2.57		
-3		91.3	91.0	0.259	1.68	2.44	0.748
-4		91.3			1.70		
-5		90.8			3.41		
BY-1	0	92.2			2.63		
-2		92.1			2.71		
-3		91.9	92.1	0.137	3.75	2.90	0.507
-4		92.2			3.22		
-5		92.3			2.77		
-6		92.1			2.32		

TABLE 3.13 (continued)

Specimen ID Number	Equivalent Exposure (years)	Trans-mittance (%)	Average	Standard Deviation	Haze (%)	Average	Standard Deviation
BY-1	1	91.9			1.43		
-2		90.7			1.75		
-3		91.6	91.6	0.469	2.48	1.90	0.347
-4		91.6			1.98		
-5		91.8			1.80		
-6		92.0			1.98		
BY-1	2	91.8			1.51		
-2		91.8			1.97		
-3		91.8	91.8	0.122	1.99	1.70	0.356
-4		91.8			1.31		
-5		91.5			2.10		
-6		91.8			1.34		
BY-1	3	92.5			1.82		
-2		92.4			1.12		
-3		92.5	92.3	0.423	2.23	1.84	0.438
-4		92.4			1.75		
-5		91.4			2.36		
-6		92.3			1.75		
CY-1	0	88.5			2.42		
-2		87.8			1.88		
-3		88.0	88.0	0.311	2.60	2.33	0.284
-4		87.7			2.23		
-5		88.1			2.50		
CY-1	1	87.5			1.59		
-2		87.2			2.33		
-3		87.0	87.36	0.270	1.89	2.23	0.332
-4		87.7			3.12		
-5		87.4			2.20		

TABLE 3.13 (continued)

Specimen ID Number	Equivalent Exposure (years)	Trans-mittance (%)	Average	Standard Deviation	Haze (%)	Average	Standard Deviation
CY-1	2	87.1			2.16		
-2		87.1			2.54		
-3		87.0	87.0	0.173	1.98	2.64	0.822
-4		86.7			4.05		
-5		87.1			2.45		
CY-1	3	86.9			2.25		
-2		86.8			2.64		
-3		86.6	86.2	1.324	2.28	3.61	2.61
-4		83.8			3.27		
-5		86.7			2.59		
DY-1	0	87.2			3.21		
-2		87.2			2.65		
-3		87.2	87.2	0.071	2.74	2.88	0.322
-4		87.1			3.25		
-5		87.3			2.57		
DY-1	1	86.9			2.91		
-2		87.2			2.97		
-3		87.1	87.0	0.114	3.08	2.94	0.089
-4		87.0			2.85		
-5		87.0			2.89		
DY-1	2	86.7			3.15		
-2		87.0			3.07		
-3		87.1	86.9	0.158	3.25	3.14	0.097
-4		86.8			3.01		
-5		86.9			3.20		

TABLE 3.13 (concluded)

Specimen ID Number	Equivalent Exposure (years)	Transmittance (%)	Average	Standard Deviation	Haze (%)	Average	Standard Deviation
DY-1	3	86.5			3.31		
-2		86.9			3.32		
-3		86.9	86.7	0.179	3.45	3.37	0.108
-4		86.6			3.26		
-5		86.7			3.52		
EY-1	0	88.2			2.71		
-2		86.2			2.83		
-3		86.6	87.0	0.750	2.91	2.83	0.074
-4		87.0			2.86		
-5		86.9			2.85		
EY-1	1	87.9			3.13		
-2		86.0			3.28		
-3		86.4	86.7	0.712	3.36	3.26	0.083
-4		86.7			3.28		
-5		86.6			3.25		
EY-1	2	87.5			3.61		
-2		86.0			3.38		
-3		86.2	86.5	0.581	3.45	3.45	0.095
-4		86.5			3.38		
-5		86.4			3.42		
EY-1	3	87.0			3.72		
-2		85.7			3.56		
-3		86.0	86.2	0.495	3.68	3.62	0.083
-4		86.3			3.52		
-5		86.0			3.60		

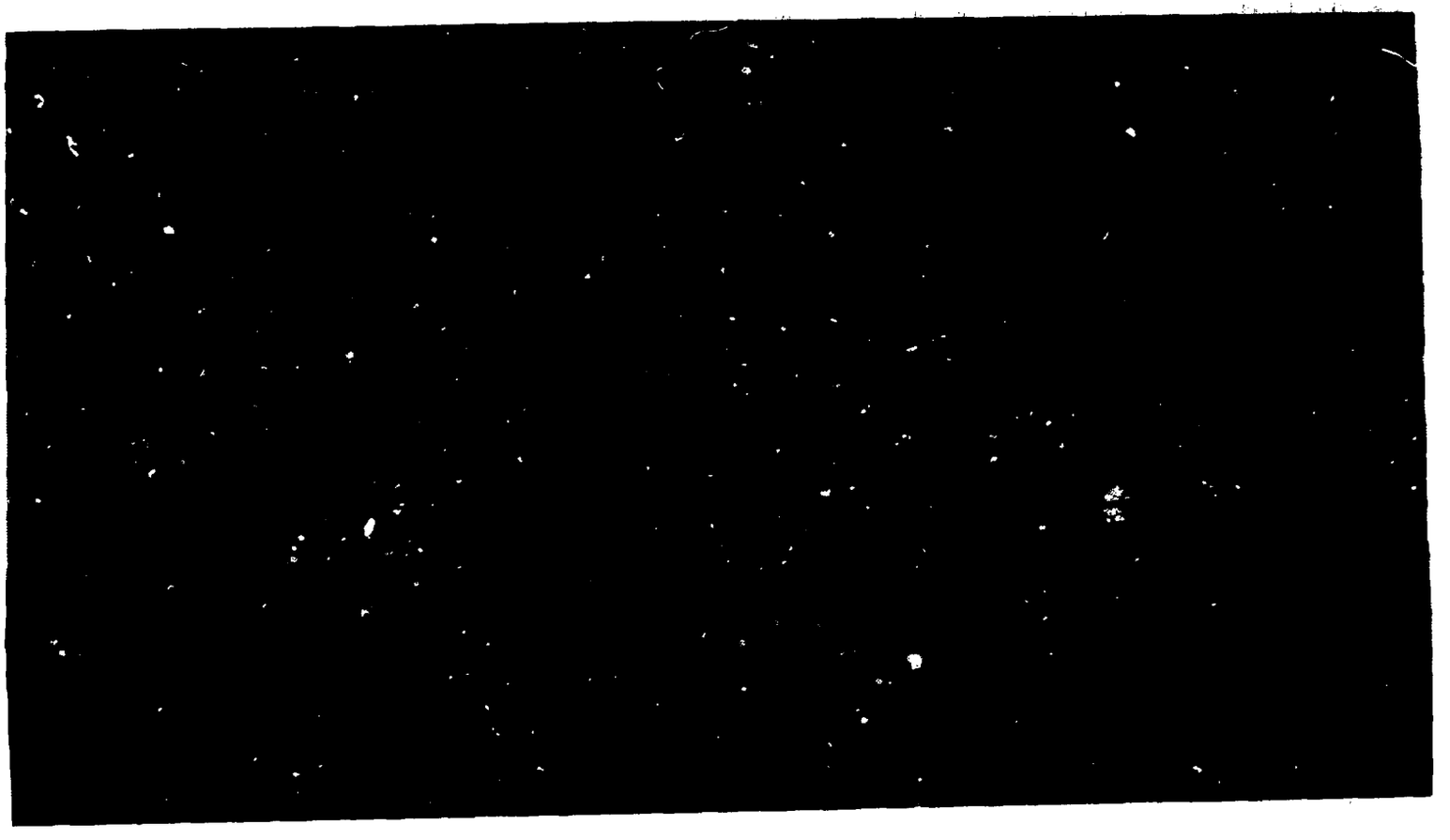

Figure 3.48. Typical Flightline Abrasion Resistance Tested Specimens.

3.9 EDGE ATTACHMENT

3.9.1 Specimen Configuration

Three-inch wide by approximately 15-inch long by as-received thickness flexure beams were cut from the transparencies so as to pick up the actual edge attachment holes in an area that minimized curvature along the beam length. Because of material limitations, specimens were cut from different edges as shown in Figures 2.2 through 2.16.

3.9.2 Test Method

The edge attachment beams were tested with the fastener end mounted in a fixture which simulated the edge fixity and attachments of the actual transparency design; the other end of the beam being simply supported. Beams were loaded at a displacement rate of 2,000 in/min using the high performance electrohydraulic closed loop MTS test machine, with the loading nose at the third point of the span (measured from the fixed end). This location was chosen to increase the shear at the fixed end (reference Figure 3.49 for test setup). The span of the beam and load location influences the magnitude of the combined tension, shear, and bending moment at the edge attachment and, therefore, can affect the failure load and/or failure mode. Three unexposed baseline beams from each of the transparencies, 9, 12, and 15 inches in length, were tested to assess possible sensitivities of beam span to the test results.

For all tests, load versus displacement data was stored in the digital memory of a transient recorder and played back at reduced speed on an X-Y recorder. Failure information for the baseline screening tests is presented in Table 3.14. Edge attachment failure modes were comparable for the different span lengths. A span length of 9 inches was chosen to minimize the effects of the severe curvature of the beams along with limitations on material availability. The shorter beams

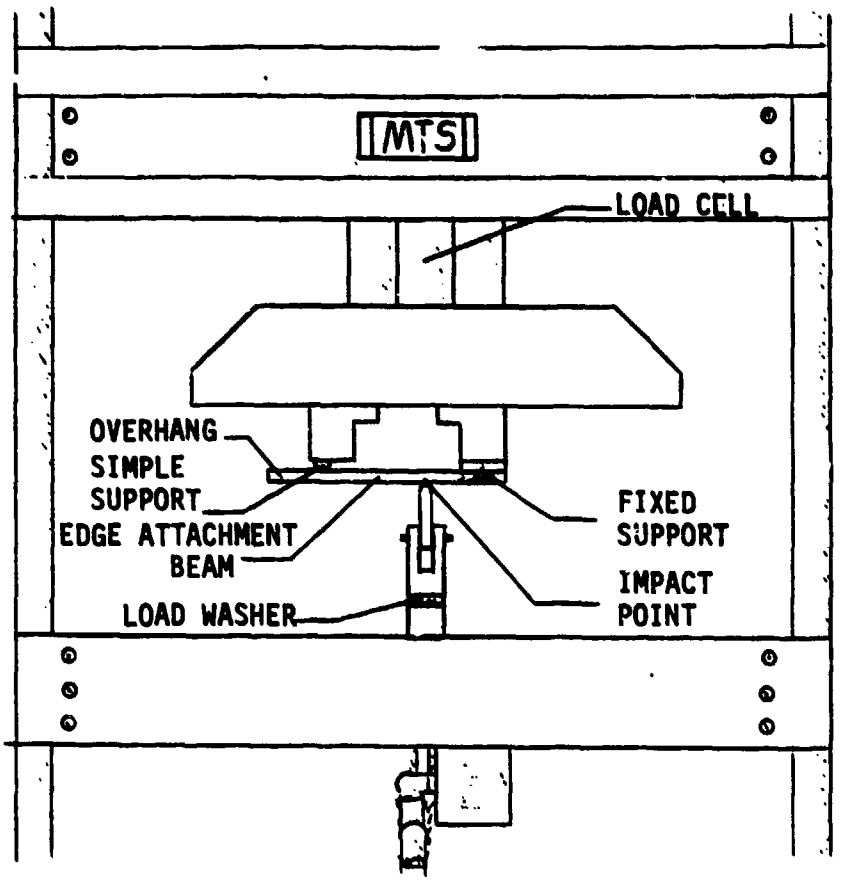

Figure 3.49. Edge Attachment Test Set-up.

BASE OF EDGE ATTACHMENT LENGTH EVALUATION

Specimen ID Number	Nominal Length (inches)	True Span (inches)	Peak Load (pounds)	Energy (ft-lbs)	Actual Loading Rate (in/min)	Failure Mode	Notes
AZ-1	9	6	5,900	47.7	825	BF	Brittle failure at impact point combined bending & torsion; threads on one bolt sheared
-2	12	8.5	>5,000	76.1	658	BF	" "
-3	15	11.5	>5,000	119.9	1547	BF	" "
BZ-1	9	6	1,300	12.9	2269	BF	Brittle failure at fixed support
-2	12	8.5	900	22.5	1850	BF	" "
-3	15	11.5	613	37.6	2092	BF	Brittle failure at support and impact point
CZ-1	9	6	5,400	517.5	2127	DF	Threads on one bolt sheared
-2	12	8.5	3,900	513.2	1668	DF	Threads on one bolt sheared; one insert partially pulled through
-3	15	11.5	2,525	1230.5	2042	D	Bolt elongation at failure threshold
DZ-1	9	6	4,575	392.5	1396	DF	Bolt elongation, inserts partially pulled through
-2	12	8.5	3,625	400.8	1745	DF	" "
-3	15	11.5	2,575	1080.	1890	D	" "
EZ-1	9	6	3,325	925.	1701	D	Inserts partially pulled through, threads on one bolt sheared
-2	12	8.5	2,850	589.2	2025	D	Inserts partially pulled through
-3	15	11.5	1,700	383.3	2025	D	Threads on one bolt sheared, other insert partially pulled through

DF denotes ductile failure (of tension surface)
BF denotes brittle failure
D denotes ductile deformation below threshold of failure

developed the highest peak loads, but because of the short spans and consequent high stiffness, the proposed loading rate of 2,000 in/min was not achieved for all of the specimens. An aluminum fixture was designed and fabricated to induce stress in the edge attachments of the beams during environmental conditioning to simulate service conditions. Due to material limitations, only 9 specimens from the F-15 canopy, 6 specimens from the coated polycarbonate F-16A canopy, and 8 specimens from the laminated F-16A canopy were available. These specimens were machined to 9 inches long, with specimen width chosen such that two fasteners would be located symmetrically on each specimen end. Two or three coupons from each design were then environmentally conditioned with stress for 1, 2, and 3 equivalent years and tested in the same manner as the baseline beams.

3.9.3 Environmental Conditioning

Three baseline beams were unexposed. In addition, three beams were exposed to 1 equivalent year of accelerated weathering under stress in accordance with Paragraph 3.3.3; similarly, three beams were exposed for 2 equivalent years, and three beams exposed for 3 equivalent years.

3.9.4 Test Data

Table 3.15 presents the results of edge attachment tests for the exposed specimens. Table 3.16 presents the comparison between baseline and environmentally conditioned edge attachment beams.

3.9.5 Data Analysis/Correlation

The edge attachment beams behaved in a manner similar to standard impact beams. Except for the laminated F-16A canopy, degradation did not appear to be significantly different than that experienced with MTS beams, nor did the edge attachments negatively influence the failure strength. The F-16A laminated canopy specimens did show a significant decrease in strength after environmental conditioning; however, this decrease

TABLE 3.15

ENVIRONMENTALLY CONDITIONED EDGE ATTACHMENT RESULTS[1]

Specimen ID No.	Equivalent Exposure (years)	Peak Load (pounds)	Energy (ft-lbs)	Average Energy (ft-lbs)	Failure[2] Mode	Notes
BE-11		1090	10.7		BF[3]	Cracks in the acrylic between
-12	1.13[4]	1000	9.6	15.1	BF	fiberglass sandwich at the fixed end prior to test
-13		1670	24.9		BF	No cracks before test
BE-14		1470	17.6		BF	No cracks before test
-15	2	920	7.2	12.1	BF	No cracks before test
-16		1100	11.6		BF	No cracks before test
BE-17		1480	17.1		BF	No cracks before test
-18	3	900	11.2	13.1	BF	No cracks before test
-19		1300	10.9		BF	No cracks before test
CE-1		5873	458.5		DF	Threads of both bolts sheared
-2	1.13	6662	591.7	525.1	DF	Threads of both bolts sheared
CE-3		6271	609.9		DF	Bolt threads sheared; insert
	2			671.7		pulled partially through
-4		6988	733.5		DF	Threads of both bolts sheared
CE-5		6811	811.4		DF	Threads of both bolts sheared
-6	3	5965	742.8	777.1	D	Bolts failed
DE-1		3830	303.5		DF	Both inserts pulled partially through
-2	1.13	43.92	380.9	333.2	DF	Both inserts pulled partially through
-3		4505	315.3		DF	Both inserts pulled partially through
DE-4		3840	384.7		DF	Both inserts pulled partially through
	2			313.3		
-5		4091	331.9		DF	Both inserts pulled partially through
DE-6		3600	345.3		DF	Both inserts pulled partially through
-7	3	4046	255.9	244.3	DF	Bolt threads sheared; insert pulled partially through
-8		3213	131.7		BF	Embrittled; both inserts pulled partially through

NOTES:

1 Nominal length of beams was 9"; the span equal to 6"; peak load, energy, and average energy values were normalized to a 3" specimen width.

Nominal loading rate of 2,000 in/min--actual loading rate not significantly different.

2 Failure modes: BF denotes brittle failure; DF denotes ductile failure (of tensile surface); D denotes ductile deformation below threshold of failure.

3 All "B" specimens failed at the fixed support at the fiberglass/acrylic surface boundary. All other specimens failed at the location of the loading nose.

4 All one-year specimens were actually exposed to 1 week and 21.5 hours of artificial weathering, equal to one year and 6.7 weeks of natural weathering.

TABLE 3.16

COMPARISON OF BASELINE AND ENVIRONMENTALLY CONDITIONED EDGE ATTACHMENT BEAMS

	BASELINE	EXPOSED		
Specimen I.D. No.	Energy (ft-lbs)	Equivalent Exposure (years)	Energy (ft-lbs)	Percent Change
BZ	12.9	1.13	15.1	+17
		2	12.1	- 6
		3	13.1	+ 2
CZ	517.5	1.13	525.1	+ 1
		2	671.7	+30
		3	777.1	+50
DZ	392.5	1.13	333.2	-15
		2	313.3	-20
		3	244.3	-38

is not necessarily related to edge attachment degradation. No visual difference could be discerned between the baseline and the exposed failure modes at the edge attachment; although, at the impact point, the polycarbonate was noticeably embrittled on at least one of the specimens which had 3 years of equivalent exposure (see Table 3.15, specimen DZ-8). The F-15 monolithic stretched acrylic canopy specimens developed closed cracks parallel to the inner and outer acrylic surface planes at the fixed end between the fiberglass sandwich during environmental conditioning plus stress. These cracks did not extend into the optical portion of the specimens and consequently could only be seen from the edge or the end view. Only one specimen (see Table 3.15, specimen BZ-13) did not develop this cracking; significantly, this specimen was exposed for only 1 equivalent year and it also had the highest energy absorption. Even with this cracking in the acrylic at the edge attachment, the specimens showed no degradation of strength compared to the baseline test. As would be expected, the coated monolithic polycarbonate F-16A canopies developed increased failure strength as more of the coating was removed by environmental conditioning, and no edge degradation or influence on failure was noted.

SECTION 4
EVALUATION OF EXISTING TEST METHODOLOGY

The durability evaluation of monolithic stretched acrylic, coated monolithic polycarbonate, and acrylic faced/polycarbonate laminated transparencies is highly dependent on a realistic accelerated weathering exposure.

For this purpose, accelerated weathering has been simulated using QUV, 120°F, 7 hour UV/5 hour condensation cycles with 168 hours run time equaling 1 equivalent year of in-service experience. Several tests used this accelerated weathering condition in combination with other parameters such as salt blast abrasion, induced stress, and normal cleaning cycles. After subjecting all material types to 3 equivalent years of the specified accelerated weathering, surface craze and haze were extreme; degradation being far in excess of proposed acceptance criteria. However, after introducing cleaning cycles into the accelerated weathering exposure condition to simulate flightline abrasion, no haze readings exceeded 4 percent after 3 equivalent years. The accelerated weathering exposure alone appears too severe; the accelerated weathering exposure combined with normal cleaning cycles appears to be representative of in-service usage.

An unexpected test result involved optical degradation of the transparency specimens. Specimens subjected only to artificial weathering (haze and transmittance, Table 3.2) showed much greater optical deterioration than the specimens which were tested for flightline abrasion resistance. The flightline specimens, which were cleaned after every 21 hours of artificial weathering (cleaning consisted of 50 cleaning operations with a 50/50 solution of water and isopropyl alcohol; see Section 3.8.2) experienced minimal deterioration in optical quality. All of the in-flight specimens except for the coated polycarbonate F-16A canopy which were subjected to 2, 4, and 8 cycles of salt blast

after each equivalent year of weathering (see Section 3.8.1) also maintained relatively good optical quality; the percent haze remained less than 5%. The percent haze for the coated polycarbonate stayed relatively low for the first 2 years of artificial weathering; however, apparently after the second year the coating seriously deteriorated, allowing moisture and UV light to directly attack the polycarbonate, seriously degrading the surface. The haze and transmittance specimens, which were only cleaned per ASTM specification FTM406, Method 3023 after each equivalent year of weathering before haze and transmittance readings were taken, were expected to show the least deterioration in optical quality. This, as noted, did not prove true. Apparently some type of surface degradation or film builds up on the specimens during QUV exposure, while cleaning or salt blasting removes this surface condition. Two possible explanations of the cause of surface irregularities on the haze and transmittance specimens are that a film buildup of minerals or impurities from the condensation in the QUV (Note: supposedly the condensation purifies the water so that this is impossible), or a breakdown in the surface molecular structure caused by UV light reacting with the long-chain polymers at the transparency surface. Because the exact nature of this surface condition was not known or understood to determine if it was removable by cleaning, the tested haze and transmittance specimens were recleaned per the ASTM specification, and haze and transmittance readings were again taken. The specimens were subjected to the flightline cleaning method of 50 cleaning operations, and then haze and transmittance readings were taken again. The resultant haze readings, presented in Table 4.1, were reduced for the monolithic specimens, stretched acrylic, and coated polycarbonate. The laminates showed little change. The haze and transmittance specimens were given another cycle of 50 cleanings to determine whether the reduction in haze and increase in transmittance achieved by cleaning the specimens was a one-time result of cleaning, or if further optical improvement could be accomplished

TABLE 4.1

HAZE AND TRANSMITTANCE SPECIMENS, 1st FLIGHTLINE CLEANING

Specimen I.D. No.	Before 50 Cleaning Cycles		After 50 Cleaning Cycles	
	Percent Haze	Transmittance	Percent Haze	Transmittance
AP-1	2.57	91.7	2.04	91.8
AP-2	2.22	91.7	1.96	91.8
AP-3	4.09	91.6	3.34	91.7
AP-4	2.38	91.6	2.05	91.7
AP-5	2.76	91.7	2.36	91.8
BP-1	2.59	92.8	2.45	92.9
BP-2	3.70	92.6	3.52	92.7
BP-3	4.10	92.6	3.88	92.7
BP-4	4.52	92.6	4.17	92.6
BP-5	5.78	92.5	5.36	92.5
BP-6	4.07	92.7	3.79	92.7
BP-7	3.26	92.8	3.02	92.9
BP-8	5.32	92.8	4.91	92.6
BP-9	7.44	92.9	6.87	92.8
CP-1	26.4	81.9	12.6	85.4
CP-2	36.3	81.8	26.7	85.2
CP-3	41.2	81.4	32.4	85.1
CP-4	29.4	82.0	15.1	85.4
CP-5	38.2	81.5	28.3	85.2
DP-1	4.22	88.0	4.42	87.8
DP-2	4.29	88.1	4.20	87.9
DP-3	5.23	87.6	5.31	87.7
DP-4	4.27	87.9	4.38	87.9
DP-5	5.33	87.4	5.26	87.6
EP-1	4.92	84.6	5.04	84.6
EP-2	6.83	84.2	6.71	84.3
EP-3	8.18	83.9	8.23	84.1
EP-4	7.57	84.1	7.44	84.1
EP-5	7.14	84.3	7.63	84.2

by additional cleaning. After the second cleaning operation, the percent haze for all of the specimens except one decreased as shown in Table 4.2. There was no significant change in percent transmittance. Each cleaning operation made significant impacts in optical quality for the stretched acrylic and the coated monolithic polycarbonate. The cast acrylic outer plies of the laminates did not show any improvement until the second cleaning.

The conclusion reached after study of this phenomenon is that proper cleaning is good for the continued optical quality of a transparency. Care must be taken to minimize the time during which the cleaning solution is in contact with the transparency to reduce the possibility of crazing; however, if the cleaning operation is performed correctly, the cleaning is advantageous. The cleaning polishes the transparency surface, reducing haze. The greatest effect was noticed with the coated polycarbonate which, without cleaning, showed severe degradation, and with cleaning did not degrade as severely.

The salt blast abrasion is extremely severe to transparent plastics unless the specified cycles are held to the proposed minimum. Thermal shock and impact requirements appear to be satisfactory as proposed. The interlaminar bond integrity tests for laminated transparencies, namely flatwise tension, torsional shear, and wedge peel, require a more comprehensive design allowables database for determining acceptance or rejection. Edge attachments are unique to each specific design.

To be more representative of actual in-service durability exposure conditions, accelerated weathering should be combined with an appropriate amount of cleaning, abrasion, thermal shock, and induced stress.

TABLE 4.2

HAZE AND TRANSMITTANCE SPECIMENS, 2nd FLIGHTLINE CLEANING

Specimen I.D. No.	Before 50 Cleaning Cycles		After 50 Cleaning Cycles	
	Percent Haze	Transmittance	Percent Haze	Transmittance
AP-1	1.92	91.8	1.73	91.8
AP-2	1.84	91.8	1.68	91.8
AP-3	2.46	91.8	2.18	91.7
AP-4	1.82	91.7	1.69	91.7
AP-5	2.27	91.8	2.23	91.7
BP-1	2.23	92.9	1.82	92.8
BP-2	2.95	92.9	2.32	92.7
BP-3	4.06	92.8	4.20	92.6
BP-4	3.44	92.9	3.06	92.8
BP-5	4.08	97.9	3.01	92.9
BP-6	2.61	93.0	2.15	92.9
BP-7	2.25	92.9	1.71	92.9
BP-8	3.06	93.0	2.69	93.0
BP-9	6.46	92.9	5.17	92.9
CP-1	12.4	95.6	10.9	85.7
CP-2	20.2	85.2	12.2	85.3
CP-3	27.3	85.1	13.4	85.4
CP-4	13.1	85.6	7.1	85.7
CP-5	23.5	85.1	15.0	85.4
DP-1	3.47	87.9	2.98	88.0
DP-2	4.89	87.6	4.85	87.7
DP-3	3.82	87.9	3.15	87.9
DP-4	3.45	87.9	2.54	88.1
DP-5	5.01	87.9	3.07	87.9
EP-1	4.28	84.6	4.16	84.6
EP-2	5.42	84.5	4.53	84.6
EP-3	6.65	84.4	4.31	84.5
EP-4	5.27	84.6	4.23	84.6
EP-5	6.07	84.6	4.27	84.6

	Percent Haze	Transmittance
Standard (Before)	7.26	92.4
Standard (After)	7.23	92.4

SECTION 5
CONCLUSIONS/RECOMMENDATIONS

5.1 CONCLUSIONS

- The existing test methodology is too severe as proposed for surface/chemical craze and haze/transmittance (without supplemental cleaning).

- The existing test methodology is satisfactory as specified for in-flight and flightline abrasion resistance, thermal shock, and impact resistance.

5.2 RECOMMENDATIONS

- Evaluate identical coupon-type specimens cut from the same five transparencies taken from the field after a known history of in-service exposure. Compare this database with the laboratory generated data.

- Generate design allowables for silicone and urethane interlayers subjected to flatwise tension, torsional shear, and wedge peel.

- Combine all durability test parameters into one combined environmental condition.

- Coordinate proposed chemical craze solvents with latest ASTM F7.08 task force recommendations.

- Implement improved procedures for reporting in-service maintenance problems and/or failures of USAF high performance transparencies to the Air Vehicle SPO, AFWAL/FIER, and appropriate transparency suppliers. Expedite the distribution of up-to-date T.O.'s relating to transparency installation and maintenance. Expand the training of field maintenance personnel through the use of video cassettes and supplier-conducted training sessions.

REFERENCES

1. West, B. S., Clayton, K. I., and Giessler, F. J., Survey of Developmental Testing and In-Service Durability of F-15, F-16, and F-111 Transparencies, AFWAL-TR-81-3151, Air Force Wright Aeronautical Laboratories, Wright-Patterson Air Force Base, Ohio, January 1982.

2. West, B. S. and Clayton, K. I., Aircraft Transparency Testing Methodology and Evaluation Criteria, AFWAL-TR-83-3045, Air Force Wright Aeronautical Laboratories, Wright-Patterson Air Force Base, Ohio, April 1983.

3. Clayton, K. I., Milholland, J. F. and Stenger, G. J., Experimental Evaluation of F-16 Polycarbonate Canopy Material, AFWAL-TR-81-4020, Air Force Wright Aeronautical Laboratories, Wright-Patterson Air Force Base, Ohio, April 1981.

4. Stenger, G. J., Structural Evaluation of a Transparency with Metallic Film Interlayer, AFWAL-TR-83-3063, Air Force Wright Aeronautical Laboratories, Wright-Patterson Air Force Base, Ohio, June 1983.

APPENDIX A

SURFACE/CHEMICAL CRAZE SUPPLEMENTAL DATA

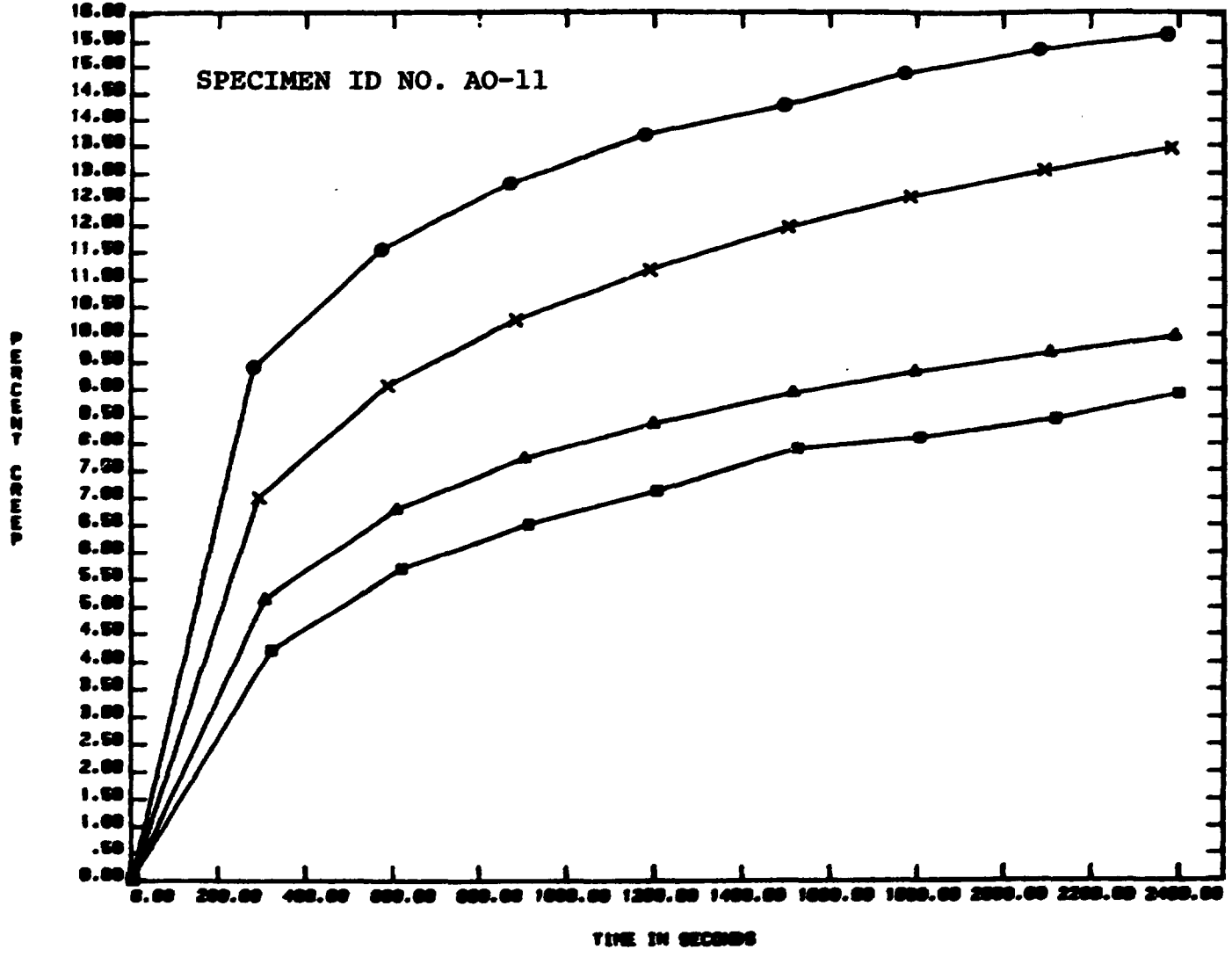

AO-11

Figure A-1. Plot of Percent Creep versus Time for F-15 Monolithic Stretched Acrylic Windshield.

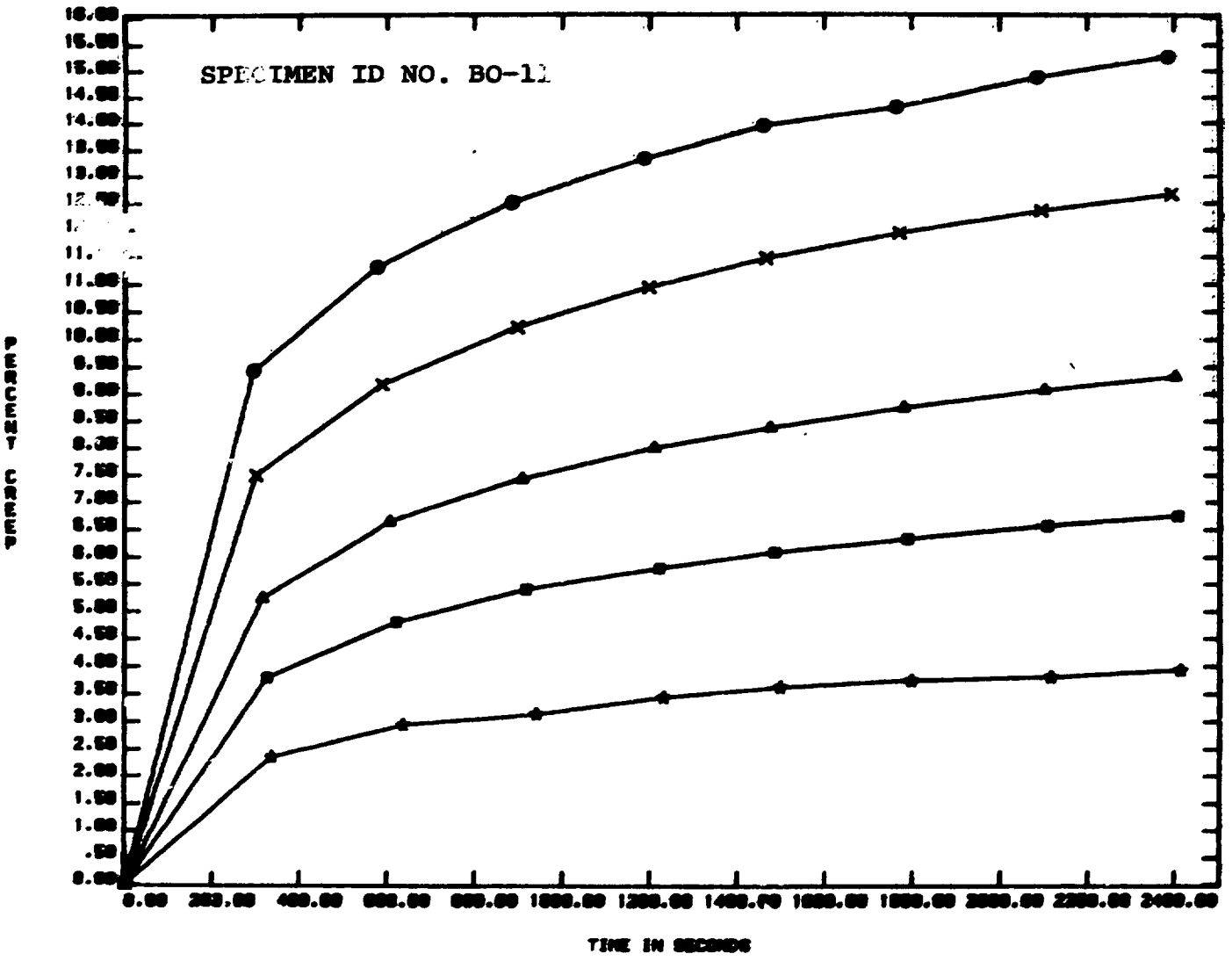

Figure A-2. Plot of Percent Creep versus Time for F-15 Stretched Acrylic Canopy.

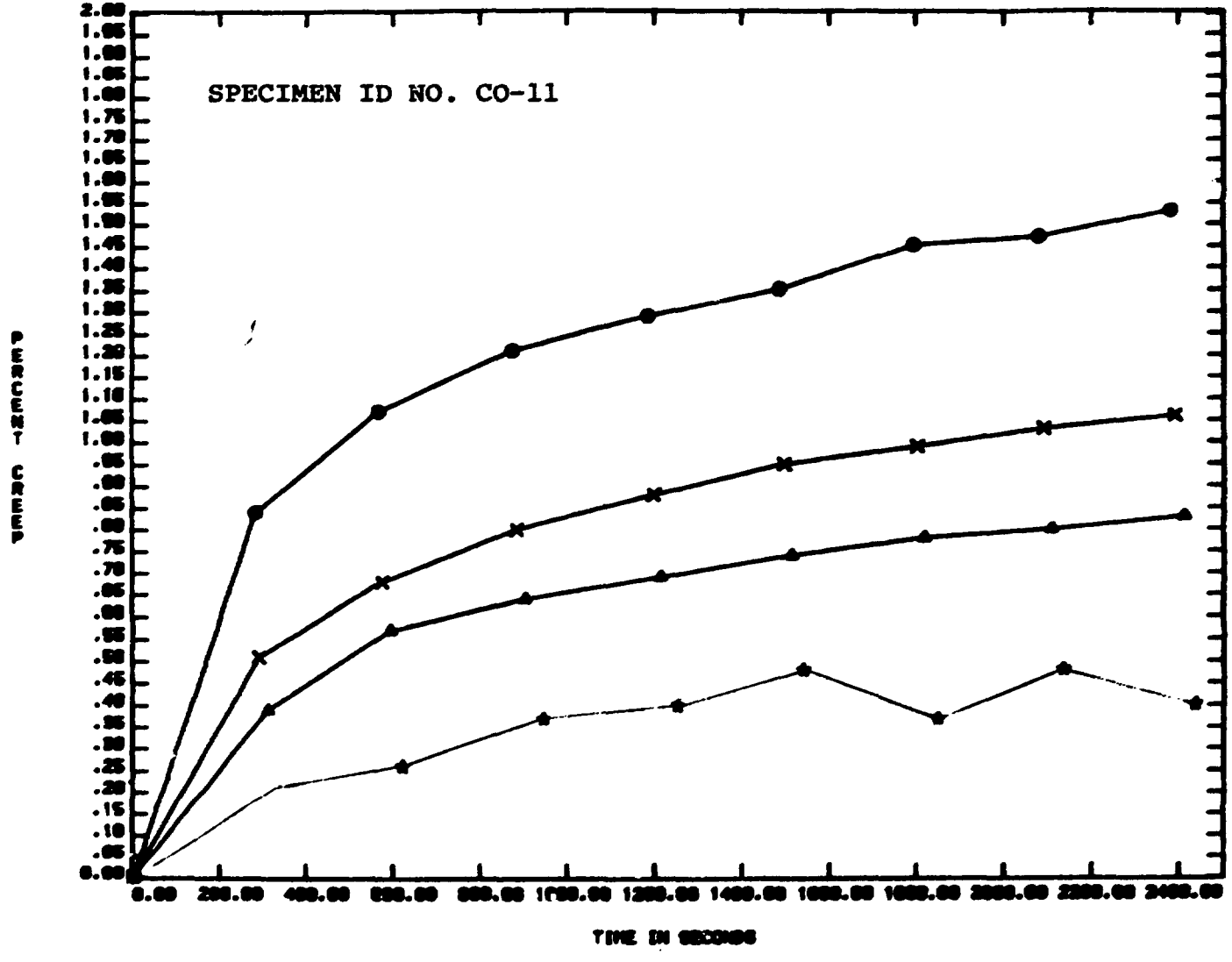

Figure A-3. Plot of Percent Creep versus Time for F-16 Coated Monolithic Polycarbonate Canopy.

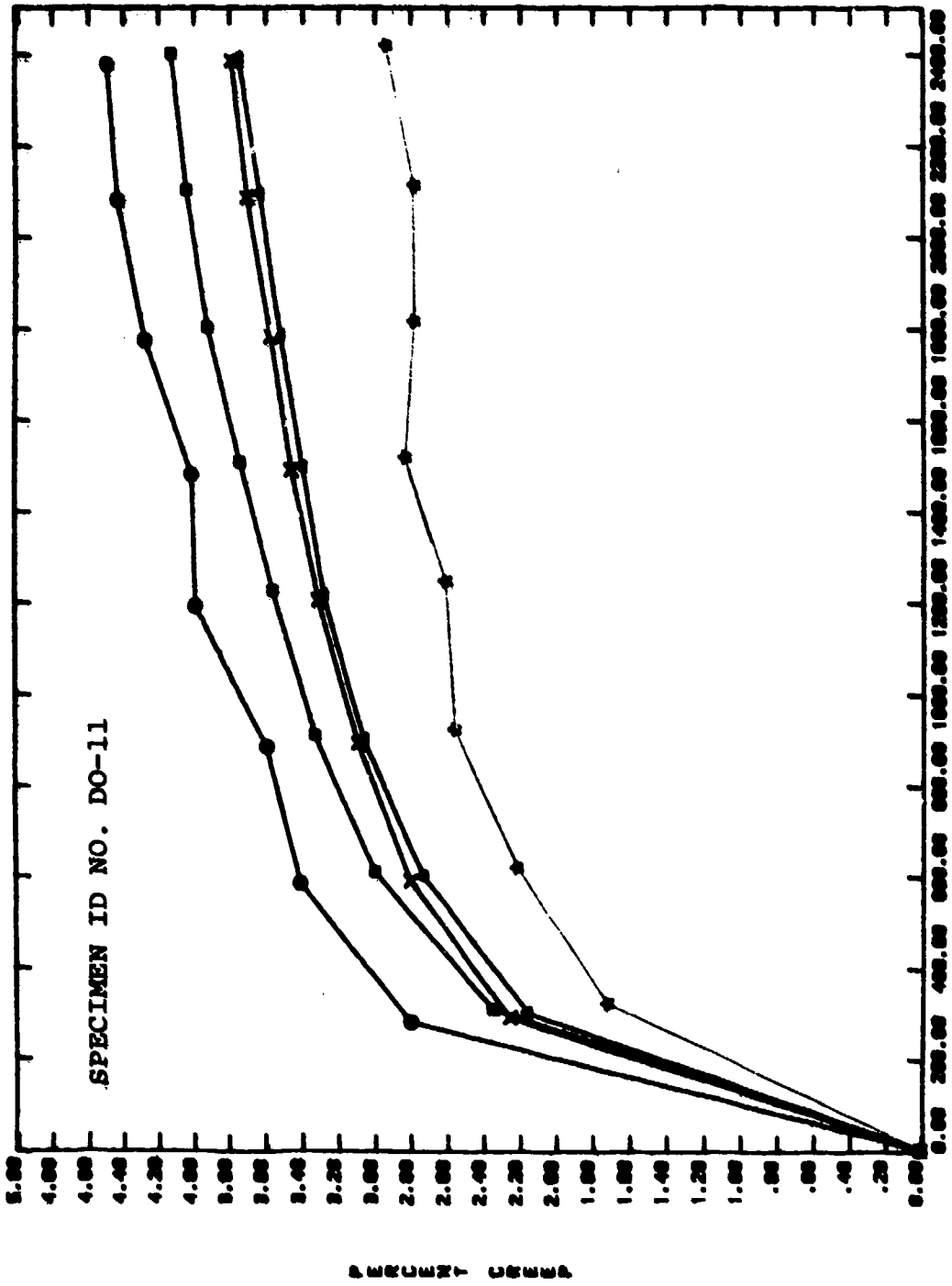

Figure A-4. Plot of Percent Creep versus Time for F-16A Laminated Canopy.

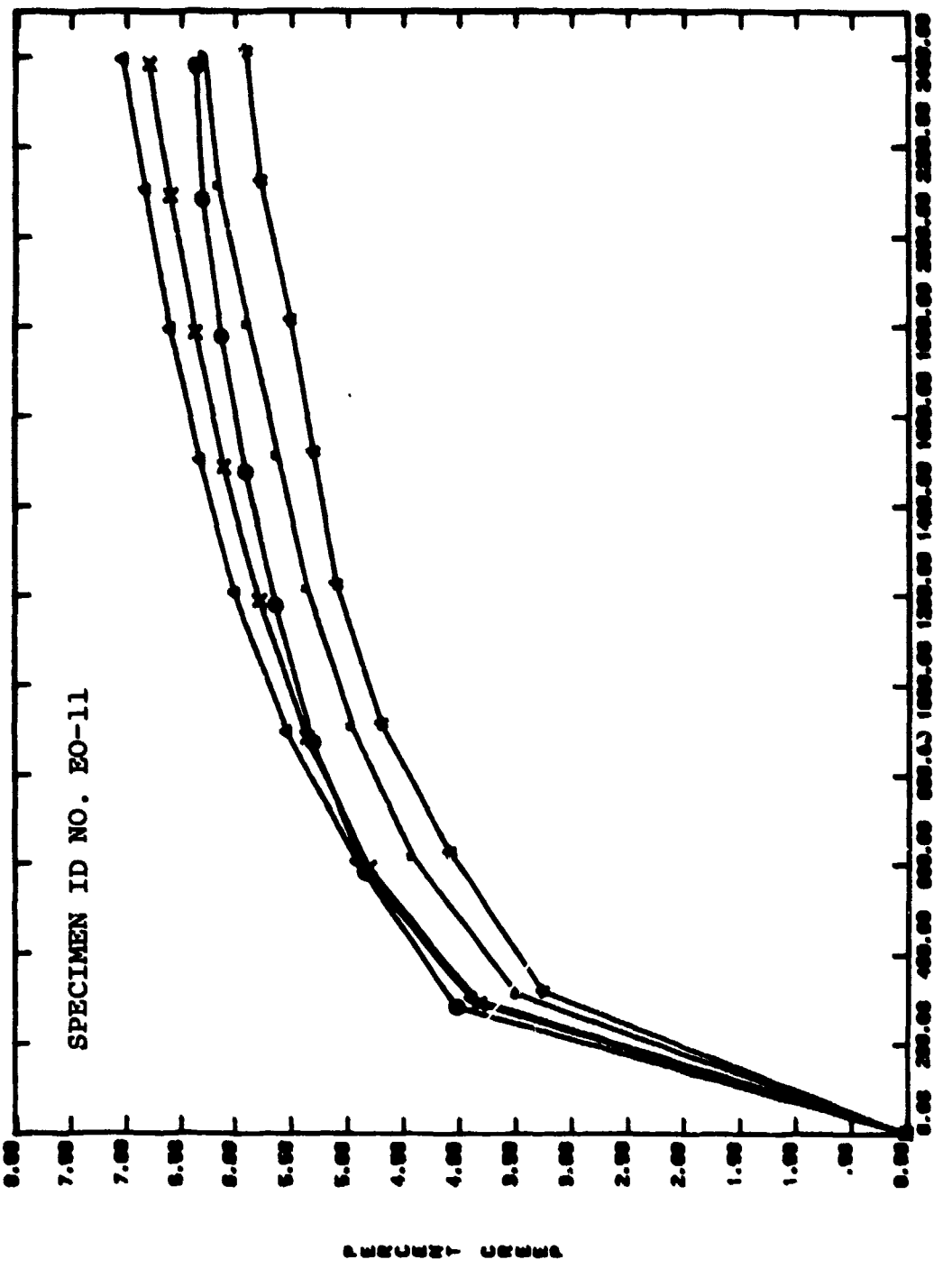

Figure A-5. Plot of Percent Creep versus Time for P-111 Laminated Windshield.

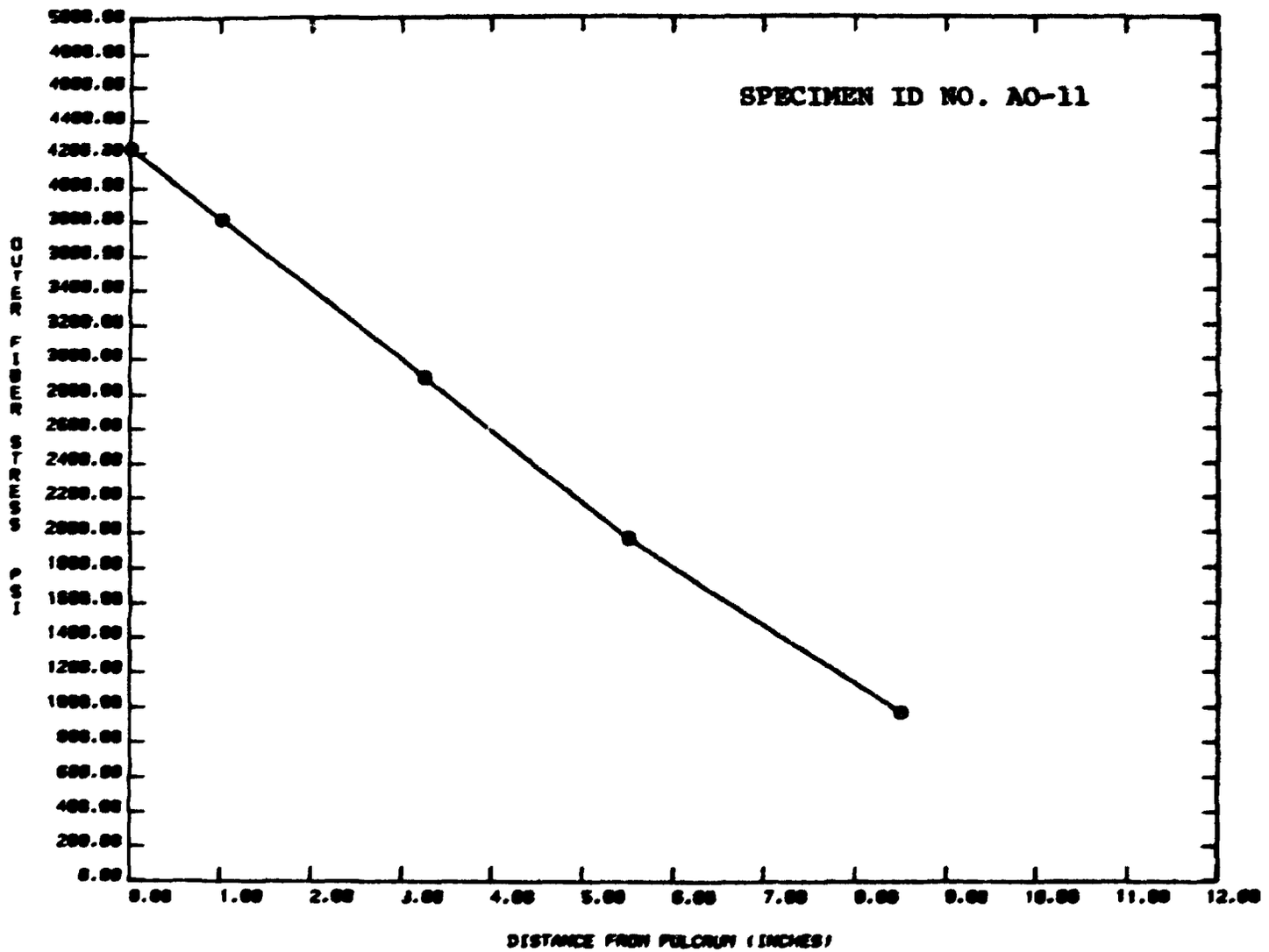

Figure A-6. Plot of Outer Fiber Stress versus Distance from the Fulcrum for the F-15 Monolithic Stretched Acrylic Windshield.

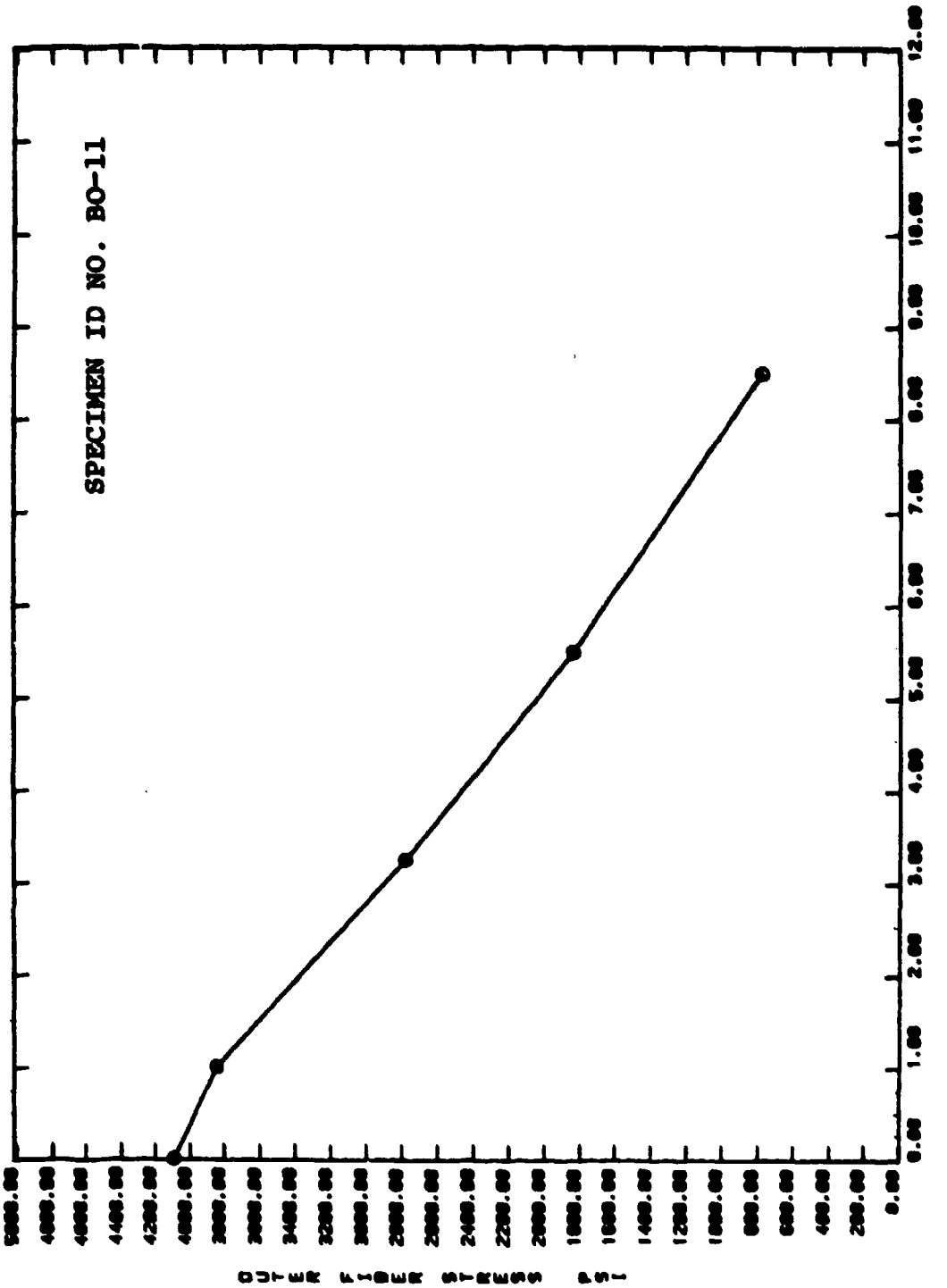

Figure A-7. Plot of Outer Fiber Stress versus Distance from the Fulcrum for the F-15 Monolithic Stretched Acrylic Canopy.

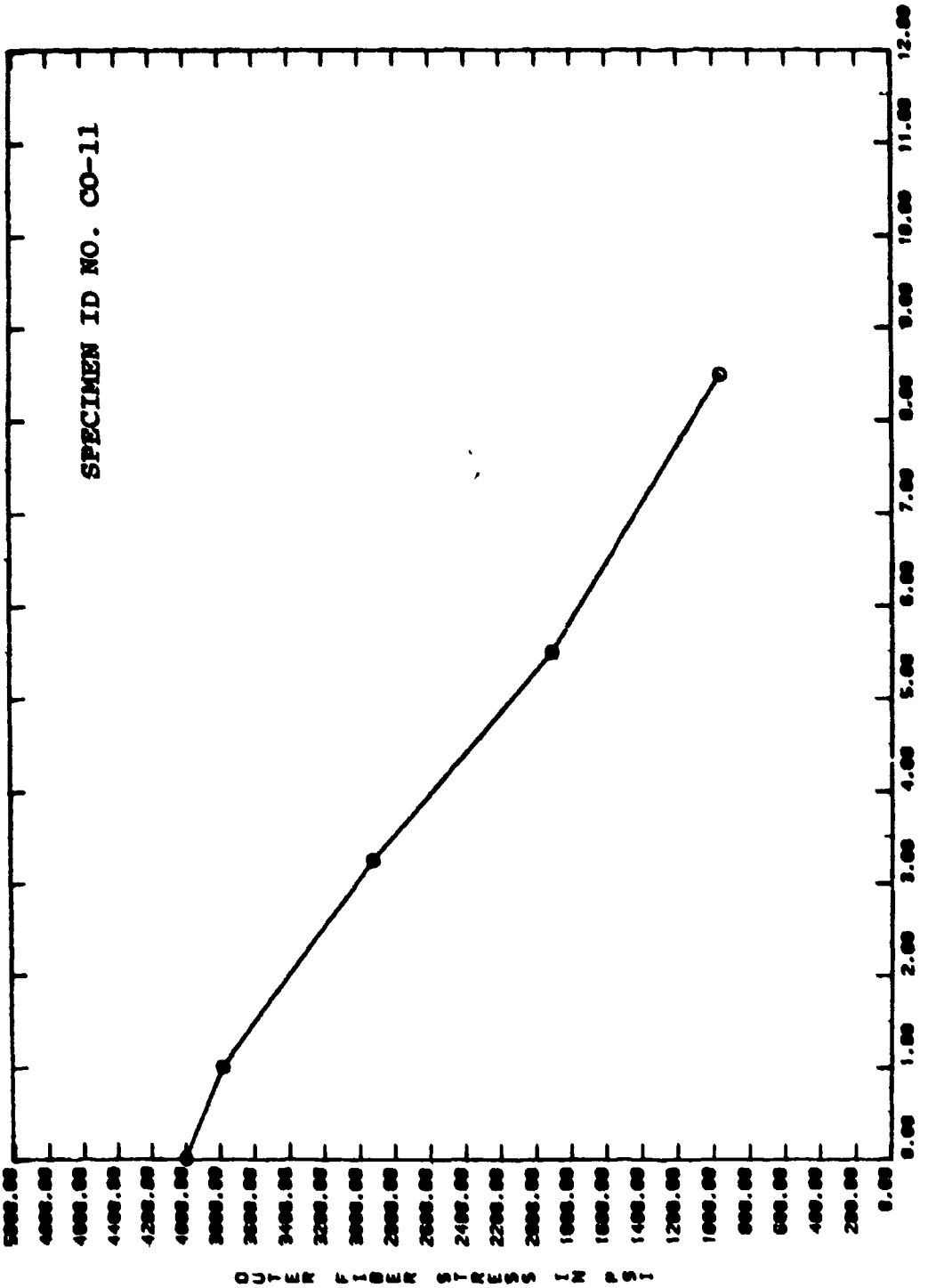

Figure A-8. Plot of Outer Fiber Stress versus Distance from the Fulcrum for the F-16A Coated Monolithic Polycarbonate Canopy.

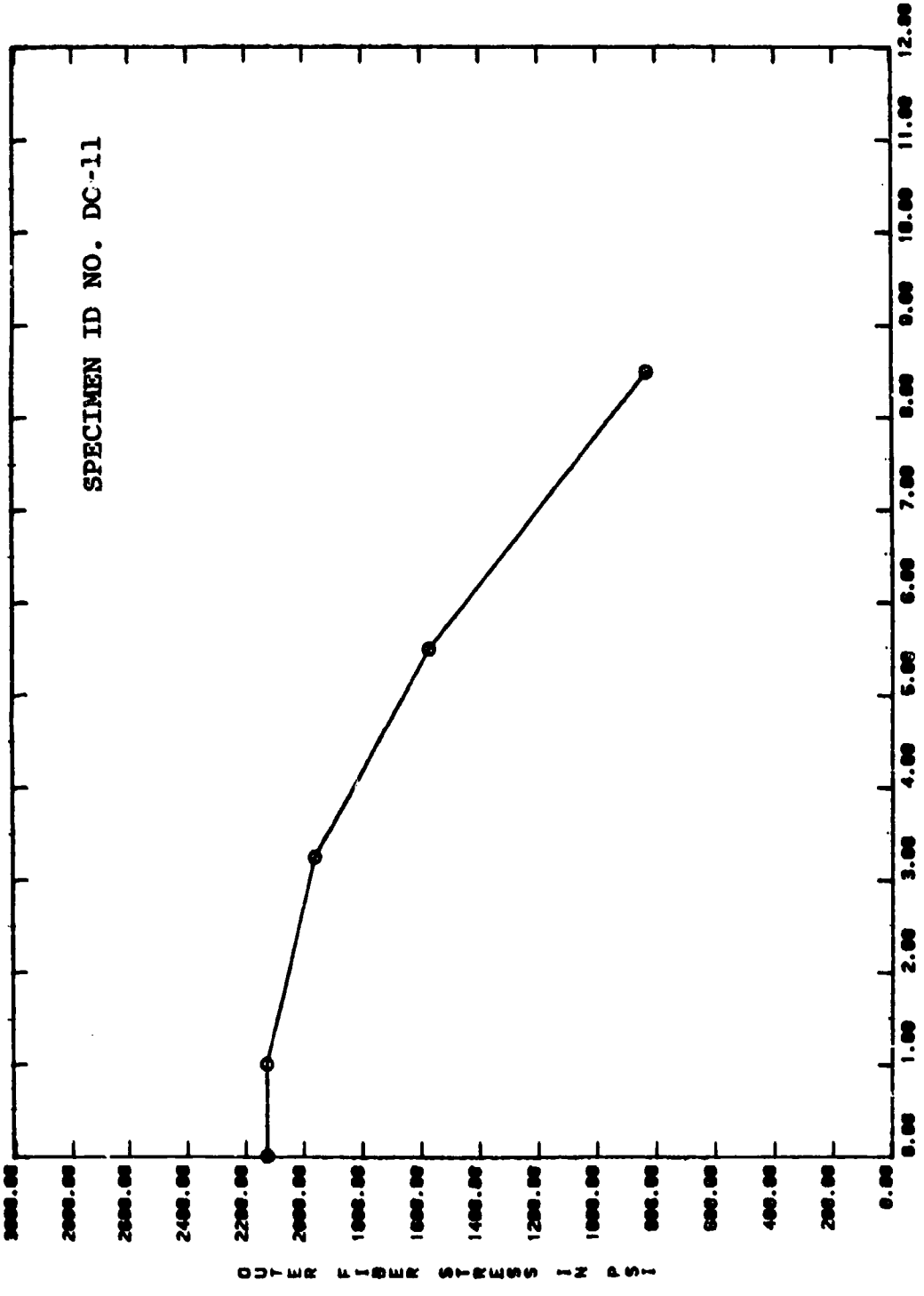

Figure A-9. Plot of Outer Fiber Stress versus Distance from the Fulcrum for the F-16A Laminated Canopy.

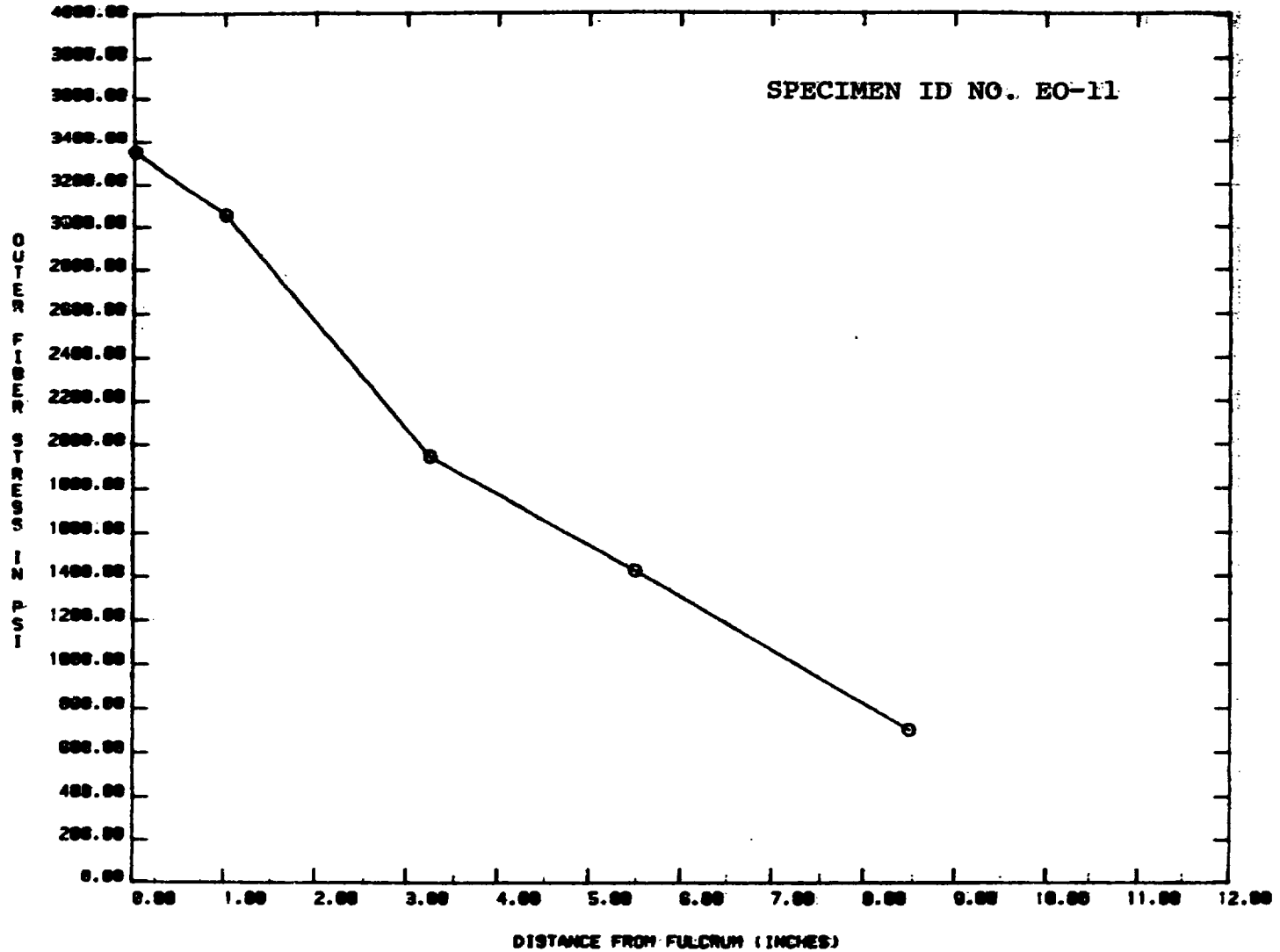

Figure A-10. Plot of Outer Fiber Stress versus Distance from the Fulcrum for the F-111 Laminated Windshield.

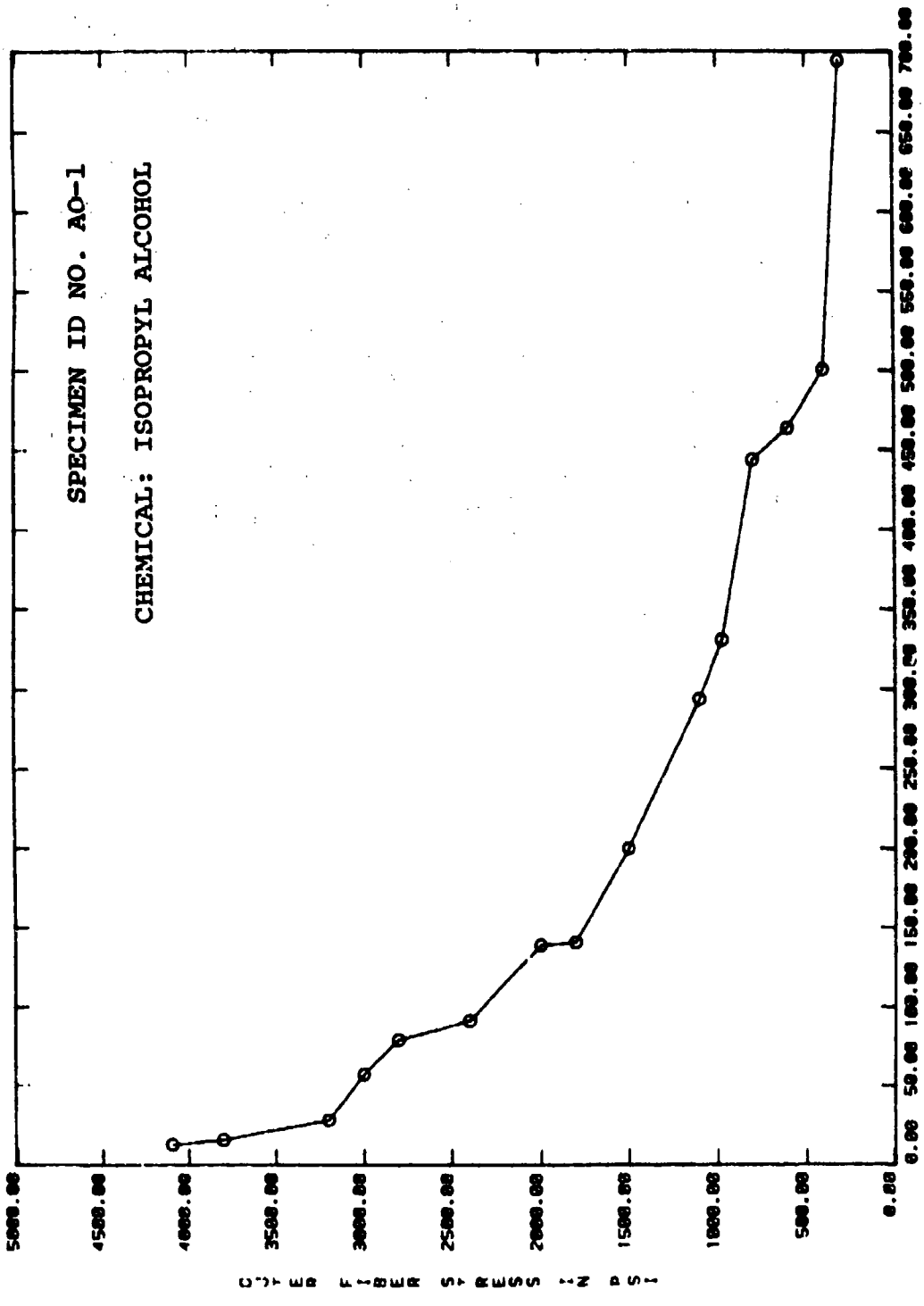

Figure A-11. Plot of Outer Fiber Stress vs. Time to Craze for the F-15 Monolithic Stretched Acrylic Windshield Specimens.

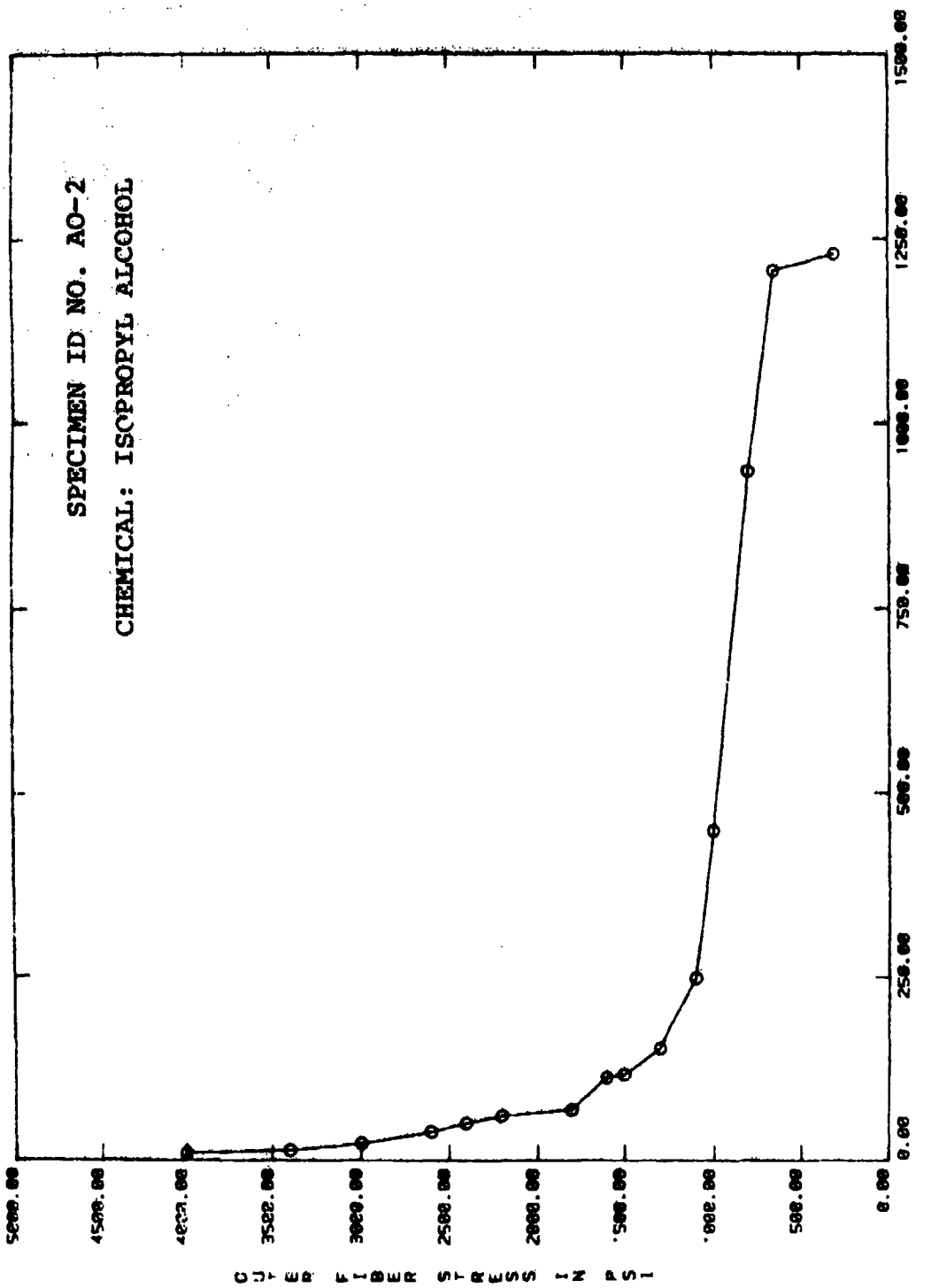

Figure A-11 (continued).

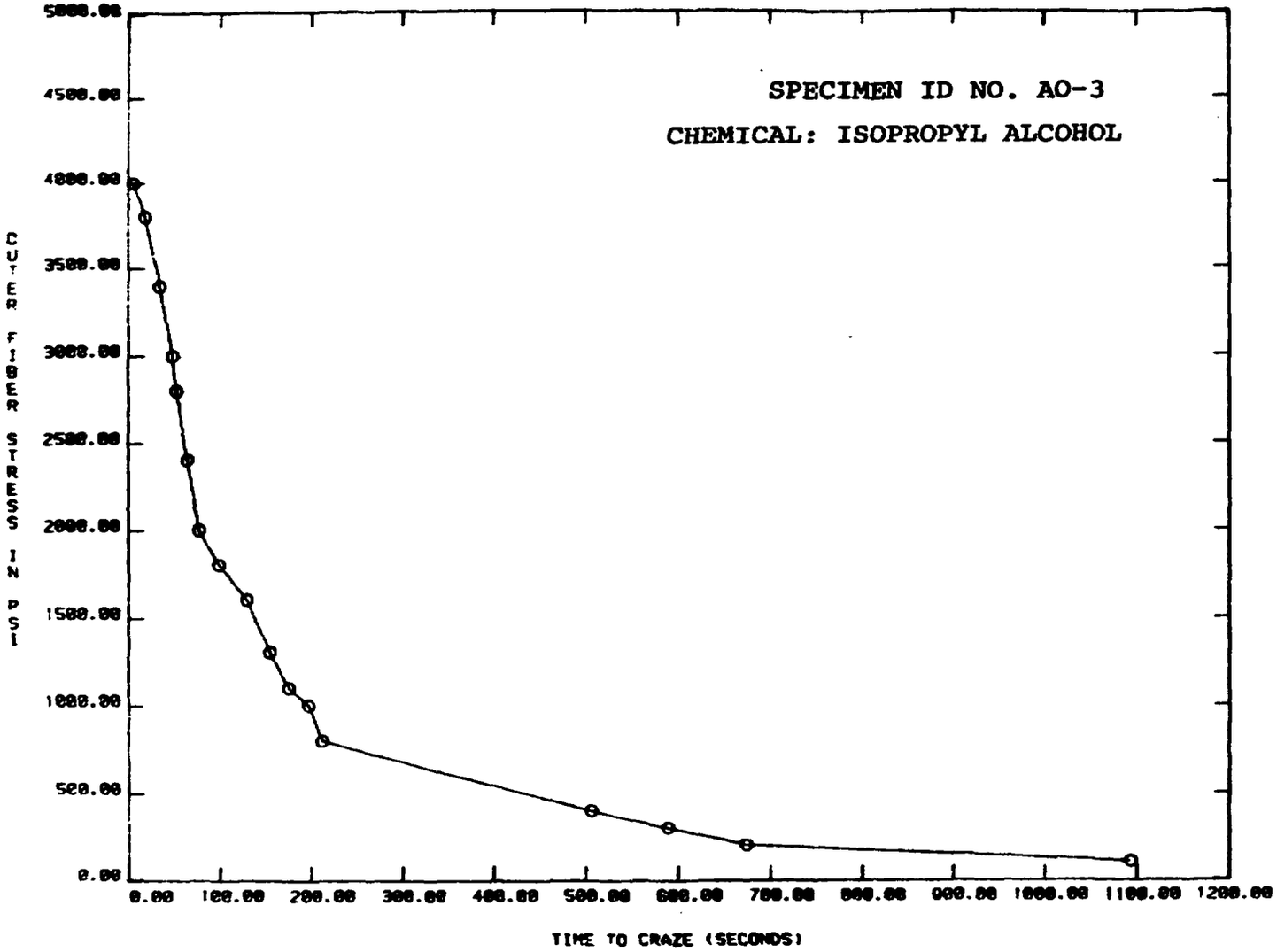

Figure A-11 (continued).

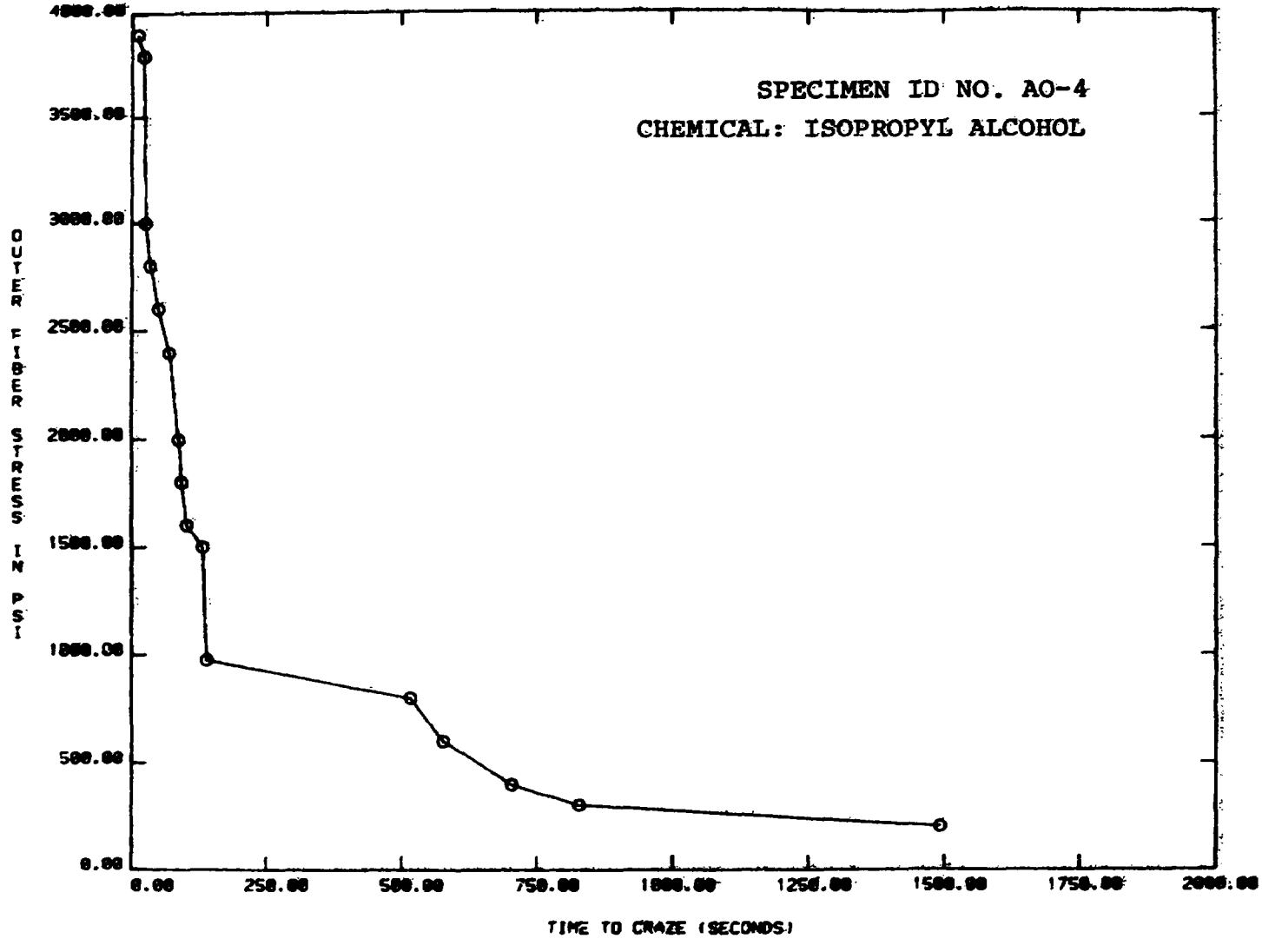

Figure A-11 (continued).

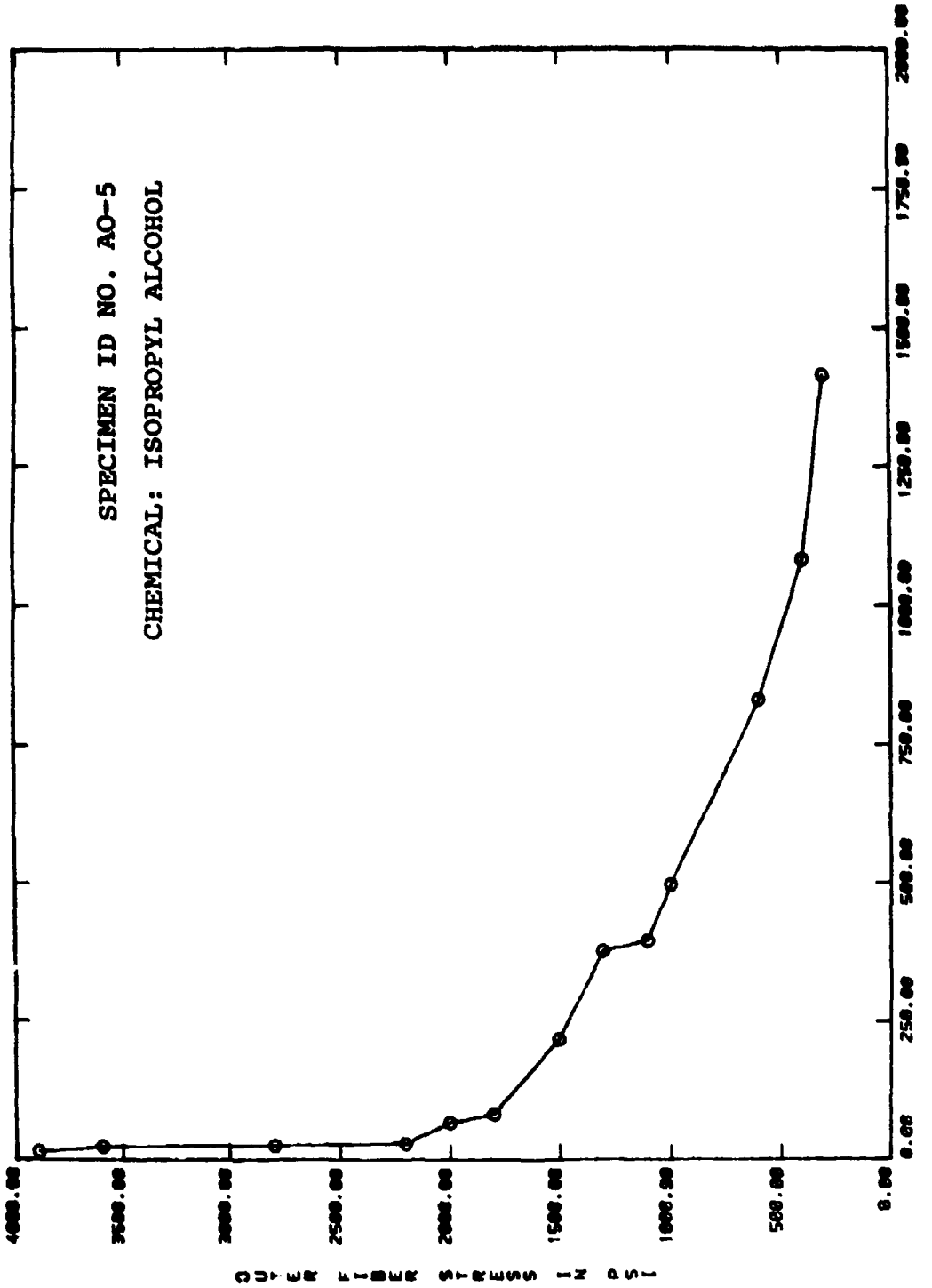

Figure A-11 (continued).

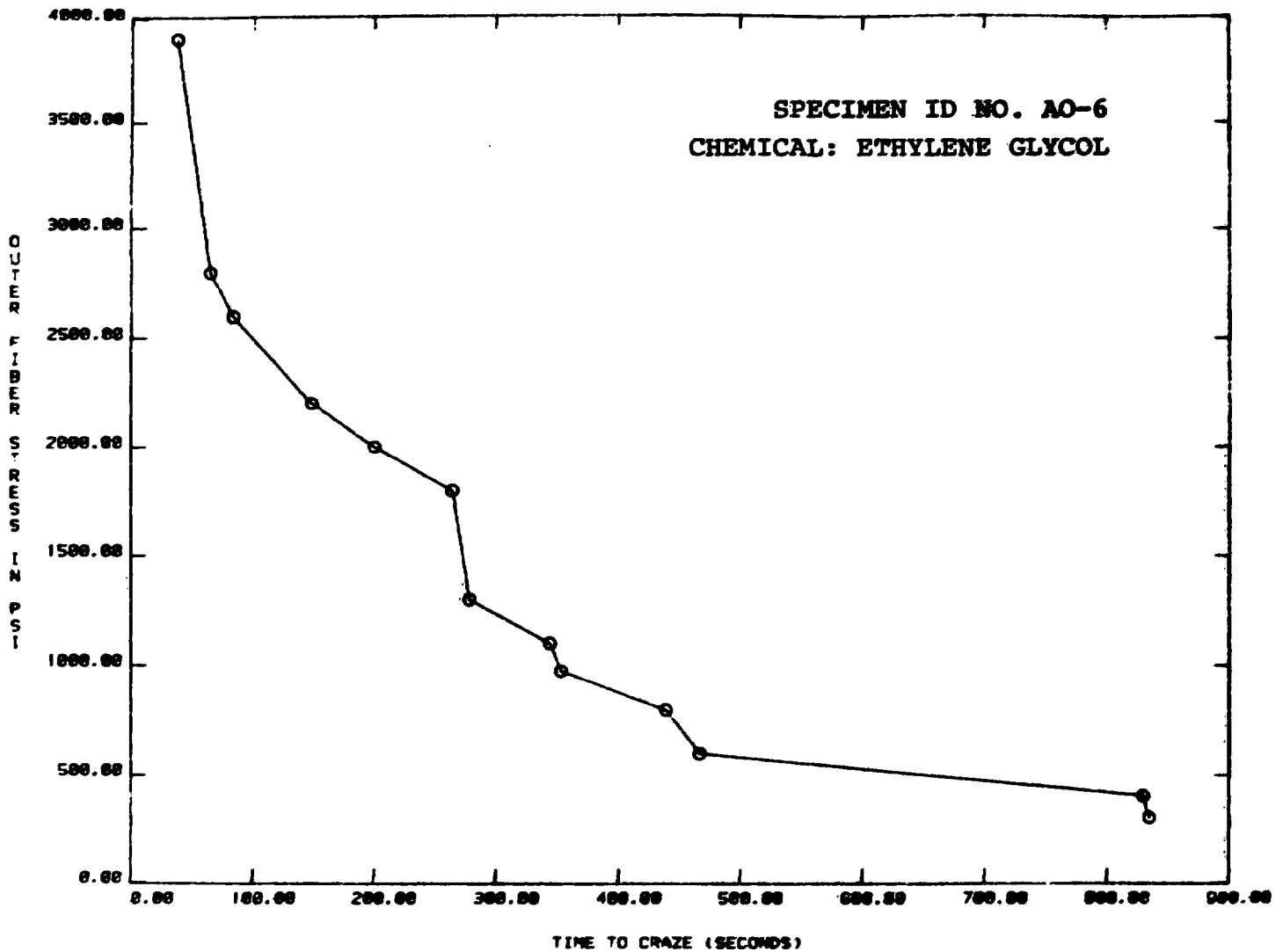

Figure A-11 (continued).

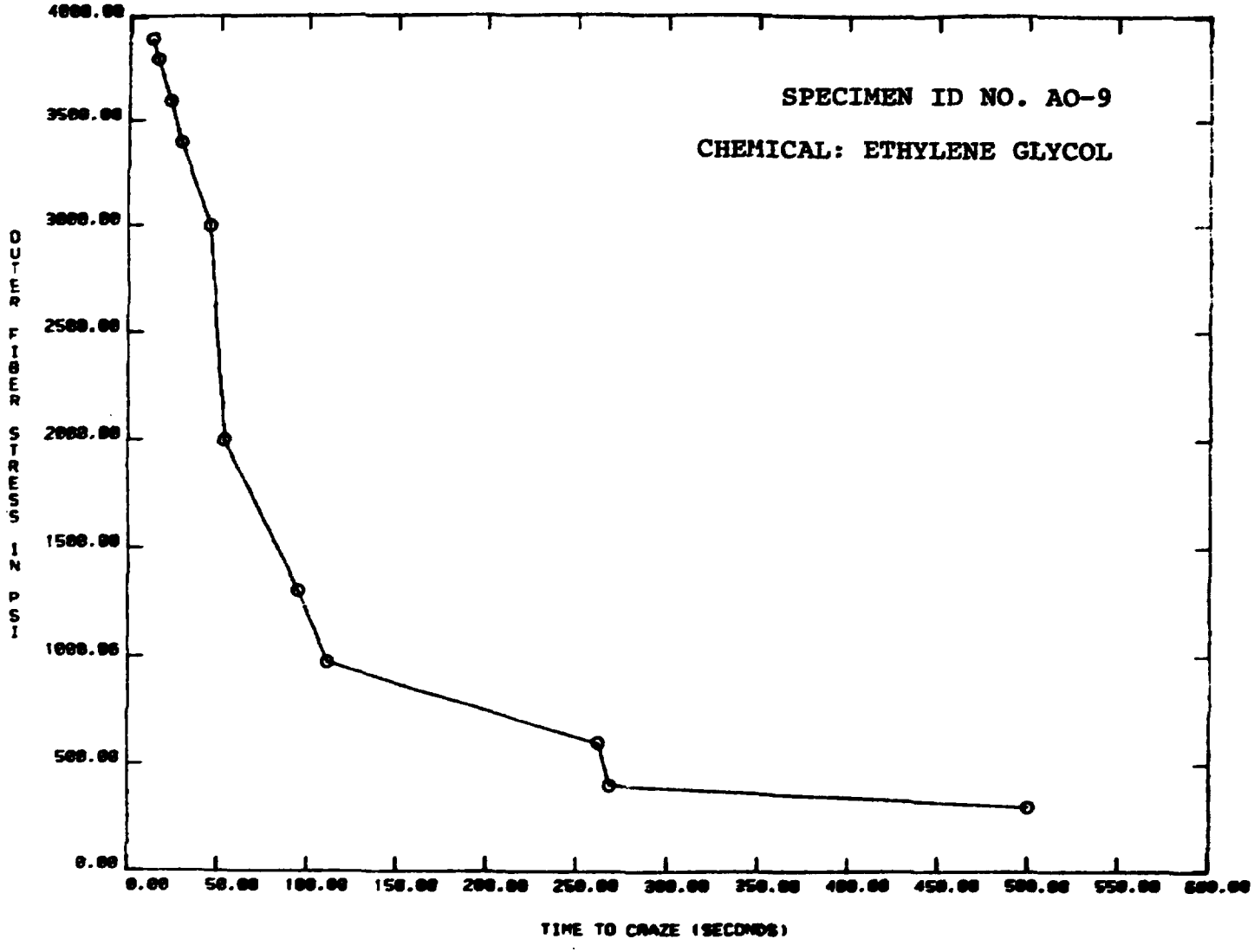

Figure A-11 (concluded).

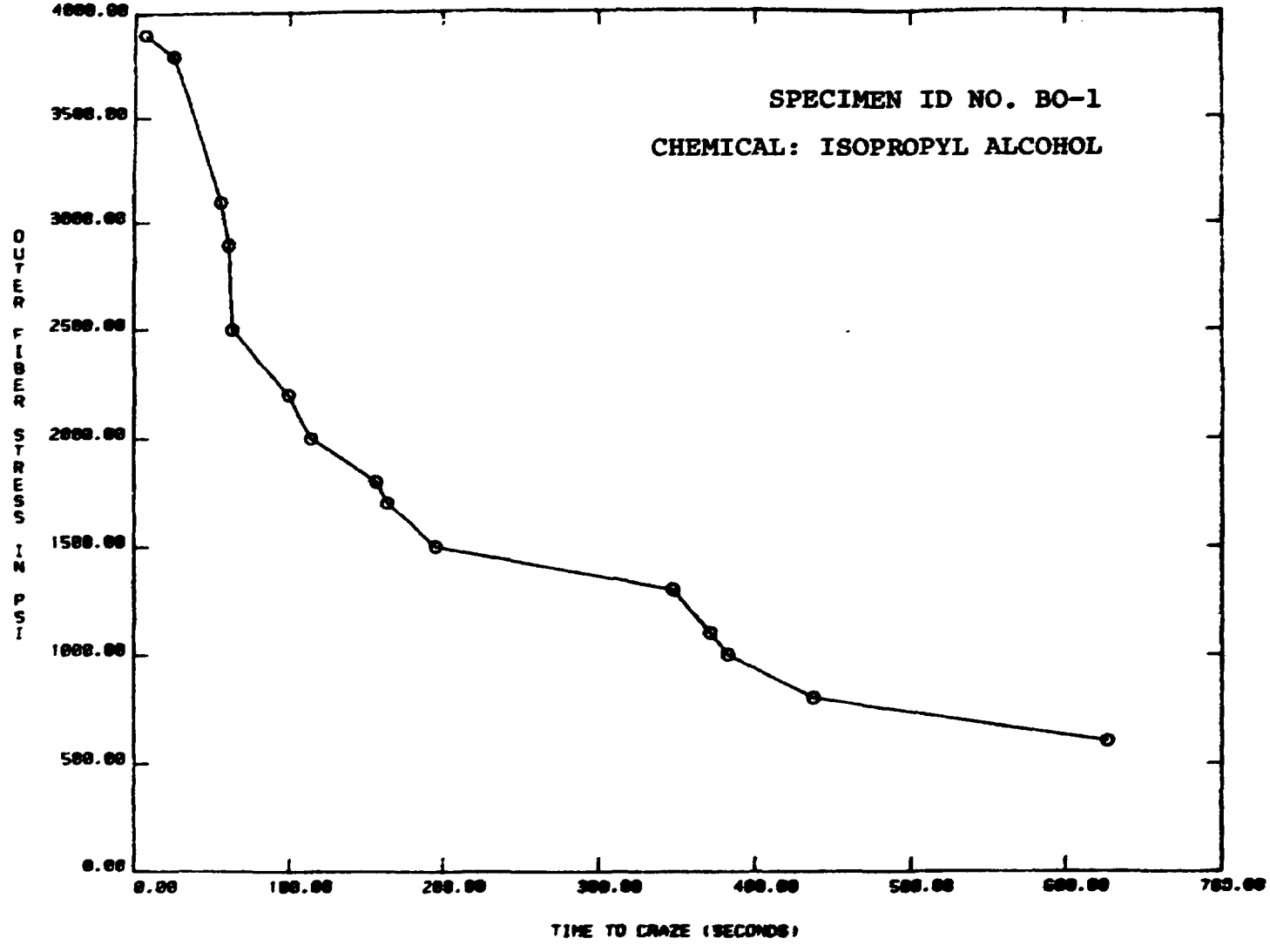

Figure A-12. Plot of Outer Fiber Stress vs. Time to Craze for the F-15 Monolithic Stretched Acrylic Canopy Specimens.

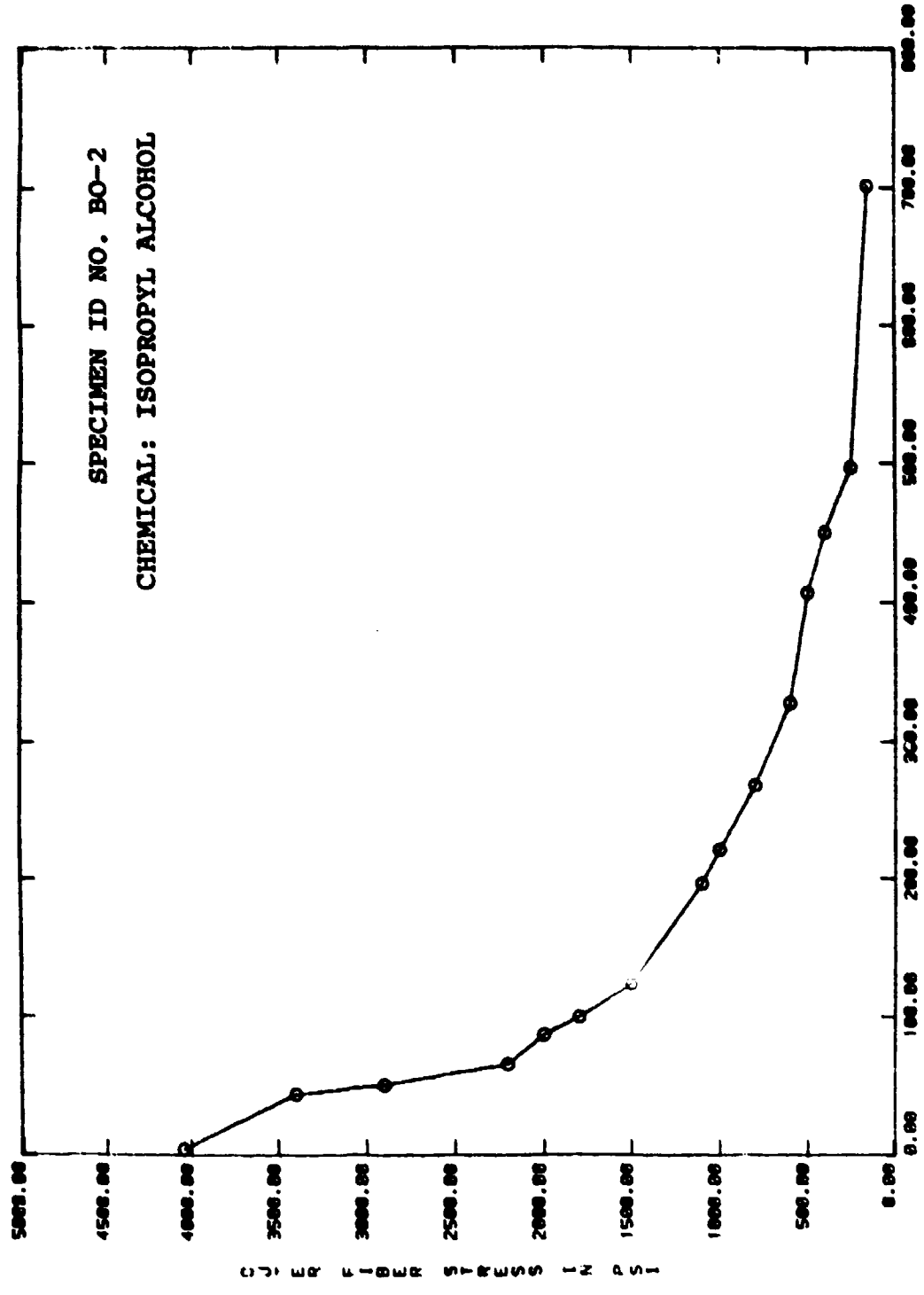

Figure A-12 (continued).

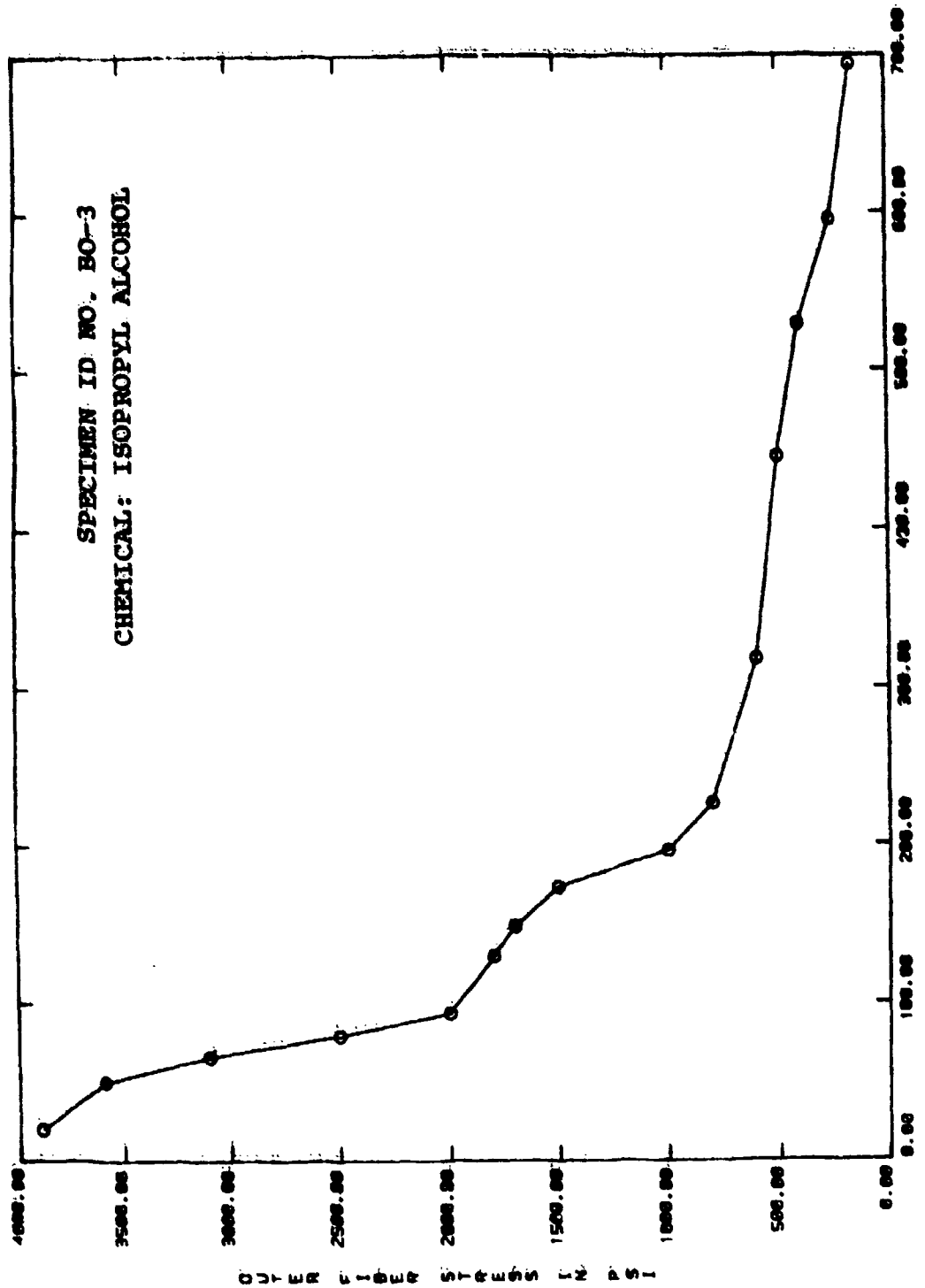

Figure A-12 (continued).

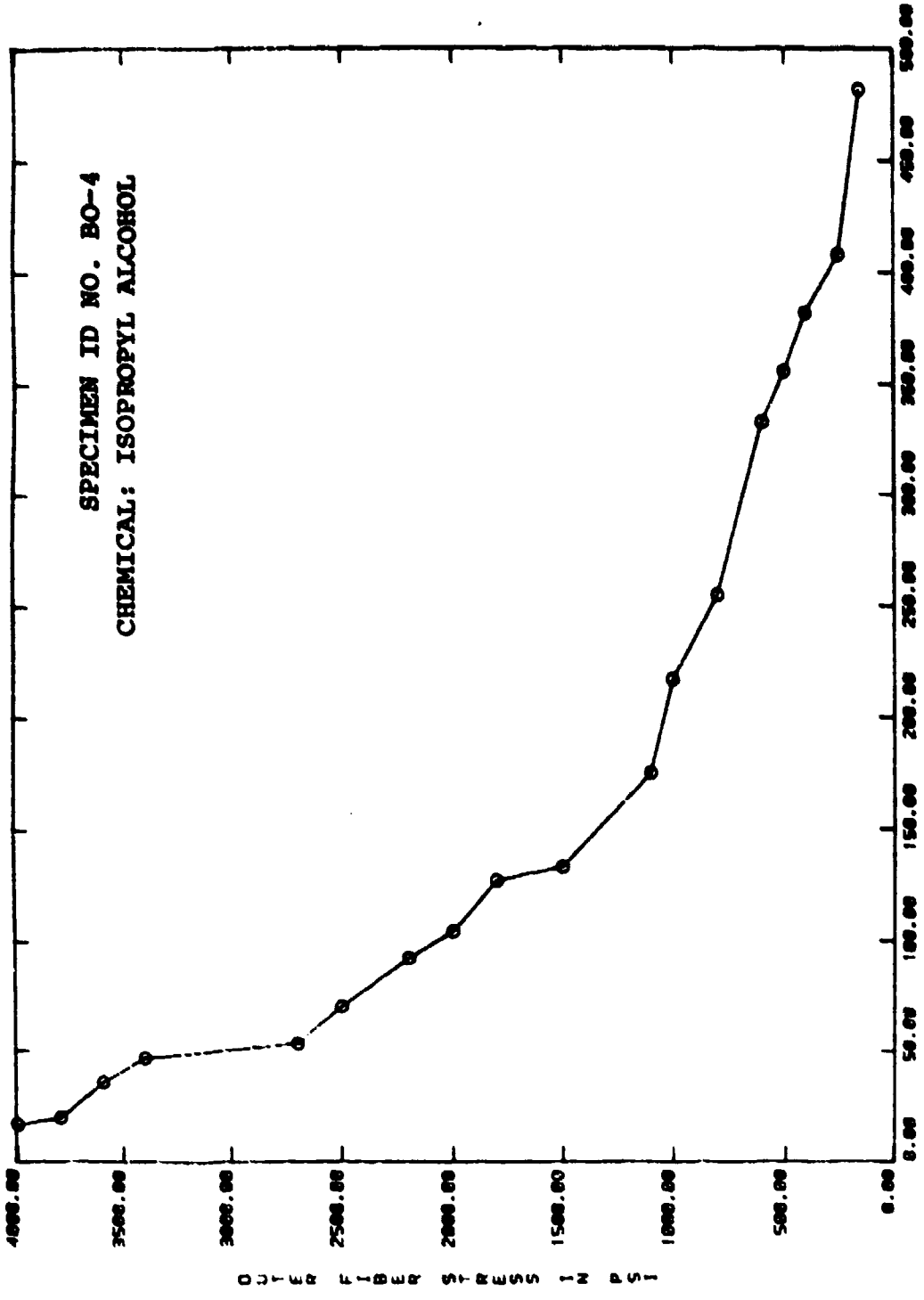

Figure A-12 (continued).

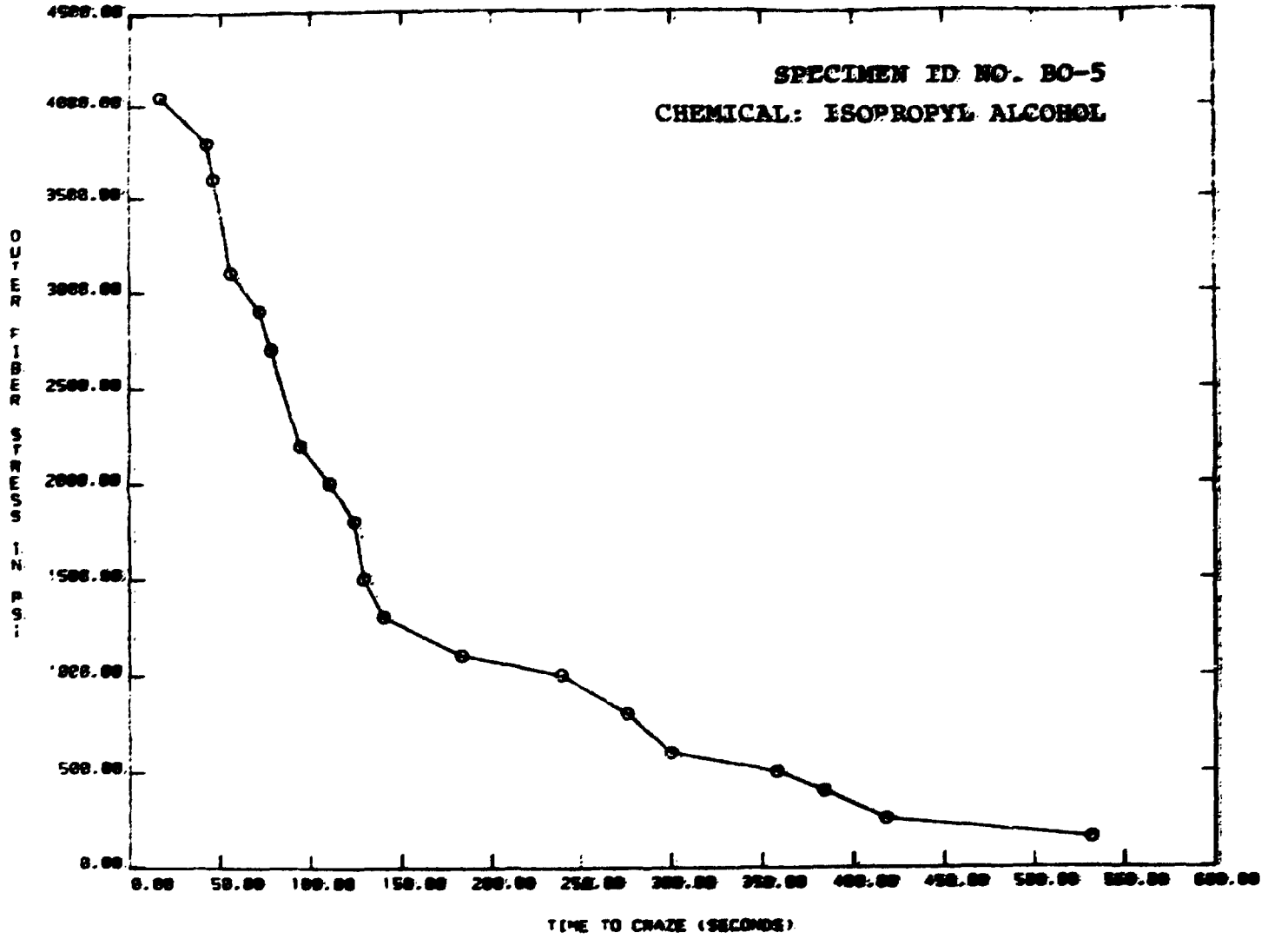

Figure A-12 (continued).

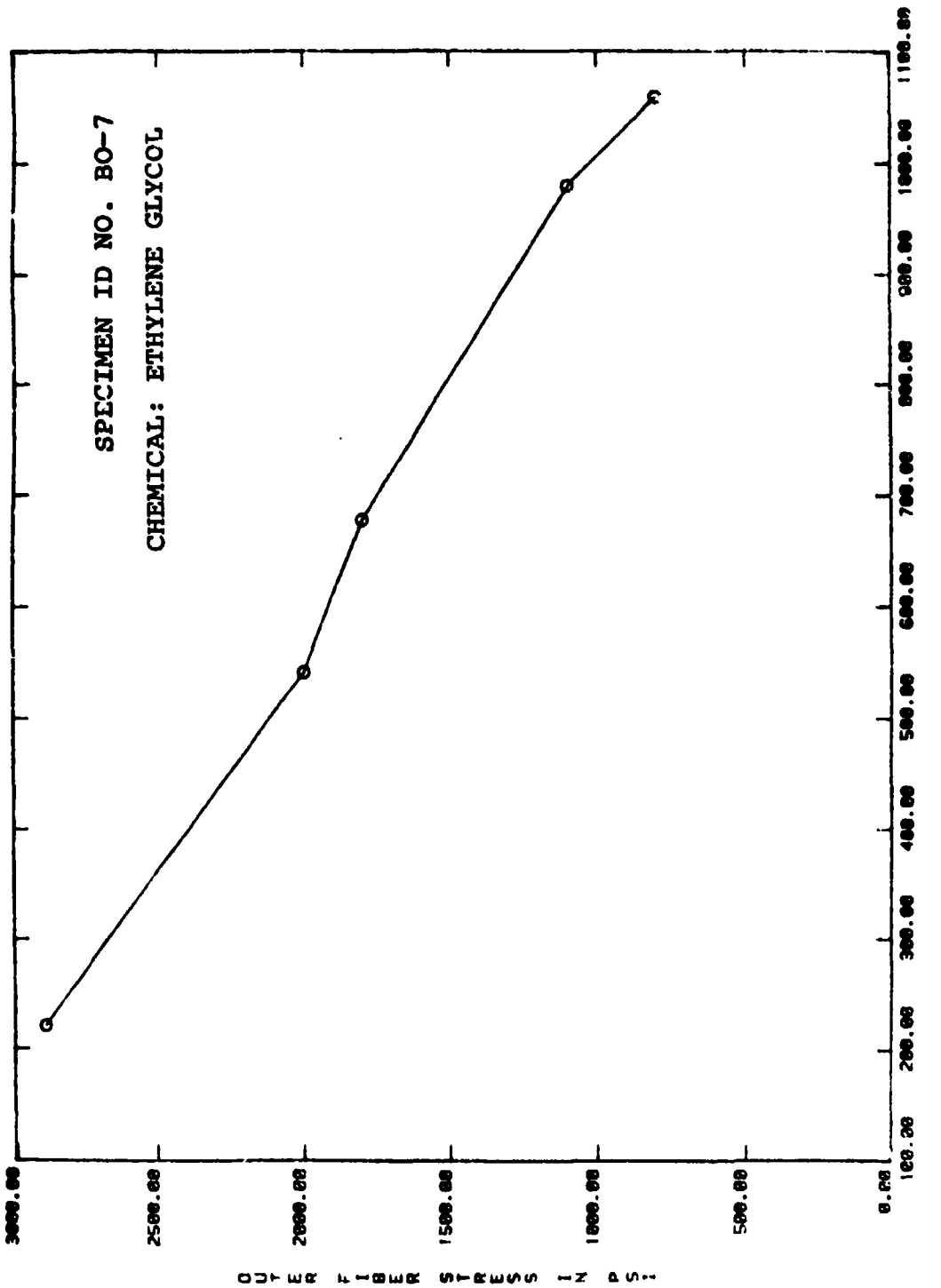

Figure A-12 (concluded).

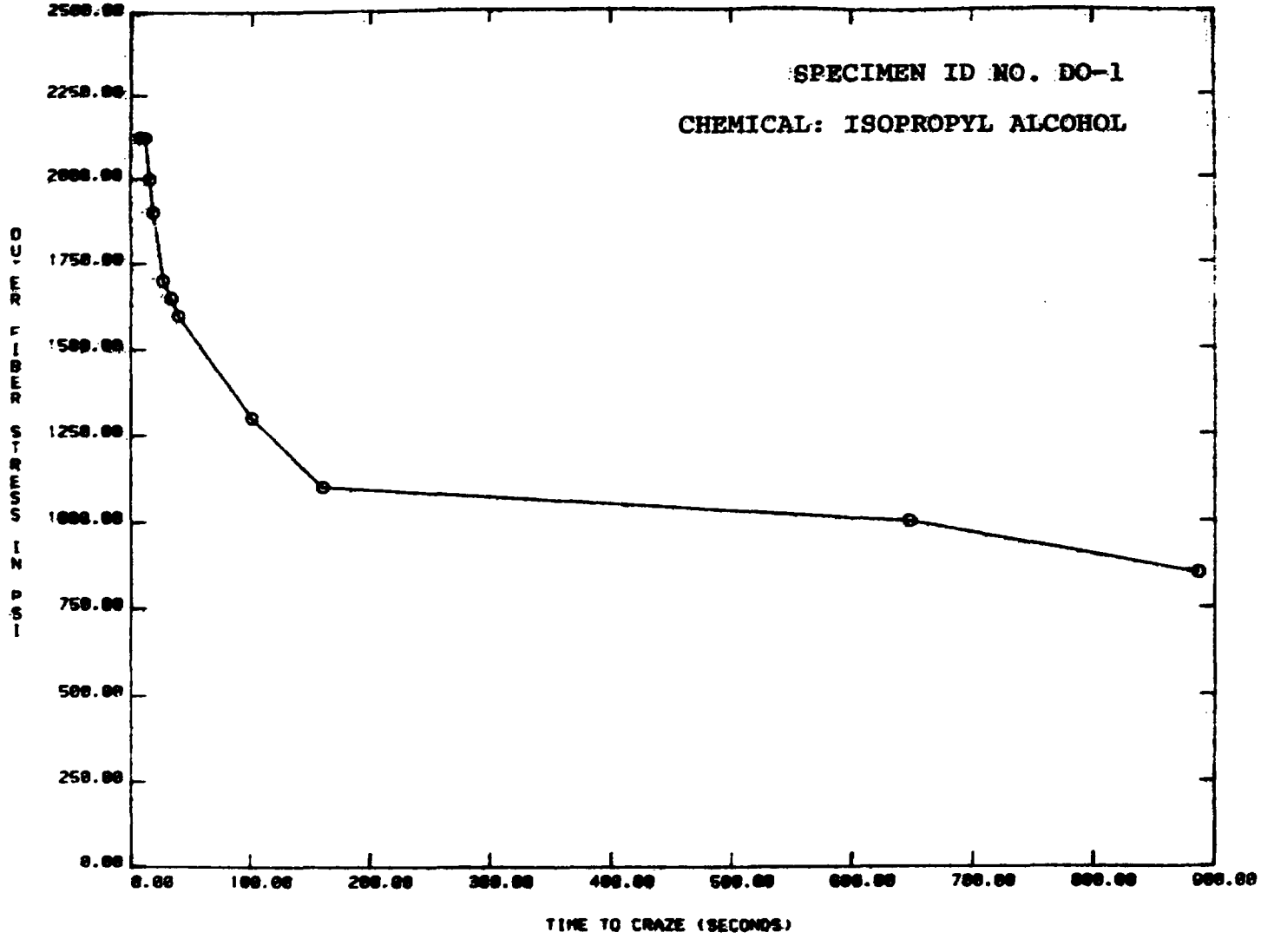

Figure A-13. Plot of Outer Fiber Stress versus Time to Craze for the F-16A Laminated Canopy Specimens.

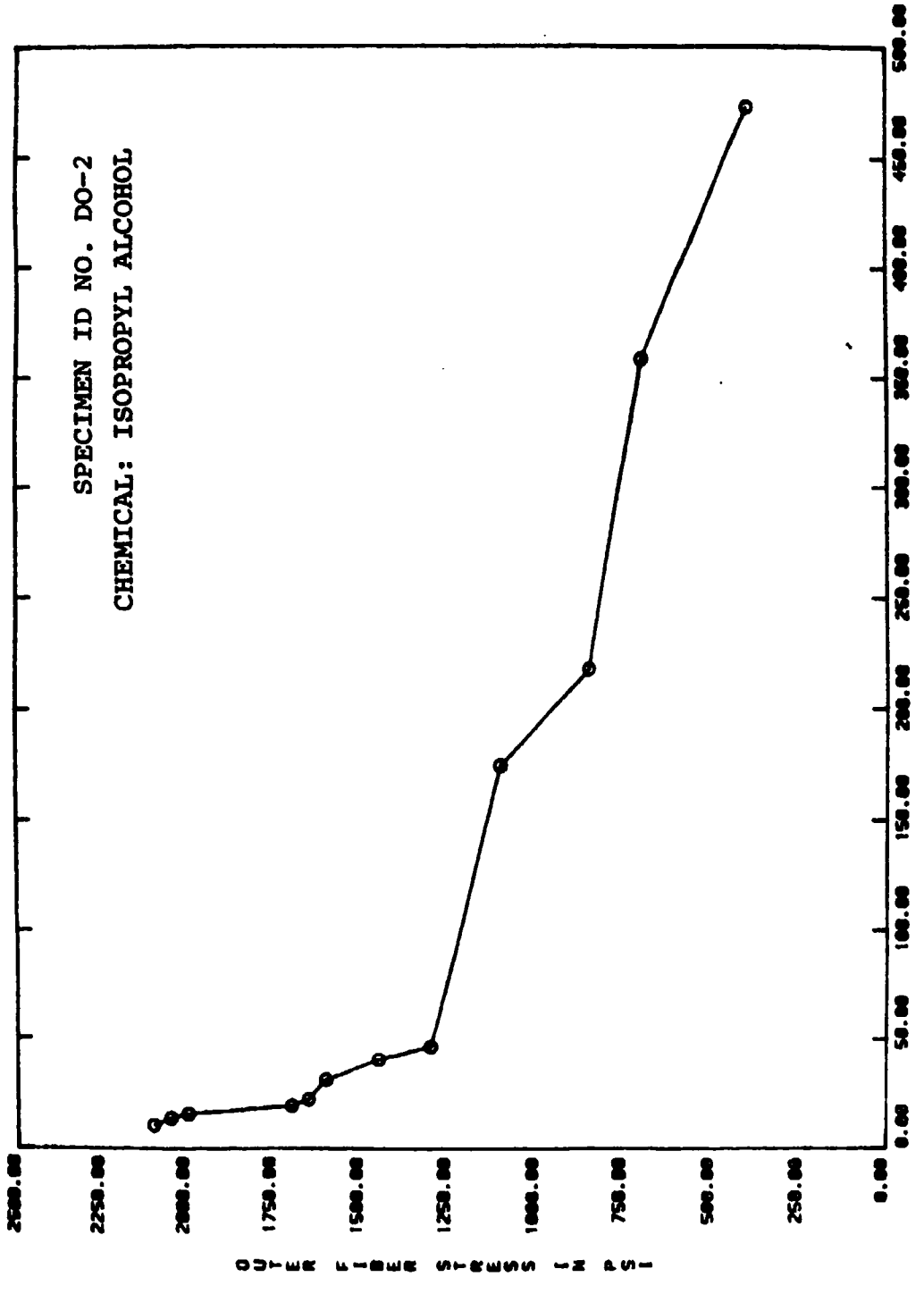

Figure A-13 (continued).

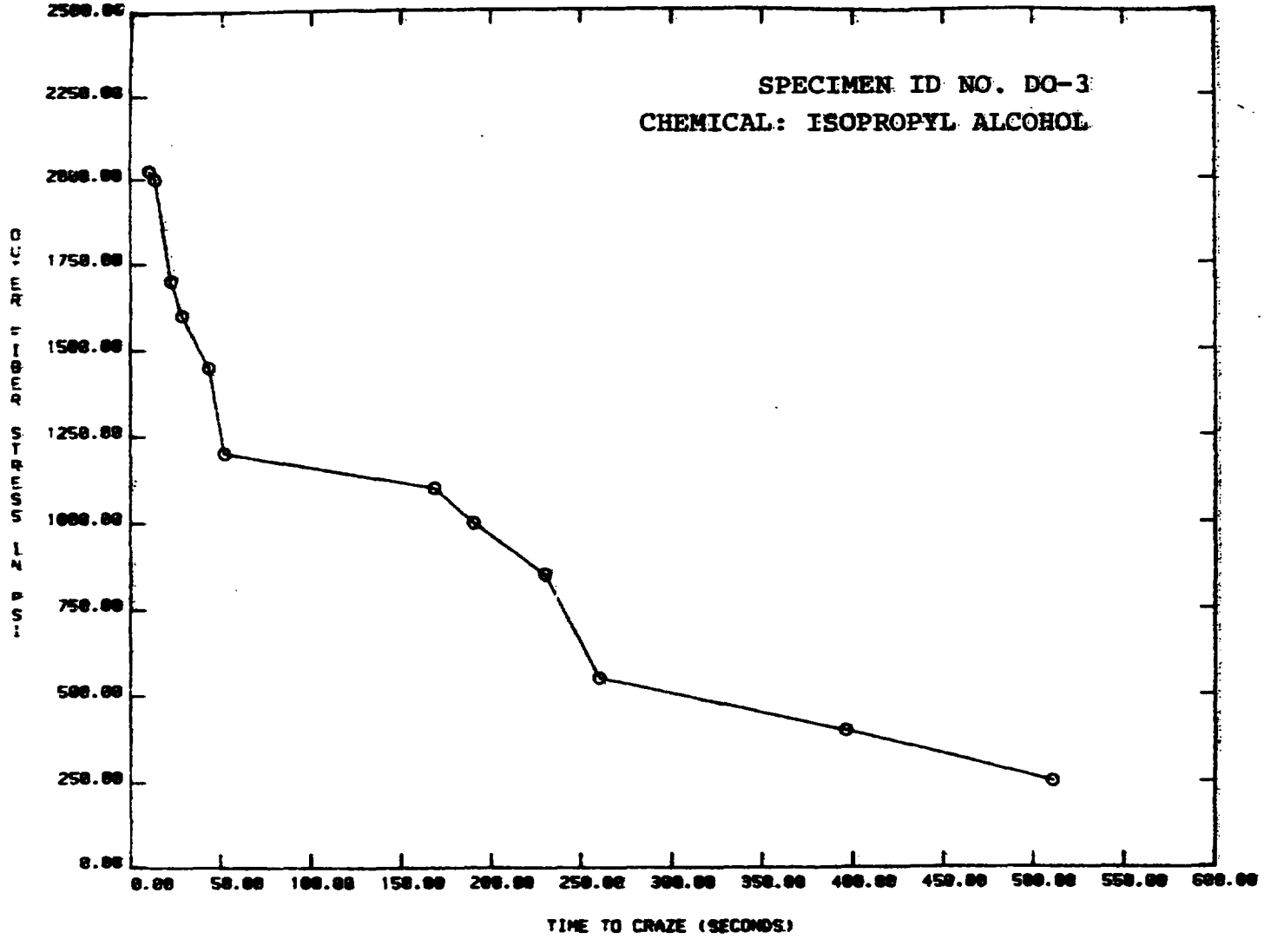

Figure A-13 (continued).

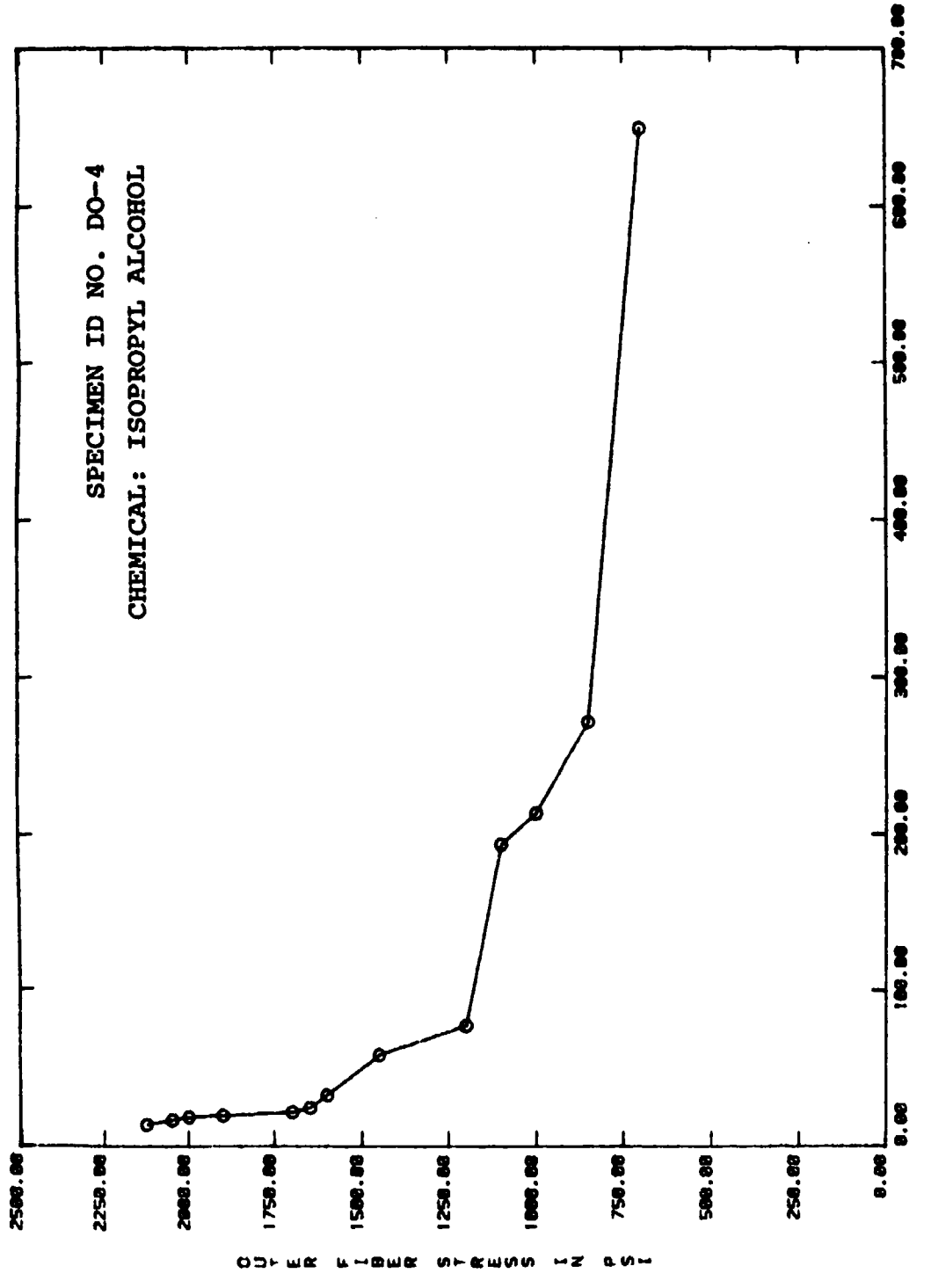

Figure A-13 (continued).

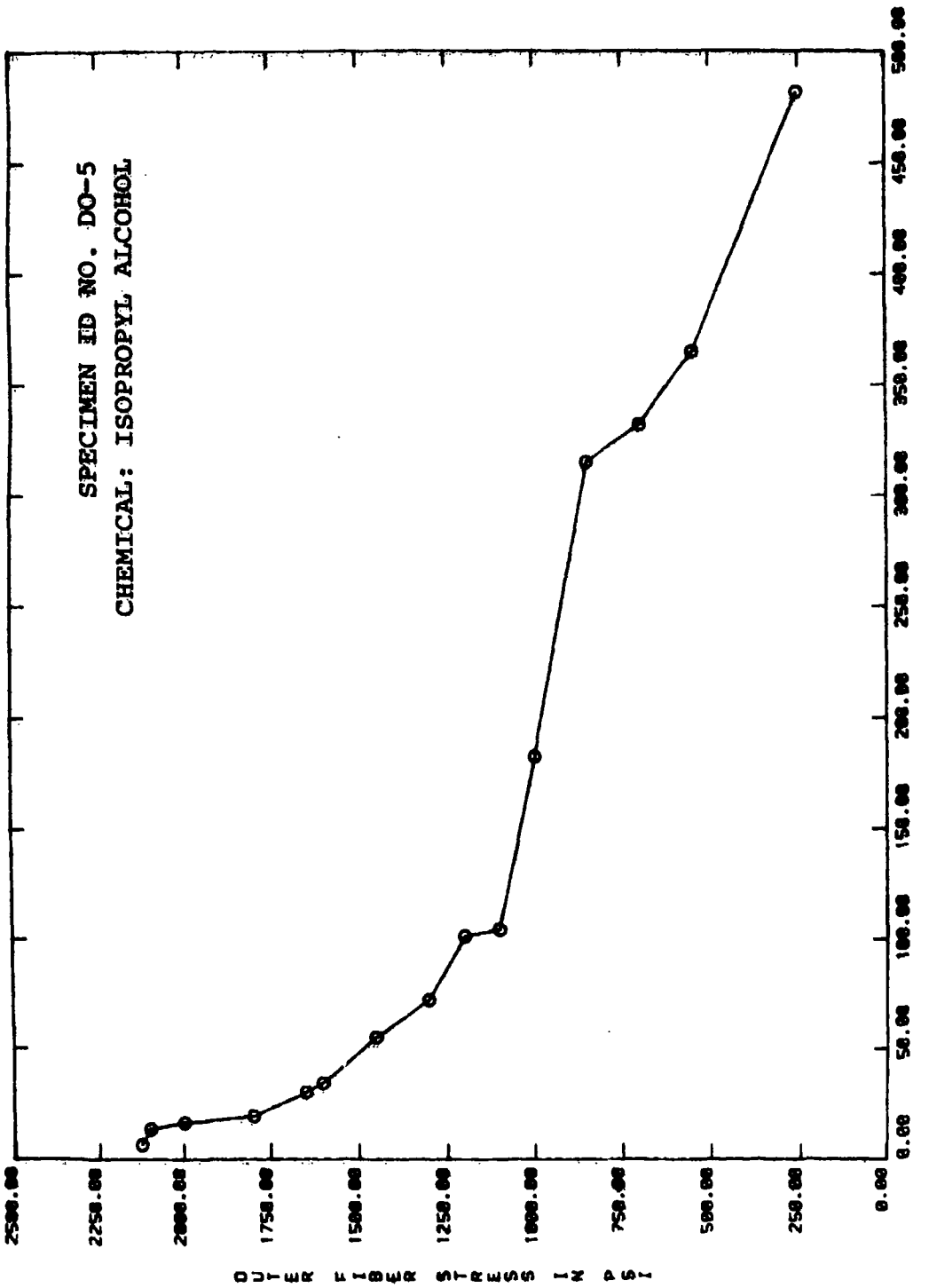

Figure A-13 (continued).

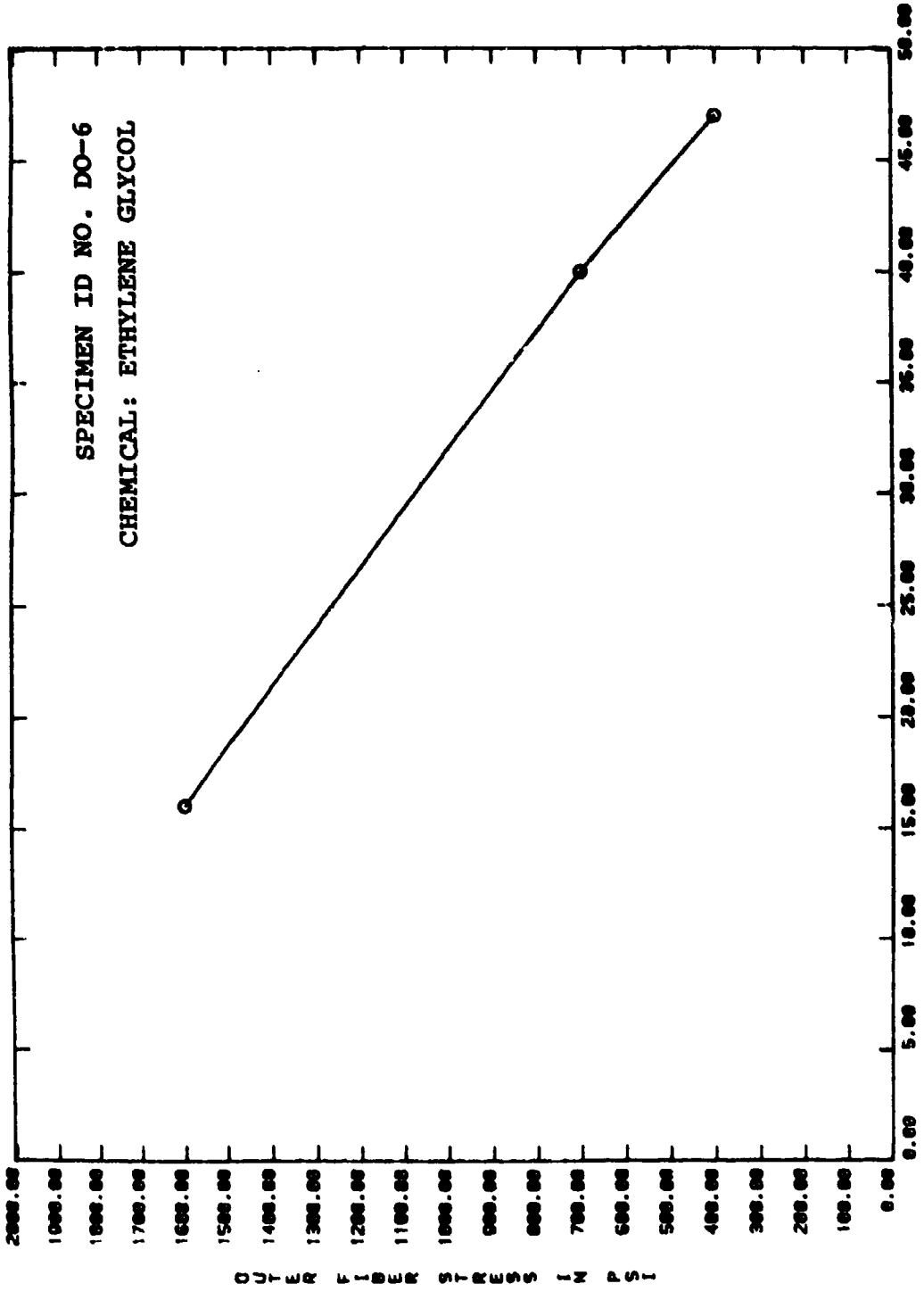

Figure A-13 (continued).

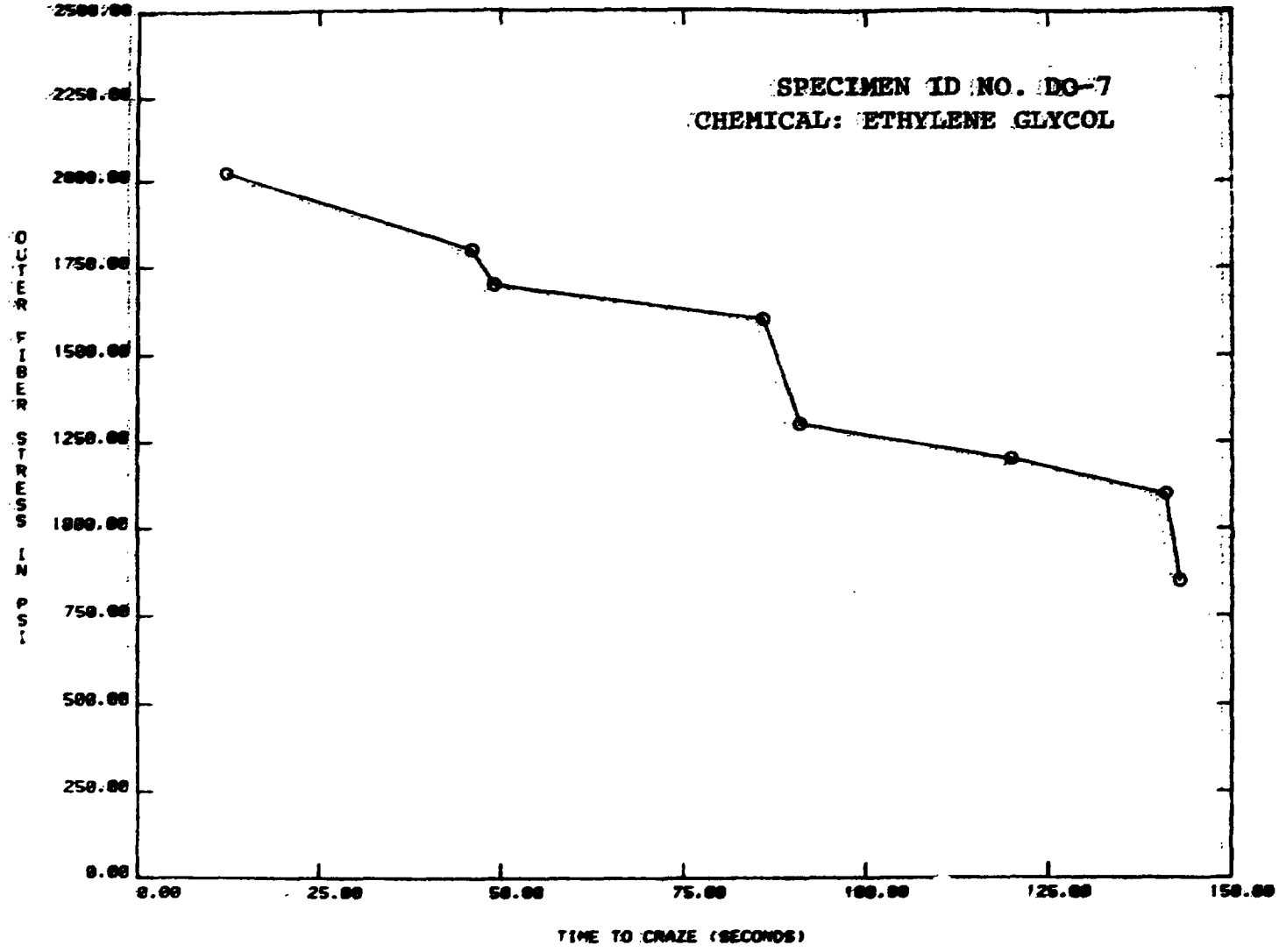

Figure A-13 (continued).

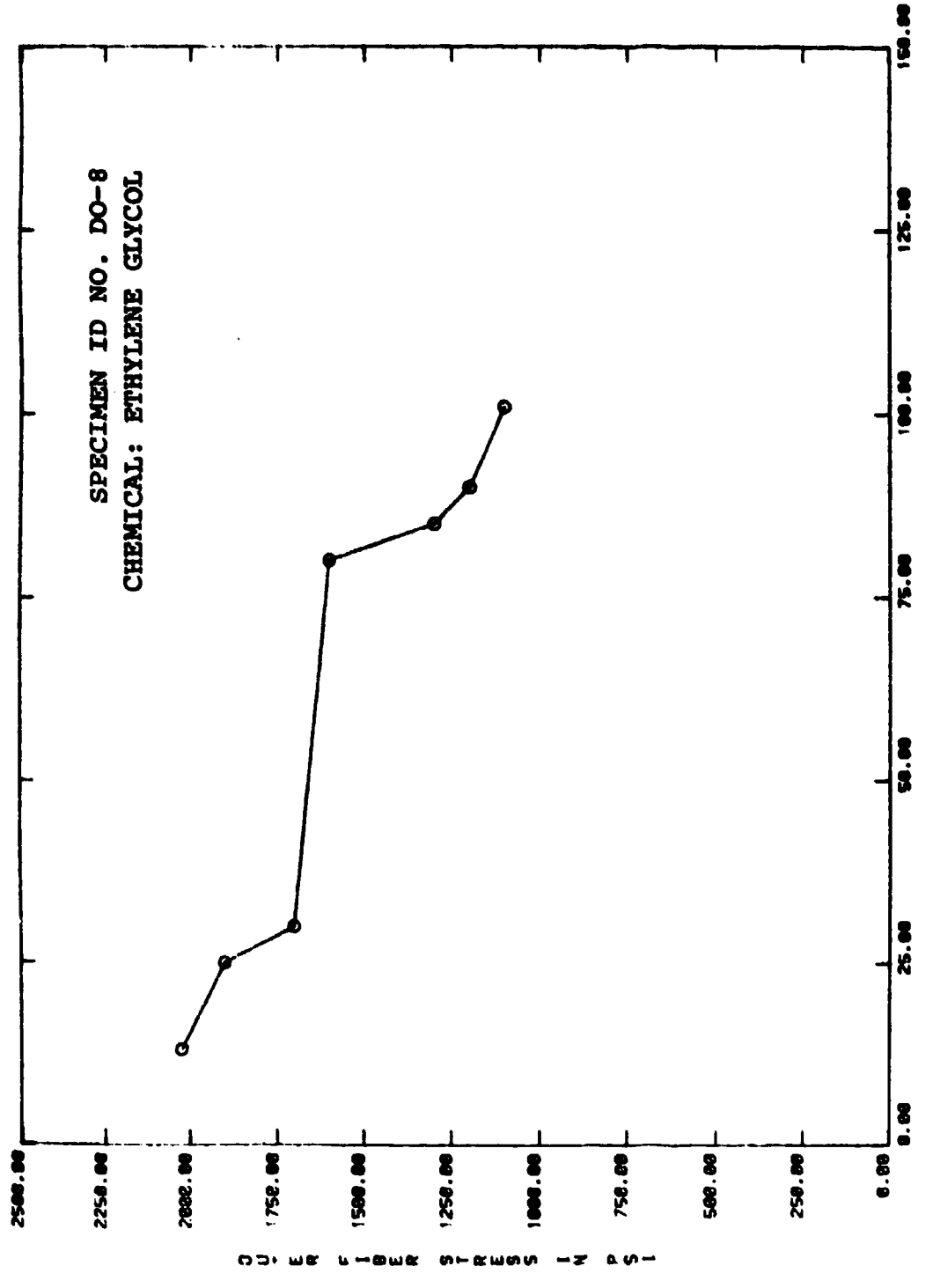

Figure A-13 (continued).

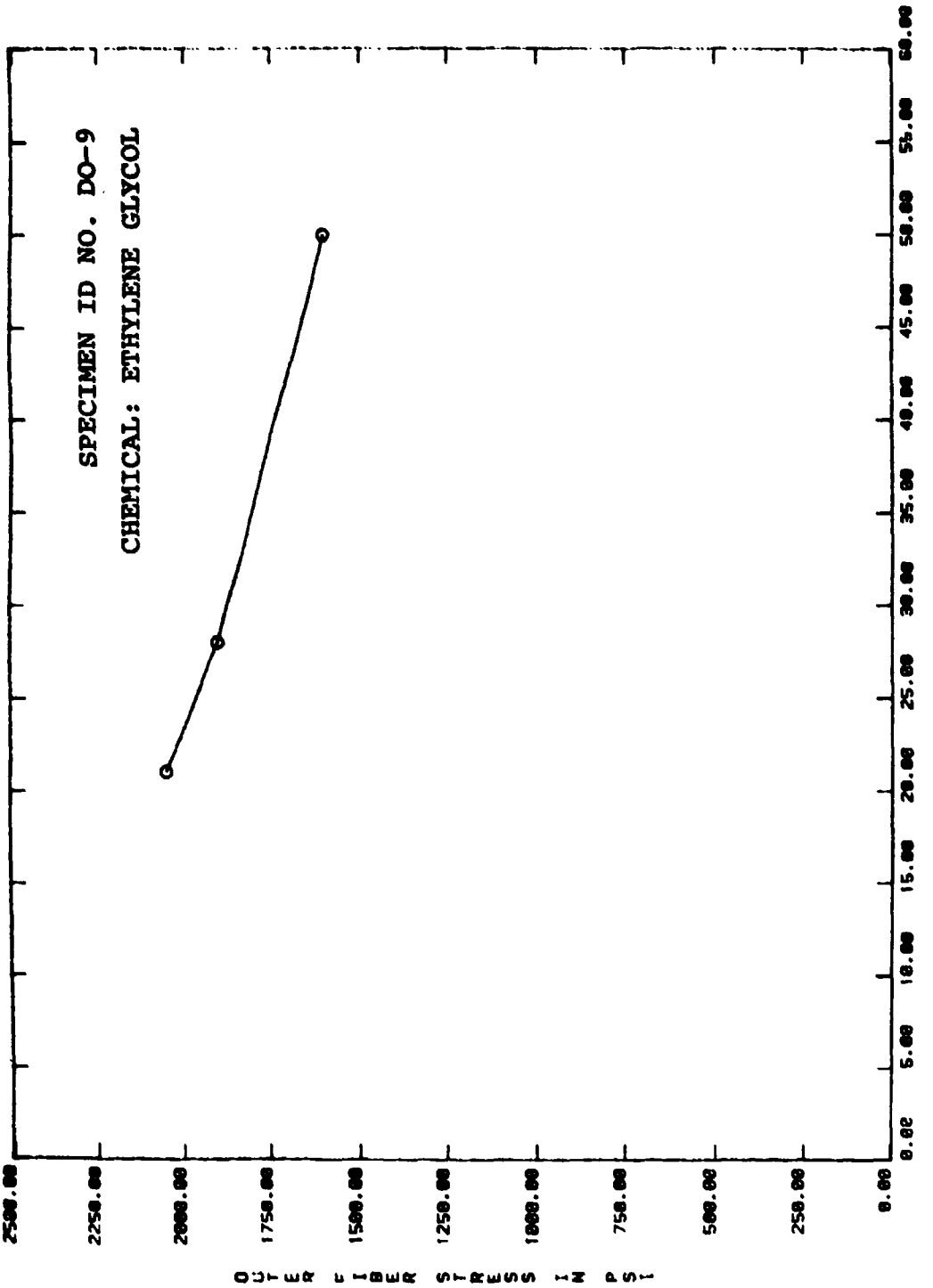

Figure A-13 (concluded).

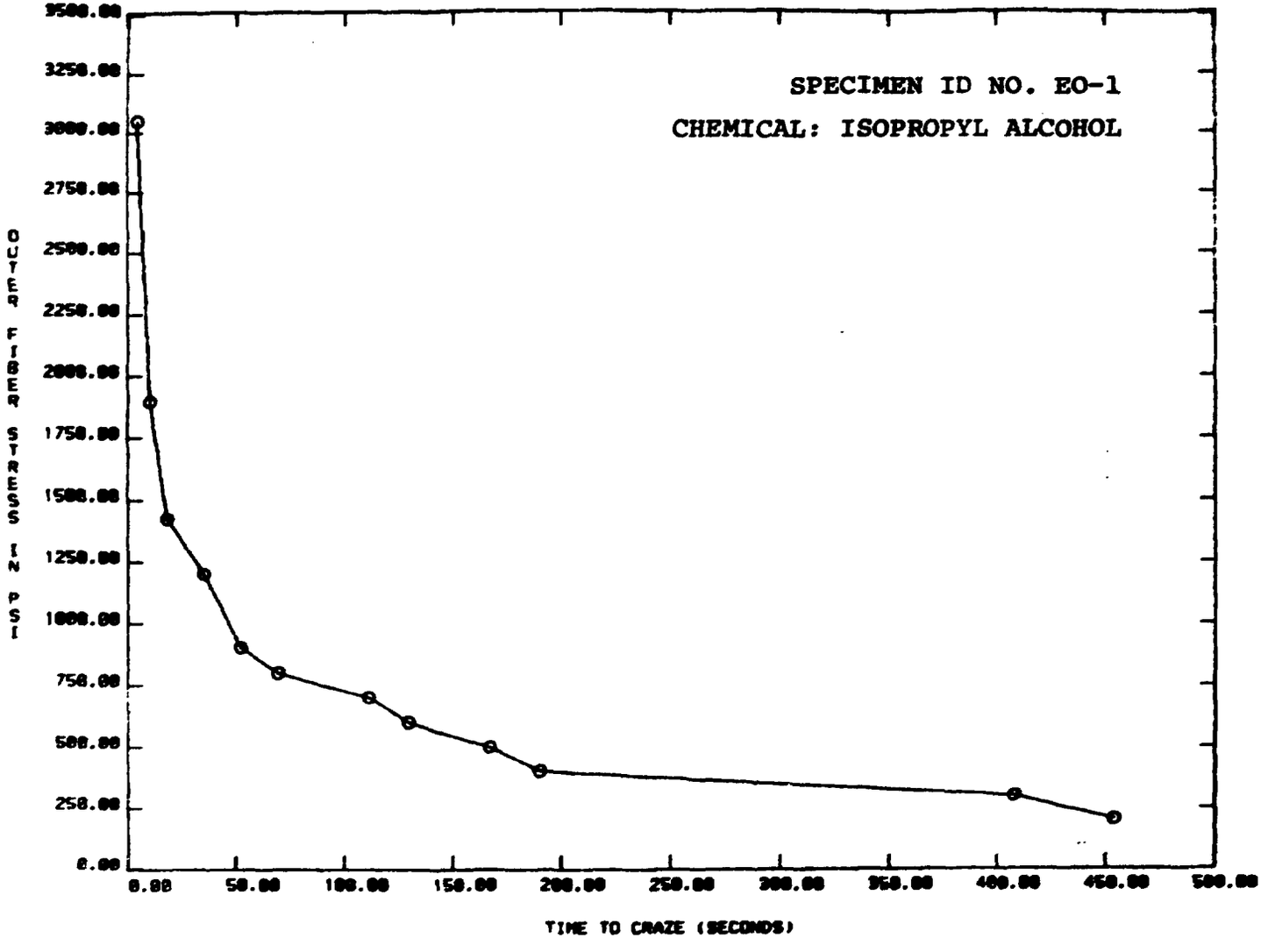

Figure A-14. Plots of Outer Fiber Stress versus Time to Craze for the F-111 Laminated Windshield Specimens.

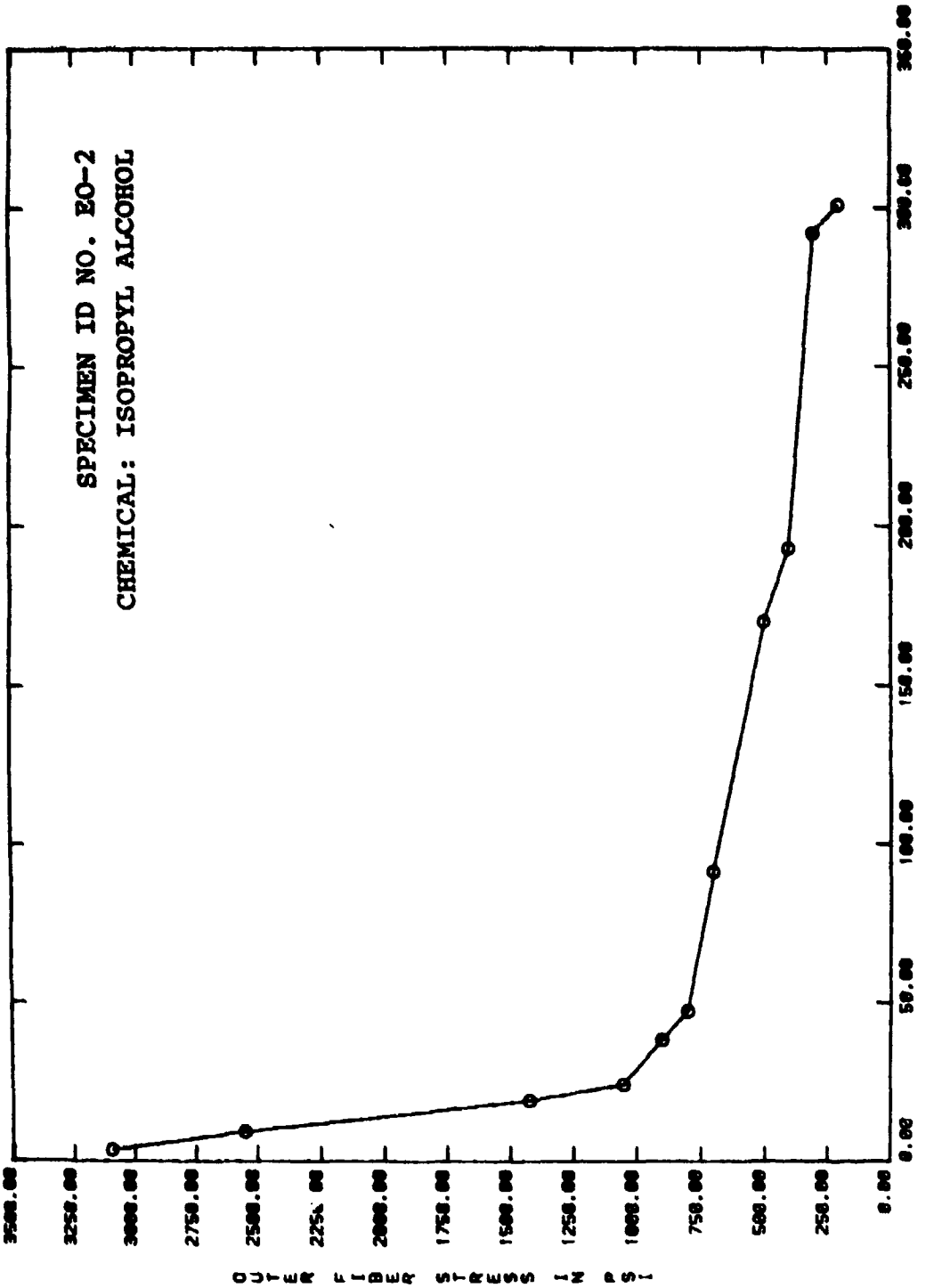

Figure A-14 (continued).

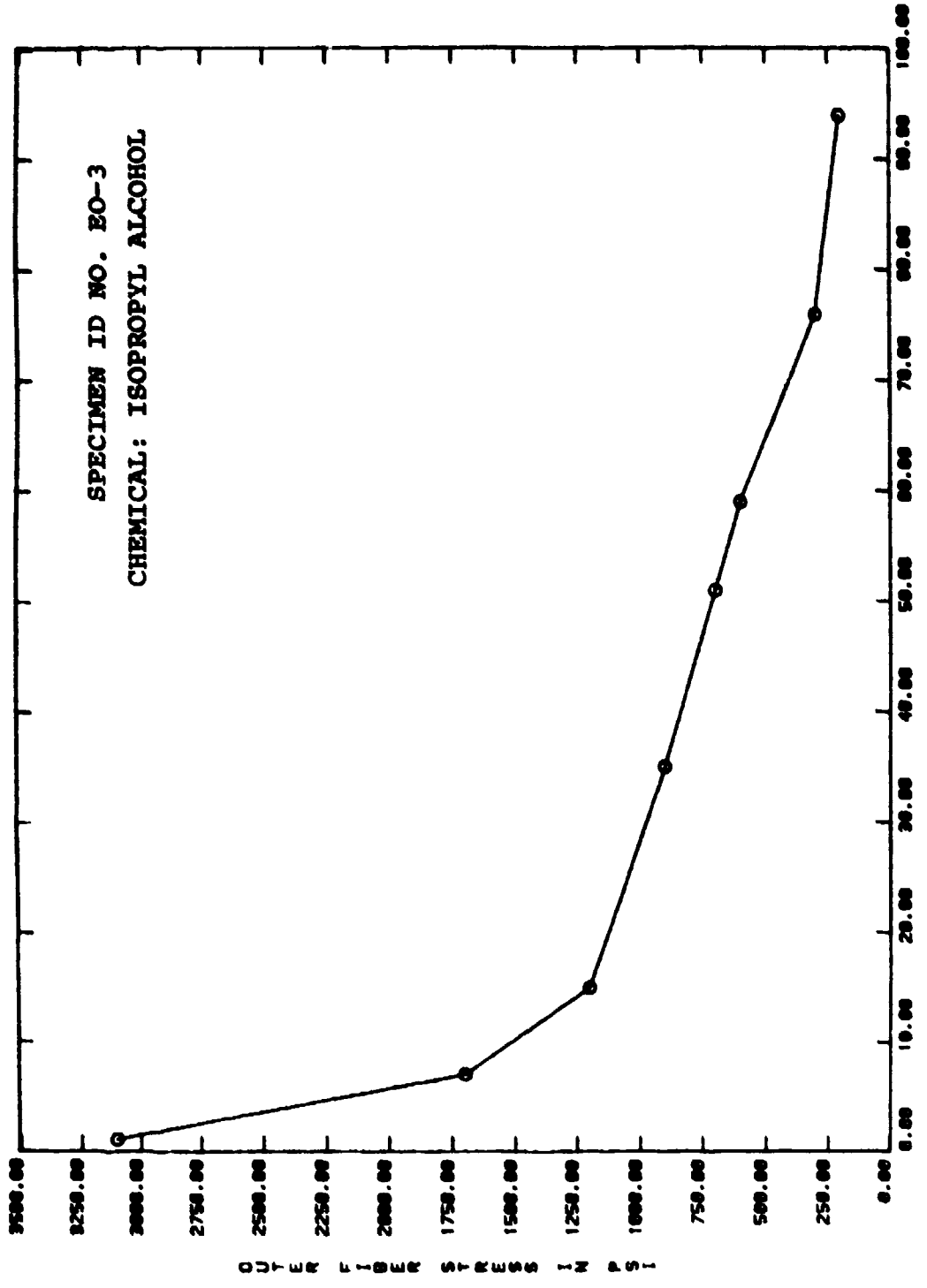

Figure A-14 (continued).

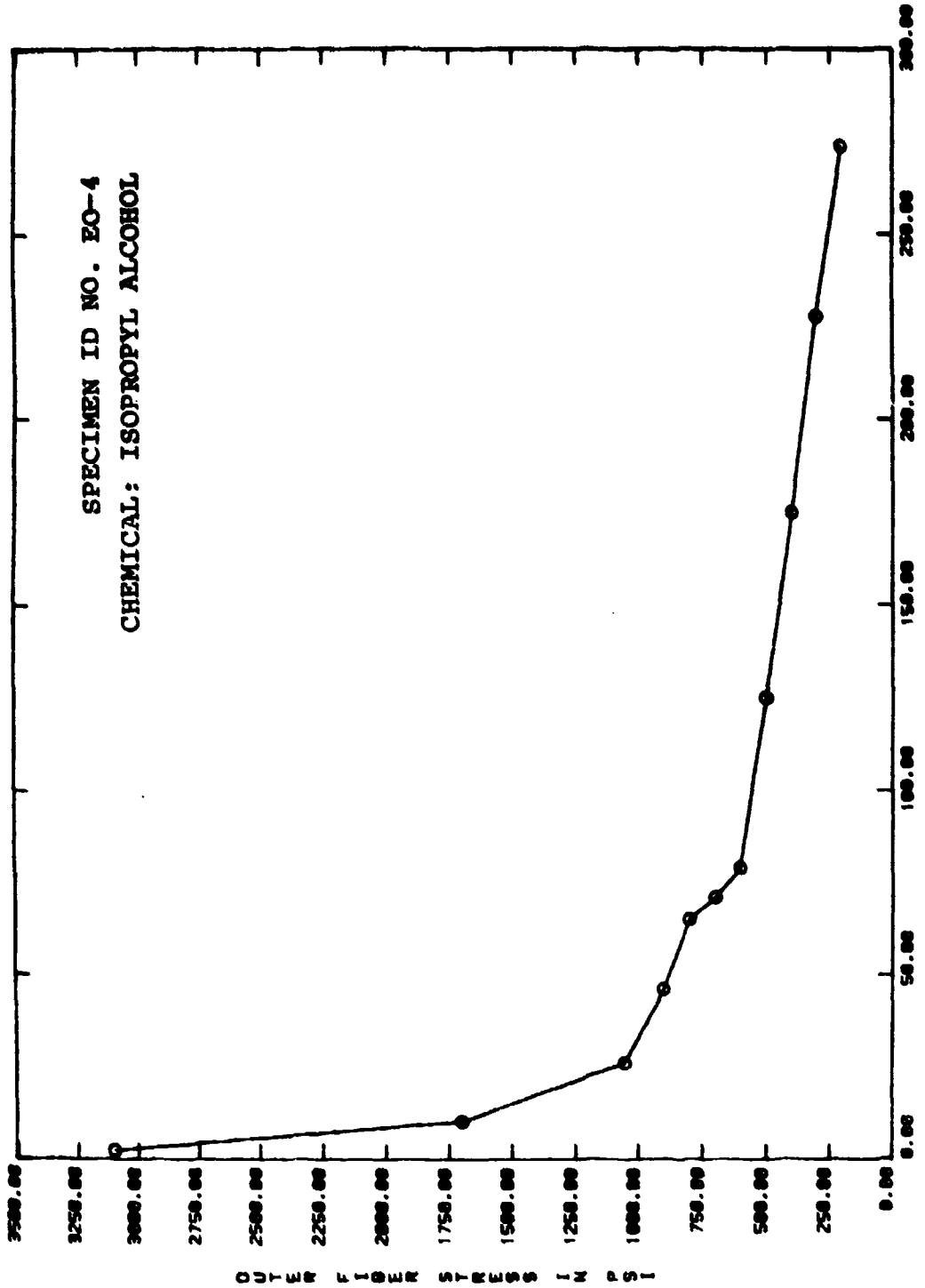

Figure A-14 (continued).

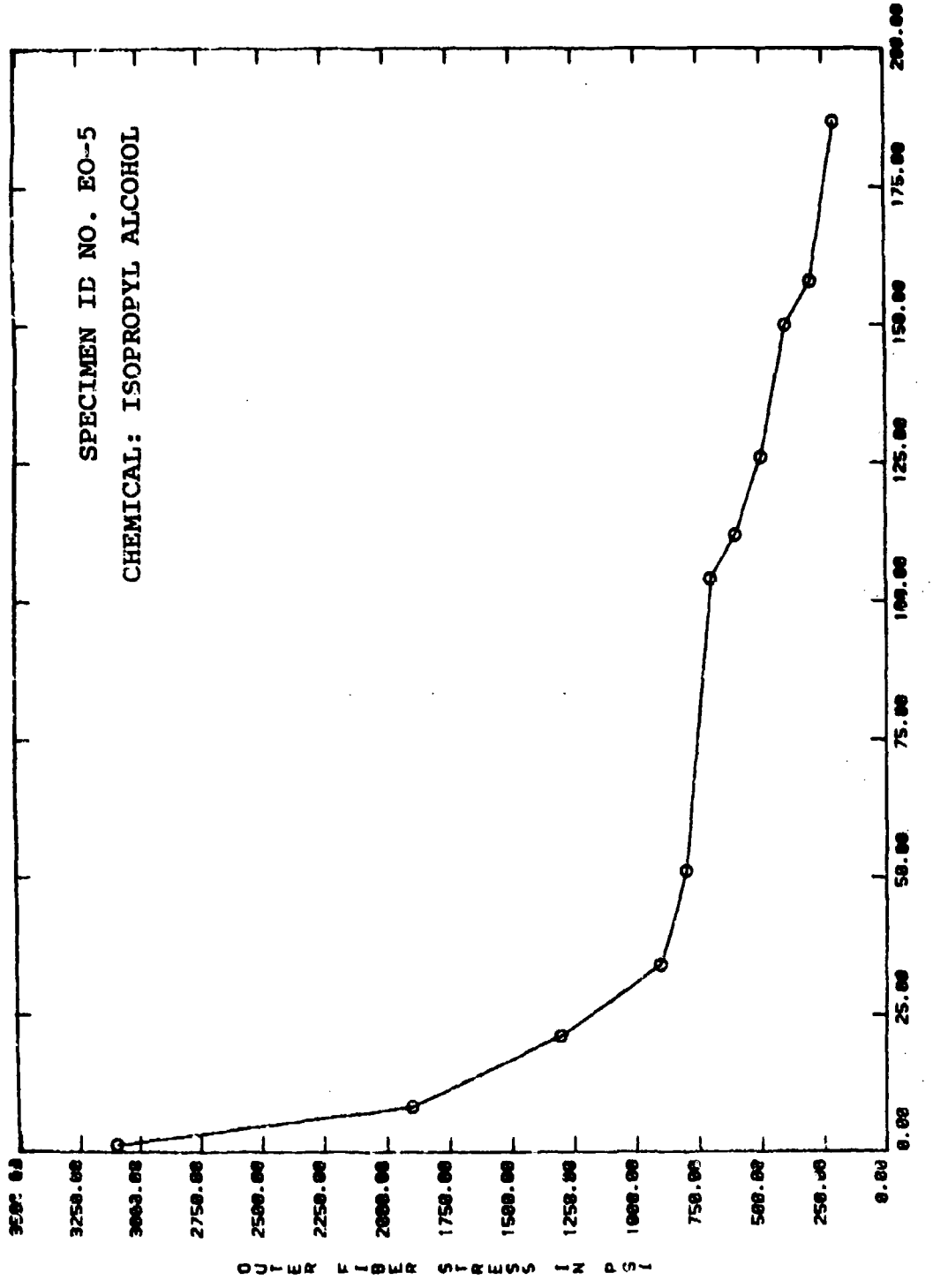

Figure A-14 (continued).

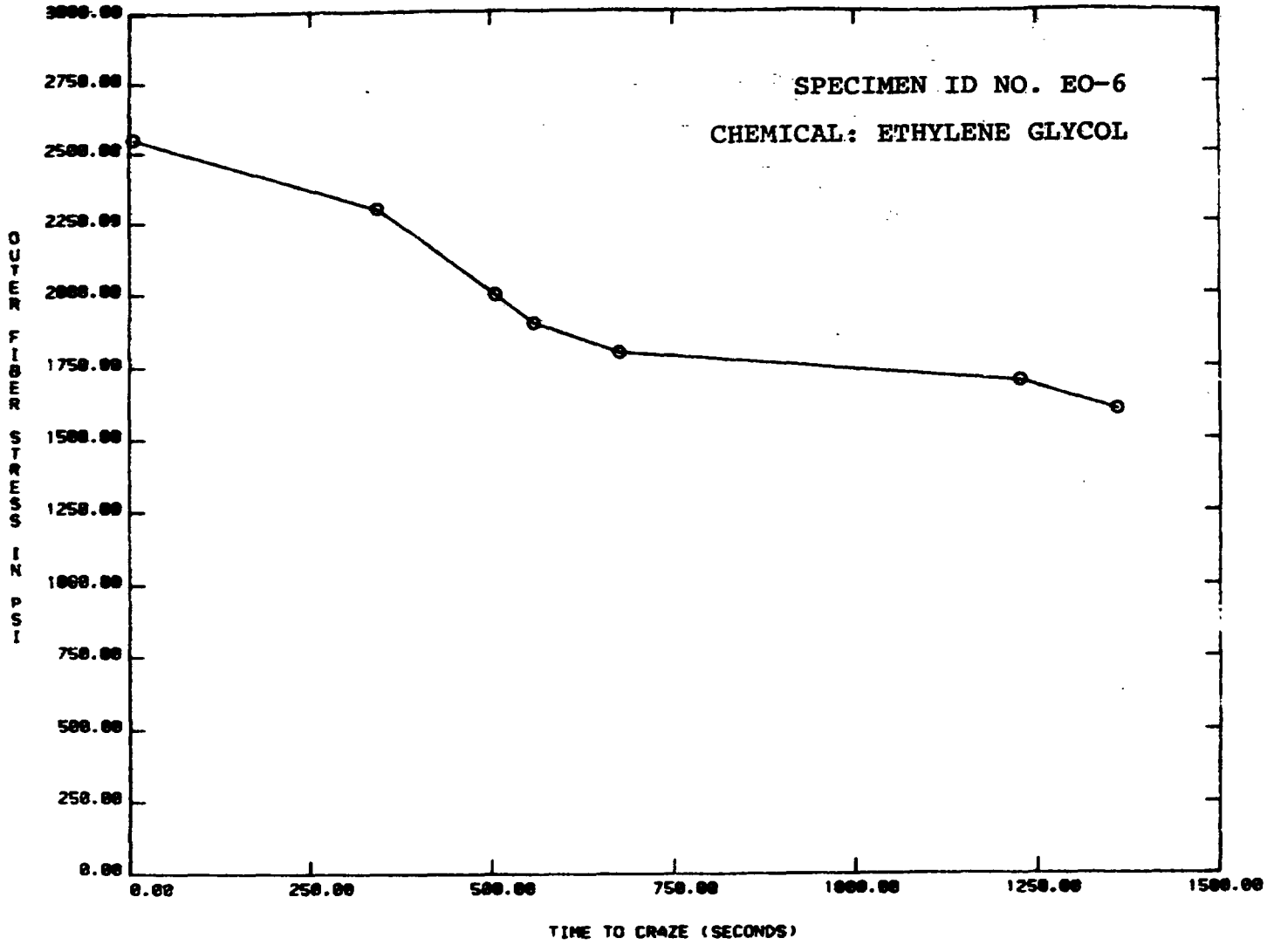

Figure A-14 (continued).

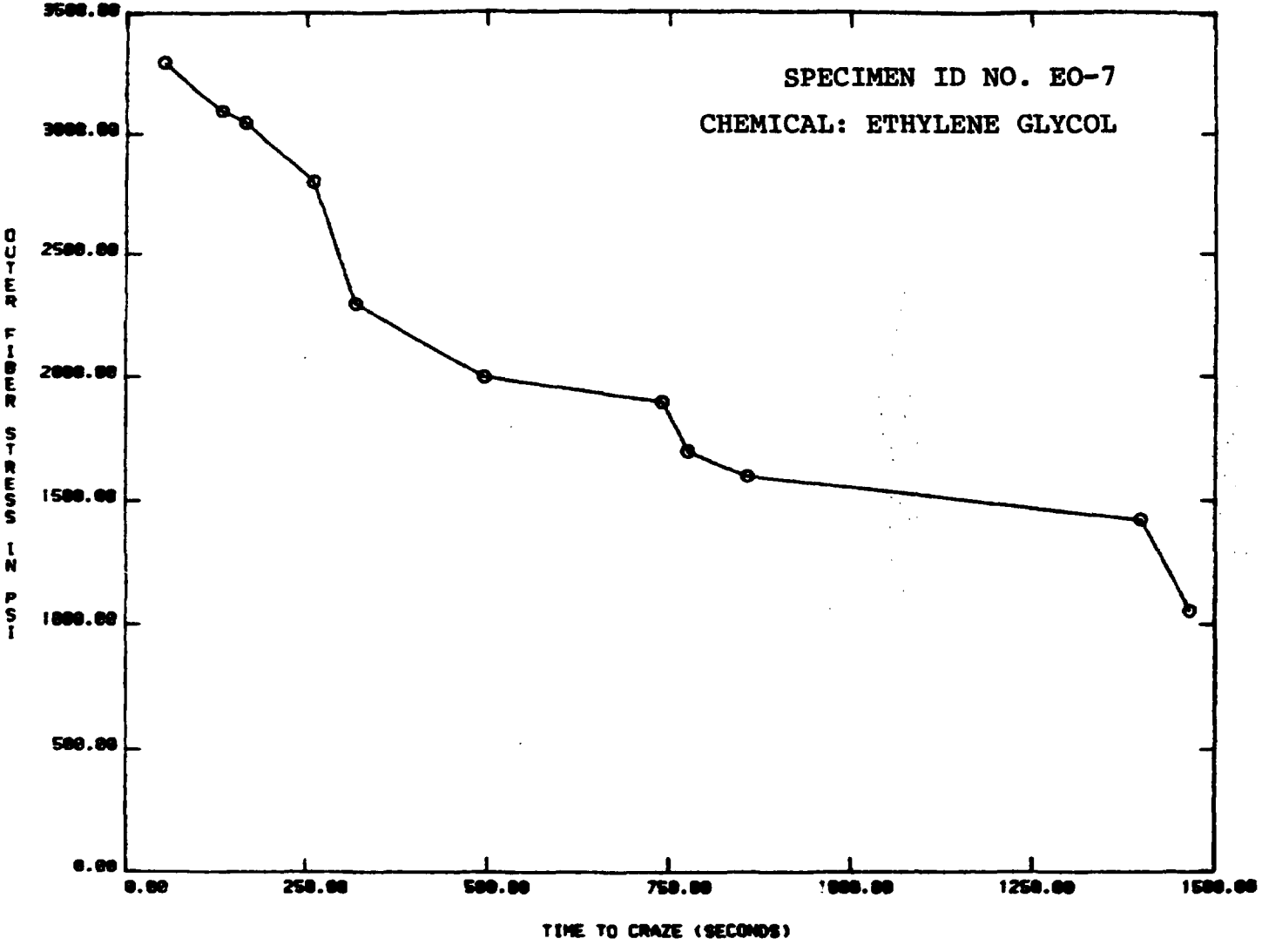

Figure A-14 (continued).

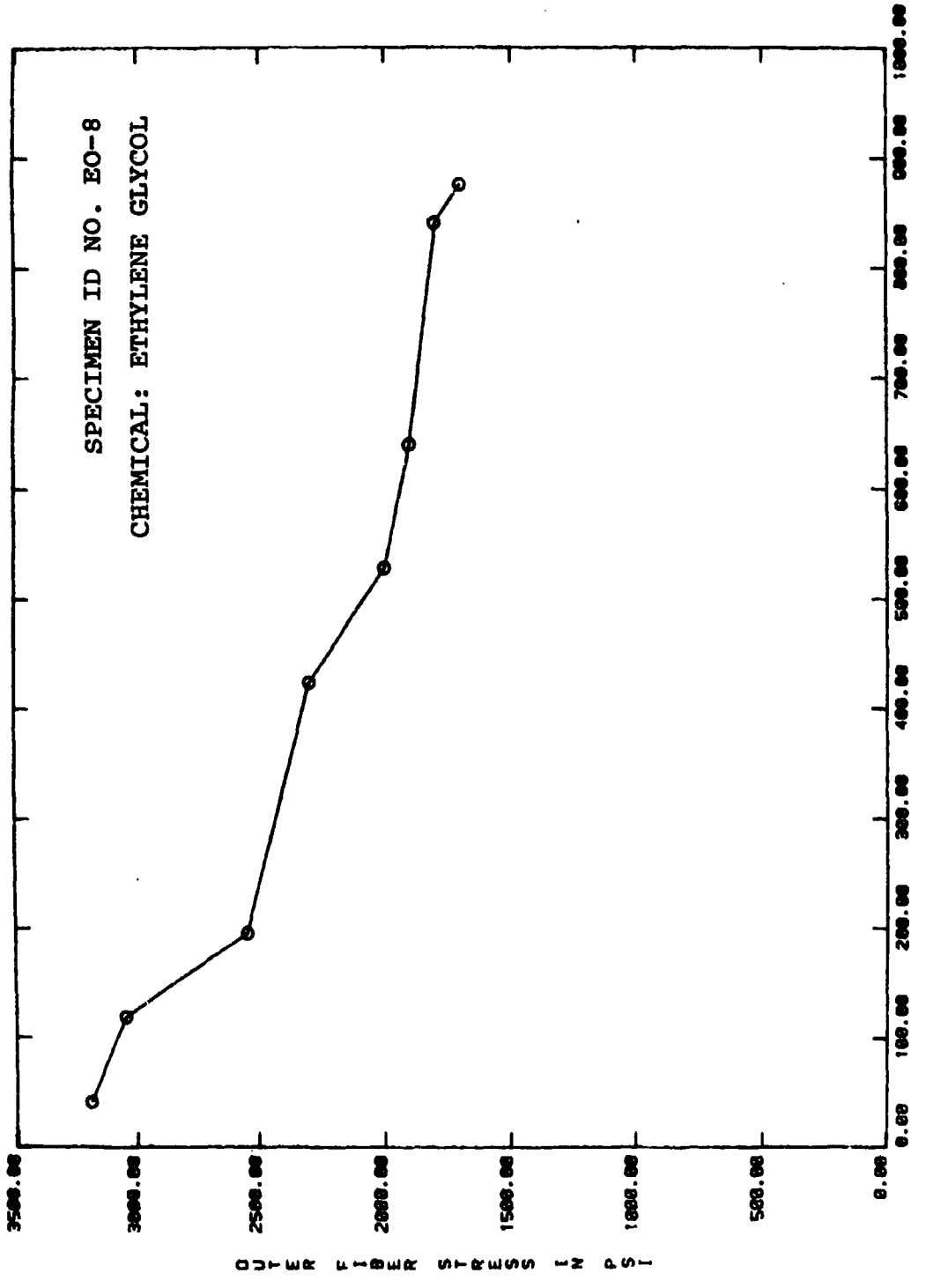

Figure A-14 (continued).

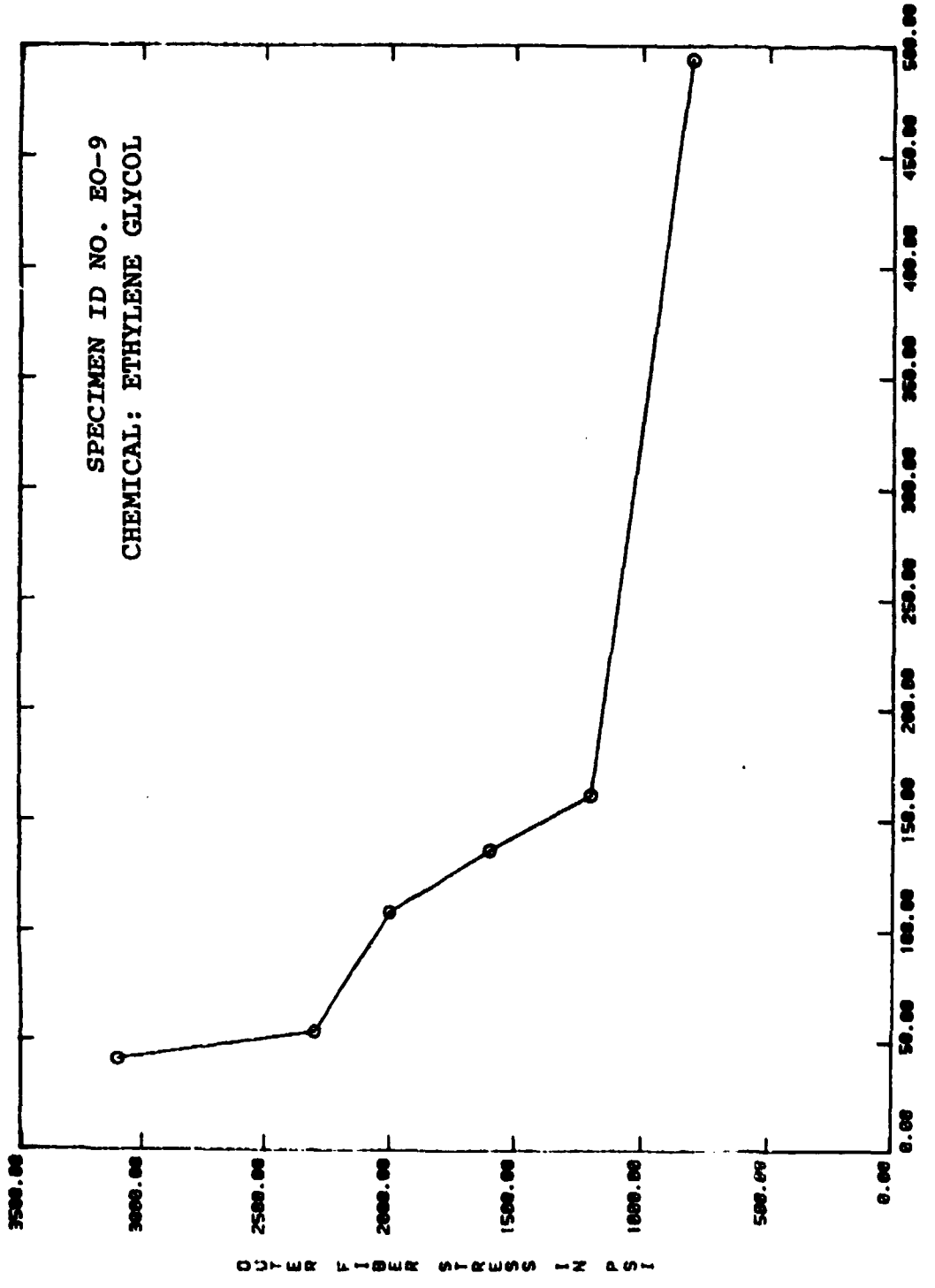

Figure A-14 (continued).

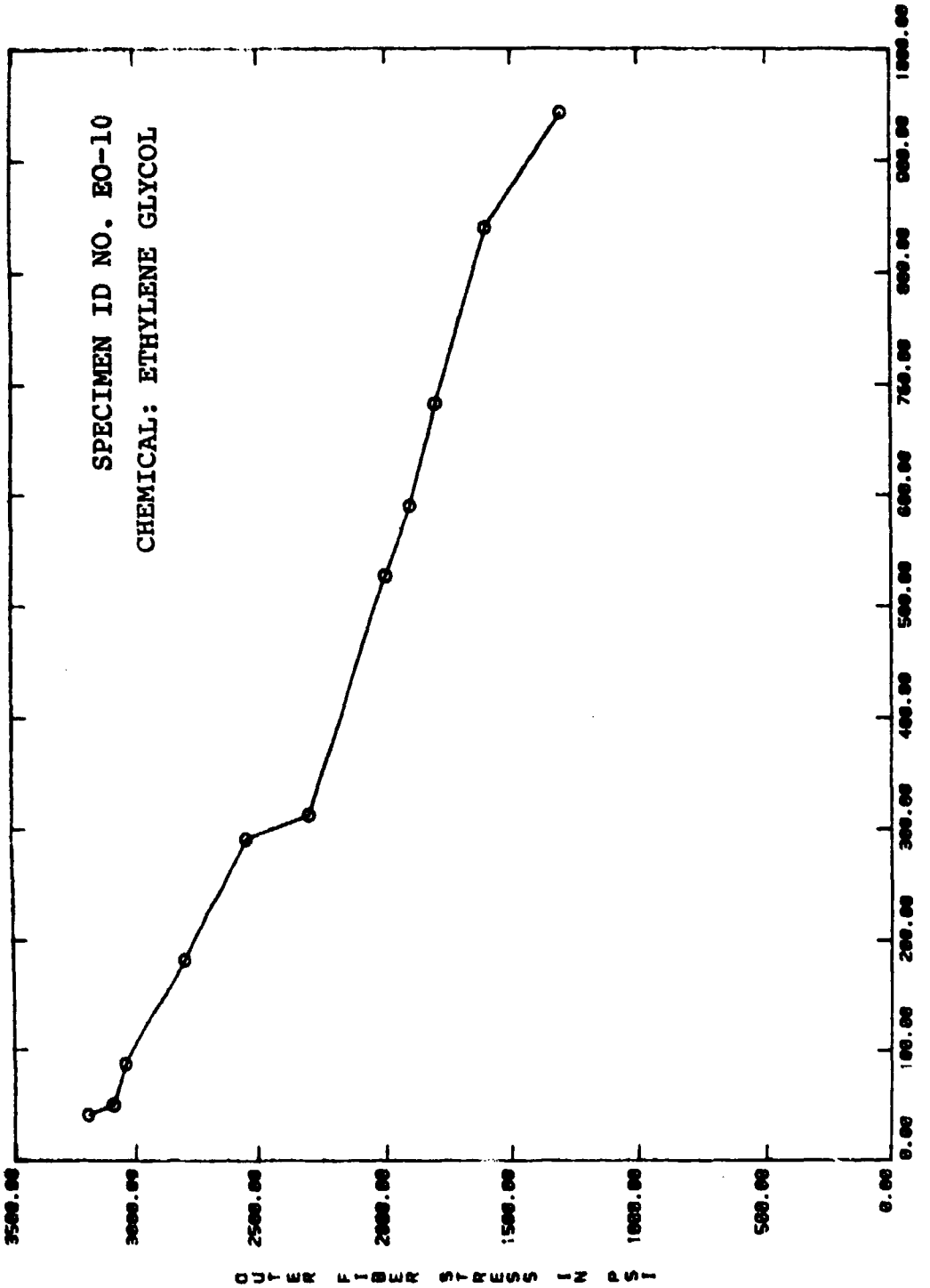

Figure A-14 (concluded).

APPENDIX B

INFLIGHT ABRASION TEST DATA
IN ACCORDANCE WITH
PROPOSED ASTM SALT ABRASION TEST METHOD

Specimen Number	Equivalent Exposure (years)	Number of Salt Blasts (total)	Average % Trans.	Standard Deviation	Average % Haze	Standard Deviation
AX 1-5	0	0	90.96	0.055	1.06	0.189
	1	0	91.76	0.055	2.21	0.385
		2	91.56	0.055	3.09	0.444
		4	91.32	0.084	4.20	0.522
		8	91.06	0.182	5.56	0.264
		16	90.92	0.192	7.65	0.762
		25	90.64	0.152	8.73	0.790
		50	89.96	0.207	13.80	0.908
		100	89.40	0.200	18.10	0.815
	2	0	90.02	0.164	14.64	1.101
		2	90.42	0.192	13.76	1.029
		4	90.48	0.192	12.94	1.623
		8	90.56	0.152	13.78	1.163
		16	90.44	0.114	14.48	0.746
		25	90.32	0.130	14.88	0.760
		50	89.74	0.089	17.98	0.661
		100	89.26	0.055	20.80	0.158
	3	0	89.74	0.134	18.84	1.067
		2	89.94	0.182	18.60	0.872
		4	89.98	0.192	17.60	0.851
		8	89.98	0.084	17.74	0.727
		16	89.94	0.055	18.10	0.764
		25	89.86	0.055	18.34	0.680
		50	89.52	0.110	20.16	0.730
		100	88.82	0.396	23.18	1.486

Specimen Number	Equivalent Exposure (years)	Number of Salt Blasts (total)	Average % Trans.	Standard Deviation	Average % Haze	Standard Deviation
BX 1-6	0	0	92.08	0.240	1.80	2.320
	1	0	92.83	0.050	2.24	0.458
		2	92.78	0.050	2.83	0.408
		4	92.73	0.050	3.51	0.211
		8	92.68	0.050	4.40	0.244
		16	92.53	0.050	6.69	0.381
		25	92.40	0.000	8.51	0.698
		50	92.15	0.058	13.03	1.320
		100	91.70	0.082	17.68	0.903
	2	0	92.27	0.327	9.47	5.941
		2	92.32	0.279	9.37	5.661
		4	92.40	0.167	9.17	4.948
		8	92.28	0.256	9.85	4.748
		16	92.15	0.281	11.50	4.496
		25	92.12	0.214	13.03	4.441
		50	92.03	0.327	15.20	4.589
		100	91.77	0.197	18.92	2.712
	3	0	91.82	0.343	16.48	4.979
		2	91.93	0.175	15.62	4.275
		4	91.95	0.243	15.47	4.034
		8	91.92	0.264	15.85	3.841
		16	92.02	0.223	15.88	3.601
		25	91.95	0.243	16.23	3.621
		50	92.12	0.147	17.52	4.012
		100	91.52	0.436	20.45	4.059

Specimen Number	Equivalent Exposure (years)	Number of Salt Blasts (total)	Average % Trans.	Standard Deviation	Average % Haze	Standard Deviation
CX 1-5	0	0	87.0	0.122	1.22	0.188
	1	0	88.56	0.167	3.65	0.430
		2	88.48	0.130	4.75	0.974
		4	88.38	0.130	5.41	0.957
		8	88.26	0.114	5.82	0.973
		16	88.16	0.152	6.81	0.838
		25	88.04	0.089	8.36	1.347
		50	87.90	0.100	13.94	1.297
	2	0	85.52	0.901	16.60	2.444
		2	85.40	0.875	16.76	2.651
		4	85.40	0.964	17.68	2.602
		8	85.32	1.038	18.44	2.643
		16	85.18	0.947	21.08	2.956
		25	85.22	1.001	23.04	3.490
		50	85.14	0.996	27.78	3.529
		100	85.32	1.013	31.56	4.289
	3	0	81.04	1.205	31.60	4.525
		2	80.94	1.410	31.96	4.181
		4	80.70	1.384	32.98	3.781
		8	80.38	1.375	35.22	3.945
		16	79.92	1.534	40.68	6.050
		25	79.68	1.585	45.14	6.352
		50	78.90	1.375	53.02	5.453
		100	77.86	1.246	61.88	4.030

Specimen Number	Equivalent Exposure (years)	Number of Salt Blasts (total)	Average % Trans.	Standard Deviation	Average % Haze	Standard Deviation
DX 1-5	0	0	86.70	0.187	2.33	0.223
	1	0	88.04	0.152	3.67	0.836
		2	87.96	0.167	4.37	0.751
		4	87.86	0.167	4.60	0.747
		8	87.70	0.158	4.76	0.769
		16	87.62	0.148	5.02	0.648
		25	87.48	0.130	5.48	0.720
		50	87.38	0.130	7.25	0.935
		100	87.06	0.167	11.32	0.536
	2	0	87.18	0.130	8.98	0.653
		2	87.24	0.114	8.38	0.832
		4	87.34	0.114	8.46	0.677
		8	87.36	0.089	8.44	1.001
		16	87.24	0.114	9.16	0.885
		25	87.20	0.071	9.84	0.879
		50	87.12	0.084	12.28	0.653
		100	86.74	0.114	15.26	0.673
	3	0	86.82	0.164	13.72	0.581
		2	86.92	0.148	13.10	0.447
		4	86.94	0.114	13.12	0.390
		8	86.92	0.148	13.26	0.336
		16	86.92	0.084	13.70	0.418
		25	86.92	0.084	13.98	0.335
		50	86.76	0.089	15.26	0.336
		100	86.60	0.071	17.40	0.245

Specimen Number	Equivalent Exposure (years)	Number of Salt Blasts (total)	Average % Trans.	Standard Deviation	Average % Haze	Standard Deviation
EX 1-5	0	0	84.30	0.158	2.53	0.103
	1	0	85.23	0.126	3.49	0.152
		2	85.12	0.045	3.84	0.125
		4	85.10	0.071	4.10	0.225
		8	85.04	0.055	4.26	0.249
		16	85.00	0.071	4.57	0.277
		25	84.86	0.089	5.28	0.497
		50	84.52	0.130	9.00	1.974
		100	84.12	0.192	12.10	1.775
	2	0	84.04	0.167	9.52	1.816
		2	84.20	0.141	8.52	1.961
		4	84.26	0.167	8.30	1.832
		8	84.24	0.152	8.46	1.837
		16	84.32	0.084	8.72	1.564
		25	84.26	0.114	9.58	1.470
		50	83.90	0.100	11.76	1.074
		100	83.70	0.141	14.00	1.065
	3	0	83.74	0.089	11.94	1.115
		2	83.90	0.100	11.56	1.422
		4	83.86	0.055	11.72	1.213
		8	83.82	0.084	11.94	1.078
		16	83.80	0.100	12.22	1.064
		25	83.76	0.089	12.60	0.954
		50	83.68	0.084	13.70	0.869
		100	83.30	0.071	15.52	0.589